

MicroRNAs in the Tumor Biology of Soft Tissue Sarcomas

Caroline Gits



The research for this thesis was performed within the framework of the Erasmus Postgraduate School Molecular Medicine at the department of Medical Oncology, Erasmus Medical Center, Erasmus MC Cancer Center, Rotterdam, The Netherlands.

The research described in this thesis was funded by EC FP6 CONTICANET Network of Excellence (LSHC-CT-2005-018806) from the European Commission.

Printing of this thesis was financially supported by

Exiqon A/S

Greiner Bio-One B.V.

ProStrakan Pharma BV

Cover design: Jan-Maarten Nachtegeller

Layout: Nikki Vermeulen, Ridderprint BV., Ridderkerk, the Netherlands

Printing: Ridderprint BV., Ridderkerk, the Netherlands

ISBN: 978-90-5335-737-8

All rights reserved. No part of this thesis may be reproduced, stored in a retrieval system of any nature, or transmitted in any form or by any means, without prior written permission of the author, or when appropriate, of the publishers of the publications.

MicroRNAs in the Tumor Biology of Soft Tissue Sarcomas

MicroRNAs in de tumor biologie van weke delen sarcomen

Proefschrift

Ter verkrijging van de graad van doctor aan de
Erasmus Universiteit Rotterdam
op gezag van de
rector magnificus

Prof.dr. H.A.P. Pols

en volgens besluit van het College voor Promoties.
De openbare verdediging zal plaatsvinden op

woensdag 13 november 2013 om 11.30 uur

door

Caroline Maria Margarita Gits

Geboren te Sittard



PROMOTIECOMMISSIE

Promotoren: Prof.dr. S. Sleijfer
Prof.dr. J. Verweij

Overige leden: Prof.dr. R. Fodde
Prof.dr. M. Debiec-Rychter
Prof.dr. G.W. Jenster

Co-promotor: dr. E.A.C. Wiemer

TABLE OF CONTENTS

Chapter 1	General introduction	7
Chapter 2	MicroRNA expression profiles distinguish liposarcoma subtypes and implicate miR-145 and miR-451 as tumor suppressors	23
Chapter 3	MicroRNAs in myxoid/round cell liposarcomas: FUS-CHOP regulated miR-497 and miR-30a target the insulin-like growth factor 1 receptor pathway	67
Chapter 4	MiR-17-92 and miR-221/222 cluster members target KIT and ETV1 in human gastrointestinal stromal tumors	99
Chapter 5	MicroRNA response to hypoxic stress in soft tissue sarcoma cells: microRNA mediated regulation of HIF3A	131
Chapter 6	General discussion	153
Chapter 7	Summary/Samenvatting	169
Chapter 8	Acknowledgements	175
	Curriculum Vitae	181
	Publication List	183
	PhD portfolio	185

Chapter 1

General introduction





SOFT TISSUE SARCOMAS

Sarcoma is a rare cancer of the connective tissue, comprising only 1% of all adult malignancies. Sarcomas are derived from mesenchymal cells, in contrast to the more commonly occurring carcinomas that originate from epithelial cells. They constitute a heterogeneous group of tumors, consisting of more than 50 histological subtypes that can occur almost anywhere in the body, such as in muscles, fat, bone, cartilage, fibrous tissue, synovial tissue and nerves. Roughly, sarcomas can be divided in two large groups: primary bone sarcomas (i.e. osteo-, chondro- and most Ewing's family of sarcomas, affecting bone or cartilage tissue), and the soft tissue sarcomas, the latter being the focus of this thesis (Table 1).¹⁻²

Table 1: Most common types of soft tissue sarcoma.

Soft Tissue Sarcoma	Site of occurrence	Incidence rate*
Gastrointestinal Stromal Tumors	Interstitial Cells of Cajal	15%
Liposarcoma	Fat tissue	15%
Leiomyosarcoma	Smooth muscle tissue	10%
Rhabdomyosarcoma	Striated muscle tissue	6%
Dermatofibrosarcoma	Fibrous tissue	6%
Kaposi sarcoma	Blood vessels of skin or mucosa	4%
Synovial sarcoma	Lining of joint cavities	2%
Angiosarcoma	Blood/lymph vessels	2%

* Age-standardized incidence rates (% of all sarcomas), World Health Organization.⁸

However, it is unclear whether sarcomas arise from the tissue in which they reside. Rhabdomyosarcomas, for instance, often arise in sites where striated muscle is sparse or absent, which suggests that they do not develop from differentiated muscle cells. Furthermore, several sarcomas are from uncertain differentiation and for most sarcomas the exact cell of origin has not been identified.³⁻⁴ Supposedly, a multipotent cell is responsible for the development of diverse sarcoma subtypes.⁴⁻⁵ It has been postulated that sarcomas originate from a mutated mesenchymal stem cell (MSC), which is vulnerable for subsequent mutations.⁴⁻⁵ Depending on the impact of the initial mutation, subsequent additional mutations, and/or the tumor microenvironment, the differentiation capacity is impaired resulting in a specific sarcoma subtype.⁵ Alternatively, sarcomas may arise from diverse differentiated cells that undergo malignant transformation, thereby acquiring stem cell like characteristics.⁶

The annual incidence of soft tissue sarcoma is approximately 30 per million, i.e. each year about 210.000 newly diagnosed patients worldwide,¹ including around 500 people per year in the Netherlands.⁷ Although the incidence rises with age, some types are more common in certain age groups. A number of soft tissue sarcoma entities (e.g. rhabdomyosarcoma, synovial sarcoma

and dermatofibrosarcoma) are particularly linked to children, where they represent 10-15% of all paediatric malignancies.

Most soft tissue sarcomas arise without clear causative factors. Only a small percentage of soft tissue sarcomas are associated with hereditary syndromes, viral infections, chemical substances or radiation exposure. For instance, the Li-Fraumeni syndrome (linked to a germline mutation in the tumor suppressor gene *p53*), Werner syndrome (characterized by premature aging caused by mutations in the *WNR* gene) and neurofibromatosis type 1 (a developmental syndrome that is caused by an inactivating mutation of the *NF1* gene), are associated with soft tissue sarcomas.⁹⁻¹⁰ Epstein-Barr virus infection is particularly associated with smooth muscle sarcomas, whereas infection with human herpesvirus 8 can cause Kaposi sarcoma, especially in immune compromised individuals, such as AIDS patients. Chemicals such as chlorophenol and phenoxy acid herbicides, but also prior radiation therapy for other tumors, are risk factors for the development of sarcomas.^{2, 11} However, for the majority of soft tissue sarcomas an apparent cause has not been identified thus far.

Because of their rarity, the large number of entities, and the heterogeneity even within a specific subtype, histological classification and prediction of clinical behaviour and prognosis in sarcomas is often a challenge.¹² Therefore, classification is usually based on a combination of histology, immunohistochemistry, primary tumor site and genetic analyses. The latter is of interest since soft tissue sarcomas usually present with specific genetic abnormalities, such as mutations (e.g. *KIT/PDGFR*A mutations in GIST), amplifications (e.g. amplification of the 12q13-15 chromosomal region in well differentiated/dedifferentiated liposarcoma), translocations (e.g. t(12;16)(q13;p11) in myxoid/round cell liposarcoma) or complex karyotypes (e.g. in pleomorphic liposarcoma). A deeper knowledge of molecular and genetic characteristics of soft tissue sarcomas can reveal new biomarkers, which can possibly aid in the diagnostic decision making.

Only half of the soft tissue sarcomas are detected in their early stages, before they have metastasized. Because of their frequently slow growth, often deep-seated localization in soft tissue, and the rare occurrence of pain or functional impairment, the tumors can grow relatively large before they are noticed. A setback of this late observation is that 10% of the patients already have detectable metastases (predominantly in the lungs) at the time of diagnosis of the primary tumor, which is associated with poor prognosis.²

Localized disease is often treated with surgery alone for low grade tumors, or a combination of surgery and radiation therapy for high grade tumors, sometimes preceded by neo-adjuvant chemotherapy in case tumor shrinkage is anticipated to facilitate the resection and/or reduce morbidity. However, overall response rates are suboptimal, and disease recurrence and the



development of metastases are common. There are few effective therapies for advanced disease and although many systemic agents give rise to improved progression free survival, median overall survival for patients with advanced soft tissue sarcoma is only 12 months.

Because of the specific genetic abnormalities in some sarcoma subtypes, research increasingly focussed on exploiting these defects as therapeutic targets. The great potential of this approach is clearly underlined by the successes of tyrosine kinase receptor targeting agents in patients with gastrointestinal stromal tumors (GIST). It was recognized that more than 90% of GIST harbor gain-of-function mutations in *c-KIT* or *PDGFRA* and that the products of these mutated genes can be inhibited by tyrosine kinase inhibitors such as imatinib and sunitinib. Since the use of these targeted drugs, the median overall survival of patients with advanced GIST has increased from only 9 months to 5 years, with at least 10% of the patients benefiting from this first line treatment for more than 10 years. So obviously, a better understanding of the biology of other soft tissue sarcoma subtypes, especially regarding driver genes and pathways, is crucial to aid the identification of therapeutic targets and the development of new targeted therapies.

The use of comparative genomic hybridization (CGH) arrays and mRNA profiling has advanced the understanding of genomic aberrations, gene expression profiles and signalling pathways involved in the pathobiology of soft tissue sarcoma. The results of these profiling studies can elucidate novel therapeutic targets, but also, in conjunction with histology, immunohistochemistry and fluorescent in situ hybridization, be of assistance in the diagnostic decision making process.¹³ Accordingly, mRNA profiling has proven to be a powerful tool for tumor classification in sarcoma.¹⁴⁻¹⁸ Recently it has become evident that microRNA (miRNA) expression profiling holds many advantages over mRNA expression profiling in human cancers, such as the superior stability in plasma and paraffin embedded tissues, and the better classification of tumors and tumor subtypes. Furthermore, since one miRNA can target and regulate multiple mRNAs, the effects of miRNAs are more widespread, and therefore deregulation of a single miRNA can be more informative than that of a single gene.¹⁹⁻²⁰ Histological sarcoma subtypes show distinct miRNA expression patterns.²¹⁻²⁴ MiRNAs that are characteristic for a specific type of soft tissue sarcoma and that are involved in the tumorigenic process, could not only be useful for sarcoma (subtype) classification, but could also be a potential target for therapy.

MIRNAS

When the human genome project, which goal was to map the human DNA and identify genes, was finished, around 20.000 protein coding genes (covering less than 2% of the genome) were identified. This was much less than previously anticipated and in the same order of magnitude as in e.g. the nematode *Caenorhabditis elegans*. However, the transcriptional output of the human

genome is at least 60%.²⁵ This led to the believe that a considerable part of what was thought to be ‘junk DNA’ should code for other regulatory structures that contribute to the complexity of the human being. Indeed, the proportion of transcribed non protein-coding sequences to coding sequences increases dramatically from nematodes to mammals.²⁵ Large numbers of regulatory elements (promoter/enhancer regions, transcription factor binding sites) and non protein coding RNA’s (ncRNAs (Table 2)), including small RNAs, were identified.²⁶ Presently, many small RNAs of different sizes and with different functions are recognized, e.g. small nuclear RNA (snRNA), small nucleolar RNA (snoRNA), transfer RNA (tRNA) and microRNA (miRNA).

Table 2: Non protein-coding RNAs in eukaryotes.³²⁻³³

RNA	Abbreviation	Size	Main function
Long non-coding RNA	long ncRNA	>200nt	Gene regulation at transcriptional and post-transcriptional level
Pseudogene RNA	-	>200nt	Lost protein coding capacity, but regulates related protein-coding gene, e.g. by acting as miRNA decoy
Ribosomal RNA	rRNA	120-5070 nt	Functions in protein synthesis in the ribosome
Small nucleolar RNA	snoRNA	60-300 nt	Modifications of other RNAs, regulates alternative splicing
Small nuclear RNA	snRNA	~150 nt	Splicing, telomere maintenance
Transfer RNA	tRNA	73-94 nt	Delivers amino acids to ribosome
Promotor-associated small RNA	PASR	20-200 nt	Regulate transcription of protein-coding genes by targeting epigenetic silencing complexes.
Centromere repeat associated small interacting RNA	crasiRNA	34-42 nt	Recruitment of heterochromatin and centromeric proteins
Piwi-interacting RNA	piRNA	26-31 nt	Transposon silencing
Telomere-specific small RNA	tel-sRNA	~24 nt	Sensors of chromatin status, regulating telomere length
Small interfering RNA	siRNA	20-25 nt	Gene regulation by mRNA degradation
MicroRNA	miRNA	19-25 nt	Gene regulation by translational repression or mRNA degradation
Transcription initiation RNA	tiRNA	~18 nt	Associated with highly expressed (preferentially GC-rich) promoters, inhibition of translation initiation

MicroRNAs (miRNAs) are evolutionarily conserved, small, non protein-coding RNA molecules. They can target (near) complementary sequences in the 3’UTR of mRNA molecules, thereby inhibiting their translation into functional proteins. A schematic representation of the miRNA biogenesis is depicted in Figure 1. Some miRNA genes are located in intragenic regions, have their own promoter and are transcribed as independent units. Most miRNAs, however, are intergenic where they reside predominantly in introns, but also in exons or on the antisense strand, of defined transcription units.²⁷ Their transcription is coupled to that of their host gene.

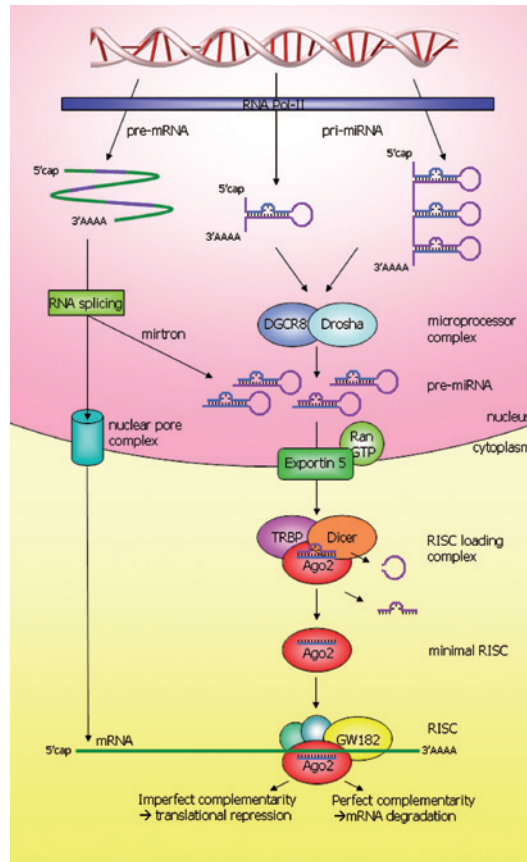


Figure 1: The miRNA biogenesis pathway. MiRNAs are transcribed by RNA Polymerase II (RNA Pol II), either alone or in clusters, and folded into typical hairpin structures, primary miRNAs (pri-miRNAs). Cleavage by the microprocessor complex (Drosha and DGCR8) results in individual precursor miRNAs (pre-miRNAs). Mirtrons are pre-miRNAs that are directly spliced from introns of precursor messenger RNA (pre-mRNA). Pre-miRNAs are transported out of the nucleus to the cytoplasm by Ran-GTP dependent Exportin 5, where they are further processed into a short miRNA duplex by components of the RISC loading complex (Dicer, TRBP and Ago2). The passenger strand is lost, while the guide strand is loaded onto Ago2 (together composing the minimal RISC). After the recruitment of additional proteins to form the complete RISC (RNA induced silencing complex), the miRNA base-pairs to complementary sequences in the 3' UTRs of target mRNAs. Perfect complementarity leads to mRNA degradation, whereas imperfect complementarity results in translational repression.

However, for about one third of the intronic miRNAs additional promoters were identified, enabling a regulation separate from that of the host gene.²⁸ Although transcription by RNA polymerase III has been described,²⁹ miRNAs are mainly transcribed by RNA polymerase II, either alone or in clusters comprising multiple miRNAs. These long transcripts, termed primary miRNAs (pri-miRNAs), are folded into typical hairpin structures, having a 5' cap and a 3' poly-A-tail. Subsequently, the pri-miRNA is recognized by the microprocessor, including the

RNA III endonuclease Drosha and the RNA binding protein DiGeorge Syndrome Critical Region 8 (DGCR8, or Pasha in invertebrates).³⁰⁻³¹ This complex processes the pri-miRNA creating one or more shorter (~70 nucleotide) structures, the precursor miRNAs (pre-miRNAs), with a 5' phosphate group and a 3' two nucleotide overhang. Some pre-miRNAs, known as mirtrons, evade the microprocessor complex and are directly spliced from short introns.³⁴ The pre-miRNAs are then actively transported from the nucleus to the cytoplasm by the Ran-GTP dependent nuclear export receptor Exportin 5.³⁵ In the cytoplasm the pre-miRNA binds the RNase III enzyme Dicer and its RNA binding co-factor TRBP (the human immunodeficiency virus transactivating response RNA-binding protein). TRBP then recruits Argonaute 2 (Ago2), completing the trimeric RISC (RNA induced silencing complex)-loading complex (RLC).³⁶⁻³⁸ Dicer cuts the loop from the hairpin structure, resulting in a miRNA-duplex of approximately 19-25 nucleotides. This can occur with or without prior cleavage of the 3' strand of the pre-miRNA by Ago2.³⁹ Following Dicer cleavage, an unknown helicase unwinds the double stranded miRNA. While Dicer and TRBP dissociate from the complex, one strand of the miRNA-duplex, the one with the less stable base pairing at the 5' end termed the guide strand, is preferentially loaded onto Ago2, together forming the minimal RISC. The other strand, the passenger strand is degraded or less efficiently loaded onto Ago2.⁴⁰ Additional proteins, such as GW182, are recruited to Ago2 to assemble the complete and active RISC complex.³⁸ The incorporated mature miRNA directs the RISC to mRNA targets with a complementary sequence in their 3'UTR. The degree of complementarity, especially in the seed sequence (position 2-8) of the miRNA, determines the action of the RISC. Perfect complementarity results in Ago2 mediated endonucleolytic cleavage (slicing) of the mRNA.⁴¹ More common in mammals is imperfect complementarity between the miRNA and the mRNA target, which leads to translational repression or mRNA destabilization. GW182 interacts with Ago2 and localizes to cytoplasmatic processing bodies (P-bodies) where mRNA turnover takes place. First, translation of the mRNA target is stalled during its early steps, presumably during translation initiation, followed by mRNA deadenylation and degradation.⁴² Interaction of GW182 with poly(A)-binding protein (PABP) and deadenylase complexes is essential for these events.⁴³⁻⁴⁴ One gene can be targeted by multiple miRNAs and a single miRNA can target many genes, which underlines the complexity and widespread effects of miRNA function. This widely conserved process of RNA silencing by small RNA molecules is called RNA interference (RNAi) or posttranscriptional gene silencing (PTGS) and is similar to mechanisms such as co-suppression in plants⁴⁵ and quelling in fungi.⁴⁶

Currently, more than 2500 miRNAs have been identified in humans (miRbase version 20).⁴⁷ The miRNAs have been numbered in order of discovery. MiRNAs with a nearly identical sequence usually get the same number followed by a different letter (e.g. miR-18a and miR-18b) and identical miRNAs which are located on different genomic locations get a numbered suffix (e.g. miR-92a-1 and miR-92a-2). Two miRNAs originating from opposing sides of the same pre-miRNA



duplex are named after the strand they are located on (e.g. miR-485-3p and miR-485-5p), or with an asterisk behind the least expressed (passenger) strand (e.g. miR-185 and miR-185*), although expression levels can vary between cell types and conditions.⁴⁸

MiRNAs have important regulatory roles in critical cellular processes like proliferation, differentiation, cell cycle regulation, apoptosis, stem cell maintenance and metabolism.⁴⁹⁻⁵² MiRNA expression is often organ and tissue specific which points at their role in tissue specialization. Furthermore, miRNA expression patterns are often changed in disease e.g. in cancer.^{24, 53} MiRNAs are frequently located in genomic regions involved in cancers, such as minimal regions of amplifications or loss of heterozygosity, fragile sites and common breakpoint areas near oncogenes or tumorsuppressors.⁵⁴ Moreover, some miRNAs even play a role as an oncogene and/or tumor suppressor gene, depending on the type of tissue and the miRNA target genes present in the respective tissue.⁵⁵⁻⁵⁹ Not surprisingly given their important role in gene expression regulation, miRNA expression profiles correlate with clinical and biological characteristics of tumors, including tissue type, differentiation, aggression, prognosis and response to therapy.⁶⁰⁻⁶² Several mechanisms can account for deregulated miRNA expression in cancer, including genomic amplifications, deletions, or mutations.⁶³⁻⁶⁵ Also epigenetic mechanisms, such as promotor hypermethylation can deregulate miRNA expression.⁶⁶⁻⁶⁸ In addition, changes in the miRNA processing could result in altered miRNA profiles.⁶⁹ Furthermore, miRNA expression can be influenced by changes in the tumor microenvironment,⁷⁰⁻⁷¹ such as tumor hypoxia.⁷²⁻⁷⁵

HYPOXIA

Hypoxia, a condition of reduced oxygen tension, induces various biological processes including proliferation, apoptosis, metabolism, angiogenesis and migration.⁷⁶ Solid tumors often encounter hypoxia when they outgrow their blood supply. Tumor hypoxia contributes to aggressive behavior, radiation- and chemotherapy resistance and poor prognosis.

A key response to hypoxia is the upregulation of HIF1, which together with HIF2 and HIF3 forms the family of hypoxia inducible factors (HIFs).⁷⁷ These transcription factors consist of an alpha and a beta subunit. The beta subunit (HIF β , or ARNT) is constitutively expressed, the alpha subunit (HIF α) is tightly controlled in an oxygen dependent manner. After dimerization they bind to hypoxia responsive elements (HREs) in the DNA, thereby inducing the transcription of genes that regulate the adaptive response to hypoxia. HREs usually consist of a 5'-[A/G]CGTG-3' consensus sequence in the promoter regions of HIF controlled genes,⁷⁸ although functional HREs without this sequence have been identified.⁷⁹⁻⁸⁰

The HIF family members all contain a N-terminal basic helix-loop-helix (bHLH) domain for DNA binding, a Per-ARNT-Sim (PAS) domain for heterodimerization, and an N-terminal and a

C-terminal transactivation domain (N-TAD, C-TAD) for transcriptional regulation (except for HIF3 α which lacks the C-TAD, which makes it a less potent transcriptional activator).⁸¹ HIF1 α , HIF2 α and some isoforms of HIF3 α also possess an oxygen dependent degradation domain. In the presence of oxygen, two conserved proline residues in the ODDD of HIF α are hydroxylated by prolyl hydroxylases (PHDs).⁸¹ Subsequently, the hydroxylated alpha subunit is recognized by the Von Hippel-Lindau (VHL) tumor suppressor, and ubiquitinated by a ubiquitin ligase complex consisting of Elongin B and C, Cullin 2, Rbx1 and VHL, which marks the protein for degradation by the 26S proteasome. In addition, during normal oxygen levels (normoxia) HIF α is hydroxylated by factor inhibiting HIF (FIH, also known as HIF1AN) at a C-terminal asparagine residu, which prevents the binding of transcriptional co-activators CBP and p300 (Figure 2, left panel). In the absence of oxygen, hydroxylation by VHL and FIH is abrogated, which stabilizes HIF and enables interaction with HIF β and co-factors, resulting in increased transcriptional activation of HIF responsive genes (Figure 2, right panel). Another mechanism resulting in HIF stabilization is called pseudohypoxia, a state in which HIF is stabilized under normoxic conditions.⁸² It may involve mutations in succinate dehydrogenase (*SDH*), a mitochondrial component that functions in the electron transport chain and in the citric acid cycle, which leads to accumulation of succinate. This in turn inhibits PHD and prevents degradation of HIF α . Another cause of pseudohypoxia involves inactivation of *VHL* (by mutations or promoter hypermethylation, as frequently observed in clear cell renal cell carcinomas), which disables HIF hydroxylation and degradation.

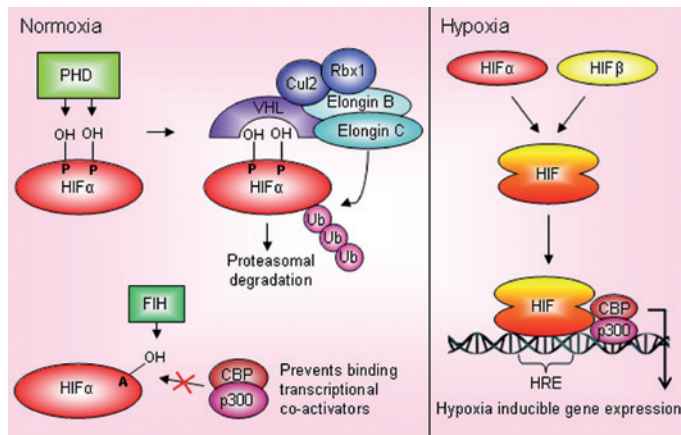


Figure 2: HIF regulation under normoxia and hypoxia. Under normoxic conditions, two proline residues (P) of HIF α are hydroxylated (OH) by prolyl hydroxylases (PHDs). Hydroxylated HIF α is recognized by Von Hippel-Lindau (VHL) and ubiquitinated (Ub) by a ubiquitin ligase complex including Elongin B and C, Cullin 2 (Cul2), Rbx1 and VHL, which marks the protein for proteasomal degradation (left panel, top). Additionally, HIF α is hydroxylated by factor inhibiting HIF (FIH) at an asparagine residu (A), which prevents the binding of transcriptional co-activators CBP and p300 (left panel, bottom). When stabilized under hypoxic conditions, HIF α dimerizes with HIF β . In the nucleus the HIF complex interacts with its co-factors, binds to hypoxia responsive elements (HREs) in the DNA and induces expression of HIF responsive genes (right panel).



Although HIF1 and HIF2 share many target genes, some targets are specifically regulated by only one of them.⁸³ HIF3 has a different function, which is not yet fully understood. Genes that are regulated by HIFs include those involved in glucose metabolism (*GLUT1*), pH regulation (*CA-IX*), angiogenesis (*VEGF*), vasodilation (*iNOS*), erythropoiesis (*EPO*), invasion (*MMP2*), metastasis (*LOX*), apoptosis (*BNIP3*), growth factors (*PDGF*), and many more. Also the expression of certain miRNAs, named hypoxia responsive miRNAs (HRMs), are involved in the cellular response to hypoxia,⁷²⁻⁷⁴ either via HIF dependent or HIF independent mechanisms.⁸⁴⁻⁸⁵ Some miRNAs are in turn involved in feedback mechanisms that regulate HIF.⁸⁶⁻⁸⁹ Most solid tumors, including soft tissue sarcomas, can present with hypoxic areas,⁹⁰⁻⁹¹ but not much is known about the involvement of miRNAs in the hypoxic signaling of these tumors.

THESIS OUTLINE

MiRNA profiling is very useful for tumor subtype classification,^{19, 24, 60, 92} and has proved to be a potent molecular diagnostic tool for sarcomas.^{21, 93} In addition, miRNA profiling and the functional characterization of miRNAs may provide more insight into the tumorigenesis and potentially lead to the identification of novel drug targets or prognostic profiles. This thesis addresses the role of miRNAs in the tumor biology of soft tissue sarcoma.

Chapter 2 of this thesis focuses on miRNA expression profiling of liposarcoma subtypes. This is the first study that examines and compares miRNA expression in all liposarcoma subtypes (i.e. well-differentiated, dedifferentiated, pleomorphic, myxoid and round cell liposarcoma), benign fat tumors (lipoma) and normal fat. We demonstrate that miRNAs can discriminate liposarcoma subtypes and identify subtype specific miRNAs which could aid diagnostics. We show that miR-145 and miR-451 may act as tumor suppressors in adipose tissue. The effects of these miRNAs on cell proliferation, cell cycle and apoptosis in liposarcoma cell lines suggest that they could be used for therapeutic purposes.

Since we found that myxoid/round cell liposarcomas (MRCLS) display a very distinct miRNA expression pattern, this is the focus of **chapter 3**. In this study we first determined the miRNA expression profile of MRCLS. In addition we examined how these differentially expressed miRNAs are associated with MRCLS biology. In particular, we determined if miRNAs are correlated with the increased chemosensitivity that MRCLS exhibit compared to other liposarcoma subtypes, which miRNAs are regulated by the MRCLS characteristic *FUS-CHOP* fusion gene and how they play a role in an important biochemical pathway in MRCLS tumorigenesis, i.e. the IGF1R pathway. In **chapter 4** we discuss the miRNA expression profile of GIST. We identified that several miR-17-92 and miR-221/222 cluster members, which are well-known oncomiRs, were significantly lower expressed in GIST compared to gastro-intestinal leiomyosarcomas, a sarcoma subtype that very closely resembles GIST in terms of morphology, and normal gastrointestinal control tissues.



Overexpression of miR-17, miR-20a and miR-222 mimics in GIST-882 and GIST-T1 cell lines strongly inhibited cell proliferation, interfered with cell cycle progression and induced apoptosis. In addition, we show that these miRNAs target both *KIT* and *ETV1* (two crucial oncogenes in GIST) in a direct and indirect manner. Delivering these miRNAs therapeutically could simultaneously repress both essential GIST oncogenes, which holds great potential for GIST management.

Chapter 5 describes the identification of hypoxia responsive miRNAs (HRMs) in sarcoma cell lines. In a panel of 12 soft tissue sarcoma cell lines we identified a number of miRNAs that are deregulated in response to hypoxic stress. The most differentially expressed HRMs contain HREs upstream of their transcription start site. Additionally, miR-210 and miR-485-5p regulate *HIF3 α* in a direct and indirect manner respectively. Finally, the role of HIF3 α , its regulation by these HRMs, and the potential clinical impact, is discussed.

The major findings from this thesis and their potential clinical relevance are being discussed in **chapter 6**.



REFERENCES

1. Fletcher CD, Unni KK, Mertens F, (Eds.). World Health Organization Classification of Tumours. Pathology and Genetics of Tumors of Soft Tissue and Bone. Lyon: IARC Press; 2002.
2. Fletcher CD, Bridge JA, Hogendoorn PC, Mertens F, (Eds.). WHO Classification of Tumours of Soft Tissue and Bone. Lyon: IARC; 2013.
3. Thway K. Pathology of soft tissue sarcomas. *Clin Oncol (R Coll Radiol)*. 2009 Nov;21(9):695-705.
4. Mackall CL, Meltzer PS, Helman LJ. Focus on sarcomas. *Cancer Cell*. 2002 Sep;2(3):175-8.
5. Mohseny AB, Hogendoorn PC. Concise review: mesenchymal tumors: when stem cells go mad. *Stem Cells*. 2011 Mar;29(3):397-403.
6. Trucco M, Loeb D. Sarcoma stem cells: do we know what we are looking for? *Sarcoma*. 2012;2012:291705.
7. Dutch Cancer Foundation. 2013; Available from: <http://www.kwfkankerbestrijding.nl>.
8. Ducimetiere F, Lurkin A, Ranchere-Vince D, Decouvelaere AV, Peoc'h M, Istier L, et al. Incidence of sarcoma histotypes and molecular subtypes in a prospective epidemiological study with central pathology review and molecular testing. *PLoS One*. 2011;6(8):e20294.
9. Ji J, Eng C, Hemminki K. Familial risk for soft tissue tumors: a nation-wide epidemiological study from Sweden. *J Cancer Res Clin Oncol*. 2008 May;134(5):617-24.
10. Evans DG, Baser ME, McGaughran J, Sharif S, Howard E, Moran A. Malignant peripheral nerve sheath tumours in neurofibromatosis 1. *J Med Genet*. 2002 May;39(5):311-4.
11. Johnson CC, Feingold M, Tilley B. A meta-analysis of exposure to phenoxy acid herbicides and chlorophenols in relation to risk of soft tissue sarcoma. *Int Arch Occup Environ Health*. 1990;62(7):513-20.
12. van de Rijn M, Fletcher JA. Genetics of soft tissue tumors. *Annu Rev Pathol*. 2006;1:435-66.
13. Beck AH, West RB, van de Rijn M. Gene expression profiling for the investigation of soft tissue sarcoma pathogenesis and the identification of diagnostic, prognostic, and predictive biomarkers. *Virchows Arch*. 2010 Feb;456(2):141-51.
14. Dei Tos AP, Doglioni C, Piccinin S, Sciort R, Furlanetto A, Boiocchi M, et al. Coordinated expression and amplification of the MDM2, CDK4, and HMGI-C genes in atypical lipomatous tumours. *J Pathol*. 2000 Apr;190(5):531-6.
15. Singer S, Socci ND, Ambrosini G, Sambol E, Decarolis P, Wu Y, et al. Gene expression profiling of liposarcoma identifies distinct biological types/subtypes and potential therapeutic targets in well-differentiated and dedifferentiated liposarcoma. *Cancer Res*. 2007 Jul 15;67(14):6626-36.
16. Gobble RM, Qin LX, Brill ER, Angeles CV, Ugras S, O'Connor RB, et al. Expression profiling of liposarcoma yields a multigene predictor of patient outcome and identifies genes that contribute to liposarcomagenesis. *Cancer Res*. 2011 Apr 1;71(7):2697-705.
17. Spitzer JI, Ugras S, Runge S, Decarolis P, Antonescu C, Tuschl T, et al. mRNA and protein levels of FUS, EWSR1, and TAF15 are upregulated in liposarcoma. *Genes Chromosomes Cancer*. 2011 May;50(5):338-47.
18. Brill E, Gobble R, Angeles C, Lagos-Quintana M, Crago A, Laxa B, et al. ZIC1 overexpression is oncogenic in liposarcoma. *Cancer Res*. 2010 Sep 1;70(17):6891-901.
19. Munker R, Calin GA. MicroRNA profiling in cancer. *Clin Sci (Lond)*. 2011 Aug;121(4):141-58.
20. Pritchard CC, Cheng HH, Tewari M. MicroRNA profiling: approaches and considerations. *Nat Rev Genet*. 2012 May;13(5):358-69.
21. Subramanian S, Lui WO, Lee CH, Espinosa I, Nielsen TO, Heinrich MC, et al. MicroRNA expression signature of human sarcomas. *Oncogene*. 2008 Mar 27;27(14):2015-26.
22. Ugras S, Brill E, Jacobsen A, Hafner M, Socci ND, Decarolis PL, et al. Small RNA sequencing and functional characterization reveals MicroRNA-143 tumor suppressor activity in liposarcoma. *Cancer Res*. 2011 Sep 1;71(17):5659-69.
23. Renner M, Czwan E, Hartmann W, Penzel R, Brors B, Eils R, et al. MicroRNA profiling of primary high-grade soft tissue sarcomas. *Genes Chromosomes Cancer*. 2012 Nov;51(11):982-96.
24. Lu J, Getz G, Miska EA, Alvarez-Saavedra E, Lamb J, Peck D, et al. MicroRNA expression profiles classify human cancers. *Nature*. 2005 Jun 9;435(7043):834-8.
25. Frith MC, Pheasant M, Mattick JS. The amazing complexity of the human transcriptome. *Eur J Hum Genet*. 2005 Aug;13(8):894-7.

26. Consortium EP, Dunham I, Kundaje A, Aldred SF, Collins PJ, Davis CA, et al. An integrated encyclopedia of DNA elements in the human genome. *Nature*. 2012 Sep 6;489(7414):57-74.
27. Rodriguez A, Griffiths-Jones S, Ashurst JL, Bradley A. Identification of mammalian microRNA host genes and transcription units. *Genome Res*. 2004 Oct;14(10A):1902-10.
28. Ozsolak F, Poling LL, Wang Z, Liu H, Liu XS, Roeder RG, et al. Chromatin structure analyses identify miRNA promoters. *Genes Dev*. 2008 Nov 15;22(22):3172-83.
29. Borchert GM, Lanier W, Davidson BL. RNA polymerase III transcribes human microRNAs. *Nat Struct Mol Biol*. 2006 Dec;13(12):1097-101.
30. Gregory RI, Chendrimada TP, Shiekhattar R. MicroRNA biogenesis: isolation and characterization of the microprocessor complex. *Methods Mol Biol*. 2006;342:33-47.
31. Gregory RI, Yan KP, Amuthan G, Chendrimada T, Doratotaj B, Cooch N, et al. The Microprocessor complex mediates the genesis of microRNAs. *Nature*. 2004 Nov 11;432(7014):235-40.
32. Sana J, Faltejškova P, Svoboda M, Slaby O. Novel classes of non-coding RNAs and cancer. *J Transl Med*. 2012;10:103.
33. Taft RJ, Pang KC, Mercer TR, Dinger M, Mattick JS. Non-coding RNAs: regulators of disease. *J Pathol*. 2010 Jan;220(2):126-39.
34. Berezikov E, Chung WJ, Willis J, Cuppen E, Lai EC. Mammalian mirtron genes. *Mol Cell*. 2007 Oct 26;28(2):328-36.
35. Lund E, Guttinger S, Calado A, Dahlberg JE, Kutay U. Nuclear export of microRNA precursors. *Science*. 2004 Jan 2;303(5654):95-8.
36. Maniatakis E, Mourelatos Z. A human, ATP-independent, RISC assembly machine fueled by pre-miRNA. *Genes Dev*. 2005 Dec 15;19(24):2979-90.
37. MacRae IJ, Ma E, Zhou M, Robinson CV, Doudna JA. In vitro reconstitution of the human RISC-loading complex. *Proc Natl Acad Sci U S A*. 2008 Jan 15;105(2):512-7.
38. Chendrimada TP, Gregory RI, Kumaraswamy E, Norman J, Cooch N, Nishikura K, et al. TRBP recruits the Dicer complex to Ago2 for microRNA processing and gene silencing. *Nature*. 2005 Aug 4;436(7051):740-4.
39. Diederichs S, Haber DA. Dual role for argonautes in microRNA processing and posttranscriptional regulation of microRNA expression. *Cell*. 2007 Dec 14;131(6):1097-108.
40. Noland CL, Ma E, Doudna JA. siRNA repositioning for guide strand selection by human Dicer complexes. *Mol Cell*. 2011 Jul 8;43(1):110-21.
41. Liu J, Carmell MA, Rivas FV, Marsden CG, Thomson JM, Song JJ, et al. Argonaute2 is the catalytic engine of mammalian RNAi. *Science*. 2004 Sep 3;305(5689):1437-41.
42. Djuranovic S, Nahvi A, Green R. miRNA-mediated gene silencing by translational repression followed by mRNA deadenylation and decay. *Science*. 2012 Apr 13;336(6078):237-40.
43. Huntzinger E, Kuzuoglu-Ozturk D, Braun JE, Eulalio A, Wohlbold L, Izaurralde E. The interactions of GW182 proteins with PABP and deadenylases are required for both translational repression and degradation of miRNA targets. *Nucleic Acids Res*. 2013 Jan;41(2):978-94.
44. Braun JE, Huntzinger E, Fauser M, Izaurralde E. GW182 proteins directly recruit cytoplasmic deadenylase complexes to miRNA targets. *Mol Cell*. 2011 Oct 7;44(1):120-33.
45. Napoli C, Lemieux C, Jorgensen R. Introduction of a Chimeric Chalcone Synthase Gene into *Petunia* Results in Reversible Co-Suppression of Homologous Genes in trans. *Plant Cell*. 1990 Apr;2(4):279-89.
46. Romano N, Macino G. Quelling: transient inactivation of gene expression in *Neurospora crassa* by transformation with homologous sequences. *Mol Microbiol*. 1992 Nov;6(22):3343-53.
47. Griffiths-Jones S. The microRNA Registry. *Nucleic Acids Res*. 2004 Jan 1;32(Database issue):D109-11.
48. Ambros V, Bartel B, Bartel DP, Burge CB, Carrington JC, Chen X, et al. A uniform system for microRNA annotation. *RNA*. 2003 Mar;9(3):277-9.
49. Carleton M, Cleary MA, Linsley PS. MicroRNAs and cell cycle regulation. *Cell Cycle*. 2007 Sep 1;6(17):2127-32.
50. Harfe BD. MicroRNAs in vertebrate development. *Curr Opin Genet Dev*. 2005 Aug;15(4):410-5.
51. Lau NC, Lim LP, Weinstein EG, Bartel DP. An abundant class of tiny RNAs with probable regulatory roles in *Caenorhabditis elegans*. *Science*. 2001 Oct 26;294(5543):858-62.
52. Boehm M, Slack FJ. MicroRNA control of lifespan and metabolism. *Cell Cycle*. 2006 Apr;5(8):837-40.



53. Volinia S, Calin GA, Liu CG, Ambs S, Cimmino A, Petrocca F, et al. A microRNA expression signature of human solid tumors defines cancer gene targets. *Proc Natl Acad Sci U S A*. 2006 Feb 14;103(7):2257-61.
54. Calin GA, Sevignani C, Dumitru CD, Hyslop T, Noch E, Yendamuri S, et al. Human microRNA genes are frequently located at fragile sites and genomic regions involved in cancers. *Proc Natl Acad Sci U S A*. 2004 Mar 2;101(9):2999-3004.
55. Chen CZ. MicroRNAs as oncogenes and tumor suppressors. *N Engl J Med*. 2005 Oct 27;353(17):1768-71.
56. Voorhoeve PM. MicroRNAs: Oncogenes, tumor suppressors or master regulators of cancer heterogeneity? *Biochim Biophys Acta*. 2010 Jan;1805(1):72-86.
57. Garofalo M, Croce CM. microRNAs: Master regulators as potential therapeutics in cancer. *Annu Rev Pharmacol Toxicol*. 2011;51:25-43.
58. Shenouda SK, Alahari SK. MicroRNA function in cancer: oncogene or a tumor suppressor? *Cancer Metastasis Rev*. 2009 Dec;28(3-4):369-78.
59. Garzon R, Calin GA, Croce CM. MicroRNAs in Cancer. *Annu Rev Med*. 2009;60:167-79.
60. Calin GA, Croce CM. MicroRNA signatures in human cancers. *Nat Rev Cancer*. 2006 Nov;6(11):857-66.
61. Calin GA, Ferracin M, Cimmino A, Di Leva G, Shimizu M, Wojcik SE, et al. A MicroRNA signature associated with prognosis and progression in chronic lymphocytic leukemia. *N Engl J Med*. 2005 Oct 27;353(17):1793-801.
62. Yanaihara N, Caplen N, Bowman E, Seike M, Kumamoto K, Yi M, et al. Unique microRNA molecular profiles in lung cancer diagnosis and prognosis. *Cancer Cell*. 2006 Mar;9(3):189-98.
63. Calin GA, Dumitru CD, Shimizu M, Bichi R, Zupo S, Noch E, et al. Frequent deletions and down-regulation of micro-RNA genes miR15 and miR16 at 13q14 in chronic lymphocytic leukemia. *Proc Natl Acad Sci U S A*. 2002 Nov 26;99(24):15524-9.
64. Ota A, Tagawa H, Karnan S, Tsuzuki S, Karpas A, Kira S, et al. Identification and characterization of a novel gene, C13orf25, as a target for 13q31-q32 amplification in malignant lymphoma. *Cancer Res*. 2004 May 1;64(9):3087-95.
65. Wu M, Jolicoeur N, Li Z, Zhang L, Fortin Y, L'Abbe D, et al. Genetic variations of microRNAs in human cancer and their effects on the expression of miRNAs. *Carcinogenesis*. 2008 Sep;29(9):1710-6.
66. Saito Y, Liang G, Egger G, Friedman JM, Chuang JC, Coetzee GA, et al. Specific activation of microRNA-127 with downregulation of the proto-oncogene BCL6 by chromatin-modifying drugs in human cancer cells. *Cancer Cell*. 2006 Jun;9(6):435-43.
67. Agirre X, Martinez-Climent JA, Odero MD, Prosper F. Epigenetic regulation of miRNA genes in acute leukemia. *Leukemia*. 2012 Mar;26(3):395-403.
68. Baer C, Claus R, Plass C. Genome-wide epigenetic regulation of miRNAs in cancer. *Cancer Res*. 2013 Jan 15;73(2):473-7.
69. Nakamura T, Canaani E, Croce CM. Oncogenic All1 fusion proteins target Drosha-mediated microRNA processing. *Proc Natl Acad Sci U S A*. 2007 Jun 26;104(26):10980-5.
70. Li X, Wu Z, Fu X, Han W. A microRNA component of the neoplastic microenvironment: microregulators with far-reaching impact. *Biomed Res Int*. 2013;2013:762183.
71. Wentz-Hunter KK, Potashkin JA. The Role of miRNAs as Key Regulators in the Neoplastic Microenvironment. *Mol Biol Int*. 2011;2011:839872.
72. Kulshreshtha R, Ferracin M, Wojcik SE, Garzon R, Alder H, Agosto-Perez FJ, et al. A microRNA signature of hypoxia. *Mol Cell Biol*. 2007 Mar;27(5):1859-67.
73. Kulshreshtha R, Davuluri RV, Calin GA, Ivan M. A microRNA component of the hypoxic response. *Cell Death Differ*. 2008 Apr;15(4):667-71.
74. Crosby ME, Devlin CM, Glazer PM, Calin GA, Ivan M. Emerging roles of microRNAs in the molecular responses to hypoxia. *Curr Pharm Des*. 2009;15(33):3861-6.
75. Kulshreshtha R, Ferracin M, Negrini M, Calin GA, Davuluri RV, Ivan M. Regulation of microRNA expression: the hypoxic component. *Cell Cycle*. 2007 Jun 15;6(12):1426-31.
76. Harris AL. Hypoxia—a key regulatory factor in tumour growth. *Nat Rev Cancer*. 2002 Jan;2(1):38-47.
77. Wang GL, Semenza GL. General involvement of hypoxia-inducible factor 1 in transcriptional response to hypoxia. *Proc Natl Acad Sci U S A*. 1993 May 1;90(9):4304-8.

78. Wenger RH, Stiehl DP, Camenisch G. Integration of oxygen signaling at the consensus HRE. *Sci STKE*. 2005 Oct 18;2005(306):re12.
79. Makino Y, Uenishi R, Okamoto K, Isoe T, Hosono O, Tanaka H, et al. Transcriptional up-regulation of inhibitory PAS domain protein gene expression by hypoxia-inducible factor 1 (HIF-1): a negative feedback regulatory circuit in HIF-1-mediated signaling in hypoxic cells. *J Biol Chem*. 2007 May 11;282(19):14073-82.
80. Tanaka T, Wiesener M, Bernhardt W, Eckardt KU, Warnecke C. The human HIF (hypoxia-inducible factor)-3alpha gene is a HIF-1 target gene and may modulate hypoxic gene induction. *Biochem J*. 2009 Nov 15;424(1):143-51.
81. Heikkila M, Pasanen A, Kivirikko KI, Myllyharju J. Roles of the human hypoxia-inducible factor (HIF)-3alpha variants in the hypoxia response. *Cell Mol Life Sci*. 2011 Dec;68(23):3885-901.
82. Sanders E. Pseudohypoxia, Mitochondrial Mutations, the Warburg Effect, and Cancer. *Biomedical Research*. 2012;23(Special Issue: Cancer Metabolism):109-31.
83. Keith B, Johnson RS, Simon MC. HIF1alpha and HIF2alpha: sibling rivalry in hypoxic tumour growth and progression. *Nat Rev Cancer*. 2012 Jan;12(1):9-22.
84. Shen G, Li X, Jia YF, Piazza GA, Xi Y. Hypoxia-regulated microRNAs in human cancer. *Acta Pharmacol Sin*. 2013 Mar;34(3):336-41.
85. Nallamshetty S, Chan SY, Loscalzo J. Hypoxia: A master regulator of microRNA biogenesis and activity. *Free Radic Biol Med*. 2013 May 24.
86. Yamakuchi M, Lotterman CD, Bao C, Hruban RH, Karim B, Mendell JT, et al. P53-induced microRNA-107 inhibits HIF-1 and tumor angiogenesis. *Proc Natl Acad Sci U S A*. 2010 Apr 6;107(14):6334-9.
87. Cha ST, Chen PS, Johansson G, Chu CY, Wang MY, Jeng YM, et al. MicroRNA-519c suppresses hypoxia-inducible factor-1alpha expression and tumor angiogenesis. *Cancer Res*. 2010 Apr 1;70(7):2675-85.
88. Ghosh G, Subramanian IV, Adhikari N, Zhang X, Joshi HP, Basi D, et al. Hypoxia-induced microRNA-424 expression in human endothelial cells regulates HIF-alpha isoforms and promotes angiogenesis. *J Clin Invest*. 2010 Nov;120(11):4141-54.
89. Taguchi A, Yanagisawa K, Tanaka M, Cao K, Matsuyama Y, Goto H, et al. Identification of hypoxia-inducible factor-1 alpha as a novel target for miR-17-92 microRNA cluster. *Cancer Res*. 2008 Jul 15;68(14):5540-5.
90. Brizel DM, Scully SP, Harrelson JM, Layfield LJ, Bean JM, Prosnitz LR, et al. Tumor oxygenation predicts for the likelihood of distant metastases in human soft tissue sarcoma. *Cancer Res*. 1996 Mar 1;56(5):941-3.
91. Nordsmark M, Hoyer M, Keller J, Nielsen OS, Jensen OM, Overgaard J. The relationship between tumor oxygenation and cell proliferation in human soft tissue sarcomas. *Int J Radiat Oncol Biol Phys*. 1996 Jul 1;35(4):701-8.
92. Barbarotto E, Schmittgen TD, Calin GA. MicroRNAs and cancer: profile, profile, profile. *Int J Cancer*. 2008 Mar 1;122(5):969-77.
93. Gougelet A, Perez J, Pissaloux D, Besse A, Duc A, Decouvelaere AV, et al. miRNA Profiling: How to Bypass the Current Difficulties in the Diagnosis and Treatment of Sarcomas. *Sarcoma*. 2011;2011:460650.

Chapter 2

MICRORNA EXPRESSION PROFILES DISTINGUISH LIPOSARCOMA SUBTYPES AND IMPLICATE MIR-145 AND MIR-451 AS TUMOR SUPPRESSORS



Caroline M.M. Gits, Patricia F. van Kuijk, Moniek B.E. Jonkers, Marcel Smid, Wilfred F. van IJcken, Jean-Michel Coindre, Frédéric Chibon, Cornelis Verhoef, Ron H.J. Mathijssen, Michael A. den Bakker, Jaap Verweij, Stefan Sleijfer, Erik A.C. Wiemer

Submitted for publication



ABSTRACT

Liposarcomas are rare, heterogeneous and malignant tumors that can be divided into four histological subtypes with different characteristics and clinical behavior. Treatment consists of surgery in combination with systemic chemotherapy, but nevertheless mortality rates are high. More insight into the biology of liposarcoma tumorigenesis is needed to devise novel therapeutic approaches. MicroRNAs (miRNAs) have been associated with carcinogenesis in many tumors and may function as tumor suppressor or oncogene. In this study we examined miRNA expression in an initial series of 57 human liposarcomas (including all subtypes), lipomas and normal fat by miRNA microarrays. Supervised hierarchical clustering of the most differentially expressed miRNAs ($p < 0.0002$) distinguished most liposarcoma subtypes and control tissues. The distinction between well differentiated liposarcomas and benign lipomas was blurred, suggesting these tumor types may represent a biological continuum. MiRNA signatures of liposarcoma subtypes were established and validated in an independent series of 58 liposarcomas and control tissues. The expression of the miR-143/145 and miR-144/451 cluster members was clearly reduced in liposarcomas compared to normal fat. Overexpression of miR-145 and miR-451 in liposarcoma cell lines decreased cellular proliferation rate, impaired cell cycle progression and induced apoptosis. In conclusion, we show that miRNA expression profiling can be used to discriminate liposarcoma subtypes, which can possibly aid in objective diagnostic decision making. In addition, our data indicate that miR-145 and miR-451 act as tumor suppressors in adipose tissue and show that re-expression of these miRNAs could be a promising therapeutic strategy for liposarcomas.



INTRODUCTION

Liposarcomas are one of the most common types of soft tissue sarcomas, representing approximately 10-15% of all mesenchymal neoplasms.¹⁻² Liposarcomas are heterogeneous tumors from adipogenic origin that, according to the latest WHO classification, can be divided into four histological subtypes: well differentiated (i.e. atypical lipomatous tumor), dedifferentiated, myxoid/round cell, and pleomorphic liposarcoma.³ These subtypes largely differ from each other in terms of pathogenesis, genetic alterations and clinical behavior.

Well differentiated liposarcoma is the most common subtype (~40%), which is frequently hard to distinguish from benign fat tumors, i.e. lipomas. Genetically they are characterized by supernumerary rings and giant chromosomes which involve amplification of the 12q13-15 chromosomal region, containing oncogenes like *MDM2*, *CDK4* and *HMGA2*.⁴⁻⁵ Well differentiated liposarcoma is locally aggressive, but shows no potential to metastasize unless the tumor undergoes dedifferentiation to a high grade tumor. Transition into dedifferentiated liposarcoma usually occurs abruptly and predominantly in tumors located in the retroperitoneum. Dedifferentiated liposarcomas also occur frequently (~40%), and are more aggressive than the well differentiated tumors they arise from.

Myxoid liposarcomas (~15%) generally harbor a t(12;16)(q13;p11) translocation, which leads to the generation of a FUS-DDIT3 (FUS-CHOP) fusion protein. Occasionally, areas in the myxoid liposarcoma transform to a high grade round cell component, which is associated with a significantly worse prognosis. This transition is gradual and represents a histological continuum. Finally, pleomorphic liposarcomas are high grade sarcomas with complex genetic characteristics. Pleomorphic liposarcomas represent the rarest (~5%) and most aggressive subtype.

In addition to tumor size and anatomic location, one of the most important determining factors for the prognosis of liposarcoma patients is the liposarcoma subtype.⁶⁻⁷ However, establishing the correct liposarcoma subtype can be laborious⁸⁻¹⁰ and requires a histological assessment together with molecular analyses using IHC, FISH, real time PCR and/or array CGH.¹¹⁻¹² Karyotypic abnormalities are common in lipomatous tumors and are often reliably correlated with morphological subtype.¹³⁻¹⁴ Also immunohistochemical analyses have increased diagnostic accuracy.¹⁵ Furthermore, mRNA expression profiling has proven to be a powerful tool for tumor classification and several genes that contribute to liposarcomagenesis have been identified by this technique.^{5, 16-19} However, the role of many genomic and cytogenetic aberrations in carcinogenesis remains unclear. Recently it has become evident that miRNA expression profiling holds many advantages over mRNA expression profiling in human cancers.²⁰⁻²¹ MiRNAs are small non-protein coding RNAs of approximately 20-25 nucleotides, which mainly target 3'-UTRs of mRNAs, thereby inhibiting their translation into functional proteins. MiRNAs have been shown to play a role in many essential biological processes such as cellular proliferation and differentiation, apoptosis and tissue specialization. Furthermore, miRNA expression is deregulated in many



cancers, and some miRNAs function as oncogene or tumor suppressor.²² MiRNA expression profiles have been reported to correlate with clinical and biological characteristics of tumors, including tissue type, differentiation status, aggressiveness and response to therapy.²³ Therefore miRNAs can be very useful for tumor (subtype) classification, including sarcomas.^{20, 23-27} In addition, miRNA profiling and the functional characterization of miRNAs may provide more insight into the process of tumorigenesis and potentially lead to the identification of novel drug targets or prognostic profiles.

The precise role of miRNAs in the biology of liposarcomas is still relatively unexplored.²⁸⁻³⁵ Most reports so far focused on deregulated miRNA expression in well differentiated and/or dedifferentiated liposarcomas compared to normal fat.³⁰⁻³⁵ Here we examined the miRNA expression in all liposarcoma subtypes, lipomas and normal fat revealing subtype specific miRNAs as well as miRNAs that were aberrantly expressed in all liposarcomas. MiR-145 and miR-451 were further investigated for their involvement in cellular proliferation, cell cycle progression and apoptosis in liposarcoma cell lines. Our results suggest that these miRNAs may function as tumor suppressors in liposarcomas.

MATERIALS & METHODS

Tumor and control tissue samples

A discovery set of 57 frozen human liposarcoma and control tissue samples were obtained from the Erasmus MC Tissue Bank: 14 well differentiated, 13 dedifferentiated, 9 myxoid, 5 round cell and 3 pleomorphic liposarcomas, together with 5 lipoma and 8 normal adipose (fat) samples as controls. For validation purposes 58 additional frozen tissue samples were obtained: 43 from the Erasmus MC Tissue Bank (11 well differentiated, 5 dedifferentiated, 4 myxoid, 4 pleomorphic liposarcomas, 9 lipomas and 9 fat samples) and 15 tumor samples were provided by Institut Bergonié, Bordeaux (2 dedifferentiated, 7 myxoid, 5 round cell and 2 pleomorphic liposarcomas). All samples were examined by expert soft tissue pathologists to verify the liposarcoma subtype classification. The percentage of tumor cells in the liposarcoma tissues was estimated at >90%. The study was approved by the Medical Ethical Review Board of the Erasmus University Medical Center.

RNA isolation

Total RNA was isolated from frozen tissues using RNeasy (Qiagen) according to the manufacturer's recommendations. The RNA concentration and quality were determined on a Nanodrop-1000 (Nanodrop Technologies).



MiRNA microarray

MiRNA profiling was performed essentially as previously described.³⁶ In brief, 1 µg total RNA was fluorescently labeled with Cy3 using the ULS™ aRNA Labeling Kit (Kreatech Diagnostics). Labeled RNA was hybridized with locked nucleic acid (LNA™) modified oligonucleotide capture probes (Exiqon) spotted in duplicate on Nexterion E slides. The capture probe set (based on miRBase version 10, annotation version 13) contains 1344 probes of which 725 are capable of detecting human miRNAs. Hybridized slides were scanned and median spot intensity was determined using ImaGene software (BioDiscovery Inc.). After background subtraction, expression values were quantile normalized using R software, bad spots were deleted, and duplicate spots were averaged. For each expression value, the ratio to the geometric mean of the miRNA was log₂ transformed. These values were used to determine differentially expressed miRNAs. Hierarchical clustering analyses were performed in Spotfire. The cluster trees were generated using cosine correlation for similarity measures and the Unweighted Pair Group Method with Arithmetic Mean (UPGMA) clustering method.

miRNA qPCR

The expression of selected miRNAs was verified by RT-PCR using TaqMan® MicroRNA Assays (Applied Biosystems). In brief, total RNA (50ng) was reverse transcribed using specific miRNA primers and the TaqMan® MicroRNA Reverse Transcription Kit (Applied Biosystems). The resulting cDNA was used as input in a quantitative real-time PCR (qPCR) using the miRNA specific primer/probe mix together with the TaqMan® Universal PCR Master Mix No AmpErase® UNG (Applied Biosystems) according to manufacturer's protocol. qPCR data were analyzed with SDS software (version 2.4, Applied Biosystems). A standard dilution series of cDNA of a sample-pool was included on every plate allowing for the absolute quantification of the miRNA expression.

Statistics

BRB-Array Tools (Microsoft-Excel plug-in) was used for identifying differentially expressed miRNAs. A univariate F-test with random variance model was used to identify miRNAs that were differentially expressed between all liposarcoma subtypes and control tissues, which were used for supervised hierarchical clustering. Two-sample t-tests with random variance model were used for comparisons between two groups. A stringent selection procedure was followed to determine subtype specific miRNAs. First, significantly differentially expressed miRNAs were determined between a single subtype and every other group (i.e. each of the remaining 4 liposarcoma subtypes, lipomas and fat) as well as between the subtype versus all other samples together (i.e. remaining samples group), which makes seven comparisons in total. A miRNA was only included in further analyses if it was differentially expressed ($p < 0.05$) in at least five out of seven comparisons, including at least the fat group and the remaining samples group. This way,



only miRNAs that discriminated one subtype from multiple other subtypes and from control tissues were included. Finally the miRNAs were sorted on expression fold change of the miRNA in the subtype compared to the remaining samples group. Since some sample groups were small, not only the p-value but also the False Discovery Rate (FDR)-adjusted p-value is indicated in the tables. Only the miRNAs that were expressed above background in both the discovery and the validation sample set are included in the tables. Spearman's rank correlation coefficients between array and qPCR data were calculated using SPSS (IBM). A student's t-test was used to determine the significance of differential miRNA expression determined by qPCR.

Cell culture

The liposarcoma cell line SW872 (ATCC, Rockville, MD, USA) and the myxoid liposarcoma cell line MLS 1765-92 (obtained from dr. P. Åman, Sahlgrenska Cancer Center, Goteborg University, Gothenburg, Sweden) were cultured in RPMI 1640/GlutaMAX (Invitrogen) supplemented with 10% fetal bovine serum, at 37 °C, 5% CO₂. STR profiles of both cell lines were determined, but as the DNA profile of these cell lines is not available in the ATCC/DSMZ data-banks we could not confirm cell line identities. However, the STR profile of the SW872 cell line matched the profile of another SW872 cell line we obtained from an independent source (Centro Nacional de Investigaciones Oncológicas, Madrid, Spain). Moreover, the SW872 cell line was included in a recent paper (Stratford E.W. et al. *Sarcoma* 2012) investigating and comparing the expression of adipocytic differentiation markers, the adipocytic differentiation potential, stem cell markers and metastasis-associated phenotypes of several liposarcoma cell lines, which shows that the SW872 cell line resembles other liposarcoma cell lines. In addition, in the MLS 1765-92 cell line we confirmed the expression of a FUS-DDIT3 fusion protein, which is specifically expressed in myxoid/round cell liposarcomas, verifying the origin of this cell line.

Transfections

MiRIDIAN microRNA mimics (Thermo Scientific) of hsa-miR-143, hsa-miR-145, hsa-miR-144 and hsa-miR-451 and miRIDIAN microRNA Mimic Negative Control #1 (Thermo Scientific) were transfected in a final concentration of 50 nM using DharmaFECT1 transfection reagent (Thermo Scientific) 24h after cell seeding, according to the manufacturer's protocol. For both cell lines transfection efficiency was optimized to >95% using fluorescent mimics.

SRB assay

Cell density was examined by a sulforhodamine B (SRB) assay 24h, 48h, 72h and 96h post-transfection. In short: cells were fixed by 10% TCA in PBS, washed, stained by 0.4% SRB in 1% acetic acid for 15 min, washed in 1% acetic acid and dried. Color was released from the cells by 10 mM Tris-Base, after which the $A_{540\text{ nm}}$ was measured in a spectrophotometer.



EdU cell proliferation assay

Cell proliferation was quantified 72h post-transfection by detection of the incorporation of 5-ethynyl-2'-deoxyuridine (EdU) during DNA synthesis using the Click-iT EdU Pacific Blue Flow Cytometry Assay Kit (Invitrogen). Briefly: cultured cells were incubated with 10 μ M EdU for 1.5h. Cells were harvested, fixed, stained and permeabilized according to the manufacturer's protocol. EdU was detected using a 405 nm laser for excitation with BP450/40 emission filter (flow cytometer FACS Aria III, BD Biosciences).

Cell cycle assay

Cells were harvested by trypsinization 72h post-transfection, fixed by 70% ethanol for 15 min, washed in PBS and resuspended in PBS/RNase/Propidium Iodide (PI) (20 μ g/ml RNase, 50 μ g/ml PI, 1% fetal bovine serum). PI staining was quantified by FACS using a 488 nm laser with emission filters LP655 and BP695/40 (flow cytometer FACS Aria III, BD Biosciences).

Apoptosis assay

Cells were harvested by trypsinization 72h post-transfection, and stained with FITC Annexin V and PI by using the FITC Annexin V Apoptosis Detection Kit I (BD Biosciences), following the manufacturer's protocol. In short: cells were washed in PBS, resuspended in Binding Buffer and stained by FITC Annexin V and PI on ice for 15 min in the dark. Cells were analyzed by FACS using a 488 nm laser with emission filters LP520 nm and BP530/30 nm (flow cytometer FACS Aria III, BD Biosciences).

RESULTS

MiRNA expression profiles identify liposarcoma subtypes

In order to determine the miRNA expression profiles of the various liposarcoma subtypes, an initial series (i.e. discovery set) of 57 human liposarcomas and control tissues (lipomas, normal fat) was analyzed on a miRNA microarray platform containing LNA™ modified oligonucleotide capture probes capable of detecting 725 human miRNAs. Patient, tumor and control tissue characteristics are listed in Table 1 (see Supplemental Table 1A for more details).

**Table 1:** Patient and tumor characteristics

Discovery set (n=57)		Liposarcomas		Validation set (n=58)	
		Gender			
19		Female		13	
25		Male		27	
62	[31-91]	Median age [range]		58	[28-74]
14		Well differentiated		11	
		Upper extremities		2	
	9	Lower extremities		6	
	4	Retroperitoneal		2	
	1	Groin			
		Hip		1	
13		Dedifferentiated		7	
		Lower extremities		1	
	10	Retroperitoneal		5	
	1	Intra-abdominal			
	1	Groin			
	1	Head			
		Hip		1	
9		Myxoid		11	
	8	Lower extremities		11	
	1	Thorax			
5		Round cell		5	
	4	Lower extremities		5	
	1	Intra-abdominal			
3		Pleomorphic		6	
	1	Upper extremities		2	
	2	Lower extremities		4	
Control Tissues					
Gender					
10		Female		8	
3		Male		10	
58	[43-84]	Median age [range]		60	[24-79]
8		Fat		9	
	4	Upper extremities			
		Lower extremities		1	
		Retroperitoneal		2	
	2	Intra-abdominal		1	
	2	Groin		3	
		Neck		1	
		Mamma		1	
5		Lipoma		9	
	4	Upper extremities		6	
	1	Lower extremities		2	
		Back		1	



Unsupervised hierarchical clustering was used to classify samples of the discovery set based on similarity in miRNA expression without prior knowledge of sample identity (Figure 1A). Most myxoid and round cell liposarcomas clustered in a separate branch, illustrating that these subtypes have a distinct miRNA expression profile compared to the other liposarcoma subtypes and control tissues (fat and lipomas). Likewise most dedifferentiated liposarcomas grouped together, as well as most control tissues. The well differentiated liposarcomas were dispersed throughout the cluster tree, and were found in all major branches among every other type of tissue, indicating that the miRNA profile of well differentiated liposarcomas is not very distinctive in this unsupervised setting. Nevertheless, we can tentatively conclude that unsupervised clustering based on miRNA expression levels is capable of discriminating between liposarcoma subtypes.

Next, it was determined which miRNAs were differentially expressed across all groups of the discovery set. The 60 most significant differentially expressed miRNAs ($p < 0.0002$; corrected for multiple testing $p < 0.002$) were used in a supervised hierarchical clustering (Figure 1B; Supplemental Table 2). The clustering gave rise to a very good discrimination between liposarcoma subtypes and control tissues. Moreover, the miRNA expression profiles appeared to correlate with genomic aberrations commonly observed in these tumors. One main branch of the cluster tree contained samples with normal and relatively simple genetic profiles, such as well differentiated and dedifferentiated liposarcomas, which both have a characteristic amplification, as well as the control samples (normal fat tissue and benign lipomas). The other major branch encompassed the translocation-related myxoid and round cell liposarcomas and the pleomorphic liposarcomas generally associated with more complex genomic alterations.

Based on miRNA expression, lipoma and normal fat tissues were poorly distinguishable from each other. Two lipoma samples clustered within the well differentiated group and although most well differentiated liposarcomas grouped in a separate branch, four clustered with the control samples. In line with the original diagnosis, the aberrantly clustered lipoma samples displayed no *MDM2* amplification whereas all four well differentiated liposarcoma samples did show *MDM2* amplification (Supplemental Table 1A). All retroperitoneal well differentiated liposarcomas, which are more prone to dedifferentiation, clustered apart from the control tissues together with well differentiated liposarcomas from other anatomic locations. However, all dedifferentiated liposarcomas clustered in a separate branch, which indicates that the miRNA profile changes significantly during dedifferentiation. The other arm of the cluster tree contained a branch with all 3 pleomorphic liposarcomas, and a branch with all myxoid and round cell liposarcomas, which have a clearly distinct miRNA profile. Since the round cell component in the analyzed round cell tumors ranged from 5-90% it was difficult to distinguish these tumors from the myxoid liposarcomas.



MiRNA signatures for liposarcoma subtypes

MiRNA signatures which are specific for each of the liposarcoma subtypes were derived from the discovery set analyses. For each subtype, the top-10 most distinct miRNAs are listed in Table 2A, sorted based on the miRNA expression fold change compared to the other samples (Table 2A, Supplemental Table 3). Subsequently, we examined whether the differential expression of these miRNAs between the various subtypes could be confirmed in an independent validation series of 58 liposarcomas and control tissues using the same microarrays (Table 2A, Supplemental Table 3; for additional patient, tumor and tissue characteristics see Table 1 and Supplemental Table 1B).

In order to further verify our microarray data, one miRNA per liposarcoma subtype was selected for validation on a qPCR platform. For each of these miRNAs, the qPCR analyses were performed in samples of the indicated liposarcoma subtype and normal fat. The relative expression levels of these miRNAs, as determined by microarray and qPCR, are shown in Figure 2A. This illustrates that, at least for the selected miRNAs, miR-27a, miR-195, miR-30a and miR-21, the microarray data obtained from the discovery set were not only reproduced in an independent validation series, but also on another miRNA detection platform, i.e. qPCR. Also, Spearman's rank correlation coefficients (Figure 2B) showed a good correlation ($p < 0.001$) between the miRNA levels as determined by microarray and qPCR. The only miRNA for which the expression data observed in the discovery set were not completely reproduced in the validation set was miR-17, discriminative for round cell liposarcomas. This may be due to the heterogeneity within this subtype, particularly the variation in the percentage of high grade round cells in a myxoid background. The expression of miR-17, but also of other miR-17 family members like miR-20a and miR-106a, was found to be higher in liposarcomas with a high round cell component (>50% round cells) than in tumors with a small round cell component (<50% round cells), normal fat and other liposarcoma subtypes (Figure 2C, Supplemental Figure 1).

Table 2: Distinct miRNA expression signatures in liposarcoma subtypes and fat.**A**

miRNA	Up/ down	Discovery set			Validation set		
		Fold change	p-value	FDR	Fold change	p-value	FDR
Myxoid liposarcoma		(n=9)			(n=11)		
hsa-miR-29a	↓	4.3	3.00E-07*	8.77E-05*	5.6	< 1e-07*	< 1e-07*
hsa-miR-485-5p	↑	4.3	9.20E-06*	0.0006727*			
hsa-miR-22	↓	2.9	1.40E-05*	0.000819*	5.4	< 1e-07*	< 1e-07*
hsa-miR-100	↓	2.6	0.0004317*	0.0132182*	2.7	0.000381*	0.005774*
hsa-miR-34b	↑	2.6	1.16E-05*	0.000754*			
hsa-miR-181a	↑	2.4	3.60E-06*	0.0004212*	3.3	< 1e-07*	< 1e-07*
hsa-miR-27a	↓	2.3	3.00E-07*	8.77E-05*	2.7	2.15E-05*	0.000682*
hsa-miR-27a*	↑	2.3	9.84E-05*	0.0038376*			
hsa-miR-593*	↑	2.2	5.31E-05*	0.0025886*	4.2	< 1e-07*	< 1e-07*
hsa-miR-92b*	↑	2.2	0.0010871*	0.0264981*	3.5	7.00E-07*	4.07E-05*
Round cell liposarcoma		(n=5)			(n=5)		
hsa-miR-422a	↑	5.6	< 1e-07*	< 1e-07*	3.0	0.002083*	0.031347*
hsa-miR-22	↓	3.5	0.0001092*	0.021294*	4.2	0.001165*	0.022584*
hsa-miR-29a	↓	3.0	0.0047013*	0.130965	4.8	0.000635*	0.015835*
hsa-miR-17	↑	2.8	0.0011601*	0.052205			
hsa-miR-106a	↑	2.8	0.0009572*	0.046664*			
hsa-miR-485-5p	↑	2.7	0.0260021*	0.292232			
hsa-miR-376a	↓	2.7	0.0076589*	0.165943			
hsa-miR-181a	↑	2.5	0.0003373*	0.032887*	2.0	0.021441*	0.111635
hsa-miR-93	↑	2.4	0.0016925*	0.066008			
hsa-miR-222	↓	2.3	0.0033618*	0.109259	4.3	1.92E-05*	0.006701*
Well differentiated liposarcoma		(n=14)			(n=11)		
hsa-miR-551b	↓	2.2	0.000552*	0.0538395	1.9	0.00047*	0.006314*
hsa-miR-628-3p	↑	1.9	0.000265*	0.0387709*	3.4	6E-07*	0.000209*
hsa-miR-17	↓	1.9	0.002763*	0.0910455	2.3	0.000317*	0.005838*
hsa-miR-106a	↓	1.8	0.003579*	0.0997007	2.3	0.000016*	0.000558*
hsa-miR-195	↓	1.8	0.001162*	0.087555	3.4	2.71E-05*	0.000822*
hsa-miR-675	↑	1.7	1.44E-05*	0.008424*	2.7	4.1E-06*	0.000321*
hsa-miR-106b	↓	1.7	9.53E-05*	0.0185835*			
hsa-miR-19a	↓	1.6	0.001528*	0.0893821	1.7	0.004991*	0.036287*
hsa-miR-602	↑	1.5	0.002296*	0.0910455	2.1	7.7E-06*	0.000399*
hsa-miR-18a	↓	1.4	0.003177*	0.0961769			
Dedifferentiated liposarcoma		(n=13)			(n=7)		
hsa-miR-338-5p	↑	3.9	< 1e-07*	< 1e-07*			
hsa-miR-221*	↑	3.6	2.00E-07*	1.95E-05*			
hsa-miR-26a-2*	↑	2.8	1.00E-07*	1.17E-05*	3.2	2.96E-05*	0.01033*
hsa-miR-21	↑	2.6	1.33E-05*	0.0004577*	2.8	0.002568*	0.074689

Table 2: Distinct miRNA expression signatures in liposarcoma subtypes and fat. (Continued)**A**

miRNA	Up/ down	Discovery set			Validation set		
		Fold change	p-value	FDR	Fold change	p-value	FDR
Dedifferentiated liposarcoma		(n=13)			(n=7)		
hsa-miR-412	↑	2.6	1.00E-07*	1.17E-05*	2.7	8.10E-05*	0.014135*
hsa-miR-938	↑	2.4	1.00E-07*	1.17E-05*			
hsa-miR-645	↑	2.4	5.70E-06*	0.0002382*	3.2	0.000257*	0.029933*
hsa-miR-155	↑	2.3	7.80E-06*	0.0003035*	2.5	0.005274*	0.131461
hsa-miR-21*	↑	2.3	1.70E-06*	0.0001105*	2.4	0.001715*	0.062202
hsa-miR-199a-5p	↑	2.2	5.00E-06*	0.0002382*			
Pleomorphic liposarcoma		(n=3)			(n=6)		
hsa-miR-143	↓	5.0	0.0002432*	0.0281483*			
hsa-miR-335	↓	3.9	0.0062123*	0.120261	8.6	8.50E-06*	0.001966*
hsa-miR-491-3p	↓	3.5	0.0102573*	0.1276706			
hsa-miR-92b*	↑	3.2	0.0036595*	0.1137679			
hsa-miR-106a	↓	3.1	0.0044468*	0.1137679			
hsa-miR-17	↓	3.0	0.0063579*	0.120261			
hsa-miR-193a-3p	↓	3.0	0.0023412*	0.096642			
hsa-miR-126	↓	2.9	0.0024321*	0.096642			
hsa-miR-130a	↓	2.7	0.0059969*	0.120261			
hsa-miR-30a	↓	2.7	0.0008934*	0.06318			

B

miRNA	Up/ down	Discovery set			Validation set		
		Fold change	p-value	FDR	Fold change	p-value	FDR
Fat		(n=8)			(n=9)		
hsa-miR-144	↑	5.9	< 1e-07*	< 1e-07*	2.8	9.16E-05*	0.007992*
hsa-miR-451	↑	3.4	0.0005016*	0.0293436*	3.2	0.000181*	0.012279*
hsa-miR-143	↑	2.9	0.0001296*	0.0108309*	3.2	0.000211*	0.012279*
hsa-miR-29c	↑	2.8	3.70E-06*	0.0005411*	2.4	0.002991*	0.113547
hsa-miR-29a	↑	2.6	0.0030355*	0.1109855			
hsa-miR-485-5p	↓	2.6	0.0092032*	0.1857617			
hsa-miR-101	↑	2.1	0.0006336*	0.033696*	1.6	0.046198*	0.327439
hsa-miR-145	↑	2.1	0.0002656*	0.017264*	3.6	5.60E-06*	0.000977*
hsa-miR-29b	↑	2.0	1.46E-05*	0.0014235*			
hsa-miR-126	↑	2.0	0.0028002*	0.1092078	2.9	7.82E-05*	0.007992*

A) MiRNAs expressed in each of the liposarcoma subtype are sorted on expression fold change compared to other liposarcomas, lipomas and fat in the discovery set (left). B) MiRNAs are sorted on expression fold change in fat compared to liposarcomas and lipomas in the discovery set (left). Arrows indicate up or downregulated miRNA expression compared to the expression in the other groups. P-values and false discovery rate (FDR) adjusted p-values are listed and significant p-values are indicated with an asterisk. MiRNAs also found differentially expressed in the validation set are indicated (right), together with the corresponding fold change and p-values. Empty rows represent miRNAs that are expressed in the validation set but are not significantly differentially expressed. MiRNAs in bold were selected for validation by qPCR.

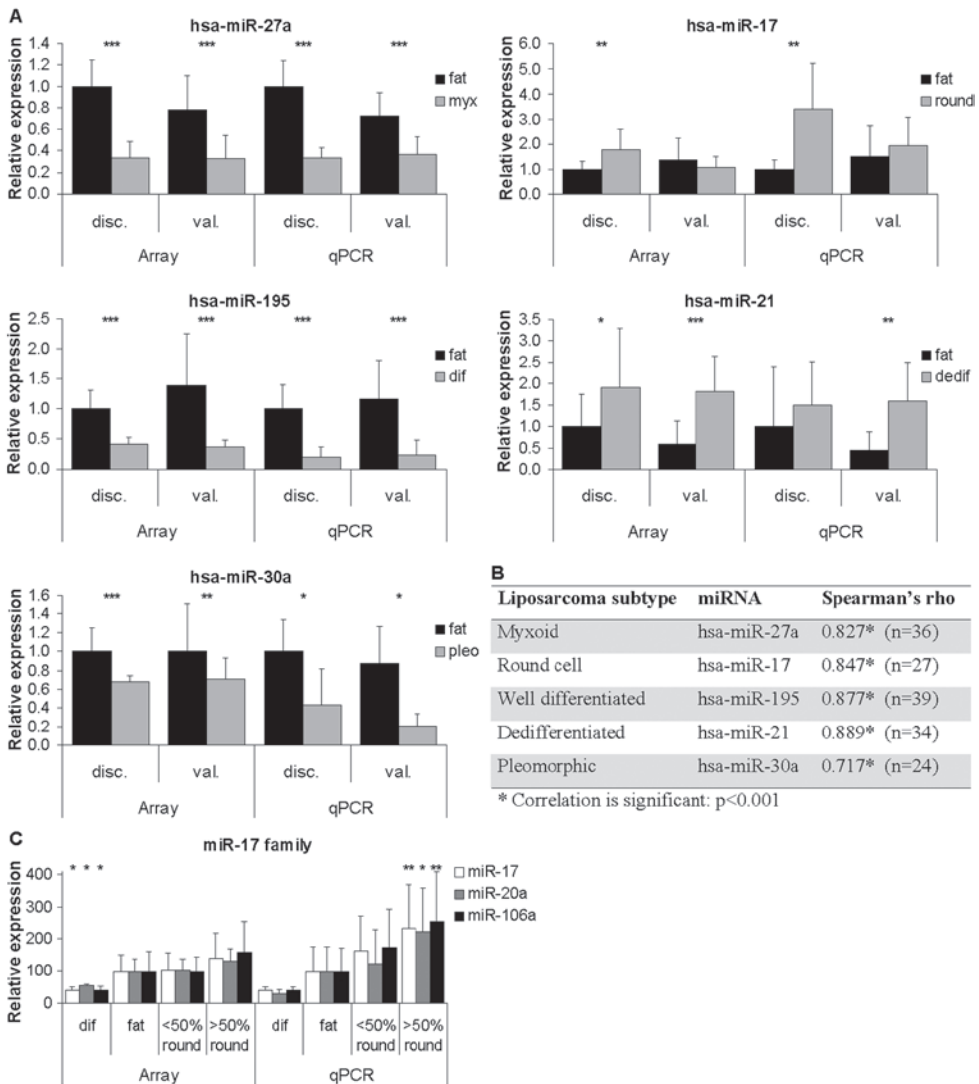


Figure 2: MiRNA expression levels are reproduced in an independent validation set and verified by qPCR. A) The miRNA expression levels of selected miRNAs as determined by microarray analysis in the discovery set (disc.) were reproduced in the validation set (val.). MiRNA expression levels are relative to the expression in fat samples (relative expression in fat in the discovery set are set to 1 in both array and qPCR data set). Liposarcoma subtypes: myx – myxoid; round – round cell; dif – well differentiated; dedif – dedifferentiated; pleo – pleomorphic. B) MiRNA expression levels determined by microarray and qPCR are correlated. Spearman's rank correlation coefficients (ρ) and statistical significance are indicated. C) MiRNA expression of miR-17, miR-20a and miR-106a was determined by microarray and qPCR and was found to be higher in high-percentage round cell tumors. MiRNA expression levels in high percentage round cell tumors (>50% round), low percentage round cell tumors (<50% round) and well differentiated liposarcomas (dif) are relative to the expression in fat samples (average expression in fat is set to 100 in both array and qPCR data set). Asterisks indicate significant difference between miRNA expression in liposarcoma subtypes compared to the normal fat group as determined by two-sample t-tests: * $p < 0.05$, ** $p < 0.005$.



MiRNAs deregulated in all liposarcomas

MiRNAs that discriminate adipocytic tumors from normal fat, rather than differentiating single subtypes of liposarcomas, are summarized in Table 2B (Supplemental Table 3). A number of the listed miRNAs arise from the same genomic location, e.g. the miR-144/451 cluster (17q11.2) and the miR-143/145 cluster (5q32), or belong to a miRNA family, e.g. the miR-29 family members. Since miR-143/145 levels are frequently decreased in human cancers (Supplemental Table 4) and are together with miR-144/451 most differentially expressed between normal fat and liposarcoma tissues, these miRNAs were selected for further functional characterization. They were shown to be highly expressed in fat, slightly downregulated (although not significant) in lipomas and even more reduced in liposarcomas (Figure 3). Moreover, it seems as if expression of miR-143, miR-145, miR-144 and miR-451 is correlated to malignancy, with a relative high expression in well differentiated liposarcomas as compared to the more malignant liposarcoma subtypes. This suggests that these miRNAs may have a tumor suppressor-like function in adipocytic tissue.

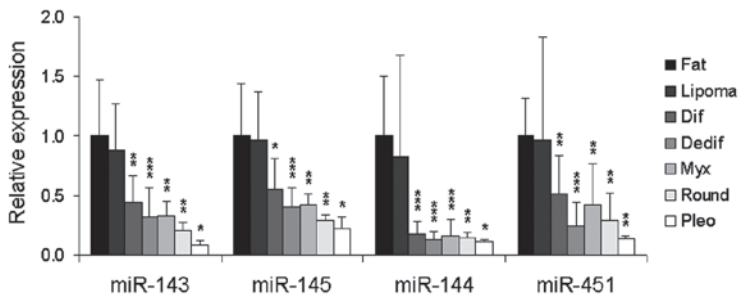


Figure 3: Deregulated expression of miR-143, miR-145, miR-144 and miR-451 in lipomas and liposarcomas. MiRNA expression, relative to the expression in normal fat, which is set to 1, was measured in the discovery sample set by microarray. Liposarcoma subtypes: dif – well differentiated; dedif – dedifferentiated; myx – myxoid; round – round cell; pleo – pleomorphic. Asterisks indicate significant differences between miRNA expression in a liposarcoma subtype compared to the normal fat group as determined by two-sample t-tests: * $p < 0.05$, ** $p < 0.005$, *** $p < 0.0005$.

MiR-145 and miR-451 inhibit cell proliferation in liposarcoma cell lines

MiRNA mimics of miR-143, miR-145, miR-144 and miR-451, as well as a scrambled control mimic (mNeg), were transfected into two liposarcoma cell lines, the SW872 undifferentiated liposarcoma cell line and the MLS 1765-92 myxoid liposarcoma cell line. Both cell lines display a low or undetectable expression, as judged by our microarray platform, of miR-143, miR-145, miR-144 and miR-451. Cell density was monitored in time at 24h, 48h, 72h and 96h post-transfection by SRB assays (Figure 4A). In both liposarcoma cell lines, overexpression of miR-145 clearly decreased the cell growth. MiR-451 overexpression led to growth arrest in the MLS 1765-92 myxoid liposarcoma cell line whereas it had no significant effect on cell density in SW872 cells. In both cell lines overexpression of miR-143 and miR-144 did not exert an effect. It was noted that



overexpression of miR-451, miR-145 and also miR-144, affected cell growth in other liposarcoma cell lines as well, indicating an important role of the miR-143/145 and miR-144/451 clusters in liposarcomas (Supplemental Figure 2).

To examine the effects of miR-145 and miR-451 on cell proliferation in SW872 and MLS 1765-92 in greater detail, liposarcoma cells were transfected with miR-145 and miR-451 mimics and a scrambled mimic as negative control. Cell proliferation was measured by EdU-incorporation as determined by FACS-analysis 72h post-transfection (Figure 4B). The percentage of EdU positive cells slightly increased when miR-145 and miR-451 were overexpressed, except in SW872 cells transfected with miR-145, indicative of increased numbers of cycling cells. However, in both cell lines overexpression of miR-145 and miR-451 led to a dramatic reduction of the levels of EdU incorporation in the EdU-positive fraction as judged by the decreased fluorescence intensity. This may point to an abnormal cell cycle progression, in which cells at some point arrest or die, not being able to complete DNA synthesis.

MiR-145 and miR-451 affect the cell cycle and induce apoptosis in liposarcoma cell lines

To determine whether miR-145 and miR-451 affect the cell cycle and cell viability, SW872 and MLS 1765-92 cells were transfected with miRNA mimics or a scrambled control mimic. Cell cycle profiles were determined by FACS-analysis 72h post-transfection (Figure 4C). In both cell lines, overexpression of miR-145 and miR-451 led to an increased sub-G1 fraction compared to the negative control, which points to DNA fragmentation indicative of cell death. The G1 fraction was decreased and the percentage of cells in the S-G2-M fraction was slightly elevated in miR-145 and miR-451 overexpressing cells, suggesting that there are more cycling cells, which is in line with the observed increased percentage of EdU positive cells. Furthermore, the cell cycle profile of miR-145 transfected SW872 cells showed distorted peaks, which might indicate DNA damage in cycling cells. In MLS 1765-92 cells overexpressing miR-145 and miR-451 the characteristic shape of the S-G2-M phase was changed. The latter may be caused by cells which cannot complete the cell cycle, confirming the results of the EdU incorporation experiments.

Induction of apoptosis was determined by Annexin V and PI stainings and FACS-analysis 72h after transfection of the mimics (Figure 4D, Supplemental Figure 3). Overexpression of miR-145 and miR-451 led to a decrease of live cells (Annexin V - / PI -) compared to the negative control. The early (Annexin V + / PI -) and late apoptotic fraction (Annexin V + / PI +) increased in both miR-145 and miR-451 transfected cell lines.

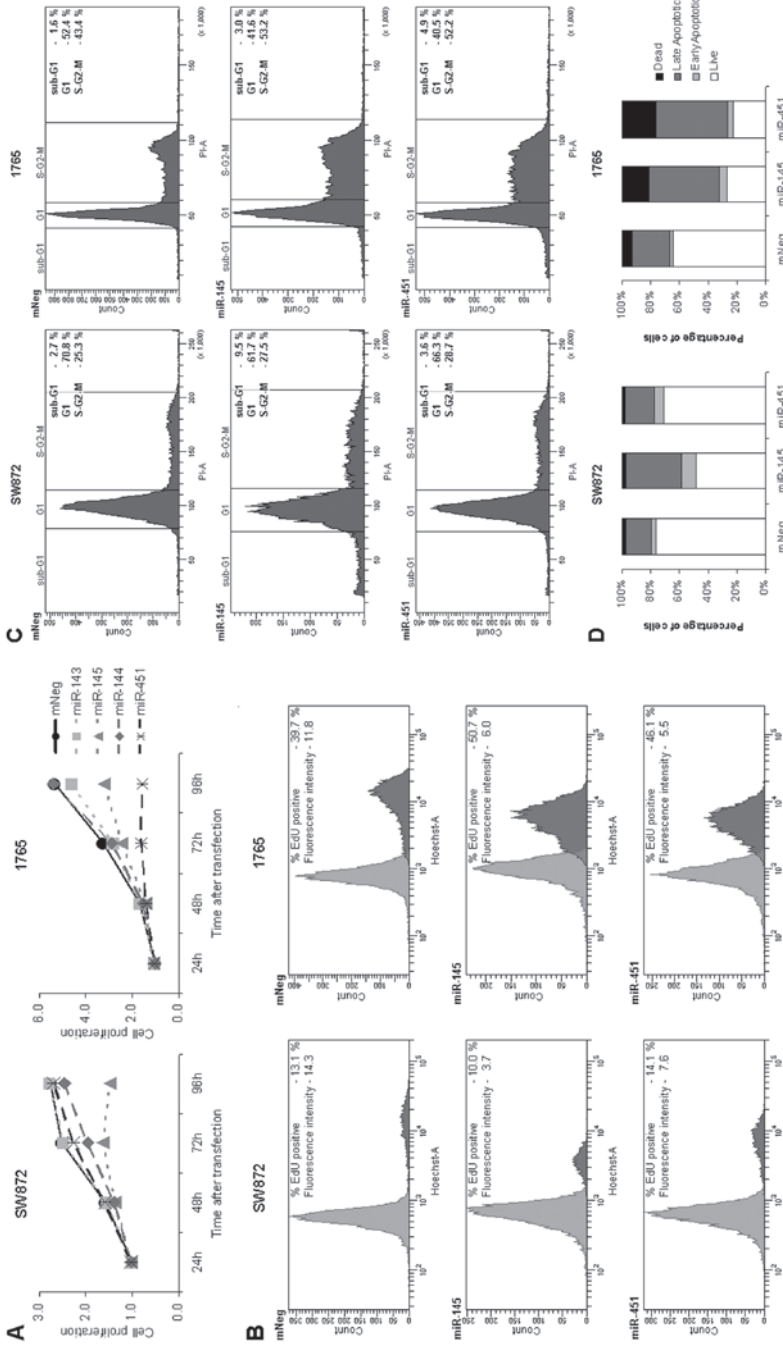


Figure 4: Overexpression of miR-145 and miR-451 affects cell proliferation, alters cell cycle profiles and induces cell death in liposarcoma cell lines. A) SW872 (liposarcoma) and MLS 1765-92 (myxoid liposarcoma) cell lines are transfected with either miR-143, miR-145, miR-144, miR-451 mimics or a negative control scrambled mimic (mNeg). Graphs indicate cell growth at 24h, 48h, 72h and 96h post-transfection, relative to the negative control at 24h, which is set at 1. B) Reduced EdU incorporation in liposarcoma cell lines SW872 and MLS 1765-92 at 72h post-transfection with miR-145 and miR-451 mimics compared to a negative control (mNeg, scrambled mimic). X-axes indicate EdU fluorescence levels, y-axes indicate cell counts. Experiments were repeated at least twice (n=2-4) and representative figures are shown. C) Cell cycle profiles were determined in liposarcoma cell lines SW872 and MLS 1765-92 transfected with miR-145, miR-451 and a negative control (mNeg) by FACS analysis 72h post-transfection. X-axes indicate PI levels, y-axes indicate cell counts. D) FACS analysis of Annexin V/PI (AnnV/PI) stained liposarcoma cell lines SW872 and MLS 1765-92 transfected with miR-145, miR-451 and a negative control (mNeg) 72h post-transfection. Live cells are presented by the Ann-/PI- fraction, early apoptotic cells by the Ann+/PI- fraction, late apoptotic cells by the Ann+/PI+ fraction and dead cells in the Ann-/PI+ fraction. Experiments were repeated at least twice (n=2-4) and representative figures are shown.



DISCUSSION

The exact diagnosis of liposarcoma subtypes has become increasingly important, not only to obtain prognostic information, but also for treatment decision making.⁶⁻⁷ For example, myxoid/round cell liposarcomas are more sensitive to radiotherapy and systemic treatments than the other subtypes.³⁷ Although some significant advances have been made concerning the treatment of sarcomas in recent years, liposarcomas are still difficult to treat. They show high recurrence and metastatic rates leading to an overall mortality of 60%.³⁷ Increased knowledge on the molecular aberrations in these tumors has aided classification of liposarcomas,¹¹⁻¹² but is also crucial to discover novel drug targets and devise new therapeutic approaches. In this study, we used miRNA expression profiling to classify liposarcoma subtypes, lipomas and adipocytic tissue. In addition we identified miRNAs that are deregulated in specific liposarcoma subtypes and provide evidence for a tumor suppressor activity of miR-145 and miR-451.

It appeared that miRNA expression profiling is able to distinguish the different liposarcoma subtypes from each other and from benign lipomas and normal fat. Our data clearly show that myxoid/round cell liposarcomas have a distinct miRNA expression profile. In an extensive soft tissue sarcoma profiling study Renner et al. found upregulation of miR-9 and miR-9* in myxoid liposarcomas versus normal fat,²⁸ which we could only verify in our round cell cohort. However, downregulation of miR-486 in TLS-CHOP expressing myxoid liposarcomas as shown by Borjigin et al.,²⁹ was validated in both our myxoid and round cell liposarcomas. In our sample set it was, however, hard to discern myxoid and round cell liposarcomas from each other. This may be due to the limited sample size, but another confounding factor is the fact that the round cell component of the myxoid/round cell liposarcomas differed and ranged from 5-100% in our sample set. Nevertheless, we show that miRNAs like miR-17, miR-20a and miR-106a are expressed at relatively high levels in myxoid tumors with a high round cell component (>50%) in comparison to normal fat and other liposarcomas subtypes. These miR-17 family members are also found overexpressed in various other cancers like colon cancer and lung cancer.³⁸ They appear to promote cell proliferation, suppress apoptosis and stimulate tumor angiogenesis³⁹ and can be linked to aggressiveness, a trait that fits the malignant nature of round cell liposarcomas.

Lipoma and normal fat tissues were poorly distinguishable from each other. This may point to an overall benign miRNA signature present in fat as well as lipomas. It is plausible that in addition to miRNA deregulation other factors and processes play a role in the transition from normal tissues to benign neoplasms. The well differentiated liposarcoma samples that cluster with lipomas and normal fat may identify a subgroup of well differentiated liposarcomas with a more favorable outcome, or indicate early stage tumors which did not yet lose their benign signature. This, however, would imply that gross miRNA deregulation is not an early event in the oncogenesis of well differentiated liposarcomas. Conversely, two lipomas clustered with the well differentiated



tumor samples. This again brings up the discussion whether lipomas and well differentiated liposarcomas are two completely separate entities or whether they represent different stages in a single biological continuum.^{5, 40-41} It will require larger tumor sets of well characterized lipomas and well differentiated liposarcomas, whose progression is preferably monitored in time in combination with in depth molecular analyses, to unravel the route of adipocytic tumor progression.

The clustering of well differentiated liposarcomas with fat and other liposarcoma subtypes has also been observed in an mRNA expression study where these tumors clustered among lipoma and fat samples as well as with dedifferentiated liposarcomas.¹⁶ This dichotomy of well differentiated liposarcomas resembling either benign lipomas/normal fat or the more malignant dedifferentiated liposarcomas, on both the mRNA and miRNA level, raises the question whether all well differentiated liposarcomas are intrinsically capable of dedifferentiation, or whether some of these tumors will always stay relatively benign. Singer et al. observed that dedifferentiation occurs more often in second-time local recurrences of well differentiated liposarcomas, which implies the acquisition of additional genomic aberrations within these tumors as they recur.⁷ Some of these additional alterations may already be present and reflected in the gene/miRNA expression profile of these tumors before the actual dedifferentiation takes place.

All dedifferentiated liposarcomas clustered in a separate branch which indicates that the miRNA profile changes significantly during dedifferentiation. Upregulation of miR-214, miR-199a-2, miR-155 and downregulation of miR-10b, miR-126 and the let-7 family in well differentiated/dedifferentiated liposarcomas compared to normal fat has been reported.³⁰⁻³² Our data confirm the upregulation of miR-214, miR-199a-3p and miR-155 in dedifferentiated liposarcomas, miR-126a in well differentiated and dedifferentiated liposarcomas, and only let-7a and let-7g in well differentiated liposarcomas. Furthermore, others described decreased levels of miR-1257, miR193b, miR-143 and miR-145 as well as increased levels of miR-21 and miR-26a in the dedifferentiated subtype.³³⁻³⁵ We also observed upregulation of miR-21 and downregulation of miR-143 and miR-145 in our dedifferentiated cohort. Although high-grade dedifferentiated liposarcomas are sometimes morphologically indistinguishable from pleomorphic liposarcoma, our miRNA profiling discriminated the two subtypes. Clustering based on matrix-CGH data could also distinguish these two liposarcoma subtypes, but a clustering using the mRNA expression data of 1600 genes failed to do so.⁴²

We identified miRNAs that were more abundantly expressed in normal fat tissue compared to lipomas and liposarcomas. Most notably, it was observed that the expression of miR-144/451 and miR-143/145 was only slightly decreased in lipomas, further reduced in well differentiated and myxoid liposarcomas and even more so in their respective high grade counterparts



dedifferentiated and round cell liposarcomas. The lowest expression was measured in pleomorphic liposarcomas, which is the most malignant subtype. Since decreased expression of these miRNAs is already observed in benign lipomas and the low grade liposarcoma subtypes, it may be an early event in tumorigenesis. The correlation of loss of miRNA expression with increasing malignant potential might be characteristic for miRNAs with a tumor suppressor function or miRNAs which suppress oncogenes. The reasons for the reduced levels of miR-143/145 and miR-144/451 in liposarcomas are not known. As far as we know, the chromosomal locations where the genes for these miRNAs reside are intact. It has been reported that the promoter region of miR-143/145 can be methylated, thereby silencing the expression of these miRNAs.⁴³⁻⁴⁴ For miR-144/451 no such epigenetic regulation has been reported.

The miR-144/451 and miR-143/145 clusters have been linked to several biological processes and have been aberrantly regulated in many tumor types (Supplemental Table 4), suggesting that they fulfil an important role in carcinogenesis. Unclear, however, is whether they operate by mediating the expression of the same set of target genes in all cancers. We are the first to describe a putative tumor suppressor like function for miR-145 and miR-451 in liposarcomas. Overexpression of miR-145 reduced cell proliferation in two different liposarcoma cell lines. MiR-451 overexpression blocked cell proliferation in MLS 1765-92 cells whereas it had only minor effects in SW872 cells. This may be due to the different genetic background of the cell lines used: SW872 is reported to be derived from an undifferentiated malignant liposarcoma, while the MLS 1765-92 cell line originates from a myxoid liposarcoma. Overexpression of both miRNAs gave rise to increased apoptosis as seen in cell cycle analyses and Annexin V/PI stainings. From these assays and the reduced levels of EdU incorporation (fluorescence intensity) it can be inferred that cells expressing miR-145 and miR-451 are unable to complete the cell cycle and consequently become apoptotic.

MiR-143 and miR-145 were both reported to be downregulated in well differentiated and dedifferentiated liposarcoma.³³ In that study, only overexpression of miR-143, and not miR-145, resulted in decreased cell proliferation and increased apoptosis in dedifferentiated liposarcoma cell lines. In contrast, in our experiments re-expression of miR-145, and not miR-143, had these effects. None of the genes putatively regulated by miR-143 (*BCL2*, *TOP2A*, *PRC1* and *PLK1*) were regulated by miR-145,³³ implying that the cellular effects we observed are mediated by different genes. Both miR-145 and miR-451 are frequently found underexpressed in cancers (Supplemental Table 4) and overexpression often affects cellular proliferation and apoptosis.⁴⁵⁻⁴⁶ Various target genes have been reported⁴⁶⁻⁴⁸ as of yet it is not known whether these targets play a role in liposarcomas. Recently Zhang et al. described that miR-155 is a liposarcoma oncogene as it was found to be significantly overexpressed in well differentiated and dedifferentiated liposarcomas compared to normal fat. They further show that miR-155 directly targets *CK1α*

thereby promoting tumor growth.³⁰ Our data confirm miR-155 upregulation in dedifferentiated liposarcomas.

The number of human miRNAs identified increases constantly, particularly because of next generation sequencing approaches. The latest version of miRBase (release 20, June 2013) lists more than 2500 mature human miRNAs. Our microarray platform, however, is only capable of detecting 725 human miRNAs, consequently the miRNA coverage of our platform is not optimal. Nevertheless from the miRNAs that we identified using our discovery set, a substantial number was verified in an independent validation set, selected miRNA expression levels were validated by qPCR, and most results from previous published studies were confirmed by our analyses.

In conclusion, we show that miRNAs are a powerful tool to discriminate liposarcoma subtypes from each other and from normal fat. In the future, liposarcoma subtype specific miRNAs could aid in objective diagnostic decision making and be of prognostic value. In addition we identified a tumor suppressive role for miR-145 and miR-451 in liposarcoma. MiRNA therapy is currently being explored.⁴⁹⁻⁵⁰ Our *in vitro* results of miR-145 and miR-451 re-expression on cell growth, proliferation and apoptosis in tumor cells suggest a possible role of these miRNAs as novel therapeutic targets for cancer therapy.

ACKNOWLEDGEMENTS

We greatly appreciated the help and technical expertise of A. Sacchetti with the FACS analyses and we thank dr. P. Åman for providing the MLS 1765-92 myxoid liposarcoma cell line. Furthermore we are grateful to the personnel of the Erasmus Medical Center Tissue Bank and Institut Bergonié for providing the tissues samples, and we thank the members the Laboratory of Translational Pharmacology for helpful discussions. This work was supported by the EC FP6 CONTICANET Network of Excellence (LSHC-CT-2005-018806) from the European Commission. The authors disclose no potential conflicts of interest.



REFERENCES

1. Ducimetiere F, Lurkin A, Ranchere-Vince D, Decouelaere AV, Isaac S, Claret-Tournier C, et al. [Incidence rate, epidemiology of sarcoma and molecular biology. Preliminary results from EMS study in the Rhone-Alpes region]. *Bull Cancer*. 2010 Jun;97(6):629-41.
2. Toro JR, Travis LB, Wu HJ, Zhu K, Fletcher CD, Devesa SS. Incidence patterns of soft tissue sarcomas, regardless of primary site, in the surveillance, epidemiology and end results program, 1978-2001: An analysis of 26,758 cases. *Int J Cancer*. 2006 Dec 15;119(12):2922-30.
3. Fletcher CD, Bridge JA, Hogendoorn PC, Mertens F, (Eds.). *WHO Classification of Tumours of Soft Tissue and Bone*. Lyon: IARC; 2013.
4. Pedeutour F, Suijkerbuijk RF, Van Gaal J, Van de Klundert W, Coindre JM, Van Haelst A, et al. Chromosome 12 origin in rings and giant markers in well-differentiated liposarcoma. *Cancer Genet Cytogenet*. 1993 Apr;66(2):133-4.
5. Dei Tos AP, Doglioni C, Piccinin S, Sciò R, Furlanetto A, Boiocchi M, et al. Coordinated expression and amplification of the MDM2, CDK4, and HMG1-C genes in atypical lipomatous tumours. *J Pathol*. 2000 Apr;190(5):531-6.
6. Dalal KM, Kattan MW, Antonescu CR, Brennan MF, Singer S. Subtype specific prognostic nomogram for patients with primary liposarcoma of the retroperitoneum, extremity, or trunk. *Ann Surg*. 2006 Sep;244(3):381-91.
7. Singer S, Antonescu CR, Riedel E, Brennan MF. Histologic subtype and margin of resection predict pattern of recurrence and survival for retroperitoneal liposarcoma. *Ann Surg*. 2003 Sep;238(3):358-70; discussion 70-1.
8. Alvegard TA, Berg NO. Histopathology peer review of high-grade soft tissue sarcoma: the Scandinavian Sarcoma Group experience. *J Clin Oncol*. 1989 Dec;7(12):1845-51.
9. Lehnhardt M, Daigeler A, Hauser J, Puls A, Soimaru C, Kuhnen C, et al. The value of expert second opinion in diagnosis of soft tissue sarcomas. *J Surg Oncol*. 2008 Jan 1;97(1):40-3.
10. Ray-Coquard I, Montesco MC, Coindre JM, Dei Tos AP, Lurkin A, Ranchere-Vince D, et al. Sarcoma: concordance between initial diagnosis and centralized expert review in a population-based study within three European regions. *Ann Oncol*. 2012 Feb 13.
11. de Vreeze RS, de Jong D, Nederlof PM, Ariaens A, Tielens IH, Frenken L, et al. Added Value of Molecular Biological Analysis in Diagnosis and Clinical Management of Liposarcoma: A 30-Year Single-Institution Experience. *Ann Surg Oncol*. 2010 Mar;17(3):686-93.
12. Sirvent N, Coindre JM, Maire G, Hostein I, Kessler F, Guillou L, et al. Detection of MDM2-CDK4 amplification by fluorescence in situ hybridization in 200 paraffin-embedded tumor samples: utility in diagnosing adipocytic lesions and comparison with immunohistochemistry and real-time PCR. *Am J Surg Pathol*. 2007 Oct;31(10):1476-89.
13. Fletcher CD, Akerman M, Dal Cin P, de Wever I, Mandahl N, Mertens F, et al. Correlation between clinicopathological features and karyotype in lipomatous tumors. A report of 178 cases from the Chromosomes and Morphology (CHAMP) Collaborative Study Group. *Am J Pathol*. 1996 Feb;148(2):623-30.
14. Bassett MD, Schuetz SM, Distche C, Norwood TH, Swisshelm K, Chen X, et al. Deep-seated, well differentiated lipomatous tumors of the chest wall and extremities: the role of cytogenetics in classification and prognostication. *Cancer*. 2005 Jan 15;103(2):409-16.
15. Binh MB, Sastre-Garau X, Guillou L, de Pinieux G, Terrier P, Lagace R, et al. MDM2 and CDK4 immunostainings are useful adjuncts in diagnosing well-differentiated and dedifferentiated liposarcoma subtypes: a comparative analysis of 559 soft tissue neoplasms with genetic data. *Am J Surg Pathol*. 2005 Oct;29(10):1340-7.
16. Singer S, Socci ND, Ambrosini G, Sambol E, Decarolis P, Wu Y, et al. Gene expression profiling of liposarcoma identifies distinct biological types/subtypes and potential therapeutic targets in well-differentiated and dedifferentiated liposarcoma. *Cancer Res*. 2007 Jul 15;67(14):6626-36.
17. Gobble RM, Qin LX, Brill ER, Angeles CV, Ugras S, O'Connor RB, et al. Expression profiling of liposarcoma yields a multigene predictor of patient outcome and identifies genes that contribute to liposarcomagenesis. *Cancer Res*. 2011 Apr 1;71(7):2697-705.
18. Spitzer JJ, Ugras S, Runge S, Decarolis P, Antonescu C, Tuschl T, et al. mRNA and protein levels of FUS, EWSR1, and TAF15 are upregulated in liposarcoma. *Genes Chromosomes Cancer*. 2011 May;50(5):338-47.
19. Brill E, Gobble R, Angeles C, Lagos-Quintana M, Crago A, Laxa B, et al. ZIC1 overexpression is oncogenic in liposarcoma. *Cancer Res*. 2010 Sep 1;70(17):6891-901.

20. Munker R, Calin GA. MicroRNA profiling in cancer. *Clin Sci (Lond)*. 2011 Aug;121(4):141-58.
21. Pritchard CC, Cheng HH, Tewari M. MicroRNA profiling: approaches and considerations. *Nat Rev Genet*. 2012 May;13(5):358-69.
22. Chen CZ. MicroRNAs as oncogenes and tumor suppressors. *N Engl J Med*. 2005 Oct 27;353(17):1768-71.
23. Calin GA, Croce CM. MicroRNA signatures in human cancers. *Nat Rev Cancer*. 2006 Nov;6(11):857-66.
24. Lu J, Getz G, Miska EA, Alvarez-Saavedra E, Lamb J, Peck D, et al. MicroRNA expression profiles classify human cancers. *Nature*. 2005 Jun 9;435(7043):834-8.
25. Barbarotto E, Schmittgen TD, Calin GA. MicroRNAs and cancer: profile, profile, profile. *Int J Cancer*. 2008 Mar 1;122(5):969-77.
26. Gougelet A, Perez J, Pissaloux D, Besse A, Duc A, Decouvelaere AV, et al. miRNA Profiling: How to Bypass the Current Difficulties in the Diagnosis and Treatment of Sarcomas. *Sarcoma*. 2011;2011:460650.
27. Subramanian S, Lui WO, Lee CH, Espinosa I, Nielsen TO, Heinrich MC, et al. MicroRNA expression signature of human sarcomas. *Oncogene*. 2008 Mar 27;27(14):2015-26.
28. Renner M, Czwan E, Hartmann W, Penzel R, Brors B, Eils R, et al. MicroRNA profiling of primary high-grade soft tissue sarcomas. *Genes Chromosomes Cancer*. 2012 Nov;51(11):982-96.
29. Borjigin N, Ohno S, Wu W, Tanaka M, Suzuki R, Fujita K, et al. TLS-CHOP represses miR-486 expression, inducing upregulation of a metastasis regulator PAI-1 in human myxoid liposarcoma. *Biochem Biophys Res Commun*. 2012 Oct 19;427(2):355-60.
30. Zhang P, Bill K, Liu J, Young E, Peng T, Bolshakov S, et al. MiR-155 is a liposarcoma oncogene that targets casein kinase-1alpha and enhances beta-catenin signaling. *Cancer Res*. 2012 Apr 1;72(7):1751-62.
31. Bianchini L, Saada E, Gjernes E, Marty M, Haudebourg J, Birtwisle-Peyrottes I, et al. Let-7 microRNA and HMGA2 levels of expression are not inversely linked in adipocytic tumors: analysis of 56 lipomas and liposarcomas with molecular cytogenetic data. *Genes Chromosomes Cancer*. 2011 Jun;50(6):442-55.
32. Tap WD, Eilber FC, Ginther C, Dry SM, Reese N, Barzan-Smith K, et al. Evaluation of well-differentiated/dedifferentiated liposarcomas by high-resolution oligonucleotide array-based comparative genomic hybridization. *Genes Chromosomes Cancer*. 2011 Feb;50(2):95-112.
33. Ugras S, Brill E, Jacobsen A, Hafner M, Socci ND, Decarolis PL, et al. Small RNA sequencing and functional characterization reveals MicroRNA-143 tumor suppressor activity in liposarcoma. *Cancer Res*. 2011 Sep 1;71(17):5659-69.
34. Taylor BS, DeCarolis PL, Angeles CV, Brenet F, Schultz N, Antonescu CR, et al. Frequent alterations and epigenetic silencing of differentiation pathway genes in structurally rearranged liposarcomas. *Cancer Discov*. 2011 Dec;1(7):587-97.
35. Hisaoka M, Matsuyama A, Nakamoto M. Aberrant calreticulin expression is involved in the dedifferentiation of dedifferentiated liposarcoma. *Am J Pathol*. 2012 May;180(5):2076-83.
36. Pothof J, Verkaik NS, van IJcken W, Wiemer EA, Ta VT, van der Horst GT, et al. MicroRNA-mediated gene silencing modulates the UV-induced DNA-damage response. *EMBO J*. 2009 Jul 22;28(14):2090-9.
37. Jones RL, Fisher C, Al-Muderis O, Judson IR. Differential sensitivity of liposarcoma subtypes to chemotherapy. *Eur J Cancer*. 2005 Dec;41(18):2853-60.
38. Volinia S, Calin GA, Liu CG, Ambs S, Cimmino A, Petrocca F, et al. A microRNA expression signature of human solid tumors defines cancer gene targets. *Proc Natl Acad Sci U S A*. 2006 Feb 14;103(7):2257-61.
39. Mendell JT. miRiad roles for the miR-17-92 cluster in development and disease. *Cell*. 2008 Apr 18;133(2):217-22.
40. Italiano A, Cardot N, Dupre F, Monticelli I, Keslair F, Piche M, et al. Gains and complex rearrangements of the 12q13-15 chromosomal region in ordinary lipomas: the "missing link" between lipomas and liposarcomas? *Int J Cancer*. 2007 Jul 15;121(2):308-15.
41. Mentzel T. Biological continuum of benign, atypical, and malignant mesenchymal neoplasms - does it exist? *J Pathol*. 2000 Apr;190(5):523-5.
42. Fritz B, Schubert F, Wrobel G, Schwaenen C, Wessendorf S, Nessling M, et al. Microarray-based copy number and expression profiling in dedifferentiated and pleomorphic liposarcoma. *Cancer Res*. 2002 Jun 1;62(11):2993-8.
43. Suh SO, Chen Y, Zaman MS, Hirata H, Yamamura S, Shahryari V, et al. MicroRNA-145 is regulated by DNA methylation and p53 gene mutation in prostate cancer. *Carcinogenesis*. 2011 May;32(5):772-8.





44. Dou L, Zheng D, Li J, Li Y, Gao L, Wang L, et al. Methylation-mediated repression of microRNA-143 enhances MLL-AF4 oncogene expression. *Oncogene*. 2012 Jan 26;31(4):507-17.
45. Sachdeva M, Mo YY. miR-145-mediated suppression of cell growth, invasion and metastasis. *Am J Transl Res*. 2010;2(2):170-80.
46. Bandres E, Bitarte N, Arias F, Agorreta J, Fortes P, Agirre X, et al. microRNA-451 regulates macrophage migration inhibitory factor production and proliferation of gastrointestinal cancer cells. *Clin Cancer Res*. 2009 Apr 1;15(7):2281-90.
47. Xu Q, Liu LZ, Qian X, Chen Q, Jiang Y, Li D, et al. MiR-145 directly targets p70S6K1 in cancer cells to inhibit tumor growth and angiogenesis. *Nucleic Acids Res*. 2012 Jan;40(2):761-74.
48. Wang R, Wang ZX, Yang JS, Pan X, De W, Chen LB. MicroRNA-451 functions as a tumor suppressor in human non-small cell lung cancer by targeting ras-related protein 14 (RAB14). *Oncogene*. 2011 Jun 9;30(23):2644-58.
49. Thorsen SB, Obad S, Jensen NF, Stenvang J, Kauppinen S. The therapeutic potential of microRNAs in cancer. *Cancer J*. 2012 May-Jun;18(3):275-84.
50. Kitade Y, Akao Y. MicroRNAs and their therapeutic potential for human diseases: microRNAs, miR-143 and -145, function as anti-oncomirs and the application of chemically modified miR-143 as an anti-cancer drug. *J Pharmacol Sci*. 2010;114(3):276-80.

SUPPLEMENTAL TABLES

Supplemental Table 1: Detailed patient and tumor characteristics.

A

Subtype	Tissue/Tumor Site	Primary/ Recurrent/ Metastatic	Neoadjuvant Therapy	MDM2 Amplification	FUS-DDIT3 Fusion Gene
Fat	Peri-colic	NA	NA	NA	NA
Fat	Axilla	NA	NA	NA	NA
Fat	Axilla	NA	NA	NA	NA
Fat	Axilla	NA	NA	NA	NA
Fat	Groin	NA	NA	NA	NA
Fat	Peri-Colic	NA	NA	NA	NA
Fat	Groin	NA	NA	NA	NA
Fat	Axilla	NA	NA	NA	NA
Lipoma	Shoulder	Primary	No	NP	NP
Lipoma	Shoulder	Primary	No	NP	NP
Lipoma	Axilla	Primary	No	NP	NP
Well differentiated	Leg	Primary	No	MDM2 ampl	NP
Well differentiated	Leg	Primary	No	MDM2 ampl	NP
Well differentiated	Leg	Primary	No	MDM2 ampl	NP
Well differentiated	Leg	Primary	No	MDM2 ampl	NP
Lipoma	Buttock	Primary	No	Not amplified	NP
Lipoma	Arm	Primary	No	Not amplified	NP
Well differentiated	Leg	Primary	No	NP	NP
Well differentiated	Leg	Primary	No	NP	NP
Well differentiated	Retroperitoneal	Primary	No	NP	NP
Well differentiated	Groin	Primary	No	NP	NP
Well differentiated	Retroperitoneal	Primary	No	NP	NP
Well differentiated	Leg	Primary	Preoperative radiotherapy	NP	NP
Well differentiated	Leg	Primary	No	NP	NP
Well differentiated	Retroperitoneal	Recurrent	No	NP	NP
Well differentiated	Retroperitoneal	Primary	No	NP	NP
Well differentiated	Leg	Primary	No	NP	NP
Dedifferentiated	Groin	Recurrent	No	NP	NP
Dedifferentiated	Retroperitoneal	Primary	No	NP	NP
Dedifferentiated	Pelvis	Recurrent	No	NP	NP
Dedifferentiated	Retroperitoneal	Recurrent	No	NP	NP
Dedifferentiated	Retroperitoneal	Recurrent	No	NP	NP
Dedifferentiated	Retroperitoneal	Recurrent	No	NP	NP
Dedifferentiated	Retroperitoneal	Recurrent	No	NP	NP
Dedifferentiated	Retroperitoneal	Recurrent	No	NP	NP
Dedifferentiated	Retroperitoneal	Primary	No	NP	NP



Supplemental Table 1: Detailed patient and tumor characteristics. (Continued)**A**

Subtype	Tissue/Tumor Site	Primary/ Recurrent/ Metastatic	Neoadjuvant Therapy	MDM2 Amplification	FUS-DDIT3 Fusion Gene
Dedifferentiated	Retroperitoneal	Primary	No	NP	NP
Dedifferentiated	Head	Recurrent	No	NP	NP
Dedifferentiated	Retroperitoneal	Recurrent	No	NP	NP
Dedifferentiated	Retroperitoneal	Recurrent	No	NP	NP
Dedifferentiated	Retroperitoneal	Primary	No	NP	NP
Myxoid	Knee Cavity	Primary	Preoperative radiotherapy	NP	Not evaluable
Myxoid	Buttock	Primary	No	NP	NP
Myxoid	Leg	Primary	No	NP	NP
Myxoid	Calf	Primary	No	NP	NP
Myxoid	Leg	Recurrent	No	NP	NP
Myxoid	Thorax	Primary	No	NP	NP
Myxoid	Leg	Recurrent	No	NP	NP
Myxoid	Leg	Primary	No	NP	NP
Round cell	Leg	Recurrent	Preoperative isolated limb perfusion	NP	NP
Round cell	Buttock	Primary	No	NP	NP
Round cell	Peri-colic	Recurrent	No	NP	NP
Round cell	Leg	Primary	No	NP	NP
Round cell	Leg	Primary	No	NP	NP
Myxoid	Leg	Primary	No	NP	NP
Pleomorphic	Leg	Primary	No	NP	NP
Pleomorphic	Arm	Recurrent	No	NP	NP
Pleomorphic	Leg	Primary	No	NP	NP

B

Subtype	Tissue/Tumor Site	Primary/ Recurrent/ Metastatic	Neoadjuvant Therapy	MDM2 Amplification	FUS-DDIT3 Fusion Gene
Fat	Leg	NA	NA	NA	NA
Fat	Groin	NA	NA	NA	NA
Fat	Groin	NA	NA	NA	NA
Fat	Retroperitoneal	NA	NA	NA	NA
Fat	Neck	NA	NA	NA	NA
Fat	Groin	NA	NA	NA	NA
Fat	Omentum	NA	NA	NA	NA
Fat	Retroperitoneal	NA	NA	NA	NA
Fat	Mamma	NA	NA	NA	NA
Lipoma	Shoulder	Primary	No	NP	NP

Supplemental Table 1: Detailed patient and tumor characteristics. (Continued)**B**

Subtype	Tissue/Tumor Site	Primary/ Recurrent/ Metastatic	Neoadjuvant Therapy	MDM2 Amplification	FUS-DDIT3 Fusion Gene
Lipoma	Arm	Primary	No	NP	NP
Lipoma	Shoulder	Primary	No	NP	NP
Lipoma	Leg	Primary	No	NP	NP
Lipoma	Leg	Primary	No	NP	NP
Lipoma	Shoulder	Primary	No	Not amplified	NP
Lipoma	Back	Primary	No	NP	NP
Lipoma	Shoulder	Primary	No	Not amplified	NP
Lipoma	Axilla	Primary	No	NP	NP
Well differentiated	Leg	Primary	No	NP	NP
Well differentiated	Leg	Primary	No	NP	NP
Well differentiated	Retroperitoneal	Recurrent	No	NP	NP
Well differentiated	Retroperitoneal	Primary	No	NP	NP
Well differentiated	Leg	Primary	No	MDM2 ampl	NP
Well differentiated	Arm	Primary	No	NP	NP
Well differentiated	Hip	Primary	No	NP	NP
Well differentiated	Leg	Primary	No	NP	NP
Well differentiated	Arm	Primary	No	MDM2 ampl	NP
Well differentiated	Leg	Recurrent	No	NP	NP
Well differentiated	Leg	Primary	No	MDM2 ampl	NP
Dedifferentiated	Retroperitoneal	Recurrent	No	NP	NP
Dedifferentiated	Leg	Recurrent	No	NP	NP
Dedifferentiated	Hip	Recurrent	No	NP	NP
Dedifferentiated	Retroperitoneal	Primary	No	MDM2 ampl	NP
Dedifferentiated	Retroperitoneal	Primary	No	MDM2 ampl	NP
Dedifferentiated*	Retroperitoneal	Primary	No	NP	NP
Dedifferentiated*	Retroperitoneal	Primary	No	NP	NP
Myxoid	Leg	Primary	Preoperative isolated limb perfusion	NP	NP
Myxoid	Leg	Recurrent	No	NP	NP
Myxoid	Leg	Primary	No	NP	FUS-DDIT3
Myxoid	Buttock	Recurrent	No	NP	NP
Myxoid*	Leg	Recurrent	No	NP	DDIT3 rearr
Myxoid*	Leg	Primary	No	NP	DDIT3 rearr
Myxoid*	Leg	Primary	No	NP	FUS-DDIT3
Myxoid*	Leg	Primary	No	NP	FUS-DDIT3
Myxoid*	Leg	Primary	No	NP	FUS-DDIT3
Myxoid*	Leg	Primary	No	NP	FUS-DDIT3
Myxoid*	Leg	Primary	No	NP	FUS-DDIT3



Supplemental Table 1: Detailed patient and tumor characteristics. (Continued)**B**

Subtype	Tissue/Tumor Site	Primary/ Recurrent/ Metastatic	Neoadjuvant Therapy	MDM2 Amplification	FUS-DDIT3 Fusion Gene
Myxoid*	Leg	Metastasis	No	NP	FUS-DDIT3
Round cell*	Leg	Metastasis	No	NP	FUS-DDIT3
Round cell*	Leg	Metastasis	No	NP	FUS-DDIT3
Round cell*	Leg	Primary	No	NP	FUS-DDIT3
Round cell*	Leg	Metastasis	No	NP	FUS-DDIT3
Round cell*	Knee	Metastasis	No	NP	FUS-DDIT3
Pleomorphic*	Leg	Recurrent	No	NP	NP
Pleomorphic*	Leg	Primary	No	NP	NP
Pleomorphic	Shoulder	Recurrent	No	Not amplified	NP
Pleomorphic	Leg	Primary	No	Not amplified	NP
Pleomorphic	Shoulder	Primary	No	NP	NP
Pleomorphic	Leg	Primary	No	NP	NP

A) Samples from the discovery set are listed in the same order as in the supervised hierarchical clustering of Figure 1b. B) Samples from the validation set. Indicated is the tumor/tissue site, whether the tumor sample was from primary, recurrent or metastatic origin, and whether the patients were treated with neo-adjuvant therapy. Furthermore molecular diagnostic marker expression: the *MDM2* status and the presence of a *FUS-DDIT3* fusion gene are indicated. The four well differentiated liposarcomas and the two lipomas from the discovery set, that clustered aberrantly (in bold) were analyzed for *MDM2* amplification. In the well differentiated liposarcomas *MDM2* amplification (*MDM2* ampl) was detected, in the lipoma samples *MDM2* was not amplified. Neo-adjuvant treatment is not a common practice; from the discovery set only one patient with well differentiated liposarcoma and one with myxoid liposarcoma received preoperative radiotherapy, and one patient with round cell liposarcoma underwent preoperative isolated limb perfusion, while from the validation set one patient with myxoid liposarcoma underwent preoperative isolated limb perfusion. Asterisks (*) indicate samples obtained from Institut Bergonié, Bordeaux, France. All other patient samples are derived from the Erasmus MC tissue bank. Abbreviations: NA = not applicable. NP = not performed. DDIT3 rearr = rearrangement of DDIT3. FUS-DDIT3 = presence of FUS-DDIT3 fusion gene.

Supplemental Table 2: The 60 most significant differentially expressed miRNAs across all groups.

miRNA	Discovery set						Validation set						
	Parametric p-value	FDR	R.E. Fat	R.E. Lipom	R.E. Dif	R.E. Dedif	R.E. Myx	R.E. Round	R.E. Pleo	Parametric p-value	FDR	Genomic location	
1	hsa-miR-29c	< 1e-07	< 1e-07	1.00	1.01	0.48	0.31	0.25	0.22	0.20	< 1e-07	< 1e-07	1-q32.2
2	hsa-miR-22	< 1e-07	< 1e-07	1.00	1.15	0.82	0.73	0.23	0.18	0.32	< 1e-07	< 1e-07	17-p13.3
3	hsa-miR-422a	< 1e-07	< 1e-07	1.00	0.87	1.09	1.62	1.95	7.68	3.74	0.0196816	0.0363433	15-q22.31
4	hsa-miR-190b	< 1e-07	< 1e-07	1.00	0.93	0.87	1.44	2.15	9.70	3.69	N.E.	N.E.	1-q21.3
5	hsa-miR-181a	< 1e-07	< 1e-07	1.00	0.98	0.96	1.29	2.79	3.04	0.68	< 1e-07	< 1e-07	1-q31.3
6	hsa-miR-144	< 1e-07	< 1e-07	1.00	0.49	0.17	0.13	0.16	0.16	0.13	0.007424	0.0166088	17-q11.2
7	hsa-miR-29a	< 1e-07	< 1e-07	1.00	0.62	0.56	0.60	0.13	0.16	0.55	< 1e-07	< 1e-07	7-q32.3
8	hsa-miR-29b	< 1e-07	< 1e-07	1.00	0.94	0.56	0.48	0.35	0.36	0.47	0.0002379	0.0013179	7-q32.3
9	hsa-miR-143	< 1e-07	< 1e-07	1.00	0.90	0.44	0.29	0.36	0.22	0.09	4.46E-05	0.0003538	5-q33.1
10	hsa-miR-202	< 1e-07	< 1e-07	1.00	0.68	1.29	1.63	1.67	3.13	2.85	N.E.	N.E.	10-q26.3
11	hsa-miR-27a	0.0000001	0.0000053	1.00	0.92	0.62	0.91	0.33	0.48	0.82	< 1e-07	< 1e-07	19-p13.12
12	hsa-miR-193a-3p	0.0000002	0.0000098	1.00	1.19	0.50	0.38	0.72	0.92	0.21	0.003565	0.0095792	17-q11.2
13	hsa-miR-338-5p	0.0000003	0.0000125	1.00	0.79	0.98	3.63	0.92	0.68	1.42	0.0046995	0.0122397	17-q25.3
14	hsa-miR-222	0.0000003	0.0000125	1.00	0.90	0.74	1.68	0.51	0.41	0.91	< 1e-07	< 1e-07	X-p11.3
15	hsa-miR-216a	0.0000004	0.0000156	1.00	0.98	1.25	1.43	5.47	5.38	1.46	N.E.	N.E.	2-p16.1
16	hsa-miR-106a	0.0000001	0.0000366	1.00	0.56	0.44	0.63	1.06	1.73	0.24	2.10E-05	0.0002094	X-q26.2
17	hsa-miR-145	0.0000012	0.0000413	1.00	0.97	0.56	0.44	0.46	0.33	0.23	7.10E-06	8.85E-05	5-q33.1
18	hsa-miR-17	0.0000018	0.0000585	1.00	0.54	0.42	0.62	1.02	1.70	0.23	1.04E-05	0.0001171	13-q31.3
19	hsa-miR-299-3p	0.0000019	0.0000585	1.00	1.45	1.30	2.32	1.14	1.00	1.68	0.0008655	0.0031954	14-q32.31
20	hsa-miR-485-5p	0.0000022	0.0000644	1.00	1.13	1.69	1.93	7.59	5.55	2.48			14-q32.31
21	hsa-miR-412	0.0000024	0.0000669	1.00	0.88	1.15	2.92	1.60	1.14	0.82	0.0004514	0.0020816	14-q32.31
22	hsa-miR-24	0.0000032	0.0000851	1.00	0.84	0.66	0.77	0.37	0.37	0.66	< 1e-07	< 1e-07	9-q22.32
23	hsa-miR-106b	0.0000037	0.0000941	1.00	0.78	0.71	1.30	1.42	1.78	0.76	0.0033579	0.0093008	7-q22.1



Supplemental Table 2: The 60 most significant differentially expressed miRNAs across all groups. (Continued)

miRNA	Discovery set						Validation set					
	Parametric p-value	FDR	R.E. Fat	R.E. Lipom	R.E. Dif	R.E. Dedif	R.E. Myx	R.E. Round	R.E. Pleo	Parametric p-value	FDR	Genomic location
24 hsa-miR-26a-2*	0.0000069	0.0001682	1.00	0.85	1.22	2.69	0.78	0.80	1.11	0.0002601	0.0013754	12-q14.1
25 hsa-miR-141	0.0000085	0.0001989	1.00	0.26	0.22	0.17	0.21	0.29	0.17	N.E.	N.E.	12-p13.31
26 hsa-miR-125a-3p	0.0000095	0.000208	1.00	0.76	1.16	1.15	1.55	1.97	1.74	0.0068734	0.0157817	19-q13.33
27 hsa-miR-92b*	0.0000096	0.000208	1.00	0.61	1.33	1.15	2.73	1.66	4.20	7.70E-06	9.07E-05	1-q22
28 hsa-miR-938	0.0000185	0.0003865	1.00	0.78	0.99	2.40	1.13	0.77	1.23	N.E.	N.E.	10-p11.23
29 hsa-miR-192	0.0000223	0.0004446	1.00	0.74	0.94	0.78	1.83	1.25	0.73	N.E.	N.E.	11-q13.1
30 hsa-miR-200b	0.0000228	0.0004446	1.00	0.60	0.41	0.40	0.41	0.56	0.47	N.E.	N.E.	1-p36.33
31 hsa-miR-23a	0.0000273	0.0005152	1.00	0.93	0.90	0.94	0.50	0.47	0.89	1.10E-06	2.13E-05	19-p13.12
32 hsa-miR-330-5p	0.0000288	0.0005265	1.00	0.80	0.99	0.95	1.44	1.31	1.52	< 1e-07	< 1e-07	19-q13.32
33 hsa-miR-221*	0.0000322	0.0005708	1.00	0.80	0.86	3.51	1.47	0.99	0.73	0.0232188	0.0409261	X-p11.3
34 hsa-miR-34b	0.0000369	0.0006349	1.00	1.14	1.15	1.46	3.32	1.22	3.09	0.0067987	0.0157136	11-q23.1
35 hsa-miR-27a*	0.0000385	0.0006435	1.00	0.64	0.93	1.22	2.44	2.10	0.83	N.E.	N.E.	19-p13.12
36 hsa-miR-550	0.0000401	0.0006516	1.00	0.96	0.88	1.06	1.55	2.00	1.57	< 1e-07	< 1e-07	7-p15.1
37 hsa-miR-23b	0.0000424	0.0006704	1.00	0.72	0.70	0.81	0.40	0.46	0.74	1.00E-07	2.70E-06	9-q22.32
38 hsa-miR-593*	0.0000442	0.0006804	1.00	0.85	1.35	0.75	2.20	1.28	0.67	1.00E-07	2.70E-06	7-q32.1
39 hsa-miR-501-5p	0.000046	0.00069	1.00	1.49	1.12	1.01	0.66	0.66	1.35	N.E.	N.E.	X-p11.23
40 hsa-miR-221	0.0000529	0.0007483	1.00	1.02	1.06	1.75	0.80	0.77	0.83	5.40E-06	6.98E-05	X-p11.3
41 hsa-miR-491-3p	0.0000534	0.0007483	1.00	1.56	0.38	1.11	0.57	0.56	0.20	0.0026256	0.0075109	9-p21.3
42 hsa-miR-652	0.000054	0.0007483	1.00	1.06	0.77	0.54	0.45	0.54	0.42	1.00E-07	2.70E-06	X-q22.3
43 hsa-miR-452	0.000055	0.0007483	1.00	1.53	1.08	0.96	0.65	0.65	0.62	1.08E-05	0.0001178	X-q28
44 hsa-miR-708*	0.0000677	0.0009001	1.00	1.05	1.26	1.39	1.39	1.63	3.21	N.E.	N.E.	11-q14.1
45 hsa-miR-27b	0.0000703	0.0009139	1.00	0.74	0.62	0.72	0.46	0.47	0.65	N.E.	N.E.	9-q22.32
46 hsa-miR-20a	0.0000939	0.0011942	1.00	0.50	0.53	0.61	1.02	1.25	0.69	0.0001961	0.0011039	13-q31.3
47 hsa-miR-567	0.0000967	0.0012036	1.00	0.56	0.76	0.94	0.92	1.16	1.70	N.E.	N.E.	3-q13.2



Supplemental Table 2: The 60 most significant differentially expressed miRNAs across all groups. (Continued)

miRNA	Discovery set										Validation set				
	Parametric p-value	R.E. Fat	R.E. Lipom	R.E. Dif	R.E. Dedif	R.E. Myx	R.E. Round	R.E. Pleo	Parametric p-value	FDR	Genomic location				
48 hsa-miR-130b	0.0000993	1.00	1.01	1.30	2.20	1.38	1.92	2.18	0.0117692	0.023606	22-q11.21				
49 hsa-miR-628-3p	0.0001103	1.00	2.00	1.76	0.81	0.70	0.88	0.91	1.50E-06	2.76E-05	15-q21.3				
50 hsa-miR-543	0.0001135	1.00	1.04	1.12	1.00	2.65	1.51	1.99	N.E.	N.E.	14-q32.31				
51 hsa-miR-130a	0.0001138	1.00	0.43	0.49	0.76	1.02	1.09	0.27	0.0014966	0.0045817	11-q12.1				
52 hsa-miR-186	0.0001143	1.00	1.07	0.99	1.44	0.84	0.93	0.73	0.0002693	0.0013821	1-p31.1				
53 hsa-miR-522	0.0001158	1.00	1.22	0.92	0.83	1.43	1.40	0.90	N.E.	N.E.	19-q13.41				
54 hsa-miR-181b	0.0001351	1.00	0.82	1.08	0.96	1.40	1.69	1.04	N.E.	N.E.	1-q31.3				
55 hsa-miR-19b	0.0001421	1.00	0.62	0.47	0.70	0.92	0.99	0.42	N.E.	N.E.	13-q31.3				
56 hsa-miR-193b	0.0001467	1.00	1.32	0.95	1.40	0.68	0.83	0.67	2.30E-06	3.65E-05	16-p13.12				
57 hsa-miR-376b	0.0001522	1.00	1.06	1.12	2.14	1.12	0.98	1.93	N.E.	N.E.	14-q32.31				
58 hsa-miR-139-3p	0.0001668	1.00	0.99	1.24	1.28	2.06	1.16	1.14	N.E.	N.E.	11-q13.4				
59 hsa-miR-146a	0.0001753	1.00	1.01	0.91	1.13	0.50	0.44	0.46	2.00E-07	5.00E-06	5-q33.3				
60 hsa-miR-21*	0.0001891	1.00	0.63	0.72	1.84	0.88	0.79	0.62	2.00E-06	3.49E-05	17-q23.1				

The 60 most significant, differentially expressed miRNAs ($p < 0.0002$) across all groups of the discovery set (liposarcoma subtypes (dif – well differentiated; dedif – dedifferentiated; myx – myxoid; round – round cell; pleo – pleomorphic), lipomas and fat samples) as used for the supervised hierarchical clustering (Figure 2). The parametric p-values (F-test) and false discovery rate (FDR)-adjusted p-values are listed. The relative miRNA expression levels (R.E.) for each group (R.E. in normal fat is set at 1), as well as the miRNA genomic locations are indicated. Note that a number of miRNAs are listed as N.E. (not expressed) in the validation set; these were miRNAs that were detected (i.e. expressed above background) in the discovery set, while they could not be detected in the validation set. Empty lanes represent miRNAs that were detected but did not have a significant parametric p-value ($p < 0.05$) in the validation set.



Supplemental Table 3: MiRNA expression signatures of liposarcoma subtypes and fat. (Continued)

	Round cell liposarcomas				Discovery set		Validation set		Fold change		Fold change		Genomic location	
	miRNA	Parametric p-value	FDR	Fold change - Down in Round	Fold change - Up in Round	Parametric p-value	FDR	Parametric p-value	FDR	Round	Round	Round	Round	
1	hsa-miR-422a	< 1e-07*	< 1e-07*	3.50	5.56	0.0020826*	0.0313472*	0.0020826*	0.0313472*	3.04	3.04	15-q22.31		
2	hsa-miR-22	0.0001092*	0.021294*	3.03	2.78	0.0011648*	0.0225842*	0.0011648*	0.0225842*	4.16	4.16	17-p13.3		
3	hsa-miR-29a	0.0047013*	0.1309648	2.66	2.75	0.0006352*	0.0158346*	0.0006352*	0.0158346*	4.78	4.78	7-q32.3		
4	hsa-miR-17	0.0011601*	0.0522045	2.26	2.70	0.0009572*	0.0466635*	0.0009572*	0.0466635*	2.05	2.05	13-q31.3		
5	hsa-miR-106a	0.0009572*	0.0466635*	2.26	2.47	0.0260021*	0.292232	0.0260021*	0.292232	4.30	4.30	X-q26.2		
6	hsa-miR-485-5p	0.0260021*	0.292232	1.95	1.87	0.0076589*	0.1659428	0.0076589*	0.1659428	2.12	2.12	14-q32.31		
7	hsa-miR-376a	0.0076589*	0.1659428	1.82	1.85	0.0003373*	0.0328868*	0.0003373*	0.0328868*	2.25	2.25	14-q32.31		
8	hsa-miR-181a	0.0003373*	0.0328868*	1.77	1.84	0.0016925*	0.0660075	0.0016925*	0.0660075	2.96	2.96	1-q31.3	9-q33.3	
9	hsa-miR-93	0.0016925*	0.0660075	1.82	1.79	0.0033618*	0.1092585	0.0033618*	0.1092585	2.96	2.96	7-q22.1		
10	hsa-miR-222	0.0033618*	0.1092585	1.82	1.85	0.0005818*	0.0410617*	0.0005818*	0.0410617*	2.11	2.11	X-p11.3		
11	hsa-miR-424*	0.0005818*	0.0410617*	1.82	1.84	0.0097894*	0.1789625	0.0097894*	0.1789625	1.88	1.88	X-q26.3		
12	hsa-miR-146a	0.0097894*	0.1789625	1.82	1.87	0.0052818*	0.1343414	0.0052818*	0.1343414	2.12	2.12	5-q33.3		
13	hsa-miR-377*	0.0052818*	0.1343414	1.82	1.85	0.0006853*	0.0410617*	0.0006853*	0.0410617*	2.25	2.25	14-q32.31		
14	hsa-miR-550	0.0006853*	0.0410617*	1.82	1.85	0.0352231*	0.3386801	0.0352231*	0.3386801	2.25	2.25	7-p15.1	7-p14.3	
15	hsa-miR-27a*	0.0352231*	0.3386801	1.82	1.84	0.006723*	0.1573182	0.006723*	0.1573182	2.96	2.96	19-p13.12		
16	hsa-miR-24	0.006723*	0.1573182	1.77	1.79	0.0051111*	0.1343414	0.0051111*	0.1343414	2.96	2.96	9-q22.32	19-p13.12	
17	hsa-miR-106b	0.0051111*	0.1343414	1.77	1.71	0.0031432*	0.1081631	0.0031432*	0.1081631	2.96	2.96	7-q22.1		
18	hsa-miR-23a	0.0031432*	0.1081631	1.77	1.71	0.0002212*	0.0308997*	0.0002212*	0.0308997*	2.96	2.96	19-p13.12		
19	hsa-miR-22*	0.0002212*	0.0308997*	1.69	1.69	0.0016614*	0.0660075	0.0016614*	0.0660075	2.96	2.96	17-p13.3		
20	hsa-miR-125a-3p	0.0016614*	0.0660075	1.69	1.69	0.0417038*	0.3511676	0.0417038*	0.3511676	2.96	2.96	19-q13.33		
21	hsa-miR-145	0.0417038*	0.3511676	1.65	1.65	0.0007653*	0.0410617*	0.0007653*	0.0410617*	2.11	2.11	5-q33.1		
22	hsa-miR-199b-5p	0.0007653*	0.0410617*	1.59	1.59	0.0075106*	0.1659428	0.0075106*	0.1659428	3.40	3.40	9-q34.11		
23	hsa-miR-656	0.0075106*	0.1659428	1.58	1.58	0.0090105*	0.1700369	0.0090105*	0.1700369	3.40	3.40	14-q32.31		
24	hsa-miR-625*	0.0090105*	0.1700369	1.52	1.52	0.0358943*	0.3386801	0.0358943*	0.3386801	3.40	3.40	14-q23.3		
25	hsa-miR-620	0.0358943*	0.3386801	1.52	1.52	0.0065057*	0.0623562	0.0065057*	0.0623562	3.40	3.40	12-q24.21		
26	hsa-miR-23b	0.0457002*	0.3564616	1.52	1.52	7.00E-05*	0.0074424*	7.00E-05*	0.0074424*	3.40	3.40	9-q22.32		



Supplemental Table 3: miRNA expression signatures of liposarcoma subtypes and fat. (Continued)

Well differentiated liposarcomas	Discovery set				Validation set					
	miRNA	Parametric p-value	FDR	Fold change - Down in Dif	Fold change - Up in Dif	Parametric p-value	FDR	Fold change - Down in Dif	Fold change - Up in Dif	Genomic location
1	hsa-miR-551b	0.0005522*	0.0538395	2.20		0.0004704*	0.0063142*	1.95		3-q26.2
2	hsa-miR-628-3p	0.0002651*	0.0387709*		1.90	6.00E-07*	0.0002094*		3.39	15-q21.3
3	hsa-miR-17	0.0027631*	0.0910455	1.87		0.0003166*	0.0058375*	2.25		13-q31.3
4	hsa-miR-106a	0.003579*	0.0997007	1.81		1.60E-05*	0.0005584*	2.34		X-q26.2
5	hsa-miR-195	0.0011624*	0.087555	1.78		2.71E-05*	0.0008215*	3.43		17-p13.1
6	hsa-miR-675	1.44E-05*	0.008424*		1.70	4.10E-06*	0.0003211*		2.67	11-p15.5
7	hsa-miR-106b	9.53E-05*	0.0185835*	1.68						7-q22.1
8	hsa-miR-19a	0.0015279*	0.0893821	1.62		0.0049908*	0.0362873*	1.67		13-q31.3
9	hsa-miR-602	0.0022955*	0.0910455		1.54	7.70E-06*	0.0003989*		2.08	9-q34.3

Dedifferentiated liposarcomas	Discovery set				Validation set					
	miRNA	Parametric p-value	FDR	Fold change - Down in Dif	Fold change - Up in Dif	Parametric p-value	FDR	Fold change - Down in Dif	Fold change - Up in Dif	Genomic location
1	hsa-miR-338-5p	< 1e-07*	< 1e-07*		3.89					17-q25.3
2	hsa-miR-221*	2.00E-07*	1.95E-05*		3.57					X-p11.3
3	hsa-miR-26a-2*	1.00E-07*	1.17E-05*		2.75	2.96E-05*	0.01033*		3.16	12-q14.1
4	hsa-miR-21	1.33E-05*	0.000458*		2.59	0.002568*	0.074689		2.82	17-q23.1
5	hsa-miR-412	1.00E-07*	1.17E-05*		2.57	8.10E-05*	0.014135*		2.70	14-q32.31
6	hsa-miR-938	1.00E-07*	1.17E-05*		2.45					10-p11.23
7	hsa-miR-645	5.70E-06*	0.000238*		2.43	0.000257*	0.029933*		3.21	20-q13.13
8	hsa-miR-155	7.80E-06*	0.000304*		2.35	0.005274*	0.131461		2.47	21-q21.3
9	hsa-miR-21*	1.70E-06*	0.000111*		2.35	0.001715*	0.062202*		2.36	17-q23.1
10	hsa-miR-199a-5p	5.00E-06*	0.000238*		2.20					19-p13.2 1-q24.3



Supplemental Table 3: MiRNA expression signatures of liposarcoma subtypes and fat. (Continued)

Dedifferentiated liposarcomas		Discovery set			Validation set				
miRNA	Parametric p-value	FDR	Fold change - Down in Dedif	Fold change - Up in Dedif	Parametric p-value	FDR	Fold change - Down in Dedif	Fold change - Up in Dedif	Genomic location
11	hsa-miR-199a-3p; hsa-miR-199b-3p	8.30E-06*	0.000304*	2.11					19-p13.2 1-q24.3
12	hsa-miR-299-3p	1.00E-07*	1.17E-05*	1.93	0.038759*	0.386483	1.52		14-q32.31
13	hsa-miR-221	8.00E-07*	5.85E-05*	1.87					X-p11.3
14	hsa-miR-193a-3p	0.001809*	0.031124*	1.81					17-q11.2
15	hsa-miR-130b	0.000283*	0.007528*	1.67					22-q11.21
16	hsa-miR-186	3.30E-06*	0.000193*	1.53					1-p31.1

Pleomorphic liposarcomas		Discovery set			Validation set				
miRNA	Parametric p-value	FDR	Fold change - Down in Pleo	Fold change - Up in Pleo	Parametric p-value	FDR	Fold change - Down in Pleo	Fold change - Up in Pleo	Genomic location
1	hsa-miR-143	0.0002432*	0.0281483*	4.96					5-q33.1
2	hsa-miR-335	0.0062123*	0.120261	3.94			8.58		7-q32.2
3	hsa-miR-491-3p	0.0102573*	0.1276706	3.52					9-p21.3
4	hsa-miR-92b*	0.0036595*	0.1137679	3.18					1-q22
5	hsa-miR-106a	0.0044468*	0.1137679	3.06					X-q26.2
6	hsa-miR-17	0.0063579*	0.120261	3.02					13-q31.3
7	hsa-miR-193a-3p	0.0023412*	0.096642	2.98					17-q11.2
8	hsa-miR-126	0.0024321*	0.096642	2.94					9-q34.3
9	hsa-miR-130a	0.0059969*	0.120261	2.71					11-q12.1
10	hsa-miR-30a	0.0008934*	0.06318	2.67					6-q13
11	hsa-miR-708	0.0015522*	0.0756698	2.56					11-q14.1
12	hsa-miR-422a	0.0341883*	0.2245724	2.44					15-q22.31
13	hsa-miR-145	0.0059055*	0.120261	2.43					5-q33.1



Supplemental Table 3: miRNA expression signatures of liposarcoma subtypes and fat. (Continued)

miRNA	Discovery set			Validation set					
	Parametric p-value	FDR	Fold change - Down in Pleo	Fold change - Up in Pleo	Parametric p-value	FDR	Fold change - Down in Pleo	Fold change - Up in Pleo	Genomic location
14 hsa-miR-659	0.0001024*	0.0154586*		2.30					22-q13.1
15 hsa-miR-637	0.025305*	0.1982958	2.20						19-p13.3
16 hsa-miR-34b	0.0411469*	0.2314513		2.16					11-q23.1
17 hsa-miR-10a	0.0095507*	0.1241591	2.04						17-q21.32
18 hsa-miR-190	0.0086197*	0.120261	2.04						15-q22.2
19 hsa-miR-92b	2.74E-05*	0.0080145*		2.02					1-q22
20 hsa-miR-29b-1*	0.0046104*	0.1137679		1.99					7-q32.3
21 hsa-miR-30b*	0.0001057*	0.0154586*		1.96					8-q24.22
22 hsa-miR-10b	0.0080369*	0.120261	1.80						2-q31.1
23 hsa-miR-510	0.002478*	0.096642		1.80					X-q27.3
24 hsa-miR-557	0.0040743*	0.1137679		1.79					1-q24.2
25 hsa-miR-671-5p	0.0087728*	0.120261		1.79					7-q36.1
26 hsa-miR-126*	0.007379*	0.120261	1.79						9-q34.3
27 hsa-miR-30e	0.0257041*	0.1982958	1.77						1-p34.2
28 hsa-miR-148a	0.0248812*	0.1982958	1.75						7-p15.2
29 hsa-miR-198	0.0131245*	0.1435211		1.75					3-q13.33
30 hsa-miR-532-3p	0.0147496*	0.1513775		1.73					X-p11.23
31 hsa-miR-194	0.0274998*	0.1986097	1.73						1-q41
32 hsa-miR-526b	0.0036508*	0.1137679		1.73					19-q13.41
33 hsa-miR-518a-5p; hsa-miR-527	0.0043139*	0.1137679		1.72					19-q13.41
34 hsa-miR-99b*	0.0046674*	0.1137679		1.72					19-q13.33
35 hsa-miR-920	0.0037155*	0.1137679		1.70					12-p12.1
36 hsa-miR-374a*	0.0222851*	0.1904709	1.68						X-q13.2
37 hsa-let-7g	0.0058201*	0.120261	1.67						3-p21.1
38 hsa-miR-488	0.0057637*	0.120261		1.60					1-q25.2
39 hsa-miR-379	0.0098084*	0.1247373	1.60						14-q32.31





Supplemental Table 3: MiRNA expression signatures of liposarcoma subtypes and fat. (Continued)

miRNA	Discovery set			Validation set					
	Parametric p-value	FDR	Fold change - Down in Fat	Fold change - Up in Fat	Parametric p-value	FDR	Fold change - Down in Fat	Fold change - Up in Fat	Genomic location
1 hsa-miR-144	< 1e-07*	< 1e-07*		5.88	9.16E-05*	0.0079921*		2.76	17-q11.2
2 hsa-miR-451	0.0005016*	0.0293436*		3.37	0.0001806*	0.012279*		3.21	17-q11.2
3 hsa-miR-143	0.0001296*	0.0108309*		2.91	0.0002111*	0.012279*		3.21	5-q33.1
4 hsa-miR-29c	3.70E-06*	0.0005411*		2.78	0.0029907*	0.1135471		2.40	1-q32.2
5 hsa-miR-29a	0.0030355*	0.1109855		2.57					7-q32.3
6 hsa-miR-485-5p	0.0092032*	0.1857617	2.56						14-q32.31
7 hsa-miR-101	0.0006336*	0.033696*		2.13	0.0461982*	0.3274393		1.62	1-p31.3
8 hsa-miR-145	0.0002656*	0.017264*		2.09	5.60E-06*	0.0009772*		3.55	5-q33.1
9 hsa-miR-29b	1.46E-05*	0.0014235*		2.04				2.94	7-q32.3
10 hsa-miR-126	0.0028002*	0.1092078		1.98	7.82E-05*	0.0079921*			9-q34.3
11 hsa-miR-193a-3p	0.0097255*	0.1872969		1.82					17-q11.2
12 hsa-miR-422a	0.042047*	0.3967338	1.74						15-q22.31
13 hsa-miR-30a	0.0059306*	0.1508435		1.70	0.0059846*	0.1305391		1.87	6-q13
14 hsa-miR-24	0.0040829*	0.1257103		1.67					9-q22.32
15 hsa-miR-10a	0.0037869*	0.1230742		1.67					17-q21.32
16 hsa-miR-27b	0.0002239*	0.0163727*		1.65					9-q22.32
17 hsa-miR-652	0.0052458*	0.1394906		1.64					X-q22.3
18 hsa-miR-130b	0.0088138*	0.1857617	1.58						22-q11.21
19 hsa-miR-23b	0.0064546*	0.1573309		1.58					9-q22.32
20 hsa-miR-126*	0.0014202*	0.063909		1.55	0.0018151*	0.0791837		2.13	9-q34.3
21 hsa-miR-30d	0.00175*	0.073125		1.51					8-q24.22

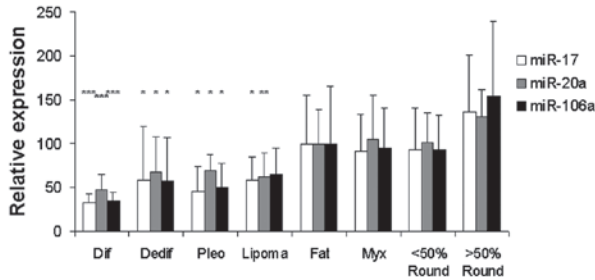
Differentially expressed miRNAs in each subtype and fat are sorted on expression fold change compared to the other samples (liposarcoma subtypes, lipomas and fat) in the discovery set (left). All miRNAs of which the expression was detected in both sample sets, and that were significantly differentially expressed ($p < 0.05$) with an expression fold change of > 1.5 in the discovery set, are listed. P-values and false discovery rate (FDR) adjusted p-values are indicated and significant p-values are signed with an asterisk. MiRNAs also found differentially expressed in the validation set are indicated (right), together with the corresponding fold change and p-values. Empty lanes represent miRNAs that did not have a significant parametric p-value ($p < 0.05$) in the validation set.



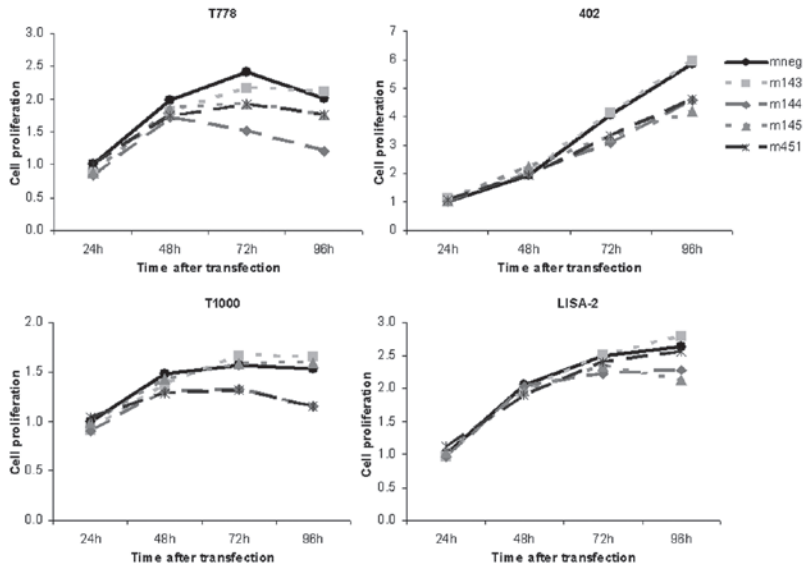
Supplemental Table 4: Deregulation of miR-144/451 and miR-143/145 cluster members in disease and biological processes.

MiRNA	Disease/biological process	Up/Down regulated	Reference
miR-144/451	Disturbed hematopoietic stem cell development	down	1
	Disturbed erythroid homeostasis	up/down	2-6
miR-144	Thyroid carcinoma	down	7
	Type 2 diabetes mellitus	up	8
miR-451	Acute Lymphoblastic Leukemia	down	9
	Non-small cell lung cancer	down	10-11
	Glioblastoma/glioma cell migration	down	12-13
	Chronic Myeloid Leukemia	down	14
	Gastric cancer	down	15
	Colorectal cancer	down	15-16
	Renal cell carcinoma	down	17
	Ovarian cancer	up	18
	Diabetic nephropathy	down	19
	Myocardial infarction	up	20
	Drug resistance	up/down	16, 21-22
miR-143/145	Migrating glioma cells	up	23
	Colorectal cancer	down	24-26
	Gastric cancer	down	27
	Lung cancer	down	28
	B-cell malignancies	down	29
	Pituitary tumors	down	30
	Vascular function	up/down	31
	Hepatocellular carcinoma	down	32
	Esophageal squamous cell carcinoma	up/down	33-34
	Esophageal adenocarcinoma	down	35
	Cervical cancer	down	36-38
	Endometriosis	up	39
	Prostate cancer	down	40-44
	Kaposi sarcoma	up	45
	Nasopharyngeal carcinoma	down	46
	Bladder cancer	down	47-50
	Smooth muscle cell differentiation	up	51
	Osteosarcoma	down	52-53
miR-143	Adipocyte differentiation	up	54
	Liposarcoma	down	55
	Pancreatic cancer	up	56
miR-145	Laryngeal squamous cell carcinoma	down	57
	Basal cell carcinoma	down	58
	Ewing's sarcoma	down	59-60
	Scleroderma	down	61
	Multiple Sclerosis	up	62
	Breast cancer	down	63-64
Ovarian cancer	down	65-67	

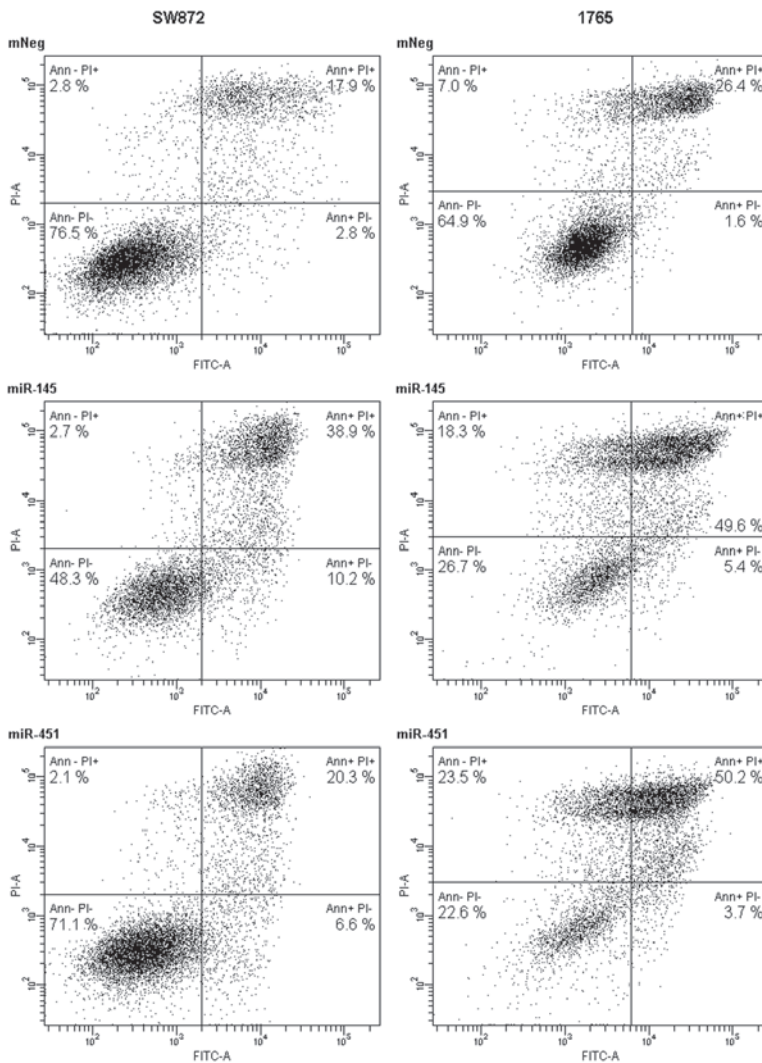
SUPPLEMENTAL FIGURES



Supplemental Figure 1: MiR-17 family members are overexpressed in high-percentage round cell tumors. MiRNA expression of miR-17, miR-20a and miR-106a was determined by microarray in the discovery set. MiRNA expression in liposarcoma subtypes are relative to the expression in fat samples (average expression in fat is set to 100). Asterisks indicate significant difference between miRNA expression in a liposarcoma subtype compared to the normal fat group as determined by two-sample t-tests: * $p < 0.05$, ** $p < 0.005$, *** $p < 0.0005$.



Supplemental Figure 2: Overexpression of miR-145, miR-451 and miR-144 affect cell proliferation. The liposarcoma cell lines LISA-2, T778, T1000 and MLS 402-91 were cultured in RPMI 1640/Glutamax (Invitrogen) supplemented with 10% fetal bovine serum (LISA-2; MLS 402-91) or 20% fetal bovine serum (T778, T1000) at 37°C, 5% CO₂. The cell lines were transfected using MiRIDIAN microRNA mimics (Thermo Scientific) of hsa-miR-143, hsa-miR-145, hsa-miR-144 and hsa-miR-451 and miRIDIAN microRNA Mimic Negative Control #1 (Thermo Scientific) in a final concentration of 50 nM using DharmaFECT1 transfection reagent (Thermo Scientific) 24h after cell seeding, according to the manufacturer's protocol. Graphs indicate cell growth at 24h, 48h, 72h and 96h post-transfection, relative to the negative control at 24h, which is set at 1. The LISA-2 cell line derived from a poorly differentiated liposarcoma was obtained from Dr. Möller and Dr. Brüderlein, Institute of Pathology, University of Ulm, Ulm, Germany. The cell lines T778 and T1000 were established from recurrent well differentiated liposarcomas, and were obtained from Dr. Pedeutour, Le Centre Hospitalier Universitaire de Nice, Nice, France. The cell line MLS 402-91 was derived from a myxoid liposarcoma and obtained from Dr. P. Åman, Sahlgrenska Cancer Center, Goteborg University, Gothenburg, Sweden. Please note that the characteristics of LISA-2, T778 and T-1000 were described by Stratford, E.W. et al. (2012) Characterization of liposarcoma cell lines for preclinical and biological studies. Sarcoma doi: 10.1155/2012/148614




Supplemental Figure 3: MiR-145 and miR-451 induce cell death in liposarcoma cell lines. Increased apoptosis in liposarcoma cell lines SW872 and MLS 1765-92, 72h post-transfection with miR-145 and miR-451 mimics compared to the negative control (mNeg, scrambled mimic). Apoptosis levels, measured by Annexin V / PI stainings, were detected by FACS. X-axes indicate FITC-Annexin V levels, y-axes indicate PI levels. Viable cells are presented by the Ann-/PI- fraction, early apoptotic cells by the Ann+/PI- fraction, late apoptotic cells by the Ann+/PI+ fraction and dead cells in the Ann-/PI+ fraction.



SUPPLEMENTAL REFERENCES

1. Papapetrou EP, Korkola JE, Sadelain M. A genetic strategy for single and combinatorial analysis of miRNA function in mammalian hematopoietic stem cells. *Stem Cells*. 2010 Feb;28(2):287-96.
2. Rasmussen KD, Simmini S, Abreu-Goodger C, Bartonicek N, Di Giacomo M, Bilbao-Cortes D, et al. The miR-144/451 locus is required for erythroid homeostasis. *J Exp Med*. 2010 Jul 5;207(7):1351-8.
3. Sangokoya C, Telen MJ, Chi JT. microRNA miR-144 modulates oxidative stress tolerance and associates with anemia severity in sickle cell disease. *Blood*. 2010 Nov 18;116(20):4338-48.
4. Dore LC, Amigo JD, Dos Santos CO, Zhang Z, Gai X, Tobias JW, et al. A GATA-1-regulated microRNA locus essential for erythropoiesis. *Proc Natl Acad Sci U S A*. 2008 Mar 4;105(9):3333-8.
5. Masaki S, Ohtsuka R, Abe Y, Muta K, Umemura T. Expression patterns of microRNAs 155 and 451 during normal human erythropoiesis. *Biochem Biophys Res Commun*. 2007 Dec 21;364(3):509-14.
6. Patrick DM, Zhang CC, Tao Y, Yao H, Qi X, Schwartz RJ, et al. Defective erythroid differentiation in miR-451 mutant mice mediated by 14-3-3zeta. *Genes Dev*. 2010 Aug 1;24(15):1614-9.
7. Rossing M, Borup R, Henao R, Winther O, Vikesaa J, Niazi O, et al. Down-regulation of microRNAs controlling tumourigenic factors in follicular thyroid carcinoma. *J Mol Endocrinol*. 2012 Feb;48(1):11-23.
8. Karolina DS, Armugam A, Tavintharan S, Wong MT, Lim SC, Sum CF, et al. MicroRNA 144 impairs insulin signaling by inhibiting the expression of insulin receptor substrate 1 in type 2 diabetes mellitus. *PLoS One*. 2011;6(8):e22839.
9. Li X, Sanda T, Look AT, Novina CD, von Boehmer H. Repression of tumor suppressor miR-451 is essential for NOTCH1-induced oncogenesis in T-ALL. *J Exp Med*. 2011 Apr 11;208(4):663-75.
10. Wang XC, Tian LL, Jiang XY, Wang YY, Li DG, She Y, et al. The expression and function of miRNA-451 in non-small cell lung cancer. *Cancer Lett*. 2011 Dec 8;311(2):203-9.
11. Wang R, Wang ZX, Yang JS, Pan X, De W, Chen LB. MicroRNA-451 functions as a tumor suppressor in human non-small cell lung cancer by targeting ras-related protein 14 (RAB14). *Oncogene*. 2011 Jun 9;30(23):2644-58.
12. Nan Y, Han L, Zhang A, Wang G, Jia Z, Yang Y, et al. MiRNA-451 plays a role as tumor suppressor in human glioma cells. *Brain Res*. 2010 Nov 4;1359:14-21.
13. Godlewski J, Nowicki MO, Bronisz A, Nuovo G, Palatini J, De Lay M, et al. MicroRNA-451 regulates LKB1/AMPK signaling and allows adaptation to metabolic stress in glioma cells. *Mol Cell*. 2010 Mar 12;37(5):620-32.
14. Lopotova T, Zackova M, Klamova H, Moravcova J. MicroRNA-451 in chronic myeloid leukemia: miR-451-BCR-ABL regulatory loop? *Leuk Res*. 2011 Jul;35(7):974-7.
15. Bandres E, Bitarte N, Arias F, Agorreta J, Fortes P, Agirre X, et al. microRNA-451 regulates macrophage migration inhibitory factor production and proliferation of gastrointestinal cancer cells. *Clin Cancer Res*. 2009 Apr 1;15(7):2281-90.
16. Bitarte N, Bandres E, Boni V, Zarate R, Rodriguez J, Gonzalez-Huarriz M, et al. MicroRNA-451 is involved in the self-renewal, tumorigenicity, and chemoresistance of colorectal cancer stem cells. *Stem Cells*. 2011 Nov;29(11):1661-71.
17. Redova M, Poprach A, Nekvindova J, Iliev R, Radova L, Lakomy R, et al. Circulating miR-378 and miR-451 in serum are potential biomarkers for renal cell carcinoma. *J Transl Med*. 2012;10:55.
18. Eitan R, Kushnir M, Lithwick-Yanai G, David MB, Hoshen M, Glezerman M, et al. Tumor microRNA expression patterns associated with resistance to platinum based chemotherapy and survival in ovarian cancer patients. *Gynecol Oncol*. 2009 Aug;114(2):253-9.
19. Zhang Z, Luo X, Ding S, Chen J, Chen T, Chen X, et al. MicroRNA-451 regulates p38 MAPK signaling by targeting of Ywhaz and suppresses the mesangial hypertrophy in early diabetic nephropathy. *FEBS Lett*. 2012 Jan 2;586(1):20-6.
20. Bostjancic E, Zidar N, Glavac D. MicroRNA microarray expression profiling in human myocardial infarction. *Dis Markers*. 2009;27(6):255-68.
21. Kovalchuk O, Filkowski J, Meservy J, Ilnytskyy Y, Tryndyak VP, Chekhun VF, et al. Involvement of microRNA-451 in resistance of the MCF-7 breast cancer cells to chemotherapeutic drug doxorubicin. *Mol Cancer Ther*. 2008 Jul;7(7):2152-9.
22. Zhu H, Wu H, Liu X, Evans BR, Medina DJ, Liu CG, et al. Role of MicroRNA miR-27a and miR-451 in the regulation of MDR1/P-glycoprotein expression in human cancer cells. *Biochem Pharmacol*. 2008 Sep 1;76(5):582-8.

- 
23. Koo S, Martin GS, Schulz KJ, Ronck M, Toussaint LG. Serial selection for invasiveness increases expression of miR-143/miR-145 in glioblastoma cell lines. *BMC Cancer*. 2012;12:143.
 24. Michael MZ, SM OC, van Holst Pellekaan NG, Young GP, James RJ. Reduced accumulation of specific microRNAs in colorectal neoplasia. *Mol Cancer Res*. 2003 Oct;1(12):882-91.
 25. Slaby O, Svoboda M, Fabian P, Smerdova T, Knoflickova D, Bednarikova M, et al. Altered expression of miR-21, miR-31, miR-143 and miR-145 is related to clinicopathologic features of colorectal cancer. *Oncology*. 2007;72(5-6):397-402.
 26. Motoyama K, Inoue H, Takatsuno Y, Tanaka F, Mimori K, Uetake H, et al. Over- and under-expressed microRNAs in human colorectal cancer. *Int J Oncol*. 2009 Apr;34(4):1069-75.
 27. Takagi T, Iio A, Nakagawa Y, Naoe T, Tanigawa N, Akao Y. Decreased expression of microRNA-143 and -145 in human gastric cancers. *Oncology*. 2009;77(1):12-21.
 28. Yanaihara N, Caplen N, Bowman E, Seike M, Kumamoto K, Yi M, et al. Unique microRNA molecular profiles in lung cancer diagnosis and prognosis. *Cancer Cell*. 2006 Mar;9(3):189-98.
 29. Akao Y, Nakagawa Y, Kitade Y, Kinoshita T, Naoe T. Downregulation of microRNAs-143 and -145 in B-cell malignancies. *Cancer Sci*. 2007 Dec;98(12):1914-20.
 30. Amaral FC, Torres N, Saggioro F, Neder L, Machado HR, Silva WA, Jr., et al. MicroRNAs differentially expressed in ACTH-secreting pituitary tumors. *J Clin Endocrinol Metab*. 2009 Jan;94(1):320-3.
 31. Norata GD, Pinna C, Zappella F, Elia L, Sala A, Condorelli G, et al. MicroRNA 143-145 deficiency impairs vascular function. *Int J Immunopathol Pharmacol*. 2012 Apr-Jun;25(2):467-74.
 32. Gramantieri L, Ferracin M, Fornari F, Veronese A, Sabbioni S, Liu CG, et al. Cyclin G1 is a target of miR-122a, a microRNA frequently down-regulated in human hepatocellular carcinoma. *Cancer Res*. 2007 Jul 1;67(13):6092-9.
 33. Akagi I, Miyashita M, Ishibashi O, Mishima T, Kikuchi K, Makino H, et al. Relationship between altered expression levels of MIR21, MIR143, MIR145, and MIR205 and clinicopathologic features of esophageal squamous cell carcinoma. *Dis Esophagus*. 2011 Sep;24(7):523-30.
 34. Wu BL, Xu LY, Du ZP, Liao LD, Zhang HF, Huang Q, et al. MiRNA profile in esophageal squamous cell carcinoma: downregulation of miR-143 and miR-145. *World J Gastroenterol*. 2011 Jan 7;17(1):79-88.
 35. Wijnhoven BP, Hussey DJ, Watson DJ, Tsykin A, Smith CM, Michael MZ. MicroRNA profiling of Barrett's oesophagus and oesophageal adenocarcinoma. *Br J Surg*. 2010 Jun;97(6):853-61.
 36. Liu L, Yu X, Guo X, Tian Z, Su M, Long Y, et al. miR-143 is downregulated in cervical cancer and promotes apoptosis and inhibits tumor formation by targeting Bcl-2. *Mol Med Report*. 2012 Mar;5(3):753-60.
 37. Lui WO, Pourmand N, Patterson BK, Fire A. Patterns of known and novel small RNAs in human cervical cancer. *Cancer Res*. 2007 Jul 1;67(13):6031-43.
 38. Wang X, Tang S, Le SY, Lu R, Rader JS, Meyers C, et al. Aberrant expression of oncogenic and tumor-suppressive microRNAs in cervical cancer is required for cancer cell growth. *PLoS One*. 2008;3(7):e2557.
 39. Ohlsson Teague EM, Van der Hoek KH, Van der Hoek MB, Perry N, Wagaarachchi P, Robertson SA, et al. MicroRNA-regulated pathways associated with endometriosis. *Mol Endocrinol*. 2009 Feb;23(2):265-75.
 40. Clape C, Fritz V, Henriquet C, Apparailly F, Fernandez PL, Iborra F, et al. miR-143 interferes with ERK5 signaling, and abrogates prostate cancer progression in mice. *PLoS One*. 2009;4(10):e7542.
 41. Szczyrba J, Loprich E, Wach S, Jung V, Unteregger G, Barth S, et al. The microRNA profile of prostate carcinoma obtained by deep sequencing. *Mol Cancer Res*. 2010 Apr;8(4):529-38.
 42. Wach S, Nolte E, Szczyrba J, Stohr R, Hartmann A, Orntoft T, et al. MicroRNA profiles of prostate carcinoma detected by multiplatform microRNA screening. *Int J Cancer*. 2012 Feb 1;130(3):611-21.
 43. Ozen M, Creighton CJ, Ozdemir M, Ittmann M. Widespread deregulation of microRNA expression in human prostate cancer. *Oncogene*. 2008 Mar 13;27(12):1788-93.
 44. Schaefer A, Jung M, Mollenkopf HJ, Wagner I, Stephan C, Jentzmik F, et al. Diagnostic and prognostic implications of microRNA profiling in prostate carcinoma. *Int J Cancer*. 2010 Mar 1;126(5):1166-76.
 45. O'Hara AJ, Wang L, Dezube BJ, Harrington WJ, Jr., Damania B, Dittmer DP. Tumor suppressor microRNAs are underrepresented in primary effusion lymphoma and Kaposi sarcoma. *Blood*. 2009 Jun 4;113(23):5938-41.
 46. Chen HC, Chen GH, Chen YH, Liao WL, Liu CY, Chang KP, et al. MicroRNA deregulation and pathway alterations in nasopharyngeal carcinoma. *Br J Cancer*. 2009 Mar 24;100(6):1002-11.

47. Lin T, Dong W, Huang J, Pan Q, Fan X, Zhang C, et al. MicroRNA-143 as a tumor suppressor for bladder cancer. *J Urol*. 2009 Mar;181(3):1372-80.
48. Han Y, Chen J, Zhao X, Liang C, Wang Y, Sun L, et al. MicroRNA expression signatures of bladder cancer revealed by deep sequencing. *PLoS One*. 2011;6(3):e18286.
49. Villadsen SB, Bramsen JB, Ostenfeld MS, Wiklund ED, Frstrup N, Gao S, et al. The miR-143/-145 cluster regulates plasminogen activator inhibitor-1 in bladder cancer. *Br J Cancer*. 2012 Jan 17;106(2):366-74.
50. Ichimi T, Enokida H, Okuno Y, Kunimoto R, Chiyomaru T, Kawamoto K, et al. Identification of novel microRNA targets based on microRNA signatures in bladder cancer. *Int J Cancer*. 2009 Jul 15;125(2):345-52.
51. Cordes KR, Sheehy NT, White MP, Berry EC, Morton SU, Muth AN, et al. miR-145 and miR-143 regulate smooth muscle cell fate and plasticity. *Nature*. 2009 Aug 6;460(7256):705-10.
52. Zhang H, Cai X, Wang Y, Tang H, Tong D, Ji F. microRNA-143, down-regulated in osteosarcoma, promotes apoptosis and suppresses tumorigenicity by targeting Bcl-2. *Oncol Rep*. 2010 Nov;24(5):1363-9.
53. Fan L, Wu Q, Xing X, Wei Y, Shao Z. MicroRNA-145 targets vascular endothelial growth factor and inhibits invasion and metastasis of osteosarcoma cells. *Acta Biochim Biophys Sin (Shanghai)*. 2012 May;44(5):407-14.
54. Esau C, Kang X, Peralta E, Hanson E, Marcusson EG, Ravichandran LV, et al. MicroRNA-143 regulates adipocyte differentiation. *J Biol Chem*. 2004 Dec 10;279(50):52361-5.
55. Ugras S, Brill E, Jacobsen A, Hafner M, Socci ND, Decarolis PL, et al. Small RNA sequencing and functional characterization reveals MicroRNA-143 tumor suppressor activity in liposarcoma. *Cancer Res*. 2011 Sep 1;71(17):5659-69.
56. Tavano F, di Mola FF, Piepoli A, Panza A, Copetti M, Burbaci FP, et al. Changes in miR-143 and miR-21 Expression and Clinicopathological Correlations in Pancreatic Cancers. *Pancreas*. 2012 Jul 25.
57. Cao P, Zhou L, Zhang J, Zheng F, Wang H, Ma D, et al. Comprehensive expression profiling of microRNAs in laryngeal squamous cell carcinoma. *Head Neck*. 2012 May 18.
58. Sand M, Skrygan M, Sand D, Georgas D, Hahn SA, Gambichler T, et al. Expression of microRNAs in basal cell carcinoma. *Br J Dermatol*. 2012 Apr 27.
59. Ban J, Jug G, Mestdagh P, Schwentner R, Kauer M, Aryee DN, et al. Hsa-mir-145 is the top EWS-FLI1-repressed microRNA involved in a positive feedback loop in Ewing's sarcoma. *Oncogene*. 2011 May 5;30(18):2173-80.
60. Mosakhani N, Guled M, Leen G, Calabuig-Farinas S, Niini T, Machado I, et al. An integrated analysis of miRNA and gene copy numbers in xenografts of Ewing's sarcoma. *J Exp Clin Cancer Res*. 2012;31:24.
61. Zhu H, Li Y, Qu S, Luo H, Zhou Y, Wang Y, et al. MicroRNA expression abnormalities in limited cutaneous scleroderma and diffuse cutaneous scleroderma. *J Clin Immunol*. 2012 Jun;32(3):514-22.
62. Keller A, Leidinger P, Lange J, Borries A, Schroers H, Scheffler M, et al. Multiple sclerosis: microRNA expression profiles accurately differentiate patients with relapsing-remitting disease from healthy controls. *PLoS One*. 2009;4(10):e7440.
63. Iorio MV, Ferracin M, Liu CG, Veronese A, Spizzo R, Sabbioni S, et al. MicroRNA gene expression deregulation in human breast cancer. *Cancer Res*. 2005 Aug 15;65(16):7065-70.
64. Sempere LF, Christensen M, Silahtaroglu A, Bak M, Heath CV, Schwartz G, et al. Altered MicroRNA expression confined to specific epithelial cell subpopulations in breast cancer. *Cancer Res*. 2007 Dec 15;67(24):11612-20.
65. Iorio MV, Visone R, Di Leva G, Donati V, Petrocca F, Casalini P, et al. MicroRNA signatures in human ovarian cancer. *Cancer Res*. 2007 Sep 15;67(18):8699-707.
66. Nam EJ, Yoon H, Kim SW, Kim H, Kim YT, Kim JH, et al. MicroRNA expression profiles in serous ovarian carcinoma. *Clin Cancer Res*. 2008 May 1;14(9):2690-5.
67. Vaksman O, Stavnes HT, Kaern J, Trope CG, Davidson B, Reich R. miRNA profiling along tumour progression in ovarian carcinoma. *J Cell Mol Med*. 2011 Jul;15(7):1593-602.



Chapter 3

MICRORNAS IN MYXOID/ROUND CELL LIPOSARCOMAS: FUS-CHOP REGULATED MIR-497 AND MIR-30A TARGET THE INSULIN-LIKE GROWTH FACTOR 1 RECEPTOR PATHWAY



Caroline M.M. Gits, Patricia F. van Kuijk, Wilfred F. van IJcken, Jean-Michel Coindre, Frédéric Chibon,
Ron H.J. Mathijssen, Michael A. den Bakker, Jaap Verweij, Stefan Sleijfer, Erik A.C. Wiemer

Manuscript in preparation

ABSTRACT

Myxoid/round cell liposarcomas (MRCLS) are characterized by a t(12;16)(q13;p11) translocation in 90% of the cases, which gives rise to a *FUS-CHOP* fusion gene. The resulting fusion oncoprotein acts as an abnormal transcription factor, inducing distinct transcriptional programs. However, not much is known about the regulation of microRNA (miRNA) expression in MRCLS and about the role of *FUS-CHOP* herein. We examined miRNA expression in MRCLS and normal fat by microarrays. Hierarchical clustering gave rise to a very good discrimination of the groups. The miR-23a~27a~24-2 and miR-23b~27b~24-1 cluster members were all significantly downregulated in MRCLS, which was validated by qPCR in an extended sample set. Overexpression of miR-24 mimics induced doxorubicin resistance in two myxoid liposarcoma cell lines (MLS 402-91 and MLS 1765-92), while miR-24 inhibitors sensitized a liposarcoma (SW872) and a rhabdomyosarcoma (RH30) cell line to doxorubicin treatment. To identify miRNAs controlled by the fusion gene, *FUS-CHOP* levels were modulated in four sarcoma cell lines. MiR-497, miR-30a and miR-34b expression was downregulated upon *FUS-CHOP* overexpression, and upregulated upon *FUS-CHOP* knockdown. Accordingly, their expression was significantly lower in MRCLS compared to normal fat, as determined by qPCR analysis. Remarkably, miR-497 and miR-30a share many predicted target genes of the insulin(-like) growth factor pathway. Overexpression of miR-497 and miR-30a considerably downregulated protein expression of IGF1R (insulin-like growth factor receptor) and its substrates IRS1 and IRS2. Luciferase reporter constructs containing wildtype and mutated 3'UTR fragments of these genes were used to demonstrate direct regulation of *IRS1* by miR-497, *IRS2* by miR-30a, and *IGF1R* by both miRNAs. MiR-497 and miR-30a overexpression had little effect on cell proliferation, but significantly sensitized myxoid liposarcoma cell lines to doxorubicin treatment, which is possibly mediated via the IGF1R pathway. Therefore, combination therapy of miR-497 and miR-30a with chemotherapeutic or targeted agents in MRCLS should be further explored.



INTRODUCTION

Liposarcomas represent the most common type of soft tissue sarcoma.¹ The major histological subtypes (well differentiated, dedifferentiated, myxoid/round cell, pleomorphic liposarcoma) are morphologically and genetically distinct.² The myxoid subtype comprises approximately 15% of the liposarcomas. Within these myxoid liposarcomas, some areas transform to a high grade round cell component, which is associated with a significantly worse prognosis.³ Although surgery and adjuvant radiotherapy are standard care for non-metastasized liposarcomas, patients with metastasized (~30%) myxoid/round cell liposarcomas (MRCLS) receive doxorubicin chemotherapy. Compared to other liposarcoma subtypes, MRCLS are particularly sensitive to radio- and chemotherapy.⁴⁻⁵ Recently, the Ras-Raf-MAPK and the PI3K-AKT pathways, activated by receptor tyrosine kinases such as RET and IGF1R, were implicated in MRCLS tumorigenesis and associated with poor prognosis.⁶⁻⁷ These genes could provide novel targets for MRCLS treatment.

A unique feature of MRCLS is that more than 90% is characterized by a t(12;16)(q13;p11) translocation, which gives rise to a *FUS-CHOP* fusion gene.⁸⁻⁹ Also t(12,22)(q13;q12) translocations have been described in which *CHOP* fuses with *EWS*, a gene closely related to *FUS*.¹⁰⁻¹¹ Both *FUS* (Fused in Sarcoma; also known as TLS (Translocated in Liposarcoma)) and *EWS* (Ewing's Sarcoma) are RNA-binding proteins which are associated with transcriptional regulation.¹²⁻¹³ *CHOP* (CCAAT/enhancer-binding protein (C/EBP) homologous protein, also known as DDIT3 (DNA-damage-inducible transcript 3)) is a transcription factor which is induced in response to stress and acts as an inhibitor of adipocytic differentiation.¹⁴ Chromosomal translocations in MRCLS are likely the primary oncogenic event. The resulting fusion oncoproteins function as abnormal transcription factors inducing distinct transcriptional programs.¹⁵⁻¹⁷ This may also result in miRNA deregulation, as indeed, miR-486 was found to be regulated by *FUS-CHOP*.¹⁸ Moreover, we identified distinct miRNA expression profiles in MRCLS compared to the other liposarcoma subtypes and normal fat, which may be related to expression of the *FUS-CHOP* fusion protein (see chapter 2 of this thesis).

MiRNAs are small, non-protein coding RNA molecules which target (near) complementary sites in 3'UTRs of mRNAs, thereby inhibiting their translation into functional proteins. MiRNAs function in many important processes such as differentiation, proliferation, apoptosis and tissue specialization. They are often deregulated in cancer and some miRNAs function as oncogenes or tumor suppressors. One gene can be targeted by multiple miRNAs and a single miRNA can target many genes, which underscores the complexity and widespread effects of miRNA function.

In this study we focus on deregulated miRNAs in MRCLS compared to normal fat. Furthermore, we examined which miRNAs are regulated by the *FUS-CHOP* fusion protein. Subsequently, we determined the involvement of MRCLS specific miRNAs in chemotherapy sensitivity and in the regulation of the IGF1R-pathway.



MATERIALS AND METHODS

Tumor and control tissue samples

Human frozen liposarcoma and control tissue samples were obtained from the Erasmus MC Tissue Bank: 9 myxoid, 5 myxoid with a round cell component (round-myx) and 8 normal fat samples. For validation purposes additional frozen tissue samples were obtained: 13 myxoid, 6 myxoid with a round cell component and 12 fat samples provided by the Erasmus MC Tissue Bank and Institut Bergonié, Bordeaux. All samples were examined by expert soft tissue pathologists to verify the liposarcoma subtype classification. The percentage of tumor cells in the liposarcoma tissues was estimated at >90%. The study was approved by the Medical Ethical Review Board of the Erasmus University Medical Center.

Cell culture

The liposarcoma cell line SW872, fibrosarcoma cell line SW684 (ATCC, Rockville, MD, USA), rhabdomyosarcoma cell line RH30 (obtained from Dr. M. Debiec-Rychter, KU Leuven, Leuven, Belgium) and the myxoid liposarcoma cell lines MLS 402-91 and MLS 1765-92 (obtained from dr. P. Åman, Sahlgrenska Cancer Center, Goteborg University, Gothenburg, Sweden) were cultured in RPMI 1640/GlutaMAX (Invitrogen) supplemented with 10% fetal bovine serum, at 37 °C, 5% CO₂.

MiRNA mimic and inhibitor transfections

MIRIDIAN microRNA mimics (Thermo Scientific) of hsa-miR-24, hsa-miR-497 and hsa-miR-30a and miRIDIAN microRNA Mimic Negative Control #1 (Thermo Scientific) were transfected in a final concentration of 50 nM using DharmaFECT1 transfection reagent (Thermo Scientific) 24h after cell seeding, according to the manufacturer's protocol. For both cell lines transfection efficiency was optimized to >95% using fluorescent mimics (Thermo Scientific).

MiRCURY LNA™ microRNA inhibitor of miR-24 and miRCURY LNA™ microRNA Inhibitor Negative Control A (Exiqon) were transfected in a final concentration of 30 nM using DharmaFECT1 transfection reagent (Thermo Scientific) 24h after cell seeding, according to the manufacturer's protocol.

RNA isolation

Total RNA was isolated from frozen tissues and cell line pellets using RNeasy (Qiagen) according to the manufacturer's recommendation. The RNA concentration and quality were determined on a Nanodrop-1000 (Nanodrop Technologies).

MiRNA microarray

MiRNA profiling was performed essentially as previously described.¹⁹ In brief, 1 µg total RNA was fluorescently labeled with Cy3 using the ULS™ aRNA Labeling Kit (Kreatech Diagnostics). Labeled

RNA was hybridized with locked nucleic acid (LNA™) modified oligonucleotide capture probes (Exiqon) spotted in duplicate on Nexterion E slides. The capture probe set (based on miRBase version 10, annotation version 13) contains 1344 probes of which 725 are capable of detecting human miRNAs. Hybridized slides were scanned and median spot intensity was determined using ImaGene software (BioDiscovery Inc.). After background subtraction, expression values were quantile normalized using R software, bad spots were deleted, and duplicate spots were averaged. For each expression value, the ratio to the geometric mean of the miRNA was log2 transformed. These values were used to determine differentially expressed miRNAs. Hierarchical clustering analyses were performed in Spotfire. The cluster trees were generated using cosine correlation for similarity measures and UPGMA clustering method.

miRNA qPCR

The expression of selected miRNAs was verified using TaqMan® MicroRNA Assays (Applied Biosystems) of miR-29a, miR-485-5p, miR-23a, miR-23b, miR-24, miR-27a, miR-27b, miR-497, miR-30a and miR-34b. In brief, total RNA (50ng) was reverse transcribed using specific miRNA primers and the TaqMan® MicroRNA Reverse Transcription Kit (Applied Biosystems). The resulting cDNA was used as input in a quantitative real-time PCR (qPCR) using the miRNA specific primer/probe mix together with the TaqMan® Universal PCR Master Mix No AmpErase® UNG (Applied Biosystems) according to manufacturer's protocol. qPCR data were analyzed with SDS software (version 2.4, Applied Biosystems). RNU43 was used as housekeeper allowing normalization using the comparative C_T -method.²⁰

SRB assay

Cell density was examined by a sulforhodamine B (SRB) assay at 24h, 48h, 72h and 96h post-transfection.²¹ In short: cells were fixed by 10% TCA in PBS, washed, stained by 0.4% SRB in 1% acetic acid for 15 min, washed in 1% acetic acid and dried. Color was released from the cells by 10 mM Tris-Base, after which the $A_{540\text{ nm}}$ was measured using a spectrophotometer.


Doxorubicin in vitro cytotoxicity assay

Doxorubicin was added to the cells in a final concentration of 50 ng/ml, 24h after transfection of mimics/inhibitors. After two days of continuous doxorubicin exposure cells were fixed, stained and analyzed by the SRB assay.

Cloning

The *FUS-CHOP* insert from pMSCV puro-FUS-CHOP v5 (obtained from dr Stamenkovic, University of Lausanne, Lausanne, Switzerland) was subcloned in a pcDNA3.1+ vector (Invitrogen) using *BglIII* (Gibco) and *KspAI* (Fermentas) restriction sites. The resulting expression construct, pcDNA3/FUS-CHOP, contained a neomycin selection marker.





Two self-designed shRNA oligo duplexes targeted against the *FUS-CHOP* specific exon 2 of *CHOP* (oligo sequences Supplemental Table 1A), with *AgeI* and *EcoRI* overhang, were cloned in a pLKO.1 vector (SCH001, Sigma-Aldrich) restricted with *AgeI* and *EcoRI*. The resulting constructs, pLKO.1/shRNA FUS-CHOP 1 and pLKO.1/shRNA FUS-CHOP 2, contained a puromycin selection marker. Fragments of the 3'UTR of *IRS1* (IRS1-1: 1175 bp fragment), *IRS2* (IRS2-1: 2428 bp fragment) and *IGF1R* (the front part: IGF1R-fr: 2377 bp fragment, the back part: IGF1R-ba: 1658 bp fragment) were PCR amplified from human genomic DNA (Promega) introducing a *XhoI* (5'-end) and a *NotI* site (3'-end). The PCR products were cloned in PCR[®]-Blunt (Invitrogen), followed by a *XhoI* and *NotI* restriction and ligation in the psiCHECK[™]-2 vector (Promega) behind a *Renilla* luciferase gene. The psiCHECK[™]-2 vector also contains a firefly luciferase gene, which was used for normalization. The resulting constructs are psiCHECK2/IRS1, psiCHECK2/IRS2, psiCHECK2/IGF1R-fr and psiCHECK2/IGF1R-ba. Site directed mutagenesis (QuickChange II XL, site directed mutagenesis kit, Agilent Technologies, Amsterdam, The Netherlands) was performed to mutate miR-497 and miR-30a target sites in the cloned 3'UTR fragments of the *IRS1*, *IRS2* and *IGF1R* constructs (Supplemental Figure 1). Primer sequences used for cloning and mutagenesis are listed in Supplemental Table 1B and 1C.

Construct transfections

pcDNA3/FUS-CHOP and pLKO.1/shRNA FUS-CHOP and corresponding empty vector control constructs were transfected using polyethylenimine 'MAX' (PEI MAX, Polysciences, Inc.) in a final concentration of 1.5 µg/ml DNA and 0.15 nmol/ml PEI MAX. Transfection medium was replaced 24h post-transfection. The cells transfected with pcDNA3 and pLKO.1 constructs were selected for stable expression of the constructs by culturing them in 500-750 µg/ml geneticin (G418 Sulfate) or 4 µg/ml puromycin (both Invitrogen) containing medium respectively, starting 48h post-transfection.

Protein extraction

Cells were harvested in MCB lysis buffer (50mM Tris-HCl pH 7.5, 50mM NaCl, 10% glycerol, 1% NP-40, 0.5% Na-deoxycholate, 20mM NaF) supplemented with a cocktail of protease and phosphatase inhibitors. Lysates were thoroughly vortexed and further lysed by two subsequent freeze-thaw cycles using liquid nitrogen. Cell debris was spun down and protein concentration was determined by a Bradford assay (BioRad).

Western blotting

Fifteen or twenty µg of total protein was subjected to SDS-PAGE. Proteins were transferred to a PVDF membrane followed by blocking of the membrane in 5% non-fat dry milk (NFDM) in PBS-Tween (PBS, 0.05% Tween'20), 5% NFDM in TBS-Tween (TBS, 0.1% Tween'20) or 5% BSA in TBS-Tween, according to recommendations for the primary antibody. Primary and secondary

antibody incubations were carried out in the same buffer using anti-CHOP (L63F7, #2895, mouse monoclonal, 1:1000, Cell Signaling Technology, Inc.), anti-IRS1 (#2382, rabbit polyclonal, 1:1000, Cell Signaling Technology, Inc.), anti-IRS2 (L1326, #3089, rabbit polyclonal, 1:1000, Cell Signaling Technology, Inc.), anti-IGF1R β (C-20, sc-713, rabbit polyclonal, 1:500, Santa Cruz Biotechnology, Inc.) and anti- β -Actin (AC-15, mouse monoclonal, 1:5000, Sigma-Aldrich) as a loading control. As secondary antibody HRP-conjugated goat-anti-mouse (1:10000, Santa Cruz Biotechnology) or goat-anti-rabbit (1:10000, Jackson ImmunoResearch) antibodies were used. Antibody incubations were followed by enhanced chemoluminescence (Supersignal West Pico Chemiluminescent Substrate, Thermo Scientific) and visualized on film (Amersham Hyperfilm ECL, GE Healthcare).

qPCR analysis of mRNAs

Total RNA (1 μ g) was reverse transcribed using the TaqMan[®] Reverse Transcription Reagents (Applied Biosystems) according to the manufacturer's protocol. The resulting cDNA was used to perform qPCR using the primer/probe mix from the TaqMan[®] Gene Expression Assays of human *IRS1*, *IRS2* and *IGF1R* (with exon spanning probes) and TaqMan[®] Universal PCR Master Mix using the 7500 Fast Real-Time PCR system (all Applied Biosystems) according to the manufacturer's recommendations. Two housekeepers (*GAPDH*, *HPRT*) were analyzed for normalization purposes using the comparative CT-method.²⁰ qPCR data was analyzed with SDS software (Applied Biosystems).

Luciferase assay

PsiCHECK[™]-2 constructs were transfected using Fugene HD transfection reagent (Promega) 24h after cell seeding, according to recommendations by the manufacturer. The next day, cells were transfected with hsa-miR-497 or hsa-miR-30a miRIDIAN mimics, or miRIDIAN microRNA Mimic Negative Control #1 (Thermo Scientific) in a final concentration of 50nM using DharmaFECT1 transfection reagent (Thermo Scientific). After 48h, cells were washed with PBS and lysed by Passive Lysis Buffer (Dual Luciferase[®] Reporter Assay System, Promega) for 30min on a shaker platform. Lysates were transferred to white 96-wells microplates. Luciferase Assay Reagent II (Dual Luciferase[®] Reporter Assay System, Promega) was added, immediately followed by quantitation of the firefly luciferase activity on a luminometer (Aspekt Fluoroskan). Subsequently, Stop & Glo[®] Reagent (Dual Luciferase[®] Reporter Assay System, Promega) was added to the mixture, immediately followed by quantitation of the *Renilla* luciferase activity. Relative luciferase signals of duplicates were averaged, after which average and standard deviations (n=3) were calculated.

Statistics

A two-sample t-test with random variance model (BRB-Array Tools, Microsoft-Excel plug-in) was used for identifying differentially expressed miRNAs in the microarray data. The p-value, the False Discovery Rate (FDR)-adjusted p-value, and the expression fold change are indicated in



the tables. A student's t-test was used to determine the significance of differential miRNA/gene expression determined by qPCR, of differences in doxorubicin sensitivity, and of differences in luciferase activity.

RESULTS

Myxoid/round cell liposarcomas have a distinct miRNA expression profile

To determine the miRNA expression profile of MRCLS, 9 myxoid, 5 myxoid with a round cell component (round-myx) and 8 normal fat samples were analyzed on miRNA microarrays which contain LNA™ modified oligonucleotide capture probes capable of detecting 725 human miRNAs. An unsupervised clustering already indicates that MRCLS have a miRNA expression profile clearly distinct from normal fat tissue (Figure 1A). Only one myxoid sample was found to group with the fat tissues and one fat samples clusters in the MRCLS branch. The myxoid sample that misclustered was derived from the only patient that received neo-adjuvant radiotherapy, which could be responsible for the aberrant miRNA profile. When the most differentially expressed miRNAs between the MRCLS and the fat samples ($p \leq 0.03$, fold change ≥ 1.7) were used in a supervised hierarchical clustering the control fat samples and MRCLS were completely distinguished (Figure 1B). Sixteen miRNAs were predominantly upregulated in MRCLS, while the other 34 miRNAs were downregulated in this liposarcoma subtype in comparison to normal fat (Supplemental Table 2). The top-15 of the most significant up- or downregulated miRNAs are listed in Table 1, with miR-485-5p being the most upregulated miRNA in the MRCLS. However, this could not be validated by qPCR in an extended set MRCLS and fat samples (Figure 2A). Conversely, the miR-29 family members (miR-29a, miR-29b, miR-29c) were among the most downregulated miRNAs in the MRCLS. qPCR analysis indeed showed a significant (>10 fold) downregulation of miR-29a levels in the myxoid and round cell liposarcomas. Furthermore, all miRNAs of the miR-23-27-24 clusters were significantly downregulated in MRCLS compared to normal fat (Table 1 and Supplemental Table 2). These miRNAs reside in two homologous clusters at different genomic locations, i.e. miR-23a, miR-27a and miR-24-2 on chromosome 19, and miR-23b, miR-27b and miR-24-1 on chromosome 9. qPCR analysis of these miRNAs in an extended sample set confirmed the microarray results. All five miRNAs showed an approximately 5 fold downregulation in the MRCLS (Figure 2B).



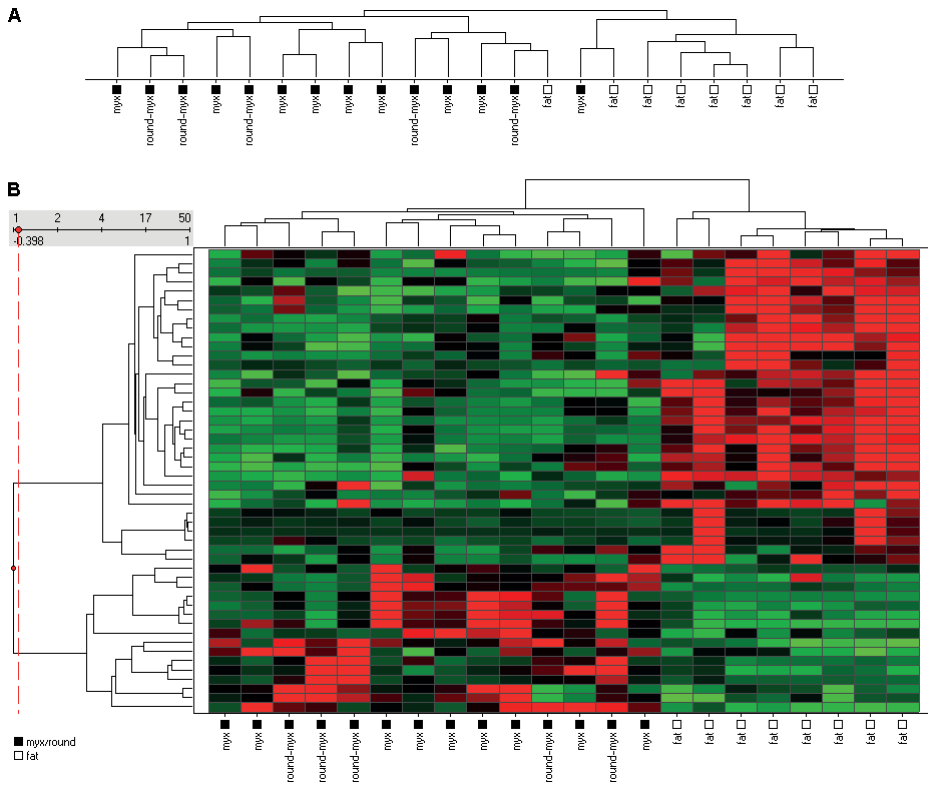


Figure 1: MRCLS show a distinct miRNA expression profile. A) MiRNA expression profiling almost completely discriminates myxoid/round cell liposarcomas from normal fat. All 585 human miRNAs with expression levels above background were used for this unsupervised hierarchical clustering. B) The 50 most differentially expressed miRNAs ($p \leq 0.03$, $\geq 1.7x$ fold change between myxoid/round cell liposarcomas and fat samples) discriminate the two groups in a supervised hierarchical clustering. Myx: myxoid liposarcoma; round-myx: myxoid liposarcoma with a round cell component.



Table 1: Top15 down-/upregulated miRNAs in myxoid/round cell liposarcoma compared to fat.

Downregulated in Myx/Round				Upregulated in Myx/Round			
miRNA	Fold-change	Parametric p-value	FDR	miRNA	Fold-change	Parametric p-value	FDR
1 hsa-miR-29a	7.10	< 1e-07	< 1e-07	hsa-miR-485-5p	6.79	< 1e-07	< 1e-07
2 hsa-miR-144	6.23	< 1e-07	< 1e-07	hsa-miR-216a	5.44	0.000018	0.000554
3 hsa-miR-22	4.64	< 1e-07	< 1e-07	hsa-miR-190b	3.69	0.000373	0.007496
4 hsa-miR-141	4.31	0.0009	0.011196	hsa-miR-422a	3.19	0.000599	0.008965
5 hsa-miR-29c	4.20	< 1e-07	< 1e-07	hsa-miR-181a	2.88	4E-07	2.34E-05
6 hsa-miR-451	3.50	0.000397	0.007496	hsa-miR-34b	2.32	0.004143	0.031888
7 hsa-miR-143	3.31	1.1E-06	5.36E-05	hsa-miR-27a*	2.31	0.000367	0.007496
8 hsa-miR-576-5p	2.92	0.002152	0.020302	hsa-miR-92b*	2.28	0.003659	0.029325
9 hsa-miR-29b	2.83	< 1e-07	< 1e-07	hsa-miR-543	2.16	0.001131	0.012978
10 hsa-miR-24	2.68	< 1e-07	< 1e-07	hsa-miR-202	2.09	0.000396	0.007496
11 hsa-miR-27a	2.65	9E-07	4.79E-05	hsa-miR-195*	2.03	0.000397	0.007496
12 hsa-miR-376a	2.56	0.000464	0.007867	hsa-miR-424*	1.97	2.7E-06	0.000122
13 hsa-miR-145	2.47	1.04E-05	0.000338	hsa-miR-377*	1.88	0.000538	0.008513
14 hsa-miR-23b	2.37	2E-07	0.000013	hsa-miR-593*	1.81	0.004315	0.032359
15 hsa-miR-146b-5p	2.31	0.001463	0.015561	hsa-miR-93	1.78	0.003114	0.0253

Fold change, p-value and FDR-adjusted p-value are indicated. The expression of the miRNAs in bold are validated by qPCR.

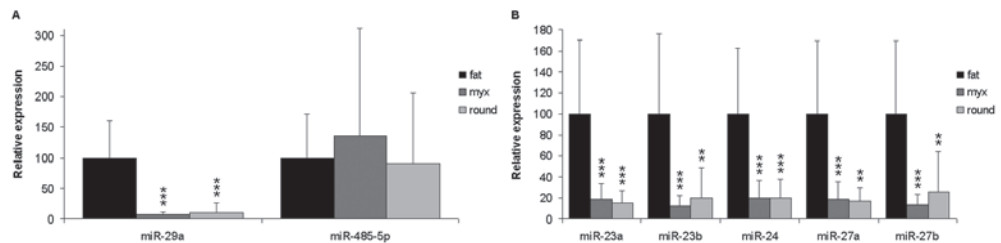


Figure 2: Validation of differentially expressed miRNAs in MRCLS. A) Expression levels of miR-29a (downregulated in myx/round) and miR-485-5p (upregulated in myx/round), are validated by qPCR in an extended sample set (myx n=22, round n=11, fat n=20). Mir-29a downregulation could be confirmed by qPCR, while miR-485-5p upregulation could not be validated. B) Validation of downregulated expression of the two miR-23-27-24 clusters in myxoid/round cell liposarcomas by qPCR in an extended sample set. Asterisks indicate statistical significant differences: * = p < 0.05, ** = p < 0.005, *** = p < 0.0005.

MiR-24 levels control sensitivity to doxorubicin

The expression of the miR-23a~27a~24-2 and miR-23b~27b~24-1 clusters is altered in many diseases, although in most cancers they are upregulated opposed to being downregulated in MRCLS.²² Furthermore, these miRNA have been implicated in drug resistance, and strikingly MRCLS are particularly sensitive to chemotherapy.^{5, 23-28} Since miR-24 is present in both miRNA

clusters and is the most differentially expressed miRNA of the two clusters, we investigated the role of miR-24 in doxorubicin sensitivity in MRCLS.

MiR-24 mimics and scrambled negative control (mNeg) mimics were transfected in two myxoid liposarcoma cell lines, after which they were exposed to 50 ng/ml doxorubicin treatment for two days. Upregulation of miR-24 in myxoid liposarcoma cell lines made the cells more resistant to doxorubicin treatment (Figure 3A). From a clinical standpoint it would be interesting to see if cells with higher endogenous levels of miR-24 could be sensitized for doxorubicin when miR-24 is inhibited. A liposarcoma cell line, SW872 (which is not of the MRCLS subtype), and a rhabdomyosarcoma cell line, RH30, exhibit higher levels of miR-24 than the two myxoid liposarcoma cell lines, MLS 402-91 and MLS 1765-92 (Figure 3B) and are more resistant to doxorubicin treatment (Figure 3C). When miR-24 levels were reduced by miR-24 LNA-inhibitors, the SW872 and RH30 cell line were slightly but significantly sensitized to doxorubicin, compared to cells transfected with a scrambled LNA-inhibitor (ctrl-inh) (Figure 3D). In the myxoid liposarcoma cell lines, which already expressed low levels of miR-24, transfections with miR-24 inhibitors did not further enhance the sensitivity to doxorubicin.

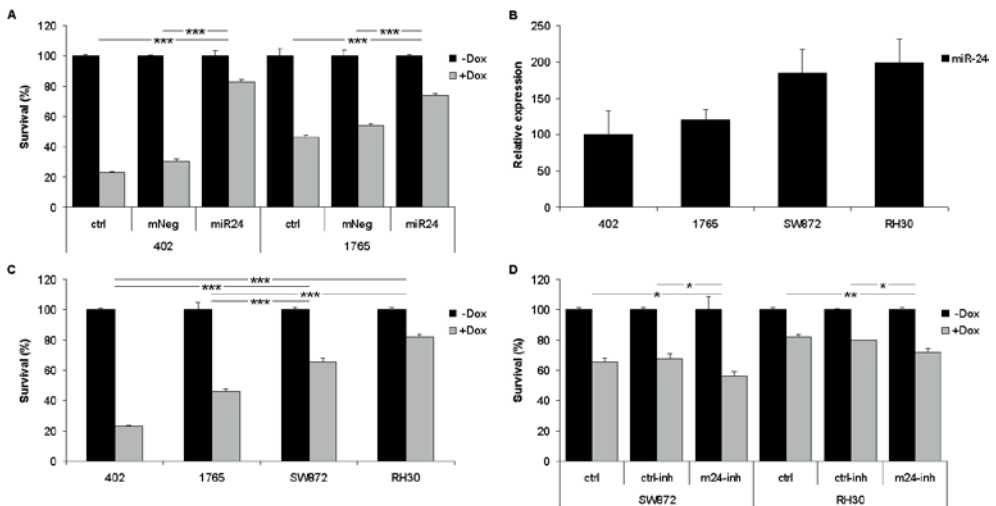


Figure 3: MiR-24 levels control sensitivity to doxorubicin. A) Overexpression of miR-24 in myxoid liposarcoma cell lines (MLS 402-91 and MLS 1765-92) induces doxorubicin resistance. Cells were untransfected (ctrl), or transfected with miR-24 mimics (miR24) or scrambled negative control (mNeg) mimics and 24h later subjected to 50ng/ml doxorubicin in medium (+Dox) or equal volume of medium (-Dox) for 2 days. B) Endogenous miR-24 levels are higher in a non-myxoid liposarcoma (SW872) and rhabdomyosarcoma (RH30) cell line than in the myxoid liposarcoma cell lines. MiR-24 levels were analyzed by qPCR, normalized to RNU43, and is relative to the expression in MLS 402-91 cells, which is set at 100. C) Untransfected SW872 and RH30 cell lines are more resistant to doxorubicin treatment (50ng/ml doxorubicin for 2 days) than the myxoid liposarcoma cell lines. D) Downregulation of miR-24 in SW872 and RH30 cell lines induces doxorubicin sensitivity. Cells were untransfected (ctrl), or transfected with miR-24 LNA-inhibitors (m24-inh) or scrambled inhibitors (ctrl-inh) and 24h later subjected to 50ng/ml doxorubicin in medium (+Dox) or an equal volume of medium (-Dox) for 2 days. Cell survival was analyzed by SRB assays. Asterisks indicate statistical significant differences: * = $p < 0.05$, ** = $p < 0.005$, *** = $p < 0.0005$.

FUSCHOP levels regulate miR-497, miR-30a and miR-34b expression

In order to identify which miRNAs are under control of the MRCLS specific *FUS-CHOP* fusion gene, FUS-CHOP levels were modulated in four sarcoma cell lines. A fibrosarcoma (SW684) and a liposarcoma (SW872) cell line, which did not express the fusion gene, were transfected with pcDNA3 empty vector (EV) as a control, and pcDNA3 FUS-CHOP constructs to induce FUS-CHOP fusion protein expression. In addition, two myxoid liposarcoma cell lines (MLS 402-91 and MLS 1765-92), which expressed the *FUS-CHOP* fusion gene endogenously, were transfected with pLKO.1 empty vector (EV) as a control, and pLKO.1 shRNA FUS-CHOP to knock-down FUS-CHOP expression.

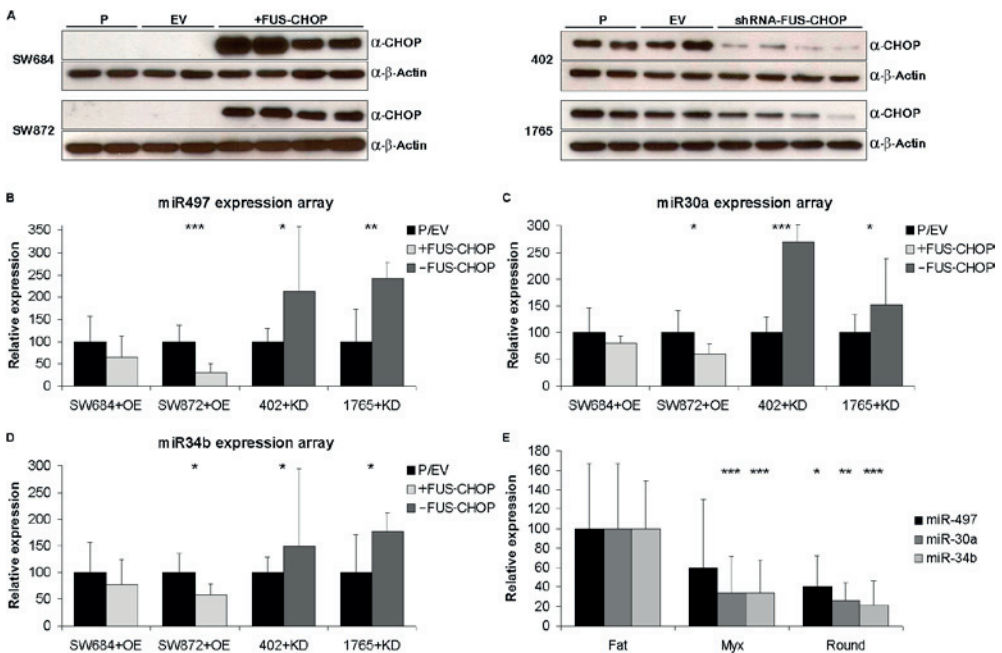


Figure 4: MiR-497, miR-30a and miR-34b are regulated by the FUS-CHOP fusion gene. A) Verification of FUS-CHOP overexpression in fibrosarcoma (SW684) and liposarcoma (SW872) cell lines (left panel) and FUS-CHOP knock-down in myxoid liposarcoma cell lines (MLS 402-91 and MLS 1765-92, right panel) after stable transfection of pcDNA3/FUS-CHOP (+FUS-CHOP) and pLKO.1/shRNA FUS-CHOP (shRNA-FUS-CHOP) respectively. FUS-CHOP protein levels were analyzed by SDS-PAGE and immunoblotting using antibodies against CHOP (α -CHOP). β -Actin was used as a loading control. MiRNA expression of these samples was measured by microarray: MiR-497 (B), miR-30a (C) and miR-34b (D) were downregulated upon FUS-CHOP overexpression (+FUS-CHOP) in SW864 and SW872 cells, and upregulated upon FUS-CHOP knock-down (-FUS-CHOP) in MLS 402-91 and MLS 1765-92 cells, as determined by microarray analyses. MiRNA expression in the overexpression/knock-down is relative to the expression in the parental/empty vector cells, which are set to 100. E) Expression of miR-497, miR-30a and miR-34b was downregulated in myxoid/round cell liposarcomas compared to normal fat as measured by qPCR (myx n=22, round n=20). MiRNA expression in myxoid and round cell liposarcomas is relative to the expression in normal fat which is set to 100. Asterisks indicate statistical significant differences: * = $p < 0.05$, ** = $p < 0.005$, *** = $p < 0.0005$.

The shRNA oligos in this construct are targeted against exon 2 of *CHOP*, which is spliced out of the regular *CHOP* transcript, but is present in the *FUS-CHOP* fusion gene, which ensures specific knock-down of FUS-CHOP and not the regular transcription factor CHOP. Figure 4A shows that FUS-CHOP protein levels were significantly induced in FUS-CHOP overexpressing fibro/liposarcoma cells (+FUS-CHOP), compared to the untransfected parental (P) and EV controls. The endogenous FUS-CHOP protein levels present in the myxoid liposarcoma cell lines (P/EV) were considerably reduced in cells with FUS-CHOP knockdown (shRNA-FUS-CHOP). Total RNA of these stable transfectants was subjected to miRNA microarray analysis and for each cell line it was determined which miRNAs were differentially expressed upon FUS-CHOP overexpression/knock-down (Supplemental Table 3). Since the fibrosarcoma cell line SW684 showed little changes in miRNA expression upon FUS-CHOP overexpression, there were no miRNAs that were significantly deregulated by FUS-CHOP overexpression or knockdown in all four cell lines. Only three miRNAs were differentially expressed in three out of four cell lines, i.e. miR-497, miR-30a and miR-34b (Figure 4B-D). These miRNAs were consistently downregulated when FUS-CHOP was overexpressed, and upregulated when FUS-CHOP was knocked-down. Accordingly, the expression of these miRNAs was significantly lower in myxoid and round cell liposarcomas (high FUS-CHOP expression) compared to normal fat (no FUS-CHOP expression), as determined by qPCR analysis (Figure 4E).

MiR-497 and miR-30a target the IGF1R-pathway

Candidate target genes for miR-497, miR-30a and miR-34b were predicted using TargetScanHuman 6.2 (<http://www.targetscan.org/>).²⁹ Remarkably, miR-497 and miR-30a, although unrelated and containing different seed sequences, share many mRNA targets. More particular, they both contain one or more potential binding sites in the 3'UTRs of several genes of the insulin(-like) growth factor pathway, e.g. *IGF1*, *IGF2*, *INSR*, *IGF1R*, *IGF2R*, *IRS1* and *IRS2* (Table 2). The IGF1R-pathway has been associated with MRCLS before.⁶⁻⁷ Therefore the effects of miR-497 and miR-30a overexpression on important players of the IGF1R pathway, i.e. IGF1R and its downstream effectors IRS1 and IRS2, are determined. The target sites of miR-497 and miR-30a in the 3'UTR of *IRS1*, *IRS2* and *IGF1R* are shown in Figure 5A. MiRNAs can exert their regulatory function either via mRNA degradation, translational repression or both. Therefore mRNA and protein levels of *IGF1R*, *IRS1* and *IRS2* were examined 72h after transfection of MLS 402-91 and MLS 1765-92 with mimics of miR-497 and miR-30a and a scrambled negative control (mneg). MiR-497 and miR-30a overexpression had little effect on mRNA levels of *IGF1R*, *IRS1* and *IRS2* (Figure 5B). The only significant changes were obtained by miR-30a overexpression, which upregulated *IGF1R* and downregulated *IRS1* mRNA expression in the MLS 402-91 cell line. Conversely, protein levels of IRS1, IRS2 and IGF1R were considerably affected in both cell lines. Protein expression of IRS1 was slightly reduced in miR-497 overexpressing cells, but severely reduced in miR-30a overexpressing cells, compared to the negative control (Figure 5C). IRS2 protein levels were moderately reduced



in miR-497 and miR-30a overexpressing cells. MiR-497 and miR-30a significantly downregulated IGF1R protein expression.

Table 2: Putative target sites of miR-497 and miR-30a in insulin (-like) growth factor pathway members.

	miR497 target sites		miR-30a target sites	
	Conserved	Poorly conserved	Conserved	Poorly conserved
IGF1 (NM_001111283)	Pos. 6088-6094		Pos. 6221-6227	
IGF2 (NM_000612)		Pos. 610-616		
IGF1R (NM_000875)	Pos. 1269-1275	Pos. 726-732 Pos. 3148-3154 Pos. 3151-3157 Pos. 3502-3508	Pos. 5629-5635	Pos. 5798-5804
IGF2R (NM_000876)	Pos. 318-324		Pos. 177-184	
INSR (NM_000208)	Pos. 577-583 Pos. 1196-1202	Pos. 228-234 Pos. 3129-3135 Pos. 3653-3659		
IRS1 (NM_005544)	Pos. 375-381	Pos. 3308-3314	Pos. 154-160	
IRS2 (NM_003749)	Pos. 2346-2352		Pos. 2069-2075	Pos. 611-617

Indicated are the positions where the miRNA seed sequence binds the 3'UTR according to TargetScanHuman 6.2.

To demonstrate that the observed downregulation of the members of the IGF1R pathway are due to the binding of the miR-497 and miR-30a to their 3'UTRs, fragments of the 3'UTRs spanning the potential miRNA target sites were cloned in a luciferase reporter construct. The resulting constructs are psiCHECK2/IRS1, psiCHECK2/IRS2, psiCHECK2/IGF1Rfr (comprising the front part of the 3'UTR of IGF1R), and psiCHECK2/IGF1Rba (comprising the back part of the 3'UTR of IGF1R) (Figure 5A, Supplemental Figure 1). MLS 1765-92 cells were transfected with these constructs, followed by a transfection with miR-497, miR-30a or a scrambled control (mneg) mimics (Figure 5D). Overexpression of miR-497 resulted in significant decrease in luciferase activity of the IRS1 construct (39%, $p < 0.0005$) and the IGF1Rfr construct (24%, $p = 0.002$). Overexpression of miR-30a significantly reduced the luciferase activity of IRS2 (52%, $p = 0.0005$) and IGF1Rba constructs (23%, $p = 0.002$), while it enhanced the luciferase activity of IRS1 (21%, $p = 0.0007$).

To demonstrate that the regulation of *IRS1*, *IRS2* and *IGF1R* is due to the direct binding of miR-497 and miR-30a to the predicted target sites in the 3'UTRs, these putative binding sites were mutated to prevent miRNA binding. All conserved miRNA binding sites were mutated, as well as one poorly conserved miR-497 site in the 3'UTR of *IGF1R*, which is positioned in the front part of the 3'UTR (Figure 5A). The resulting mutant constructs are illustrated in Supplemental Figure 1. A mutated miR-497 site in IRS1 completely rescued the luciferase activity (from 61% to 101%, $p < 0.0005$) (Figure 5E). Overexpression of miR-30a enhanced luciferase activity of the WT IRS1 construct and further increased it (from 121% to 143%, $p = 0.01$) when the miR-30a site was mutated.

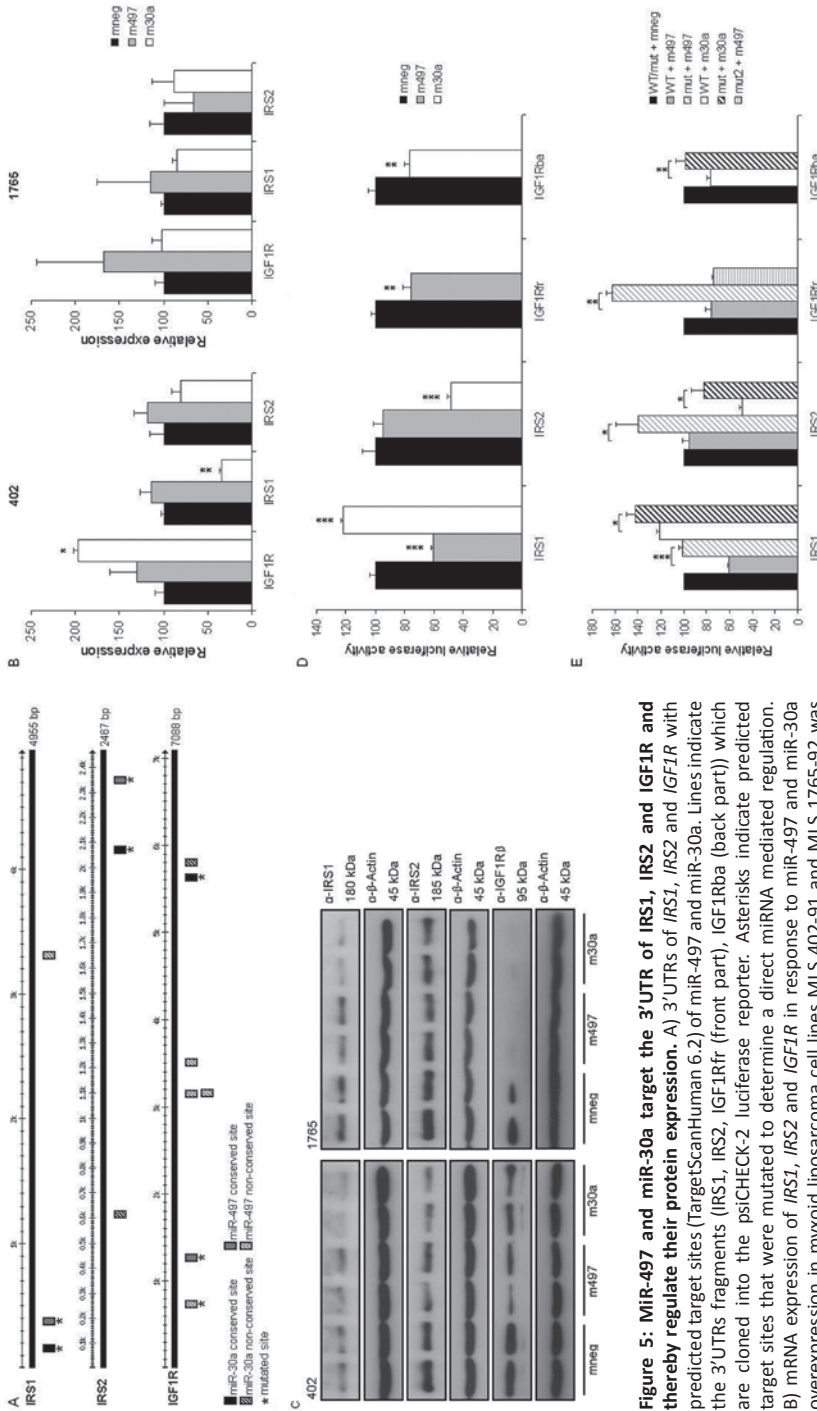


Figure 5: miR-497 and miR-30a target the 3'UTR of IRS1, IRS2 and IGF1R and thereby regulate their protein expression. A) 3'UTRs of *IRS1*, *IRS2* and *IGF1R* with predicted target sites (TargetScanHuman 6.2) of miR-497 and miR-30a. Lines indicate the 3'UTRs fragments (*IRS1*, *IRS2*, *IGF1R* (front part), *IGF1R*β (back part)) which are cloned into the psiCHECK-2 luciferase reporter. Asterisks indicate predicted target sites that were mutated to determine a direct miRNA mediated regulation. B) mRNA expression of *IRS1*, *IRS2* and *IGF1R* in response to miR-497 and miR-30a overexpression in myxoid liposarcoma cell lines MLS 402-91 and MLS 1765-92 was determined by qPCR and normalized to two housekeepers (*GAPDH*, *HPRT*). Shown are average values \pm SD (n=2), values are relative to expression of mneg (scrambled negative control mimic) which is set at 100. C) *IRS1*, *IRS2* and *IGF1R* protein expression in response to overexpression of miR-497, miR-30a and scrambled control (mneg) mimics, was determined by SDS-PAGE and immunoblotting. β -Actin was used as loading control D) Myxoid liposarcoma MLS 1765-92 cells were transfected with psiCHECK2-*IRS1*, -*IRS2*, -*IGF1R* or -*IGF1R*β, followed 24h later by transfection of scrambled (mneg), miR-497 or miR-30a mimics. (E) MLS 1765-92 cells were transfected with psiCHECK-2 constructs containing wild-type (WT) and mutated (mut) 3'UTR sequences of *IRS1*, *IRS2*, *IGF1R* or *IGF1R*β, followed 24h later by transfection of scrambled (mneg), miR-497 or miR-30a mimics. The *Renilla* luciferase activity was measured and normalized using firefly luciferase activity 48h after final transfection. The relative luciferase activity with scrambled mimic was set at 100. Shown are average values \pm SD (n=3). Statistical significance between scrambled control and miRNA mimics was tested by two-sample t-test. * = p<0.05, ** = p<0.005, *** = p<0.0005.



A mutated miR-30a site in *IRS2* significantly restored the luciferase activity (from 48% to 82%, $p=0.008$), while a mutated miR-497 site increased the luciferase activity (from 95% to 140%, $p=0.01$). Mutation of the conserved miR-497 site in *IGF1Rfr* rescued the luciferase activity (from 76% to 162%, $p<0.0005$), while mutation of the non-conserved miR-497 site (mut2) did not. A mutated miR-30a site in *IGF1Rba* completely restored the luciferase activity (from 76% to 99%, $p=0.01$).

These results suggest that *IRS1* and *IRS2* are directly regulated by miR-497 and miR-30a respectively, while *IGF1R* is directly regulated by both miRNAs. As judged from the results of qPCR and immunoblotting, regulation predominantly takes place via translational repression, rather than via mRNA degradation.

Overexpression of miR-497 and miR-30a affect cell proliferation and enhance sensitivity to doxorubicin

IGF1R signalling has been implicated in tumor cell proliferation and therapy resistance.³⁰⁻³⁶ Therefore we determined the effect of miR-497 and miR-30a, which can regulate the expression of IGF1R pathway members, on cell proliferation and doxorubicin sensitivity of myxoid liposarcoma cells.

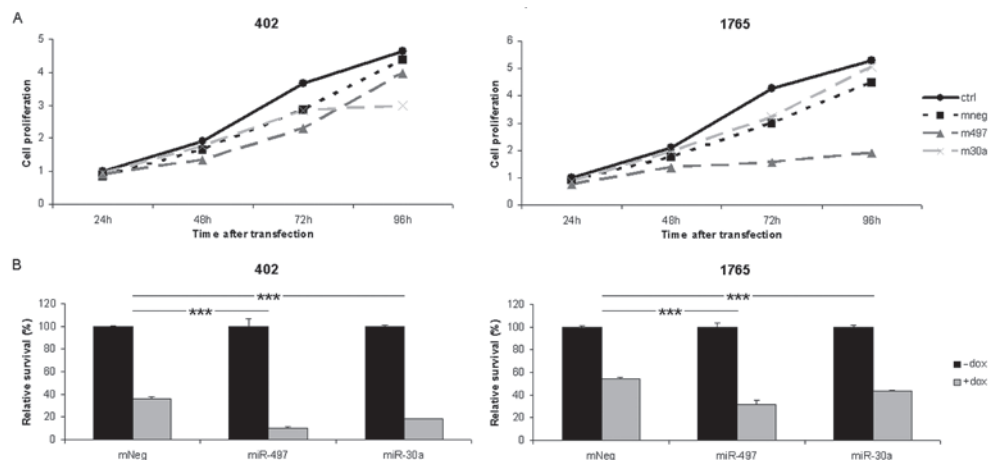


Figure 6: Overexpression of miR-497 and miR-30a affects cell proliferation and sensitizes myxoid liposarcoma cells to doxorubicin. A) MLS 402-91 and MLS 1765-92 myxoid liposarcoma cell lines are either untransfected (ctrl), or transfected with miR-497, miR-30a or a scrambled negative control mimic (mneg). Graphs indicate cell proliferation at 24h, 48h, 72h and 96h post-transfection, relative to the control at 24h, which is set at 1. B) Overexpression of miR-497 and miR-30a sensitizes MLS 402-91 and MLS 1765-92 cells to doxorubicin. Cells were transfected with miR-497, miR-30a and scrambled negative control (mNeg) mimics and 24h later subjected to 50ng/ml doxorubicin in medium (+Dox) or equal volume of medium (-Dox) for 2 days. Cell proliferation is analyzed by SRB assays. Asterisks indicate statistical significant differences: * = $p<0.05$, ** = $p<0.005$, *** = $p<0.0005$.

MiRNA mimics of miR-497 and miR-30a, as well as a scrambled control mimic (mneg), were transfected into MLS 402-91 and MLS 1765-92 myxoid liposarcoma cell lines, after which cell density was monitored in time at 24h, 48h, 72h and 96h post-transfection by SRB assays (Figure 6A). In MLS 402-91 cells miR-30a overexpression resulted in decreased cell density 96h after transfection, which was consistently observed in independent experiments. MiR-497 overexpression hardly had an effect on cell growth in MLS 402-91 cells, but significantly inhibited cell density in MLS 1765-92 cells. MiR-30a overexpression did not exert an effect in MLS 1765-92 cells.

To investigate the effect of miR-497 and miR-30a overexpression on doxorubicin sensitivity, mimics and scrambled negative control (mNeg) mimics were transfected in the two myxoid liposarcoma cell lines, after which they were subjected to 50 ng/ml doxorubicin treatment for two days. In both cell lines, upregulation of both miRNAs significantly sensitized the cells to doxorubicin treatment.


DISCUSSION

MRCLS represent a unique group of liposarcomas, characterized by a t(12;16)(q13;p11) translocation in >90% of the cases. This translocation gives rise to a *FUS-CHOP* fusion gene, which acts as an abnormal transcription factor, inducing distinct transcriptional programs.¹⁵⁻¹⁷ Furthermore, MRCLS are more sensitive to radio- and chemotherapy than the other liposarcoma subtypes.⁴⁻⁵ We previously identified that MRCLS also represent a unique group of liposarcomas on the basis of miRNA expression (Chapter 2 of this thesis).

In this study, we examined the role of MRCLS-specific miRNAs in the characteristic biology of MRCLS.

Hierarchical clustering showed that the miRNA expression profile of MRCLS is distinct from that of normal fat tissue. Remarkably, all members of the homologous miR-23a~27a~24-2 and miR-23b~27b~24-1 clusters were significant differentially expressed between MRCLS and fat, with at least a two fold downregulation in the MRCLS group. Validation of these microarray data by qPCR even showed an average five fold reduction of miR-23a, miR-23b, miR-24, miR-27a and miR-27b. The expression of these miRNA cluster members is deregulated in many tumor types, although not consistently up- or downregulated.²² They are, for example, upregulated in acute myeloid leukemia, gastric cancer, and hepatocellular carcinoma, while they are downregulated in melanoma and oral squamous cell carcinoma.²² Furthermore, although these miRNAs have been linked to cell proliferation, differentiation, angiogenesis, apoptosis, and cell cycle control, they have been shown to give rise to contrasting phenotypes in different cell types.²² Moreover, miR-23a/b, miR-27a/b and miR-24 have been implicated in drug resistance,²³⁻²⁸ but in some studies resistance is associated with high levels of these miRNAs, while in other studies it is





related to low levels. Since MRCLS are particularly sensitive to chemotherapy,⁵ and miR-24 is the most differentially expressed miRNA in MRCLS and is expressed from both miRNA clusters, we examined the role of miR-24 in doxorubicin sensitivity, a commonly used drug in the first line therapy of MRCLS. In myxoid liposarcoma cell lines with low endogenous miR-24 levels, miR-24 overexpression induced doxorubicin resistance, while miR-24 inhibition in more resistant cell lines that expressed relatively high endogenous miR-24 levels sensitized the cells to doxorubicin treatment. Therefore, miR-24 levels can potentially be of predictive value for the response to doxorubicin treatment. The relevance of combination therapy of miR-24 inhibition and doxorubicin should be further investigated. Before a miRNA can be used therapeutically, it is of importance to know its target genes in order to prevent unwanted side effects. Some target genes of miR-24 are identified, e.g. *ARNT*, *BIM*, *H2AX*, *p16* and *p27*.³⁷⁻⁴⁰ However, further target prediction and validation could be complicated by the fact that miR-24 can target transcripts via binding to seedless miRNA response elements (i.e. highly complementary binding of targets without involvement of the miRNA seed region).⁴¹ Seedless miR-24 target genes are enriched in DNA repair and cell-cycle regulating genes, and include *CCNA2*, *CDK4*, *E2F2*, *FEN1* and *MYC*.⁴¹ Furthermore, miR-24 expression has been shown to inhibit VEGFA signaling in endothelial cells, and miR-24 decoy increased angiogenesis in mice cardiomyocytes.⁴²⁻⁴³ If the same holds true in tumor tissues, this would imply that low miR-24 levels may enhance tumor vascularity and blood flow, which could be beneficial for the effectiveness of systemic therapy.

In MRCLS, the N-terminal part of RNA binding protein FUS, containing potent transactivation domains, is fused to the C-terminal part of transcription factor CHOP.⁴⁴ In the fusion protein, the RNA-binding domain of FUS is replaced by the DNA-binding and leucine zipper dimerization domain of CHOP. Consequently, FUS-CHOP functions as an abnormal transcription factor, inducing distinct transcriptional programs.¹⁵⁻¹⁷ The translocation and subsequent formation of the fusion gene is considered the genetic event that causes malignant transformation and initiates MRCLS tumor formation.¹⁷ However, the definite mechanisms of FUS-CHOP in MRCLS tumorigenesis and progression, including the regulation of miRNA and gene expression, have not been completely elucidated. We investigated which miRNAs are regulated by the fusion protein, by modulating FUS-CHOP levels in two myxoid liposarcoma cell lines with high endogenous FUS-CHOP expression, and a fibrosarcoma and a liposarcoma cell line without endogenous FUS-CHOP expression. Three miRNAs, in particular miR-497, miR-30a and miR-34b, were significantly regulated by FUS-CHOP in three out of four cell lines. Their expression was induced when FUS-CHOP expression was knocked-down in the myxoid liposarcoma cell lines, and reduced when FUS-CHOP was overexpressed in the liposarcoma cell line. The same trend, although not significant, was observed in the fibrosarcoma cell line. These results were in line with the relative low expression of these miRNAs in MRCLS samples compared to normal fat tissue as determined by qPCR. Most of the MRCLS specific miRNAs we identified earlier were

not regulated by FUS-CHOP. This implies that other mechanisms, independent of FUS-CHOP expression, are responsible for (de)regulating miRNA expression in MRCLS. The only miRNA from the miR-23a~27a~24-2 and miR-23b~27b~24-1 clusters that was found to be regulated by the fusion protein, was miR-23a which was significantly upregulated in the MLS 402-91 cell line upon FUS-CHOP knock-down. Since the other cluster members are not identified in our analysis, while the downregulation of these miRNAs in MRCLS was substantial, their expression is probably not regulated by FUS-CHOP. Recently, Borjigin et al. found that miR-486 expression was repressed in FUS-CHOP-expressing NIH3T3 fibroblasts and MLS tissues.¹⁸ Although we found that miR-486 was significantly downregulated in MRCLS compared to fat, miR-486 expression was not regulated by FUS-CHOP in our analysis. Renner et al. identified that miR-9 and miR-9* were upregulated in myxoid liposarcomas versus normal fat.⁴⁵ In our analysis however, miR-9* was upregulated in MLS 402-91 myxoid liposarcoma cells upon FUS-CHOP knock-down.

Although miR-497 and miR-30a consist of completely different sequences, even within the seed, they share many predicted target genes that are implicated in the insulin(-like) growth factor pathway, e.g. *IGF1*, *IGF2*, *INSR*, *IGF1R*, *IGF2R*, *IRS1* and *IRS2*. Insulin and insulin like growth factor (IGF) 1 and 2 can bind the insulin receptor (INSR) and insulin like growth factor receptors (IGF1R and IGF2R) with varying affinity. Upon ligand binding, IGF1R activates insulin receptor substrate (IRS) 1 and 2, which act in downstream signalling. The tyrosine kinase receptor IGF1R and its downstream players have been associated with MRCLS before. Cheng et al. demonstrated that immunohistochemical stainings of tissue microarrays identified much higher expression levels of IGF1R, IGF2 and RET in myxoid liposarcomas compared to other liposarcoma subtypes, lipomas and fat, which significantly associated with aggressive behavior and poor prognosis.⁶ Involvement of IGF1R and its downstream targets in MRCLS has been verified by Demicco et al.⁷ Low levels of miR-497 and miR-30a in MRCLS could allow for high expression of IGF1R pathway members. We demonstrated that miR-497 and miR-30a overexpression reduced protein levels of IGF1R and its substrates IRS1 and IRS2. Luciferase reporter assays showed that IRS1 is predominantly regulated by miR-497, IRS2 is regulated by miR-30a, and IGF1R expression is controlled by both miRNAs. However, miR-30a overexpression also had an effect on IRS1 protein expression, miR-497 slightly reduced IRS2 protein levels, and IGF1R expression was drastically reduced by both miRNAs. Therefore, next to direct regulation of IGF1R pathway members by miR-497 and miR-30a, indirect effects are likely to play a role as well.

The kinases PI3K, Akt and mTOR, which are often overactive in cancer, can be activated via the IGF1R pathway, or alternatively by other tyrosin kinase receptors, such as RET, by mutations in *PI3K*, or by loss of *PTEN*. Although *RET* contains two putative miR-497 binding sites in its 3'UTR and may thus potentially be regulated by this miRNA, the other genes do not contain predicted target sites for miR-497 or miR-30a. However, *PI3K* mutations have been implicated in only 14%



of MRCLS (predominantly round cell liposarcomas), and loss of *PTEN* was observed in 12% of MRCLS.⁷ We therefore believe that the overall effect of IGF1R-pathway inhibition by miR-497 and miR-30a will be relevant in the majority of MRCLS.

The functional implications of IGF1R signalling in MRCLS are not yet clearly understood. In other tumor types, IGF1R expression stimulates tumor cell proliferation and associates with radio- and chemotherapy resistance.³⁰⁻³¹ IGF1R inhibition leads to decreased tumor growth and can sensitize various tumor types to multiple agents.^{30, 32-35} In the two myxoid liposarcoma cell lines tested, miR-497 and miR-30a overexpression had only minor effects on cell proliferation, except for miR-497 overexpression in MLS 1765-92 cells which inhibited cell proliferation considerably. The effect of miR-497 and miR-30a overexpression on doxorubicin sensitivity, however, was significant. In both cell lines, upregulation of both miRNAs significantly sensitized the cells to doxorubicin treatment. Although myxoid liposarcomas are more sensitive to radiotherapy and systemic treatments than other liposarcoma subtypes, the response rate to first line chemotherapy is only 48%.⁵ Future research should identify whether the IGF1R pathway is over-activated in the poor responders. If that is the case, combination therapy of doxorubicin and miR-497/30a can be promising for myxoid liposarcomas which do not respond well to standard treatment initially.

Since inhibition of the IGF1R pathway showed great therapeutic potential in several tumor types, a number of strategies to target this pathway are in development. Monoclonal antibodies against IGF1 and IGF2 prevent interaction with their receptors, while monoclonal antibodies against IGF1R hinder ligand binding.^{34, 46} Tyrosine kinase inhibitors prevent IGF1R and IR activation,⁴⁷ while shRNA against *IGF1R* downregulates expression of the receptor.³⁶ Furthermore, inhibitors of PI3K, Akt and mTOR have been developed to inhibit downstream signalling.⁴⁸ Many of these drugs, however, only target one gene within the IGF1R pathway, and showed varying degrees of success in sarcomas. When IGF1R signalling is inhibited, compensatory signalling via IR or EGFR has been observed.⁴⁹⁻⁵⁰ which may lead to resistance. Therefore, combination therapies, e.g. with miRNA-based therapeutics, should be considered. MiR-497 and miR-30a can target *IGF1R*, *IRS1* and *IRS2*, and potentially many other related genes, as putative binding sites for these miRNAs have been found in *IGF1*, *IGF2*, *INSR*, *RET* and *EGFR*. Although the effect of miR-497 and miR-30a on these individual genes has not yet been determined, the cumulative effect of simultaneous inhibition of these genes has great potential. Furthermore, miR-497 and miR-30a overexpression can sensitize MRCLS to doxorubicin treatment. Hence, combination therapy of miR-497 and miR-30a with chemotherapeutic or targeted agents should be further explored.



ACKNOWLEDGEMENTS

We thank Dr. M. Debiec-Rychter for providing the RH30 rhabdomyosarcoma cell line, and dr. P. Åman for providing the MLS 402-91 and MLS 1765-92 myxoid liposarcoma cell lines. Furthermore we are grateful to the personnel of the Erasmus Medical Center Tissue Bank and Institut Bergonié for providing the tissues samples, and we thank the members the Laboratory of Translational Pharmacology for helpful discussions. This work was supported by the EC FP6 CONTICANET Network of Excellence (LSHC-CT-2005-018806) from the European Commission. The authors disclose no potential conflicts of interest.



REFERENCES

1. Dei Tos AP. Liposarcoma: new entities and evolving concepts. *Ann Diagn Pathol.* 2000 Aug;4(4):252-66.
2. Fletcher CD, Bridge JA, Hogendoorn PC, Mertens F, (Eds.). WHO Classification of Tumours of Soft Tissue and Bone. Lyon: IARC; 2013.
3. Haniball J, Sumathi VP, Kindblom LG, Abudu A, Carter SR, Tillman RM, et al. Prognostic factors and metastatic patterns in primary myxoid/round-cell liposarcoma. *Sarcoma.* 2011;2011:538085.
4. Pitson G, Robinson P, Wilke D, Kandel RA, White L, Griffin AM, et al. Radiation response: an additional unique signature of myxoid liposarcoma. *Int J Radiat Oncol Biol Phys.* 2004 Oct 1;60(2):522-6.
5. Jones RL, Fisher C, Al-Muderis O, Judson IR. Differential sensitivity of liposarcoma subtypes to chemotherapy. *Eur J Cancer.* 2005 Dec;41(18):2853-60.
6. Cheng H, Dodge J, Mehl E, Liu S, Poulin N, van de Rijn M, et al. Validation of immature adipogenic status and identification of prognostic biomarkers in myxoid liposarcoma using tissue microarrays. *Hum Pathol.* 2009 Sep;40(9):1244-51.
7. Demicco EG, Torres KE, Ghadimi MP, Colombo C, Bolshakov S, Hoffman A, et al. Involvement of the PI3K/Akt pathway in myxoid/round cell liposarcoma. *Mod Pathol.* 2012 Feb;25(2):212-21.
8. Crozat A, Aman P, Mandahl N, Ron D. Fusion of CHOP to a novel RNA-binding protein in human myxoid liposarcoma. *Nature.* 1993 Jun 17;363(6430):640-4.
9. Rabbitts TH, Forster A, Larson R, Nathan P. Fusion of the dominant negative transcription regulator CHOP with a novel gene FUS by translocation t(12;16) in malignant liposarcoma. *Nat Genet.* 1993 Jun;4(2):175-80.
10. Dal Cin P, Sciot R, Panagopoulos I, Aman P, Samson I, Mandahl N, et al. Additional evidence of a variant translocation t(12;22) with EWS/CHOP fusion in myxoid liposarcoma: clinicopathological features. *J Pathol.* 1997 Aug;182(4):437-41.
11. Panagopoulos I, Hoglund M, Mertens F, Mandahl N, Mitelman F, Aman P. Fusion of the EWS and CHOP genes in myxoid liposarcoma. *Oncogene.* 1996 Feb 1;12(3):489-94.
12. Bertolotti A, Lutz Y, Heard DJ, Chambon P, Tora L. hTAF(II)68, a novel RNA/ssDNA-binding protein with homology to the pro-oncoproteins TLS/FUS and EWS is associated with both TFIID and RNA polymerase II. *EMBO J.* 1996 Sep 16;15(18):5022-31.
13. Tan AY, Manley JL. TLS inhibits RNA polymerase III transcription. *Mol Cell Biol.* 2010 Jan;30(1):186-96.
14. Batchvarova N, Wang XZ, Ron D. Inhibition of adipogenesis by the stress-induced protein CHOP (Gadd153). *EMBO J.* 1995 Oct 2;14(19):4654-61.
15. Thelin-Jarnum S, Lassen C, Panagopoulos I, Mandahl N, Aman P. Identification of genes differentially expressed in TLS-CHOP carrying myxoid liposarcomas. *Int J Cancer.* 1999 Sep 24;83(1):30-3.
16. Schwarzbach MH, Koesters R, Germann A, Mechttersheimer G, Geisbill J, Winkler S, et al. Comparable transforming capacities and differential gene expression patterns of variant FUS/CHOP fusion transcripts derived from soft tissue liposarcomas. *Oncogene.* 2004 Sep 2;23(40):6798-805.
17. Riggi N, Cironi L, Provero P, Suva ML, Stehle JC, Baumer K, et al. Expression of the FUS-CHOP fusion protein in primary mesenchymal progenitor cells gives rise to a model of myxoid liposarcoma. *Cancer Res.* 2006 Jul 15;66(14):7016-23.
18. Borjigin N, Ohno S, Wu W, Tanaka M, Suzuki R, Fujita K, et al. TLS-CHOP represses miR-486 expression, inducing upregulation of a metastasis regulator PAI-1 in human myxoid liposarcoma. *Biochem Biophys Res Commun.* 2012 Oct 19;427(2):355-60.
19. Pothof J, Verkaik NS, van IJcken W, Wiemer EA, Ta VT, van der Horst GT, et al. MicroRNA-mediated gene silencing modulates the UV-induced DNA-damage response. *EMBO J.* 2009 Jul 22;28(14):2090-9.
20. Schmittgen TD, Livak KJ. Analyzing real-time PCR data by the comparative C(T) method. *Nat Protoc.* 2008;3(6):1101-8.
21. Keepers YP, Pizao PE, Peters GJ, van Ark-Otte J, Winograd B, Pinedo HM. Comparison of the sulforhodamine B protein and tetrazolium (MTT) assays for in vitro chemosensitivity testing. *Eur J Cancer.* 1991;27(7):897-900.
22. Chhabra R, Dubey R, Saini N. Cooperative and individualistic functions of the microRNAs in the miR-23a~27a~24-2 cluster and its implication in human diseases. *Mol Cancer.* 2010;9:232.
23. Zhang H, Li M, Han Y, Hong L, Gong T, Sun L, et al. Down-regulation of miR-27a might reverse multidrug resistance of esophageal squamous cell carcinoma. *Dig Dis Sci.* 2010 Sep;55(9):2545-51.

24. Husted S, Sokilde R, Rask L, Cirera S, Busk PK, Eriksen J, et al. MicroRNA expression profiles associated with development of drug resistance in Ehrlich ascites tumor cells. *Mol Pharm*. 2011 Dec 5;8(6):2055-62.
25. Zhu H, Wu H, Liu X, Evans BR, Medina DJ, Liu CG, et al. Role of MicroRNA miR-27a and miR-451 in the regulation of MDR1/P-glycoprotein expression in human cancer cells. *Biochem Pharmacol*. 2008 Sep 1;76(5):582-8.
26. Singh R, Saini N. Downregulation of BCL2 by miRNAs augments drug-induced apoptosis--a combined computational and experimental approach. *J Cell Sci*. 2012 Mar 15;125(Pt 6):1568-78.
27. Chhabra R, Adlakha YK, Hariharan M, Scaria V, Saini N. Upregulation of miR-23a-27a-24-2 cluster induces caspase-dependent and -independent apoptosis in human embryonic kidney cells. *PLoS One*. 2009;4(6):e5848.
28. Miller TE, Ghoshal K, Ramaswamy B, Roy S, Datta J, Shapiro CL, et al. MicroRNA-221/222 confers tamoxifen resistance in breast cancer by targeting p27Kip1. *J Biol Chem*. 2008 Oct 31;283(44):29897-903.
29. Lewis BP, Burge CB, Bartel DP. Conserved seed pairing, often flanked by adenosines, indicates that thousands of human genes are microRNA targets. *Cell*. 2005 Jan 14;120(1):15-20.
30. Jones RA, Campbell CI, Wood GA, Petrik JJ, Moorehead RA. Reversibility and recurrence of IGF-IR-induced mammary tumors. *Oncogene*. 2009 May 28;28(21):2152-62.
31. Turner BC, Haffty BG, Narayanan L, Yuan J, Havre PA, Gumbs AA, et al. Insulin-like growth factor-I receptor overexpression mediates cellular radioresistance and local breast cancer recurrence after lumpectomy and radiation. *Cancer Res*. 1997 Aug 1;57(15):3079-83.
32. Zhang YW, Yan DL, Wang W, Zhao HW, Lu X, Wu JZ, et al. Knockdown of insulin-like growth factor I receptor inhibits the growth and enhances chemo-sensitivity of liver cancer cells. *Curr Cancer Drug Targets*. 2012 Jan;12(1):74-84.
33. Hurbin A, Wislez M, Busser B, Antoine M, Tenaud C, Rabbe N, et al. Insulin-like growth factor-1 receptor inhibition overcomes gefitinib resistance in mucinous lung adenocarcinoma. *J Pathol*. 2011 Sep;225(1):83-95.
34. Mayeenuddin LH, Yu Y, Kang Z, Helman LJ, Cao L. Insulin-like growth factor 1 receptor antibody induces rhabdomyosarcoma cell death via a process involving AKT and Bcl-x(L). *Oncogene*. 2010 Dec 2;29(48):6367-77.
35. Beauchamp MC, Knafo A, Yasmeen A, Carboni JM, Gottardis MM, Pollak MN, et al. BMS-536924 sensitizes human epithelial ovarian cancer cells to the PARP inhibitor, 3-aminobenzamide. *Gynecol Oncol*. 2009 Nov;115(2):193-8.
36. Wang YH, Xiong J, Wang SF, Yu Y, Wang B, Chen YX, et al. Lentivirus-mediated shRNA targeting insulin-like growth factor-1 receptor (IGF-1R) enhances chemosensitivity of osteosarcoma cells in vitro and in vivo. *Mol Cell Biochem*. 2010 Aug;341(1-2):225-33.
37. Lal A, Pan Y, Navarro F, Dykxhoorn DM, Moreau L, Meire E, et al. miR-24-mediated downregulation of H2AX suppresses DNA repair in terminally differentiated blood cells. *Nat Struct Mol Biol*. 2009 May;16(5):492-8.
38. Qian L, Van Laake LW, Huang Y, Liu S, Wendland MF, Srivastava D. miR-24 inhibits apoptosis and represses Bim in mouse cardiomyocytes. *J Exp Med*. 2011 Mar 14;208(3):549-60.
39. Giglio S, Cirombella R, Amodeo R, Portaro L, Lavra L, Vecchione A. MicroRNA miR-24 promotes cell proliferation by targeting the CDKs inhibitors p27(Kip1) and p16(INK4a.). *J Cell Physiol*. 2013 Oct;228(10):2015-23.
40. Oda Y, Nakajima M, Mohri T, Takamiya M, Aoki Y, Fukami T, et al. Aryl hydrocarbon receptor nuclear translocator in human liver is regulated by miR-24. *Toxicol Appl Pharmacol*. 2012 May 1;260(3):222-31.
41. Lal A, Navarro F, Maher CA, Maliszewski LE, Yan N, O'Day E, et al. miR-24 Inhibits cell proliferation by targeting E2F2, MYC, and other cell-cycle genes via binding to "seedless" 3'UTR microRNA recognition elements. *Mol Cell*. 2009 Sep 11;35(5):610-25.
42. Kasza Z, Fuchs PF, Tamm C, Eriksson AS, O'Callaghan P, Heindryckx F, et al. MicroRNA-24 suppression of N-deacetylase/N-sulfotransferase-1 (NDST1) reduces endothelial cell responsiveness to VEGFA. *J Biol Chem*. 2013 Jul 24.
43. Meloni M, Marchetti M, Garner K, Littlejohns B, Sala-Newby G, Xenophontos N, et al. Local Inhibition of MicroRNA-24 Improves Reparative Angiogenesis and Left Ventricle Remodeling and Function in Mice With Myocardial Infarction. *Mol Ther*. 2013 Jul;21(7):1390-402.
44. Sanchez-Garcia I, Rabbitts TH. Transcriptional activation by TAL1 and FUS-CHOP proteins expressed in acute malignancies as a result of chromosomal abnormalities. *Proc Natl Acad Sci U S A*. 1994 Aug 16;91(17):7869-73.
45. Renner M, Czwan E, Hartmann W, Penzel R, Brors B, Eils R, et al. MicroRNA profiling of primary high-grade soft tissue sarcomas. *Genes Chromosomes Cancer*. 2012 Nov;51(11):982-96.



46. Olmos D, Postel-Vinay S, Molife LR, Okuno SH, Schuetze SM, Paccagnella ML, et al. Safety, pharmacokinetics, and preliminary activity of the anti-IGF-1R antibody figitumumab (CP-751,871) in patients with sarcoma and Ewing's sarcoma: a phase 1 expansion cohort study. *Lancet Oncol.* 2010 Feb;11(2):129-35.
47. Haisa M. The type 1 insulin-like growth factor receptor signalling system and targeted tyrosine kinase inhibition in cancer. *J Int Med Res.* 2013 Apr;41(2):253-64.
48. Blay JY. Updating progress in sarcoma therapy with mTOR inhibitors. *Ann Oncol.* 2011 Feb;22(2):280-7.
49. Buck E, Gokhale PC, Koujak S, Brown E, Eyzaguirre A, Tao N, et al. Compensatory insulin receptor (IR) activation on inhibition of insulin-like growth factor-1 receptor (IGF-1R): rationale for cotargeting IGF-1R and IR in cancer. *Mol Cancer Ther.* 2010 Oct;9(10):2652-64.
50. Haluska P, Carboni JM, TenEyck C, Attar RM, Hou X, Yu C, et al. HER receptor signaling confers resistance to the insulin-like growth factor-I receptor inhibitor, BMS-536924. *Mol Cancer Ther.* 2008 Sep;7(9):2589-98.



SUPPLEMENTAL TABLES AND FIGURES

Supplemental Table 1: shRNA oligonucleotides and primers used for cloning and mutagenesis.

A

Duplex	Oligo	Sequence
1	1	<u>CCGGAAGGAAGTGTATCTTCATACACTCGAGTGTATGAAGATACACTTCCTTTTTTT</u>
	2	<u>AATTAAAAAAGGAAGTGTATCTTCATACACTCGAGTGTATGAAGATACACTTCCTTT</u>
2	1	<u>CCGGTACATCACACACCTGAAAGCAGCTCGAGCTGCTTTCAGGTGTGGTATGATTTTTT</u>
	2	<u>AATTAAAAATACATCACACACCTGAAAGCAGCTCGAGCTGCTTTCAGGTGTGGTATGTA</u>

B

Gene	Primer	Sequence	Product size
<i>IRS1</i> 3'UTR	Forward primer	CGCTCGAGA AATGAAGACCTAAATGACCTC	1175 bp
	Reverse primer	AT GCGGCCG CATTCTGGTTAGCAACAGC	
<i>IRS2</i> 3'UTR	Forward primer	CGCTCGAG AGATCTGTCTGGCTTATCAC	2428 bp
	Reverse primer	AT GCGGCCG CTATTAAGGAGGGCATCCAT	
<i>IGF1R</i> 3'UTR	Forward primer1	CGCTCGAG TCTTGGATCCTGAATCTG	2377 bp
	Reverse primer 1	AT GCGGCCG CAGTGGGACAAACTGCTGAC	
	Forward primer 2	CGCTCGAG TGAGATCGATGGGTGAGAA	1658 bp
	Reverse primer 2	AT GCGGCCG CTACGTATCTTCGGGGTCT	

C

Gene	Primer	Sequence
IRS1-m30a-mut	Forward primer	5'-GGTACGATGCATCCATTTTCAGTTTGATATCTTTTCAATCCTCAGGATTTTCAT
	Reverse primer	5'-ATGAAATCCTGAGGATTGGATAAAGATATCAAAGTAAATGGATGCATCGTACC
IRS1-m497-mut	Forward primer	5'-ACTCTCAATGCATTTTCAAGATACATTTTCATCTCGAGCTGAAACTGTGTACGA
	Reverse primer	5'-TCGTACACAGTTTCAGCTCGAGATGAAATGTATCTTGAAAATGCATTGAGAGT
IRS2-m30a-mut	Forward primer	5'-TTTCAAAAAAGGCATATGCAATATTTACATTTTAAATTTAGAATTCAGAATGGAACC AAAAATGATAAATGTTATG
	Reverse primer	5'-CATAACATTTATACATTTTGGTTCCATTCTGAATTCTAAATAAAAATGAAATATTGCA TATGCCTTTTTGTGAAA
IRS2-m497-mut	Forward primer	5'-ATATAGGGGTCAATGTGATGCTCGAGGAGACGAGAATAAACTGGA
	Reverse primer	5'-TCCAGTTTATTCTCGTCTCCTCGAGCATCACATTGACCCCTATAT
IGF1Rfr-m497pc-mut	Forward primer	5'-CTGCCCTGCTGTGGTACCAAGGCCACAGGCA
	Reverse primer	5'-TGCCTGTGCCTTGGGTACCAACAGCAGGGGCGAG
IGF1Rfr-m497c-mut	Forward primer	5'-TTCATCTATACGTCTGTACAGAAAAAAGGTACCATTTTTTTTGTCTGATCTTT GTGGATTTAA
	Reverse primer	5'-TTAAATCCACAAAGATCAAGAACAAAAAATGGTACCTTTTTTTTTCTGTACAGA CGTATAGATGAA
IGF1Rba-m30a-mut	Forward primer	5'-GGGTAGTCAGTTGACGAAGATCTGGATATCAAGAATAATTAATGTTTCATTGC
	Reverse primer	5'-GCAATGAAACATTTAATTAGTTCTTGATATCCAGATCTTCGTCAACTGACTACCC

A) Oligonucleotides that were used to create shRNA oligo duplexes with Age1 and EcoR1 overhangs (underlined sequences) and were cloned in a pLKO.1 vector. The shRNAs were targeted (bold sequence) against a sequence in CHOP exon 2 which is only transcribed in the FUS-CHOP fusion gene transcripts and not in endogenous CHOP. Sequence in italics represents the shRNA loop. B) Primer sequences used to PCR-amplify fragments of *IRS1*, *IRS2* and *IGF1R* (front (fr) and back (ba) part) from human genomic DNA, introducing Xho1 and Not1 restriction sites (bold). C) Primers used for site mutagenesis of predicted miR-497 and miR-30a binding sites in *IRS1*, *IRS2*, *IGF1Rfr* and *IGF1Rba* 3'UTR constructs.



Supplemental Table 2: Differentially expressed miRNAs between myxoid/round cell liposarcomas and normal fat.

	miRNA	Down in MyxRound vs. Fat	Up in MyxRound vs. Fat	Parametric p-value	FDR	Genomic Location
1	hsa-miR-29a	7.10		< 1e-07	< 1e-07	7-q32.3
2	hsa-miR-485-5p		6.79	< 1e-07	< 1e-07	14-q32.31
3	hsa-miR-144	6.23		< 1e-07	< 1e-07	17-q11.2
4	hsa-miR-216a		5.44	1.80E-05	0.000554	2-p16.1
5	hsa-miR-22	4.64		< 1e-07	< 1e-07	17-p13.3
6	hsa-miR-141	4.31		0.0009	0.011196	12-p13.31
7	hsa-miR-29c	4.20		< 1e-07	< 1e-07	1-q32.2
8	hsa-miR-190b		3.69	0.000373	0.007496	1-q21.3
9	hsa-miR-451	3.50		0.000397	0.007496	17-q11.2
10	hsa-miR-143	3.31		1.10E-06	5.36E-05	5-q33.1
11	hsa-miR-422a		3.19	0.000599	0.008965	15-q22.31
12	hsa-miR-576-5p	2.92		0.002152	0.020302	4-q25
13	hsa-miR-181a		2.88	4.00E-07	2.34E-05	1-q31.3; 9-q33.3
14	hsa-miR-29b	2.83		< 1e-07	< 1e-07	7-q32.3; 1-q32.2
15	hsa-miR-24	2.68		< 1e-07	< 1e-07	9-q22.32; 19-p13.12
16	hsa-miR-27a	2.65		9.00E-07	4.79E-05	19-p13.12
17	hsa-miR-376a	2.56		0.000464	0.007867	14-q32.31
18	hsa-miR-145	2.47		1.04E-05	0.000338	5-q33.1
19	hsa-miR-23b	2.37		2.00E-07	1.30E-05	9-q22.32
20	hsa-miR-34b		2.32	0.004143	0.031888	11-q23.1
21	hsa-miR-27a*		2.31	0.000367	0.007496	19-p13.12
22	hsa-miR-146b-5p	2.31		0.001463	0.015561	10-q24.32
23	hsa-miR-101	2.29		2.05E-05	0.0006	1-p31.3; 9-p24.1
24	hsa-miR-92b*		2.28	0.003659	0.029325	1-q22
25	hsa-miR-126	2.25		0.001629	0.016561	9-q34.3
26	hsa-miR-200b	2.19		0.000813	0.010808	1-p36.33
27	hsa-miR-543		2.16	0.001131	0.012978	14-q32.31
28	hsa-miR-27b	2.16		1.00E-07	7.30E-06	9-q22.32
29	hsa-miR-200a	2.13		0.000965	0.011763	1-p36.33
30	hsa-miR-222	2.12		5.00E-06	0.000195	X-p11.3
31	hsa-miR-146a	2.09		4.30E-06	0.00018	5-q33.3
32	hsa-miR-202		2.09	0.000396	0.007496	10-q26.3
33	hsa-miR-652	2.07		6.80E-06	0.000249	X-q22.3
34	hsa-miR-23a	2.05		8.50E-06	0.000293	19-p13.12
35	hsa-miR-100	2.03		0.001332	0.014701	11-q24.1
36	hsa-miR-195*		2.03	0.000397	0.007496	17-p13.1
37	hsa-miR-424*		1.97	2.70E-06	0.000122	X-q26.3
38	hsa-miR-10a	1.96		0.000149	0.003477	17-q21.32

Supplemental Table 2: Differentially expressed miRNAs between myxoid/round cell liposarcomas and normal fat. (Continued)

miRNA	Down in MyxRound vs. Fat	Up in MyxRound vs. Fat	Parametric p-value	FDR	Genomic Location
39 hsa-miR-30a	1.95		8.12E-05	0.002159	6-q13
40 hsa-miR-142-3p	1.93		0.000114	0.002897	17-q22
41 hsa-miR-377*		1.88	0.000538	0.008513	14-q32.31
42 hsa-miR-200c	1.88		0.008704	0.05378	12-p13.31
43 hsa-miR-593*		1.81	0.004315	0.032359	7-q32.1
44 hsa-miR-16	1.80		5.14E-05	0.001432	13-q14.3; 3-q26.1
45 hsa-miR-638	1.80		0.020927	0.103749	19-p13.2
46 hsa-miR-93		1.78	0.003114	0.0253	7-q22.1
47 hsa-miR-491-3p	1.78		0.030547	0.129971	9-p21.3
48 hsa-miR-26a	1.76		0.000772	0.010506	3-p22.2; 12-q14.1
49 hsa-miR-631		1.71	0.002513	0.021694	15-q24.2
50 hsa-miR-126*	1.70		0.000471	0.007867	9-q34.3

Listed are all 50 miRNAs ($p \leq 0.03$, fold change $\geq 1.7x$) that are differentially expressed between myxoid/round cell liposarcomas and fat, and are used in supervised hierarchical clustering (Figure 1B). P-values of two-sample t-test and false discovery rate p-value (FDR), as well as fold change in miRNA expression and miRNA genomic locations are indicated.

Supplemental Table 3: FUS-CHOP regulated miRNAs.

SW684	Parametric p-value	Fold change down in FUS-CHOP OE	Fold change up in FUS-CHOP OE	miRNA	Genomic Location
1	0.008811	2.00		hsa-miR-381	14-q32.31
2	0.017735	1.91		hsa-miR-377*	14-q32.31
3	0.031524		1.66	hsa-miR-634	17-q24.2
4	0.038615		1.63	hsa-miR-518a-3p	19-q13.41

SW872	Parametric p-value	Fold change down in FUS-CHOP OE	Fold change up in FUS-CHOP OE	miRNA	Genomic Location
1	0.00012	2.79		hsa-miR-671-5p	7-q36.1
2	0.000266	3.59		hsa-miR-497	17-p13.1
3	0.00404	2.01		hsa-miR-135b*	1-q32.1
4	0.004128		1.92	hsa-let-7e	19-q13.33
5	0.004491	1.99		hsa-miR-185*	22-q11.21
6	0.005937	2.07		hsa-miR-146b-5p	10-q24.32
7	0.008486	2.21		hsa-miR-490-3p	7-q33
8	0.009074	2.13		hsa-miR-214	1-q24.3
9	0.013218	2.26		hsa-miR-922	3-q29

Supplemental Table 3: FUS-CHOP regulated miRNAs. (Continued)

SW872	Parametric p-value	Fold change down in FUS-CHOP OE	Fold change up in FUS-CHOP OE	miRNA	Genomic Location
10	0.013691	1.62		hsa-miR-31	9-p21.3
11	0.01395		1.69	hsa-miR-574-5p	4-p14
12	0.014656		1.71	hsa-miR-221*	X-p11.3
13	0.016005	1.63		hsa-miR-16	13-q14.3; 3-q26.1
14	0.016041		2.19	hsa-miR-412	14-q32.31
15	0.01667	1.96		hsa-miR-320	8-p21.3
16	0.020105		1.59	hsa-miR-520c-3p	19-q13.41
17	0.023293	1.59		hsa-miR-30c	1-p34.2; 6-q13
18	0.02402	1.72		hsa-miR-107	10-q23.31
19	0.02498	1.66		hsa-miR-30a	6-q13
20	0.026118		1.64	hsa-miR-503	X-q26.3
21	0.03055	1.62		hsa-miR-432	14-q32.31
22	0.033925		1.47	hsa-miR-302c*	4-q25
23	0.035117	1.60		hsa-miR-146a	5-q33.3
24	0.035442		1.73	hsa-miR-574-3p	4-p14
25	0.037393		1.50	hsa-miR-146b-3p	10-q24.32
26	0.03977	1.70		hsa-miR-25*	7-q22.1
27	0.041437		1.64	hsa-miR-328	16-q22.1
28	0.041566		1.56	hsa-miR-16-2*	3-q26.1
29	0.041924	1.67		hsa-miR-34b	11-q23.1
30	0.042249		1.50	hsa-miR-656	14-q32.31
31	0.043397	1.56		hsa-miR-124	8-p23.1; 8-q12.3; 20-q13.33
32	0.046193		1.54	hsa-miR-765	1-q23.1

402	Parametric p-value	Fold change down in shRNA FUS-CHOP	Fold change up in shRNA FUS-CHOP	miRNA	Genomic Location
1	< 1e-07	34.32		hsa-miR-886-3p	5q31.2
2	< 1e-07	40.99		hsa-miR-886-5p	5q31.2
3	0.000238		2.17	hsa-miR-183*	7-q32.2
4	0.000298		2.76	hsa-miR-30a	6-q13
5	0.000448		1.94	hsa-miR-103	5-q35.1; 20-p13
6	0.000473	2.09		hsa-miR-7-2*	15-q26.1
7	0.000629		1.76	hsa-miR-320	8-p21.3
8	0.000886		2.04	hsa-miR-9*	1-q22; 5-q14.3; 15-q26.1
9	0.001222		1.69	hsa-miR-145*	5-q33.1
10	0.00126		1.78	hsa-miR-130b	22-q11.21

Supplemental Table 3: FUS-CHOP regulated miRNAs. (Continued)

402	Parametric p-value	Fold change down in shRNA FUS-CHOP	Fold change up in shRNA FUS-CHOP	miRNA	Genomic Location
11	0.002593		2.24	hsa-miR-766	X-q24
12	0.00271		1.84	hsa-miR-149*	2-q37.3
13	0.002945		1.68	hsa-miR-23a	19-p13.12
14	0.003861		1.94	hsa-miR-638	19-p13.2
15	0.00427		2.12	hsa-miR-574-3p	4-p14
16	0.004279		1.62	hsa-miR-491-3p	9-p21.3
17	0.004757		2.32	hsa-miR-193a-3p	17-q11.2
18	0.005035		1.77	hsa-miR-30c	1-p34.2; 6-q13
19	0.005066	1.55		hsa-miR-142-5p	17-q22
20	0.005075		2.17	hsa-miR-765	1-q23.1
21	0.005344		1.79	hsa-miR-503	X-q26.3
22	0.006289	1.66		hsa-miR-526b*	19-q13.41
23	0.006923		1.66	hsa-miR-720	3-q26.1
24	0.008388		1.57	hsa-miR-363*	X-q26.2
25	0.008701	1.55		hsa-miR-524-5p	19-q13.41
26	0.010185	1.63		hsa-miR-625	14-q23.3
27	0.011373		1.68	hsa-miR-26b	2-q35
28	0.012259	1.80		hsa-miR-920	12-p12.1
29	0.012898		1.44	hsa-miR-542-3p	X-q26.3
30	0.01859	1.47		hsa-miR-600	9-q33.2
31	0.018933	1.53		hsa-miR-136	14-q32.31
32	0.019128	1.45		hsa-miR-553	1-p21.2
33	0.020097		1.51	hsa-miR-490-5p	7-q33
34	0.020315		1.67	hsa-miR-21	17-q23.1
35	0.020432		1.90	hsa-miR-32*	9-q31.3
36	0.020451		1.66	hsa-miR-21*	17-q23.1
37	0.022828		1.67	hsa-miR-488	1-q25.2
38	0.023006		2.05	hsa-miR-634	17-q24.2
39	0.023116	1.64		hsa-miR-620	12-q24.21
40	0.024036	1.47		hsa-miR-662	16-p13.3
41	0.024651		1.48	hsa-miR-140-5p	16-q22.1
42	0.024746		1.54	hsa-miR-129-5p	7-q32.1; 11-p11.2
43	0.025106		1.89	hsa-miR-671-5p	7-q36.1
44	0.026323	1.58		hsa-miR-551b*	3-q26.2
45	0.026465		1.43	hsa-miR-328	16-q22.1
46	0.027103	1.42		hsa-miR-526b	19-q13.41
47	0.028605	1.49		hsa-miR-100	11-q24.1



Supplemental Table 3: FUS-CHOP regulated miRNAs. (Continued)

402	Parametric p-value	Fold change down in shRNA FUS-CHOP	Fold change up in shRNA FUS-CHOP	miRNA	Genomic Location
48	0.029046		1.67	hsa-miR-93	7-q22.1
49	0.029942	1.47		hsa-miR-185	22-q11.21
50	0.032694		1.68	hsa-miR-574-5p	4-p14
51	0.032917	1.74		hsa-miR-922	3-q29
52	0.034757		1.44	hsa-miR-877*	6-p21.33
53	0.034984	1.50		hsa-miR-425*	3-p21.31
54	0.035529		1.56	hsa-miR-30b*	8-q24.22
55	0.03575		1.53	hsa-miR-523	19-q13.41
56	0.035923		1.53	hsa-miR-620	12-q24.21
57	0.036309		1.89	hsa-miR-497	17-p13.1
58	0.037261		1.45	hsa-miR-19a	13-q31.3
59	0.037345		1.36	hsa-miR-30d	8-q24.22
60	0.038628		1.41	hsa-miR-500	X-p11.23
61	0.038896		1.36	hsa-miR-548b-3p	6-q22.31
62	0.039386	1.38		hsa-miR-214	1-q24.3
63	0.039967		1.44	hsa-miR-148b	12-q13.13
64	0.040324		1.51	hsa-miR-34b	11-q23.1
65	0.041748		1.68	hsa-miR-130a	11-q12.1
66	0.044842		1.33	hsa-miR-371-3p	19-q13.41
67	0.045232	1.37		hsa-miR-338-3p	17-q25.3
68	0.046412	1.61		hsa-miR-549	15-q25.1
69	0.048085		1.41	hsa-miR-656	14-q32.31
70	0.049013		1.60	hsa-miR-1908	11-q12.2
71	0.049648		1.45	hsa-miR-296-5p	20-q13.32


1765	Parametric p-value	Fold change down in shRNA FUS-CHOP	Fold change up in shRNA FUS-CHOP	miRNA	Genomic Location
1	0.000867		2.79	hsa-miR-497	17-p13.1
2	0.002031		2.13	hsa-miR-135b*	1-q32.1
3	0.002992		2.04	hsa-let-7a	9-q22.32; 11-q24.1; 22-q13.31
4	0.003821	1.74		hsa-miR-424*	X-q26.3
5	0.007186		2.09	hsa-miR-222	X-p11.3
6	0.007694	1.67		hsa-miR-125a-3p	19-q13.33
7	0.008446	1.73		hsa-miR-7-2*	15-q26.1
8	0.00884		1.73	hsa-miR-708	11-q14.1
9	0.011712	1.52		hsa-miR-654-5p	14-q32.31

Supplemental Table 3: FUS-CHOP regulated miRNAs. (Continued)

1765	Parametric p-value	Fold change down in shRNA FUS-CHOP	Fold change up in shRNA FUS-CHOP	miRNA	Genomic Location
10	0.011754		1.71	hsa-let-7d*	9-q22.32
11	0.011775		1.59	hsa-miR-31	9-p21.3
12	0.012743		1.59	hsa-miR-888*	X-q27.3
13	0.012974		1.69	hsa-miR-155	21-q21.3
14	0.014579	1.65		hsa-miR-29b-1*	7-q32.3
15	0.016245	1.74		hsa-miR-936	10-q25.1
16	0.017242	1.74		hsa-miR-939	8-q24.3
17	0.019098	1.56		hsa-miR-132*	17-p13.3
18	0.021473	1.54		hsa-let-7i	12-q14.1
19	0.022689	1.59		hsa-miR-30c-2*	6-q13
20	0.022718	1.57		hsa-miR-629	15-q23
21	0.023112	1.94		hsa-miR-32*	9-q31.3
22	0.023393	1.59		hsa-miR-298	20-q13.32
23	0.024217	1.46		hsa-miR-576-5p	4-q25
24	0.027633	1.44		hsa-miR-16-1*	13-q14.3
25	0.028691		1.85	hsa-miR-203	14-q32.33
26	0.02915	1.46		hsa-miR-526b	19-q13.41
27	0.029261	1.47		hsa-miR-376a*	14-q32.31
28	0.031656		1.40	hsa-miR-135b	1-q32.1
29	0.035559		1.78	hsa-miR-185*	22-q11.21
30	0.035907	1.51		hsa-miR-198	3q13.33
31	0.036872	1.62		hsa-miR-16-2*	3-q26.1
32	0.037336		1.72	hsa-miR-34b	11-q23.1
33	0.040544	1.65		hsa-miR-98	X-p11.22
34	0.041688		1.53	hsa-miR-331-5p	12-q22
35	0.042704		1.40	hsa-miR-601	9-q33.2
36	0.042719	1.51		hsa-miR-559	2-p21
37	0.043629	1.47		hsa-miR-106a*	X-q26.2
38	0.045993	1.43		hsa-miR-302c*	4-q25
39	0.046331	1.42		hsa-miR-338-5p	17-q25.3
40	0.047285		1.52	hsa-miR-30a	6-q13

Differentially expressed miRNAs ($p < 0.05$) between pcDNA3 empty vector control and pcDNA3/FUS-CHOP transfected SW684 (fibrosarcoma) and SW872 (liposarcoma) cell lines, and between pLKO.1/empty vector control and pLKO.1/shRNA FUS-CHOP transfected MLS 402-91 and MLS 1765-92 (myxoid liposarcoma) cell lines, as determined by microarray analysis. For each cell line it was determined which miRNAs were significantly deregulated during FUS-CHOP overexpression or knock-down. P-values of two-sample t-test, fold change in miRNA expression, and genomic location of the miRNA are indicated. MiR-497, miR-30a and miR-34b, which are deregulated in SW872, MLS 402-91 and MLS 1765-92 cells upon modulation of FUS-CHOP levels, are indicated in bold.





```

IRS1 – miR-30a conserved site: position 139-161
5' GCATCCATTTCAGTTTGTACT IRS1 – WT m30a site
   ||||| | || |||||
3' GAAGGUCAGCUCCUACAAAUGU miR-30a
   ||||| | || ||X|XX|
5' GCATCCATTTCAGTTTGATATCT IRS1-m30a-mut

IRS1 – miR-497 conserved site: position 360-382
5' AAGATACATTTTCATCTGCTGCTG IRS1 – WT m497 site
   | | | | | | | | | |
3' UGUUUGGUGUCACACGACGAC miR-497
   | | | | | | | | | |
5' AAGATACATTTTCATCTCGAGCTG IRS1-m497-mut

IRS2 – miR-30a conserved site: position 2054-2076
5' TACATTTTAAATTTAGTTTACAG IRS2 – WT m30a site
   | | | | | | | | | |
3' GAAGGUCAGCUCCUACAAAUGU miR30a
   | | | | | | | | | |
5' TACATTTTAAATTTAGAATTCAG IRS2-m30a-mut

IRS2 – miR-497 conserved site: position 2331-2353
5' TAGGGGTCAATGTGATGCTGCTG IRS2 – WT m497 site
   | | | | | | | | | |
3' UGUUUGGUGUCACACGACGAC miR-497
   | | | | | | | | | |
5' TAGGGGTCAATGTGATGCTCGAG IRS2-m497-mut

IGF1R – miR-497 conserved site: position 1254-1277
5' TACAGAAAAAAAAAAGCTGCTAT IGF1Rfr – WT m497 site
   ||| | | | | | | | | |
3' UGUUUGGUGUCACACGACGAC miR-497
   ||| | | | | | | | | |
5' TACAGAAAAAAAAAAGGTACCAT IGF1Rfr-m497-mut

IGF1R – miR-497 poorly conserved site: position 711-733
5' CGACTGCCCTGCTGTGCTGCTC IGF1Rfr – WT m497 site 2
   || || | | | | | | | |
3' UGUUUGGUGUCACACGACGAC miR-497
   || || | | | | | | | |
5' CGACTGCCCTGCTGTGGTACCC IGF1Rfr-m497-mut2

IGF1R – miR-30a conserved site: position 5614-5636
5' GTTGACGAAGATCTGGTTACAA IGF1Rba – WT m30a site
   || | | | | | | | | | |
3' GAAGGUCAGCUCCUACAAAUGU miR-30a
   || | | | | | | | | | |
5' GTTGACGAAGATCTGGATATCAA IGF1Rba-m30a-mut

```

Supplemental Figure 1: 3'UTRs of IRS1, IRS2 and IGF1R with predicted target sites for miR-497 and miR-30a.

Predicted 3'UTR target sites in IRS1, IRS2 and IGF1R for miR-497 and miR-30a and the mutations that have been generated in the target site sequence where the miRNA seed sequence (bold) binds. Only conserved miRNA binding sites were mutated, as well as one poorly conserved miR-497 site in the 3'UTR of IGF1R, which is positioned in the front part of the 3'UTR. The wild-type (WT) and mutated (mut) sites are indicated. The vertical lines represent possible base pairing between miRNA and 3'UTR target site, and the x's indicate abrogated base pairing where nucleotides are mutated. The resulting mutated 3'UTR fragments were cloned into the psiCHECK-2 luciferase reporter.

Chapter 4

MIR-17-92 AND MIR-221/222 CLUSTER MEMBERS TARGET KIT AND ETV1 IN HUMAN GASTROINTESTINAL STROMAL TUMORS



Caroline M.M. Gits, Patricia F. van Kuijk, Moniek B.E. Jonkers, Antonius W.M. Boersma, Wilfred F.J. van IJcken, Agnieszka Wozniak, Raf Sciot, Piotr Rutkowski, Patrick Schöffski, Takahiro Taguchi, Ron H.J. Mathijssen, Jaap Verweij, Stefan Sleijfer, Maria Debiec-Rychter, Erik A.C. Wiemer

ABSTRACT

Background: Gastrointestinal stromal tumors (GIST) are characterized by high expression of KIT and ETV1, which cooperate in GIST oncogenesis. Our aim was to identify microRNAs that are deregulated in GIST, play a role in GIST pathogenesis, and could potentially be used as therapeutic tool.

Methods: Differentially expressed microRNAs between primary GIST (n=50) and gastrointestinal leiomyosarcomas (GI-LMS, n=10) were determined using microarrays. Selected microRNA mimics were transfected into GIST-882 and GIST-T1 cell lines to study the effects of microRNA overexpression on GIST cells. Luciferase reporter assays were used to establish regulation of target genes by selected microRNAs.

Results: MiR-17-92 and miR-221/222 cluster members were significantly ($p < 0.01$) lower expressed in GIST *versus* GI-LMS and normal gastrointestinal control tissues. MiR-17/20a/222 overexpression in GIST cell lines severely inhibited cell proliferation, affected cell cycle progression, induced apoptosis and strongly downregulated protein and – to a lesser extent – mRNA levels of their predicted target genes *KIT* and *ETV1*. Luciferase reporter assays confirmed direct regulation of *KIT* and *ETV1* by miR-222 and miR-17/20a, respectively.

Conclusion: MicroRNAs that may play an essential role in GIST pathogenesis were identified, in particular miR-17/20a/222 that target *KIT* and *ETV1*. Delivering these microRNAs therapeutically could hold great potential for GIST management, especially in imatinib-resistant disease.



INTRODUCTION

Gastrointestinal stromal tumors (GIST) are the most common mesenchymal tumors of the gastrointestinal (GI) tract. GIST originate from the interstitial cells of Cajal (ICC), or their precursor stem cells.¹⁻³ ICC operate as pacemaker cells of the GI-tract inducing the peristaltic movements. They show immunophenotypical and ultrastructural features of both smooth muscle and neuronal differentiation and reside between the circular and longitudinal muscle layers of the GI-tract.⁴⁻⁶ Therefore, GIST were initially commonly classified as gastrointestinal leiomyosarcomas (GI-LMS).

In contrast to GI-LMS and other soft tissue sarcomas, a common (>95%) feature of GIST is the expression of v-kit Hardy-Zuckerman 4 feline sarcoma viral oncogene homolog (KIT), a tyrosine kinase receptor.^{3, 6-7} KIT expression is also a characteristic of ICC and other cell types like hematopoietic stem cells, melanocytes, mast cells and germ cells. In all these cells ligand-dependent activation of KIT signalling is important for proliferation, differentiation and survival. In addition to KIT expression, spontaneous gain-of-function mutations in *KIT* (~80%) or platelet-derived growth factor receptor alpha (*PDGFRA*; ~10%) are frequently found in GIST. These mutations, which are mutually exclusive and have similar biological functions, are considered oncogenic drivers of GIST.^{3, 5-6, 8-10} The mutant receptors display constitutive kinase activity, which is independent of growth factor binding. Thereby downstream signaling pathways like the RAS-RAF-MAPK pathway, the PI3K-AKT pathway and the STAT3 transcription factor are activated, giving rise to increased cell proliferation and survival.

In a small subset of GIST without mutations in *KIT* and *PDGFRA* (wild-type (WT)-GIST), other genes are thought to play a role in the tumorigenesis. Mutated genes found in WT-GIST include *BRAF*^{V600E} and succinate dehydrogenase subunits B, C and D (*SDHB*, *SDHC*, *SDHD*).¹⁴⁻¹⁵

Recently, another factor was identified to play a role in the tumor biology of GIST. ETV1 cooperates with KIT and is essential both in normal ICC development as well as in GIST oncogenesis.¹⁶ ETV1 is a member of the ETS family of transcription factors, which are frequently deregulated in human malignancies and have a characteristic highly conserved DNA-binding (ETS) domain.¹⁷ Like KIT, ETV1 is highly expressed in ICC and GIST, where it is a master regulator of ICC/GIST-specific transcriptional networks. Normal WT-KIT and ETV1 levels will ensure natural ICC development. Mutated KIT prolongs ETV1 protein stability, thereby leading to over-activation of ETV1 mediated transcriptional programs, which induce hyperplasia and finally GIST formation.¹⁶

Although many aspects of the tumor biology of GIST have been elucidated, some issues remain. One of these is the underlying mechanism causing overexpression of KIT and ETV1. Since KIT (and most likely ETV1) overexpression is rarely caused by gene amplification, it is postulated



that other mechanisms like transcriptional or translational regulation, or processes that act on RNA stability may be involved.¹⁸ MicroRNAs (miRNAs) may influence KIT and/or ETV1 expression as they are non-protein coding RNAs, that bind to (partially) complementary sites in 3'UTRs of target mRNAs causing translational inhibition and/or mRNA degradation. In recent years miRNAs have been implicated in a wide range of important cellular processes like proliferation, differentiation, apoptosis and stem cell maintenance. Their expression is cell type specific and often deregulated in disease, including cancer, in which miRNAs can function as oncogene or tumor suppressor.¹⁹⁻²¹ MiRNA expression patterns of GIST have been associated with genomic changes and biological behavior.²²⁻²³ Downregulation of miR-494, as well as the miR-221/222 cluster, have been correlated with KIT protein expression in GIST.²⁴⁻²⁵

In this study we aimed to get more insight into the potential role of miRNAs in GIST. We compared the miRNA expression profiles of GIST and GI-LMS samples to identify miRNAs that could be of biological importance in GIST. We focussed on the differentially expressed miR-17-92 and miR-221/222 clusters, which have relatively low expression levels in GIST and potentially target both KIT and ETV1.

MATERIALS & METHODS

Tumor samples

Frozen specimens of 50 primary GIST and 10 GI-LMS were obtained from the tissue banks of the Department of Pathology of University Hospital of Leuven, Belgium, and the Department of Soft Tissue / Bone Sarcoma and Melanoma, Institute of Oncology, Warsaw, Poland. All patients gave written informed consent and approval was obtained from the University Hospital Leuven ethics committee (ML7481) and Institute of Oncology, Warsaw, Poland. Diagnosis of GI-LMS was based on morphological features and immunophenotype (desmin and h-caldesmon immunopositive; S100, CD34, CD117/KIT and DOG1 immunonegative). GIST diagnosis was based on histological features and immunostaining (CD117/KIT and DOG1 immunopositive) and the presence of KIT or PDGFRA mutations. Tumor samples contained >80% tumor cells. In addition, frozen specimens of five normal gastric and five normal small intestinal control tissues were obtained from the Erasmus MC Tissue Bank. The study was approved by the Medical Ethical Review Board of the Erasmus University Medical Center.

RNA isolation

Total RNA was isolated by standard RNeasy (Qiagen, Crawley, UK) extraction. In short, frozen tissues were homogenized in RNeasy lysis buffer after which chloroform was added. Phase separation by centrifugation was followed by RNA precipitation using isopropanol. The RNA pellet was washed twice in 75% EtOH and dissolved in nuclease free water. RNA concentration and quality were tested on Nanodrop-1000 (Nanodrop Technologies, Wilmington, DE, USA).

MiRNA microarray

One μg total RNA was fluorescently labeled with Cy3 using Kreatech ULS™ aRNA Labeling Kit (Kreatech Diagnostics, Amsterdam, Netherlands) following the standard protocol. Labeled RNA was hybridized in a Tecan HS4800 hybridization station to in-home spotted array slides²⁶ with locked nucleic acid (LNA™) modified oligonucleotide capture probes (Exiqon, Vedbaek, Denmark) capable of detecting 725 human miRNAs in duplicate. Slides were scanned using a Tecan LS Reloaded scanner and median spot intensity was determined using ImaGene software (BioDiscovery Inc., Hawthorne, CA, USA). After background subtraction, values were quantile normalized by R software, bad spots were deleted, and duplicate spots were averaged. For each value, the ratio to the geometric mean of the miRNA was log₂ transformed. These values were used to determine differentially expressed miRNAs and to perform statistical testing by a two-sample t-test in BRB-Array Tools (Microsoft Excel plug-in). Hierarchical clustering analyses were performed in Spotfire (Spotfire DecisionSite 9.1, Tibco Software, Somerville, MA, USA). Boxplots were created in SPSS (IBM Corporation, Armonk, NY, USA).

qPCR analysis of miRNAs

RNA (50ng) was reverse transcribed by using specific miRNA primers from the TaqMan® MicroRNA Assays for hsa-miR-17, hsa-miR-20a, hsa-miR-222 and RNU48 and reagents from the TaqMan® MicroRNA Reverse Transcription Kit (both Applied Biosystems, Nieuwerkerk aan den IJssel, Netherlands) according to the manufacturer's protocol. The resulting cDNA was used in a Quantitative Real-Time PCR (qPCR) with the primer/probe mix from the TaqMan® MicroRNA Assay together with the TaqMan® Universal PCR Master Mix No AmpErase® UNG using the 7500 Fast Real-Time PCR system (all Applied Biosystems) according to the manufacturer's protocol. qPCR data were analyzed with SDS software (Applied Biosystems). MiRNA expression was normalized using RNU48 expression and the comparative C_T -method.²⁷

qPCR analysis of mRNAs

RNA (1 μg) was reverse transcribed using the TaqMan® Reverse Transcription Reagents (Applied Biosystems) according to the manufacturer's protocol. The resulting cDNA was used to perform qPCR using the primer/probe mix from the TaqMan® Gene Expression Assays of human *KIT* and *ETV1* (with exon spanning probes) and TaqMan® Universal PCR Master Mix using the 7500 Fast Real-Time PCR system (all Applied Biosystems) according to the manufacturer's protocol. Three housekeepers (*GAPDH*, *HPRT* and *HMBS*) were analyzed for normalization purposes using the comparative C_T -method.²⁷ qPCR data was analyzed with SDS software (Applied Biosystems).

Cell culture

The GIST-T1 cell line was provided by Dr. T. Taguchi (Kochi University, Japan). This *KIT* exon 11 mutant cell line is characterized by a heterozygous deletion of 57 bases.²⁸ The GIST-882 was



kindly provided by Dr. J. Fletcher (Dana-Farber Cancer Institute, Boston, MA, USA). This cell line is characterized by a *KIT* exon 13 missense mutation, resulting in a single amino acid K642E substitution in the proximal part of the cytoplasmic split tyrosine kinase domain.²⁹ Both cell lines were cultured in RPMI 1640 (Invitrogen, Bleiswijk, Netherlands) supplemented with 10% fetal bovine serum, at 37°C, 5% CO₂. The imatinib resistant GIST-T1-R cell line was provided by Dr. S. Bauer (West-German Cancer Center, University Duisburg-Essen, University Hospital Essen, Germany). The GIST-T1-R is derived from GIST-T1 and contains secondary *KIT* exon 17 mutations causing imatinib resistance. GIST-T1-R is cultured in RPMI/HAM-F12 (Invitrogen), supplemented with 20% fetal bovine serum, in the presence of 1µM imatinib, at 37°C, 5% CO₂.

4

Mimic transfections

MIRIDIAN microRNA mimics (Thermo Scientific, Etten-Leur, Netherlands) of hsa-miR-17, hsa-miR-20a, and hsa-miR-222 and miRIDIAN microRNA Mimic Negative Control #1 (Thermo Scientific) were transfected in a final concentration of 50 nM using DharmaFECT1 transfection reagent (Thermo Scientific) 24h after cell seeding. For both cell lines transfection efficiency was optimized to >95% using fluorescent mimics and increased expression levels of miR-17, miR-20a and miR-222 in transfected cells were verified by qPCR.

SRB assay

Cell density was monitored by a sulforhodamine B (SRB) assay at 24h, 48h, 72h and 96h post-transfection.³⁰ In short, cells were fixed by 10% TCA in PBS, washed with half warm tap water, stained by 0.4% SRB in 1% acetic acid for 15min, washed in 1% acetic acid and dried. Color was released from the cells by 10 mM Tris-Base, after which A540nm was measured on a spectrophotometer. Three independent experiments were performed, and representative graphs are shown.

Cell cycle assay

Cells were harvested by trypsinization 72h post-transfection, fixed in 70% ethanol for 15min, washed in PBS and resuspended in PBS/RNase/Propidium Iodide (PI) (20 µg/ml RNase, 50 µg/ml PI, 1% fetal bovine serum). PI staining was FACS-analyzed using a 488 nm laser with emission filters LP655 and BP695/40 (flowcytometer FACS Aria III, BD Biosciences, Breda, Netherlands) and analyzed by FlowJo software (Tree Star, Inc., Ashland, USA). Experiments were performed three times and representative figures are shown.

Apoptosis assay

Cells were harvested by trypsinization 72h post-transfection, and stained with FITC-Annexin V and PI by using the FITC-Annexin V Apoptosis Detection Kit I (BD Biosciences), following the manufacturer's protocol. In short, cells were washed in PBS and resuspended in 1x Binding

Buffer. FITC-Annexin V and PI were added to the solution ($\sim 10^5$ cells) and incubated on ice for 15min in the dark. More binding buffer was added before analysis using a 488nm laser with emission filters LP520 nm and BP530/30 nm (flowcytometer FACS Aria III, BD Biosciences). Three independent experiments were performed and representative figures are shown.

Protein extraction

Cells were harvested in MCB lysis buffer (50mM Tris-HCl pH 7.5, 50mM NaCl, 10% glycerol, 1% NP-40, 0.5% Na-deoxycholate, 20mM NaF) supplemented with a cocktail of protease and phosphatase inhibitors. Lysates were thoroughly vortexed and further lysed by two subsequent freeze-thaw cycles using liquid nitrogen. Cell debris was spun down and protein concentration was determined by a Bradford assay (BioRad, Veenendaal, Netherlands).

Western blotting

Thirty μ g of total protein was subjected to SDS-PAGE. Proteins were transferred to a PVDF membrane followed by blocking of the membrane in 5% non-fat dry milk in PBS-Tween (PBS, 0.05% Tween 20) to prevent non-specific antibody binding. Primary and secondary antibody incubations were carried out in the same buffer using anti-CD117/c-kit (YR145, rabbit monoclonal, 1:500, Cell Marque, Rocklin, CA, USA), anti-ER81/ETV1 (ab81086, rabbit polyclonal, 1:1000, Abcam, Cambridge, UK) and anti- β -Actin (AC-15, mouse monoclonal, 1:5000, Sigma-Aldrich, Zwijndrecht, Netherlands) as a loading control. As secondary antibody HRP-conjugated goat-anti-mouse (1:10000, Santa Cruz Biotechnology, Heidelberg, Germany) or goat-anti-rabbit (1:10000, Jackson Immunoresearch, Suffolk, UK) antibodies were used. Antibody incubations were followed by enhanced chemoluminescence (Supersignal West Pico Chemiluminescent Substrate, Thermo Scientific) and visualized on film (Amersham Hyperfilm ECL, GE Healthcare, Diegem, Belgium).

Cloning

Fragments of the 3'UTR of *ETV1* (ETV1short: 708bp fragment, ETV1long: 3721bp fragment) and *KIT* (KITshort: 1263bp fragment, KITlong: 2055bp fragment) were PCR amplified from human genomic DNA (Promega, Leiden, Netherlands) introducing a XhoI (5'-end) and a NotI site (3'-end). The PCR products were cloned in PCR[®]-Blunt (Invitrogen), followed by a XhoI and NotI restriction and ligation in the psiCHECK[™]-2 vector (Promega) behind a *Renilla* luciferase gene. The psiCHECK[™]-2 vector also contains a firefly luciferase gene, which was used for normalization. The resulting constructs are psiCHECK2/ETV1short, psiCHECK2/ETV1long, psiCHECK2/KITshort and psiCHECK2/KITlong. Site-directed mutagenesis (QuikChange II XL, site directed mutagenesis kit, Agilent Technologies, Amsterdam, The Netherlands) was performed to mutate miR-17/20a and miR-222 target sites in the 3'UTR of KIT and ETV1 (Supplemental Figure 1). Primer sequences used for cloning and mutagenesis are listed in Supplemental Table 1.



Luciferase assay

PsiCHECK™-2 constructs were transfected using Fugene HD transfection reagent (Promega) 24h after cell seeding, according to recommendations by the manufacturer. The next day, cells were transfected with hsa-miR-17, hsa-miR-20a, and hsa-miR-222 miRIDIAN mimics, a mixture of these three mimics, and miRIDIAN microRNA Mimic Negative Control #1 (Thermo Scientific) to a final concentration of 50nM using DharmaFECT1 transfection reagent (Thermo Scientific). After 48h, protein lysates were prepared in which firefly and *Renilla* luciferase activities were quantified using the Dual Luciferase® Reporter Assay System (Promega). *Renilla* luciferase expression was normalized on the firefly luciferase expression and relative luciferase signals of duplicates were averaged. Two independent experiments were normalized after which average and standard deviations were calculated. Significant differences in luciferase activity were determined by two-sample t-tests.

RESULTS

Identification of differentially expressed microRNAs between GIST and GI-LMS

In order to identify miRNAs that are specifically deregulated in GIST we compared the miRNA expression profile of primary GIST (n=50) and GI-LMS (n=10). Patients' and tumors' characteristics are listed in Table 1.

Table 1: Patients' and tumors' characteristics.

GIST		n=50			
Gender		Mutation status	Location	Risk of relapse ¹	
Male	32	KIT	Gastric	36	Overtly malignant ² 12
Female	18	- Exon 9	4 Non-gastric	High	12
		- Exon 11	26 - Colon	1 Intermediate	14
Median age [range]	65 [41-85]	- Exon 17	1 - Duodenum	2 Low	12
			- Esophagus	1	
		PDGFRA	- Small intestine	10	
		- Exon 12	1		
		- Exon 14	1		
		- Exon 18	17		
Leiomyosarcoma		n=10			
Gender			Location	Malignancy	
Male	4		Gastric	7	Overtly malignant ² 10
Female	6		Non-gastric		
			- Small intestine	3	
Median age [range]	45 [36-71]				

1. Tumor risk assessment was performed using AFIP criteria³¹

2. Recurrent or metastatic disease during clinical follow-up

MiR-17-92 and miR-221/222 cluster members distinguish GIST from GI-LMS

Strikingly, the list of differentially expressed miRNAs between GIST and GI-LMS contained a number of miRNA clusters, e.g. members of the miR-17-92 cluster (i.e. miR-17, miR-18a, miR-19a and miR-20a) and the miR-221/222 cluster (all $p < 0.01$, corrected for multiple testing $p < 0.05$). Of note, miR-494, which was previously found to inversely correlate with KIT expression,²⁵ was not differentially expressed between our groups. We focused on the miR-17-92 and miR-221/222 clusters since the latter is known for its association with KIT expression in GIST,²⁴ whereas the miR-17-92 cluster is notorious for its oncogenic role in many tumor types.³²⁻³⁵ The expression levels of these cluster members were significantly lower in GIST compared to GI-LMS (Figure 2a). Moreover, these miRNAs are predicted to target both KIT and ETV1, which are key players in GIST oncogenesis. Therefore, the loss of expression of these miRNAs in GIST could be of importance for the molecular pathogenesis of these tumors, which makes them meaningful candidates for further research.

Inhibition of cell proliferation in miR-17, miR-20a and miR-222 overexpressing cells

Three miRNAs, miR-17, miR-20a and miR-222, were selected for functional characterization, since these were the miRNAs with the highest expression fold change between GI-LMS and GIST compared to their cluster members. The downregulation of these miRNAs in GIST *versus* GI-LMS was validated by qPCR (Figure 2b, left panel). In addition, these miRNAs were downregulated in GIST compared to normal gastrointestinal tissues (Figure 2b, right panel). In contrast, in other tumor types, e.g. colorectal cancer and non-small cell lung cancer, these miRNAs were upregulated or unaltered (Supplemental Figure 2). MiRNA mimics and a scrambled control mimic were transfected into two well characterized GIST cell lines, i.e. GIST-T1 and GIST-882. Cell proliferation was monitored by SRB assays at 24h, 48h, 72h and 96h after transfection (Figure 3). In GIST-882 cells miR-17 and miR-20a induced a strong inhibition of cell proliferation compared to the negative control, whereas miR-222 only slightly reduced cell proliferation within the time frame of the experiment. In GIST-T1 cells miR-17, miR-20a and miR-222 overexpression caused a total proliferation arrest. These miRNAs also inhibited cell proliferation in GIST-T1-R cells that exhibit resistance to imatinib due to secondary *KIT* mutations (Supplemental Figure 3).



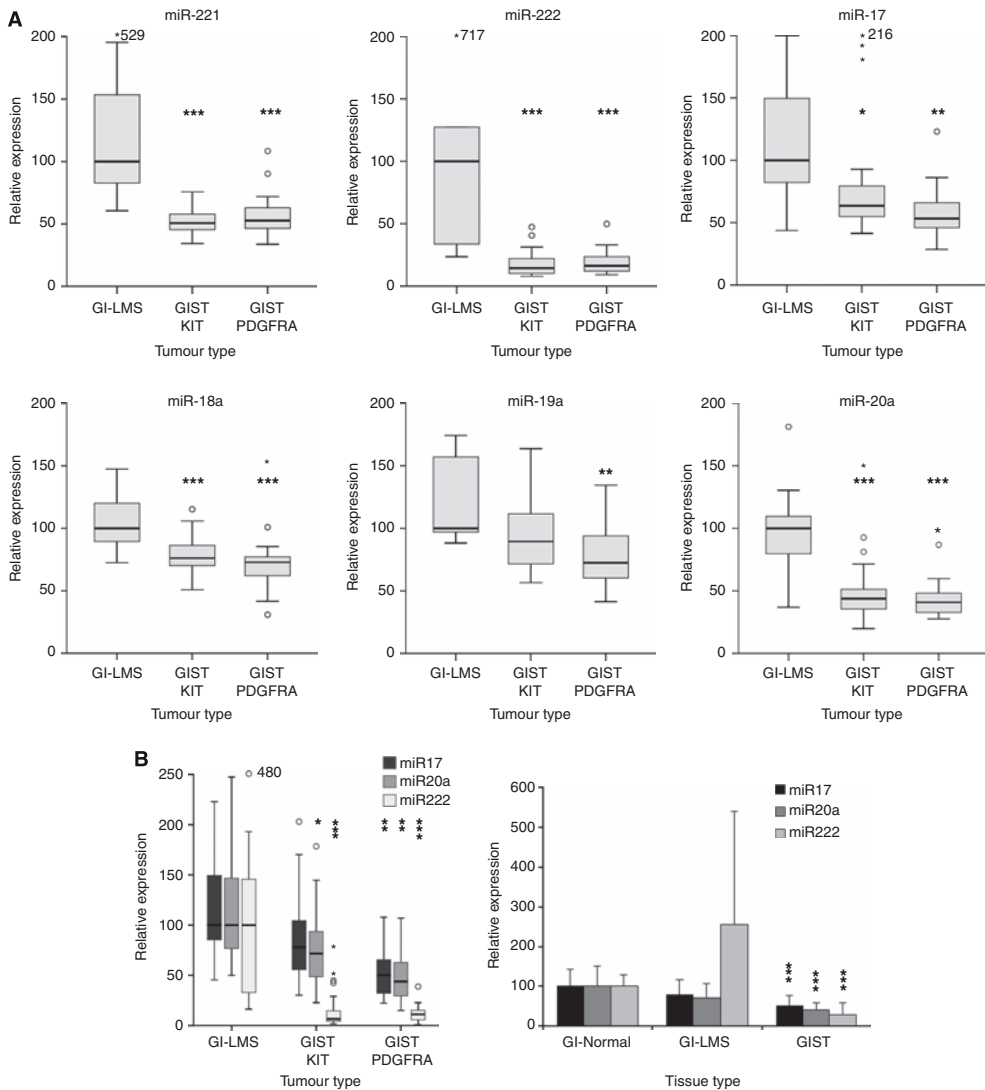


Figure 2: MiR-221/222 and miR-17-92 cluster members are downregulated in GIST compared to GI-LMS and normal GI tissues. (A) Boxplots represent miRNA microarray expression data of miR-221, miR-222, miR-17, miR-18a, miR-19a and miR-20a in GIST (n=50, either *KIT* or *PDGFRA* mutants) versus GI-LMS (n=10, median GI-LMS set at 100). (B) left panel: MiR-17, miR-20a and miR-222 downregulation in GIST versus GI-LMS is validated by qPCR. Boxes represent 25th-75th percentile, line in the box represents median (50th percentile), whiskers represent lowest and highest values within 1.5x the interquartile range, circles are outliers (between 1.5-3x interquartile range), small asterisks are extreme values (>3x interquartile range). Numbers next to circles/asterisks correspond to values beyond scale. Significant differences in miRNA levels between GI-LMS and *KIT*- or *PDGFRA*-mutant GIST is determined by Mann Whitney U tests. Right panel: MiR-17, miR-20a and miR-222 are significantly downregulated in GIST compared to normal gastrointestinal tissues (GI-normal). MiRNA expression levels of GIST/GI-LMS are relative to normal gastric (n=5) and intestinal tissues (n=5) (average GI-normal set at 100). Significant differences in miRNA levels between GIST (n=50) or GI-LMS (n=10) and GI-normal are determined by student t-tests. * = p<0.05, ** = p<0.005, *** = p<0.0005.



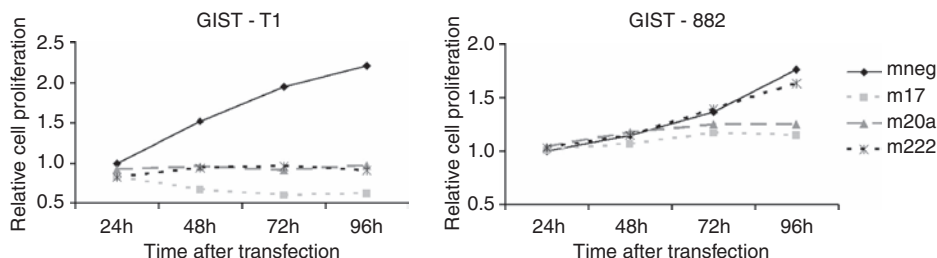


Figure 3: Reduced cell proliferation of GIST cell lines transfected with miR-17, miR-20a and miR-222 mimics. Graphs depict average cell density ($n=3$) of GIST-T1 and GIST-882 cell lines at 24h, 48h, 72h and 96h post-transfection, relative to the negative control (mneg; transfected with scrambled mimic) at 24h, which is set at 1.

Overexpression of miR-17, miR-20a and miR-222 affects the cell cycle and induces apoptosis in GIST cells

Cell cycle profiles were determined 72h post-transfection of the miR-17, miR-20a and miR-222 mimics and scrambled control mimic (Figure 4a). GIST-T1 cells showed a small but consistent decrease in the percentage of cells in G1 and G2-M when miR-17 or miR-20a were overexpressed. At the same time there was an increased sub-G1 fraction, indicative of cell death. A different effect was seen when miR-222 was overexpressed: there were just slightly more cells in the sub-G1 fraction, while there was a considerable decrease of cells in G1-phase. In addition, we observed an increased G2-M fraction indicating that cycling cells arrest in the G2-M phase when miR-222 is overexpressed.

In GIST-882 cells similar observations were made, albeit less pronounced. Since these cells proliferate less vigorously than GIST-T1 cells the G1 peak is relatively high, which influences the cell cycle profile drastically. Nevertheless, there was still an increased sub-G1 fraction and a decreased G1 fraction in miR-17 and miR-20a overexpressing cells. In miR-222 overexpressing cells there was a subtle decrease in the G1 peak, accompanied by an increased cell fraction in S-G2-M phase.

To determine the effect of miR-17, miR-20a and miR-222 overexpression on cell viability and apoptosis, GIST cells were transfected with miRNA mimics and a scrambled control mimic. Apoptosis was measured by Annexin V and PI staining determined by FACS-analysis 72h post-transfection (Figure 4b, for FACS plots see Supplemental Figure 4). In GIST-T1 cells, overexpression of the miRNAs led to a decreased population of live cells (Ann-/PI-) compared to the negative control. The early (Ann+/PI-) and late apoptotic fraction (Ann+/PI+) increased in the miRNA mimic expressing cells. These results were similar for the GIST-882 cell line, although again the effects were less pronounced. However, regardless of the increased dead cell fraction (Ann-/PI+), miR-222 overexpression did not lead to increased levels of early and late apoptotic cells in this cell line, consistent with the results from the cell proliferation and cell cycle assays.

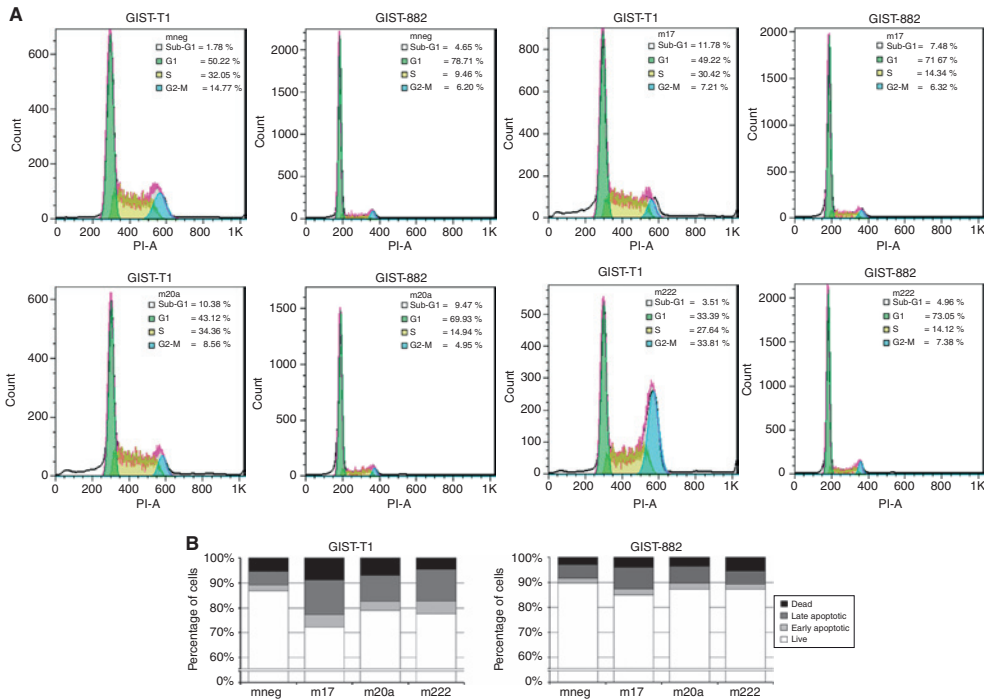


Figure 4: Overexpression of miR-17, miR-20a and miR-222 affects cell cycle progression and induces cell death. GIST-T1 and GIST-882 cell lines were transfected with scrambled (mneg), miR-17, miR-20a and miR-222 mimics. (A) Cell cycle profiles were determined by FACS analyses 72h post-transfection and analyzed by FlowJo software. Sub-G1 cells are depicted in white, cells in G1-phase in green, cells in S-phase in yellow and G2-M-phase cells in blue. Percentages of cells in distinct stages of the cell cycle are depicted on the right. (B) FACS analysis of Annexin V/PI (Ann/PI) stained cells, 72h post-transfection. Live cells are presented by the Ann-/PI- fraction, early apoptotic cells by the Ann+/PI- fraction, late apoptotic cells by the Ann+/PI+ fraction and dead cells are detected in the Ann-/PI+ fraction.

MiR-17, miR-20a target *ETV1* and miR-222 targets *KIT*

Candidate target genes for miR-17, miR-20a and miR-222 were predicted using TargetScanHuman 6.2 (<http://www.targetscan.org/>).³⁶ Interestingly, as mentioned, all miRNAs have potential binding sites in the 3'UTR of *KIT* and *ETV1*, which are important players in GIST oncogenesis (Figure 5). Indeed *KIT* and *ETV1* mRNA expression was significantly higher in GIST compared to GI-LMS (Supplemental Figure 5).



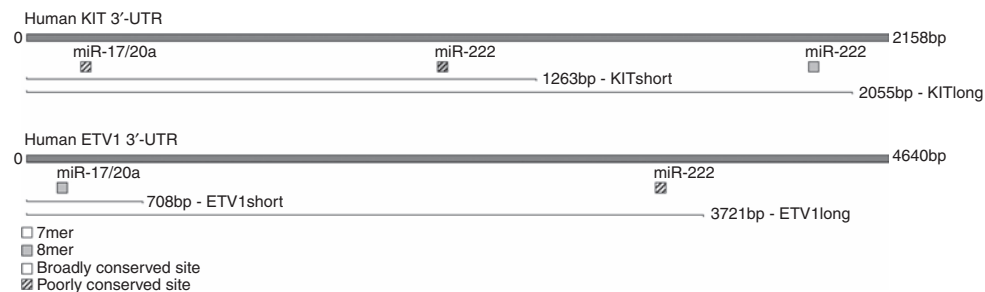


Figure 5: 3'UTR of *KIT* and *ETV1* and predicted target sites (TargetScanHuman 6.2) of miR-17, miR-20a and miR-222. Lines indicate the 3'UTRs fragments (KITshort/long, ETV1short/long) which are cloned into the psiCHECK-2 luciferase reporter.

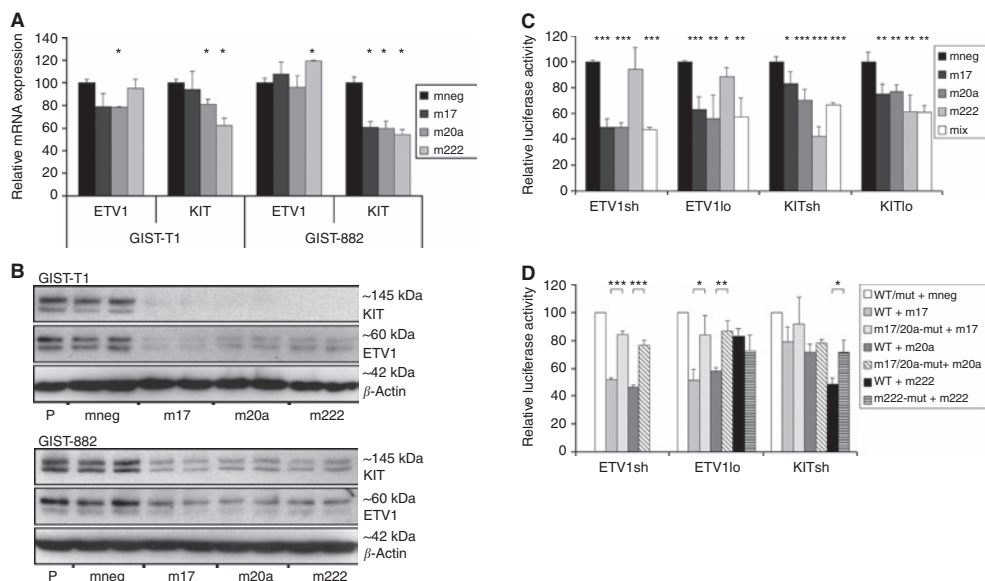


Figure 6: MiR-17, miR-20a and miR-222 target the 3'UTR of *KIT* and *ETV1* and thereby reduce their mRNA and protein levels. GIST-T1 and GIST-882 cell lines were transfected with scrambled (mneg), miR-17, miR-20a and miR-222 mimics and protein and RNA was isolated 72h post-transfection. (A) *KIT* and *ETV1* mRNA expression was determined by qPCR and normalized to three housekeepers (*GAPDH*, *HPRT* and *HMBS*). Shown are average values \pm SD (n=2), average expression of mneg is set at 100. (B) *KIT* and *ETV1* protein expression was determined by SDS-PAGE and immunoblotting. Parental untransfected control GIST cell lines are indicated by P. β -Actin was used as loading control. (C) GIST-T1 cells were transfected with psiCHECK 2 constructs containing short (sh) and long (lo) fragments of 3'UTR sequences of *ETV1* and *KIT* (n=4), followed 24h later by transfection of scrambled (mneg), miR-17, miR-20a or miR-222 mimics, or a mixture of these miRNA mimics (mix). (D) GIST-T1 cells were transfected with psiCHECK 2 constructs containing wild-type (WT) and mutated (mut) 3'UTR sequences of ETVshort (sh), ETVlong (lo) and KITshort, followed 24h later by transfection of scrambled (mneg), miR-17, miR-20a or miR-222 mimics. The *Renilla* luciferase activity was measured and normalized using firefly luciferase activity 48h after final transfection. The relative luciferase activity of cells transfected with scrambled mimic was set at 100. Shown are average values \pm SD (n=3). Statistical significance between scrambled control and miRNA mimics or between WT and mut was tested by two-sample t-test. * = $p < 0.05$, ** = $p < 0.005$, *** = $p < 0.0005$.

MiRNAs can exert their regulatory function either *via* mRNA degradation, translational repression or both. To determine the effects of miR-17, miR-20a and miR-222 overexpression on KIT and ETV1 both mRNA and protein levels were examined 72h after transfection of GIST cell lines with the miRNA mimics and a negative control. In GIST-T1 cells *ETV1* mRNA levels were 21% downregulated when miR-17 or miR-20a ($p=0.01$ for miR-20a) was overexpressed (Figure 6a). Overexpression of miR-222 barely changed *ETV1* mRNA levels. *KIT* mRNA levels were hardly affected by miR-17, but significantly downregulated by miR-20a (19% decrease, $p=0.04$) and miR-222 (38% decrease, $p=0.02$). In GIST-882 cells *ETV1* expression was not downregulated significantly upon mimic transfection, but *KIT* mRNA levels were reduced by 39% in miR-17 ($p=0.02$), 40% in miR-20a ($p=0.02$) and 46% in miR-222 ($p=0.01$) overexpressing cells. Protein expression of both KIT and ETV1 was easily detectable by immunoblotting in both untransfected GIST cell lines and cells transfected with a scrambled control mimic (Figure 6b). However, cells overexpressing miR-17, miR-20a or miR-222 clearly showed diminished KIT and ETV1 protein levels in both cell lines.

To demonstrate that the observed downregulation of KIT and ETV1 is due to the binding of the miRNAs to their 3'UTRs, fragments of the 3'UTRs spanning the potential miRNA target sites were cloned in a luciferase reporter construct. GIST cells were transfected with these constructs and miRNA mimics (Figures 6c). GIST-T1 cells with the *ETV1*short construct, containing binding sites for miR-17 and miR-20a, showed a 50% decreased luciferase activity ($p<0.0005$) when these miRNAs were overexpressed compared to the negative control. There was, however, no decreased luciferase activity when miR-222 was overexpressed, which agrees with the absence of a miR-222 binding site in the *ETV1*short construct. When a potential miR-222 binding site was introduced, as is the case in the *ETV1*long construct, miR-222 overexpression led to a small but significant decrease (12%, $p=0.02$) of the luciferase activity.

Both KIT constructs comprise potential binding sites for miR-17/20a and miR-222. Using both constructs, overexpression of miR-17 and miR-20a resulted in a 17%-30% decrease ($p<0.02$) in luciferase activity, whereas miR-222 showed a stronger inhibition of luciferase activity (39% -58% decrease, $p<0.002$). The presence of an additional distal miR-222 site in the *KIT*long construct did not further decrease luciferase activity. For all 3'UTR constructs, a combination of miR-17, miR-20a and miR-222 mimic (mix) did not have a synergistic effect on the reduction of luciferase activity, compared to the overexpression of individual miRNAs.

To examine whether the regulation of KIT and ETV1 is due to direct miRNA binding to target sites in the 3'UTRs, the putative binding sites were mutated in the *ETV1*short, *ETV1*long and *KIT*short constructs (Figure 6d, Supplemental Figure 1). GIST-T1 cells transfected with the *ETV1*short construct containing a mutated miR17/20a site, showed a significantly higher luciferase activity when transfected with miR-17 (84% vs 52%, $p<0.0005$) and miR-20a (77% vs 47%, $p<0.0005$) compared to cells transfected with the wild-type *ETV1*short construct. Similarly, in *ETV1*long,



mutation of the miR-17/20a target site significantly restored luciferase activity (miR-17: $p=0.03$; miR-20a: $p=0.002$). It was noted that luciferase activities were never restored to the levels obtained in cells transfected with the mneg control mimic. This may be caused by the severe effects overexpression of the miR-17/20a mimics have on GIST-T1 cell proliferation and survival. Apparently miR-222 does not directly regulate ETV1, as mutation of the miR-222 binding site did not lead to increased luciferase activity. Similarly, it can not be firmly concluded that miR-17 and miR-20a directly regulate KIT. In contrast, mutation of the miR-222 binding site in the KIT 3'UTR did significantly abolish regulation by miR-222 (72% vs 49%, $p=0.01$).

Since the reduction in luciferase activity upon miRNA overexpression is more prominent than the downregulation of KIT and ETV1 mRNA levels, the miRNA mediated inhibition of these genes apparently takes place *via* translational repression rather than *via* mRNA degradation. The marked decrease in KIT and ETV1 protein levels upon miR-17, miR-20a and miR-222 overexpression in GIST cell lines supports this theory.

DISCUSSION

Deregulation of miRNA expression can contribute to tumorigenesis and often the deregulated miRNA expression patterns are tumor type specific. In order to identify miRNAs that are specifically deregulated in GIST, miRNA expression was compared to that of GI-LMS, another mesenchymal tumor type with similar morphological features which occurs at the same anatomical sites. Here we showed that there is a large disparity in miRNA expression between GIST and GI-LMS.

The expression levels of the miR-221/222 cluster and the miR-17-92 cluster were significantly lower in GIST compared to GI-LMS. This was confirmed by qPCR, which also showed that the expression of miR-17, miR-20a and miR-222 was lower in GIST than in normal GI-tissues. In order to explain the reduced levels of these miRNAs in GIST, we checked if chromosome 13 loss, which is frequently observed in advanced GIST, correlated to lowered expression of miR-17 and miR-20a of which the genes are located on 13-q31.3. In our sample set no such correlation could be observed. An alternative explanation may be epigenetic silencing which has been reported for the miR-17-92 cluster in macrophages and lung tissue.³⁷⁻³⁸ Interestingly, members of the miR-17-92 cluster are often found higher expressed in human malignancies, including gastric and colon cancers, neuroblastoma and B-cell lymphomas relative to normal tissue.³²⁻³⁵ Also the miR-221/222 cluster is known to be upregulated in various cancers such as glioblastoma, and hepatocellular, pancreatic and prostate carcinoma.³⁹⁻⁴² In line with our data, it was previously reported that the expression of miR-221 and miR-222 are significantly downregulated in GIST in comparison to peripheral non-tumorous tissue.²⁴ MiRNAs belonging to both clusters have been considered to act as either a tumor suppressor or an oncogene, depending on the tumor type.⁴³⁻⁴⁴

Being important oncomiRs, the relatively low expression of the miR-221/222 and miR-17-92 cluster members could contribute to GIST development. In support of this notion, increased expression of miR-17, miR-20a and miR-222 in two different, well-characterized GIST cell lines resulted in cell growth inhibition and apoptosis induction. In addition, cells overexpressing miR-222 showed an elevated G2-M peak. This could be the result of a mitotic block, or a forced entrance to G2/M while the cells are not ready to undergo mitosis, which subsequently leads to cell death.

MiR-221/222 is reported to inhibit cell proliferation *via* KIT down-modulation in erythropoiesis and erythroleukemic cells.⁴⁵ In GIST, downregulation of miR-221 and miR-222 is correlated with pronounced KIT expression.²⁴ However, in that study, functional experiments to investigate the cellular effects of miR-221/222 repletion in GIST cells were not performed. MiR-494 has been demonstrated to target and downregulate KIT thereby inhibiting GIST cell growth and inducing apoptosis.²⁵ Interestingly, target prediction algorithms not only identified potential miRNA binding sites in the *KIT*-3'UTR for miR-221/222, but also for miR-17-92 cluster members. The upregulation of miR-17, miR-20a or miR-222 in our GIST cell lines resulted in downregulation of *KIT* mRNA and markedly reduced protein levels. Luciferase reporter assays showed clear regulation of a *KIT*-3'UTR controlled luciferase signal by miR-222, confirming that miR-222 directly targets *KIT*. As we could not demonstrate direct regulation of *KIT* by miR-17/20a we consider the observed reduction of KIT protein in GIST cells transfected with miR-17/20a to be an indirect secondary effect, possibly mediated through downregulation of additional target genes.

Recently ETV1 was found to be highly expressed in GIST and required for GIST development. We observed that the upregulation of miR-17, miR-20a or miR-222, not only affected KIT expression, but also resulted in the downregulation of ETV1 protein levels in two GIST cell lines. We show that miR-17 and miR-20a directly target *ETV1* whereas miR-222 does not seem regulate ETV1 in a direct manner. Since it is known that mutated KIT prolongs ETV1 stability,¹⁶ it may be that the lowered KIT levels caused by miR-222 affect the stability – and hence protein levels – of ETV1. Alternatively, KIT independent factors, possibly other miR-222 target genes, could be responsible for the reduced ETV1 protein levels.

In addition to miR-17 and miR-20a, other members of the miR-17-92 cluster, which were also downregulated in GIST, have potential target sites in *KIT* and *ETV1*. The 3'UTR of *KIT* contains putative target sites for miR-18a (and the closely related miR-18b from another cluster, but belonging to the miR-17 family) and miR-19a/b, while the *ETV1*-3'UTR contains a potential miR-19a/b site. Future research will demonstrate whether these miRNAs are capable of regulating KIT and ETV1 levels *via* these putative target sites. It was also noted that the 3'UTR of *PDGFRA* contains two potential miR-17/20a target sites. Therefore, overexpression of miR-17 and miR-20a potentially also has an effect on *PDGFRA*-mutant GIST.



Although miR-17 and miR-20a regulate ETV1 and miR-222 regulates KIT, they will most likely also target additional genes in the context of GIST cells. The cumulative effect of all target genes will eventually explain the cellular phenotype observed, including the differences between the miR-17/20a and miR-222 effects.

Since GIST cells are dependent on the continued high expression of KIT and ETV1, miRNAs that target these genes present a promising therapeutic opportunity. Despite the enormous successes obtained with KIT-targeting tyrosine kinase inhibitors (TKIs) such as imatinib and sunitinib, the vast majority of patients with metastatic GIST will eventually become resistant against these drugs, e.g. due to secondary mutations in the tyrosine kinase receptors. Moreover, the majority of WT-GIST and *PDGFRA*-D842V-mutant GIST are not sensitive to imatinib in the first place. Therefore, inhibition of KIT activity alone is unlikely to cure GIST.⁴⁶ We confirm miR-222 as a regulator of KIT, and are the first to demonstrate that miR-17 and miR-20a regulate ETV1, another key player in GIST development. Moreover, we present evidence that overexpression of these miRNAs in GIST cell lines dramatically inhibits cell proliferation, affects cell cycle progression and induces apoptosis. Remarkably, our results demonstrate that miR-17/20a clearly affect, in an indirect manner, KIT expression; likewise, miR-222 has a pronounced effect on ETV1 expression. As of yet it is unclear which genes and molecular mechanisms underlie these observations. Although miRNA therapy is still in its infancy and further *in vivo* research needs to be done, our findings could hold great therapeutic potential.⁴⁷⁻⁴⁹ When miRNA-treatment becomes available, targeted overexpression of members of the miR-221/222 and miR-17-92 clusters in GIST might significantly suppress ETV1 and KIT levels. The joined repression of both essential GIST oncogenes could be promising for GIST treatment, especially for imatinib-resistant disease.

ACKNOWLEDGMENTS

We thank the members of the Laboratory of Translational Pharmacology for helpful discussions. We greatly appreciated the help and technical expertise of A. Sacchetti with the FACS analyses. Furthermore we thank the Trapman laboratory, dept. of Pathology, Erasmus University Medical Center for the ETV1 antibody. This work was supported by the EC FP6 CONTICANET network of excellence (LSHC-CT-2005-018806) from the European Commission, the Life Raft Group Grant (M.D-R) and the Concerted Action Grant (GOA/11/2010) from KU Leuven.

REFERENCES

1. Kindblom LG, Remotti HE, Aldenborg F, Meis-Kindblom JM. Gastrointestinal pacemaker cell tumor (GIPACT): gastrointestinal stromal tumors show phenotypic characteristics of the interstitial cells of Cajal. *Am J Pathol.* 1998 May;152(5):1259-69.
2. Sircar K, Hewlett BR, Huizinga JD, Chorneyko K, Berezin I, Riddell RH. Interstitial cells of Cajal as precursors of gastrointestinal stromal tumors. *Am J Surg Pathol.* 1999 Apr;23(4):377-89.
3. Hirota S, Isozaki K, Moriyama Y, Hashimoto K, Nishida T, Ishiguro S, et al. Gain-of-function mutations of c-kit in human gastrointestinal stromal tumors. *Science.* 1998 Jan 23;279(5350):577-80.
4. Tornillo L, Terracciano LM. An update on molecular genetics of gastrointestinal stromal tumours. *J Clin Pathol.* 2006 Jun;59(6):557-63.
5. Liegl-Atzwanger B, Fletcher JA, Fletcher CD. Gastrointestinal stromal tumors. *Virchows Arch.* 2010 Feb;456(2):111-27.
6. Corless CL, Barnett CM, Heinrich MC. Gastrointestinal stromal tumours: origin and molecular oncology. *Nat Rev Cancer.* 2011 Dec;11(12):865-78.
7. Sarlomo-Rikala M, Kovatich AJ, Barusevicius A, Miettinen M. CD117: a sensitive marker for gastrointestinal stromal tumors that is more specific than CD34. *Mod Pathol.* 1998 Aug;11(8):728-34.
8. Heinrich MC, Corless CL, Duensing A, McGreevey L, Chen CJ, Joseph N, et al. PDGFRA activating mutations in gastrointestinal stromal tumors. *Science.* 2003 Jan 31;299(5607):708-10.
9. Lasota J, Miettinen M. KIT and PDGFRA mutations in gastrointestinal stromal tumors (GISTs). *Semin Diagn Pathol.* 2006 May;23(2):91-102.
10. Lasota J, Jasinski M, Sarlomo-Rikala M, Miettinen M. Mutations in exon 11 of c-Kit occur preferentially in malignant versus benign gastrointestinal stromal tumors and do not occur in leiomyomas or leiomyosarcomas. *Am J Pathol.* 1999 Jan;154(1):53-60.
11. Hostein I, Faur N, Primois C, Boury F, Denard J, Emile JF, et al. BRAF mutation status in gastrointestinal stromal tumors. *Am J Clin Pathol.* 2010 Jan;133(1):141-8.
12. Agaram NP, Wong GC, Guo T, Maki RG, Singer S, Dematteo RP, et al. Novel V600E BRAF mutations in imatinib-naïve and imatinib-resistant gastrointestinal stromal tumors. *Genes Chromosomes Cancer.* 2008 Oct;47(10):853-9.
13. Agaimy A, Terracciano LM, Dirnhofer S, Tornillo L, Foerster A, Hartmann A, et al. V600E BRAF mutations are alternative early molecular events in a subset of KIT/PDGFR α wild-type gastrointestinal stromal tumours. *J Clin Pathol.* 2009 Jul;62(7):613-6.
14. Pasini B, McWhinney SR, Bei T, Matyakhina L, Stergiopoulos S, Muchow M, et al. Clinical and molecular genetics of patients with the Carney-Stratakis syndrome and germline mutations of the genes coding for the succinate dehydrogenase subunits SDHB, SDHC, and SDHD. *Eur J Hum Genet.* 2008 Jan;16(1):79-88.
15. Janeway KA, Kim SY, Lodish M, Nose V, Rustin P, Gaal J, et al. Defects in succinate dehydrogenase in gastrointestinal stromal tumors lacking KIT and PDGFRA mutations. *Proc Natl Acad Sci U S A.* 2011 Jan 4;108(1):314-8.
16. Chi P, Chen Y, Zhang L, Guo X, Wongvipat J, Shamu T, et al. ETV1 is a lineage survival factor that cooperates with KIT in gastrointestinal stromal tumours. *Nature.* 2010 Oct 14;467(7317):849-53.
17. Seth A, Watson DK. ETS transcription factors and their emerging roles in human cancer. *Eur J Cancer.* 2005 Nov;41(16):2462-78.
18. Tabone S, Theou N, Wozniak A, Saffroy R, Deville L, Julie C, et al. KIT overexpression and amplification in gastrointestinal stromal tumors (GISTs). *Biochim Biophys Acta.* 2005 Jun 30;1741(1-2):165-72.
19. Chen CZ. MicroRNAs as oncogenes and tumor suppressors. *N Engl J Med.* 2005 Oct 27;353(17):1768-71.
20. Zhang B, Pan X, Cobb GP, Anderson TA. microRNAs as oncogenes and tumor suppressors. *Dev Biol.* 2007 Feb 1;302(1):1-12.
21. Di Leva G, Croce CM. Roles of small RNAs in tumor formation. *Trends Mol Med.* 2010 Jun;16(6):257-67.
22. Choi HJ, Lee H, Kim H, Kwon JE, Kang HJ, You KT, et al. MicroRNA expression profile of gastrointestinal stromal tumors is distinguished by 14q loss and anatomic site. *Int J Cancer.* 2010 Apr 1;126(7):1640-50.
23. Haller F, von Heydebreck A, Zhang JD, Gunawan B, Langer C, Ramadori G, et al. Localization- and mutation-dependent microRNA (miRNA) expression signatures in gastrointestinal stromal tumours (GISTs), with a cluster of co-expressed miRNAs located at 14q32.31. *J Pathol.* 2010 Jan;220(1):71-86.



24. Koelz M, Lense J, Wrba F, Scheffler M, Dienes HP, Odenthal M. Down-regulation of miR-221 and miR-222 correlates with pronounced Kit expression in gastrointestinal stromal tumors. *Int J Oncol.* 2011 Feb;38(2):503-11.
25. Kim WK, Park M, Kim YK, Tae YK, Yang HK, Lee JM, et al. MicroRNA-494 downregulates KIT and inhibits gastrointestinal stromal tumor cell proliferation. *Clin Cancer Res.* 2011 Dec 15;17(24):7584-94.
26. Pothof J, Verkaik NS, van IW, Wiemer EA, Ta VT, van der Horst GT, et al. MicroRNA-mediated gene silencing modulates the UV-induced DNA-damage response. *EMBO J.* 2009 Jul 22;28(14):2090-9.
27. Schmittgen TD, Livak KJ. Analyzing real-time PCR data by the comparative C(T) method. *Nat Protoc.* 2008;3(6):1101-8.
28. Taguchi T, Sonobe H, Toyonaga S, Yamasaki I, Shuin T, Takano A, et al. Conventional and molecular cytogenetic characterization of a new human cell line, GIST-T1, established from gastrointestinal stromal tumor. *Lab Invest.* 2002 May;82(5):663-5.
29. Tuveson DA, Willis NA, Jacks T, Griffin JD, Singer S, Fletcher CD, et al. STI571 inactivation of the gastrointestinal stromal tumor c-KIT oncoprotein: biological and clinical implications. *Oncogene.* 2001 Aug 16;20(36):5054-8.
30. Keepers YP, Pizao PE, Peters GJ, van Ark-Otte J, Winograd B, Pinedo HM. Comparison of the sulforhodamine B protein and tetrazolium (MTT) assays for in vitro chemosensitivity testing. *Eur J Cancer.* 1991;27(7):897-900.
31. Miettinen M, Lasota J. Gastrointestinal stromal tumors: pathology and prognosis at different sites. *Semin Diagn Pathol.* 2006 May;23(2):70-83.
32. Guo J, Miao Y, Xiao B, Huan R, Jiang Z, Meng D, et al. Differential expression of microRNA species in human gastric cancer versus non-tumorous tissues. *J Gastroenterol Hepatol.* 2009 Apr;24(4):652-7.
33. Volinia S, Calin GA, Liu CG, Ambs S, Cimmino A, Petrocca F, et al. A microRNA expression signature of human solid tumors defines cancer gene targets. *Proc Natl Acad Sci U S A.* 2006 Feb 14;103(7):2257-61.
34. Schulte JH, Marschall T, Martin M, Rosenstiel P, Mestdagh P, Schlierf S, et al. Deep sequencing reveals differential expression of microRNAs in favorable versus unfavorable neuroblastoma. *Nucleic Acids Res.* 2010 Sep;38(17):5919-28.
35. He L, Thomson JM, Hemann MT, Hernando-Monge E, Mu D, Goodson S, et al. A microRNA polycistron as a potential human oncogene. *Nature.* 2005 Jun 9;435(7043):828-33.
36. Lewis BP, Burge CB, Bartel DP. Conserved seed pairing, often flanked by adenosines, indicates that thousands of human genes are microRNA targets. *Cell.* 2005 Jan 14;120(1):15-20.
37. Dakhllallah D, Batte K, Wang Y, Cantemir-Stone CZ, Yan P, Nuovo G, et al. Epigenetic regulation of miR-17~92 contributes to the pathogenesis of pulmonary fibrosis. *Am J Respir Crit Care Med.* 2013 Feb 15;187(4):397-405.
38. Pospisil V, Vargova K, Kokavec J, Rybarova J, Savvulidi F, Jonasova A, et al. Epigenetic silencing of the oncogenic miR-17-92 cluster during PU.1-directed macrophage differentiation. *EMBO J.* 2011 Nov 2;30(21):4450-64.
39. Gillies JK, Lorimer IA. Regulation of p27Kip1 by miRNA 221/222 in glioblastoma. *Cell Cycle.* 2007 Aug 15;6(16):2005-9.
40. Fornari F, Gramantieri L, Ferracin M, Veronese A, Sabbioni S, Calin GA, et al. MiR-221 controls CDKN1C/p57 and CDKN1B/p27 expression in human hepatocellular carcinoma. *Oncogene.* 2008 Sep 25;27(43):5651-61.
41. Lee EJ, Gusev Y, Jiang J, Nuovo GJ, Lerner MR, Frankel WL, et al. Expression profiling identifies microRNA signature in pancreatic cancer. *Int J Cancer.* 2007 Mar 1;120(5):1046-54.
42. Galardi S, Mercatelli N, Giorda E, Massalini S, Frajese GV, Ciafre SA, et al. miR-221 and miR-222 expression affects the proliferation potential of human prostate carcinoma cell lines by targeting p27Kip1. *J Biol Chem.* 2007 Aug 10;282(32):23716-24.
43. Garofalo M, Quintavalle C, Romano G, Croce CM, Condorelli G. miR221/222 in cancer: their role in tumor progression and response to therapy. *Curr Mol Med.* 2012 Jan;12(1):27-33.
44. O'Donnell KA, Wentzel EA, Zeller KI, Dang CV, Mendell JT. c-Myc-regulated microRNAs modulate E2F1 expression. *Nature.* 2005 Jun 9;435(7043):839-43.
45. Felli N, Fontana L, Pelosi E, Botta R, Bonci D, Facchiano F, et al. MicroRNAs 221 and 222 inhibit normal erythropoiesis and erythroleukemic cell growth via kit receptor down-modulation. *Proc Natl Acad Sci U S A.* 2005 Dec 13;102(50):18081-6.
46. Rubin BP. Bioinformatic mining of gene expression datasets identifies ETV1 as a critical regulator of oncogenesis in gastrointestinal stromal tumors. *Cancer Cell.* 2010 Nov 16;18(5):407-8.
47. Cho WC. MicroRNAs in cancer - from research to therapy. *Biochim Biophys Acta.* 2010 Apr;1805(2):209-17.

48. Thorsen SB, Obad S, Jensen NF, Stenvang J, Kauppinen S. The Therapeutic Potential of MicroRNAs in Cancer. *Cancer J*. 2012 May;18(3):275-84.
49. Kasinski AL, Slack FJ. Epigenetics and genetics. MicroRNAs en route to the clinic: progress in validating and targeting microRNAs for cancer therapy. *Nat Rev Cancer*. 2011 Dec;11(12):849-64.



SUPPLEMENTAL TABLES AND FIGURES

Supplemental Table 1: Primers used for cloning.

A

<i>ETV1</i> 3'UTR	Forward primer	5'-GCCTCGAGTAACACAAGTGACAGTCAAGCAGGG
	Reverse primer - short	5'-GAGCGGCCGCCTATGACTCAGTTTGGGCCAG
	Reverse primer - long	5'-GAGCGGCCGCATGATAAGATCACATAGTAACC
<i>KIT</i> 3'UTR	Forward primer	5'-GACTCGAGCAGAATCAGTGTGGGTCAC
	Reverse primer - short	5'-GAGCGGCCGCTTCTGGTAAGCTACTCTAG
	Reverse primer - long	5'-GAGCGGCCGCTTATGTATTTACACATAAAG

B

ETVsh m17/20a-mut	Forward primer	5'-GGTCTGCCATGGACTGTGAAGCTTATTTGAGGGTGGGTGG
	Reverse primer	5'-CCACCCACCCTCAAATAAGCTTTCACAGTCCATGGCAGACC
ETVlo m222-mut	Forward primer	5'-CCGCACGGAGGAGGAAGACTGGATATCAAAGACTCTAATTGATTACT
	Reverse primer	5'-AGTAAATCAATTAGAGTCTTTGATATCCAGTCTTCTCCTCCGTGCGG
KITsh m17/20a-mut	Forward primer	5'-TGCAATCCTGTCTTTCTGAGCAAAGCTTAGTGCCGATGATTTTGTCT
	Reverse primer	5'-GACAAAAATCATCGGCCACTAAGCTTTGCTCAGAAAGACAGGATTGCA
KITsh m222-mut	Forward primer	5'-GGAAAACACTGCCATCTTAGTTTGGATTCTTAGATATCAGGAAATAAAG TATAGGTTTAG
	Reverse primer	5'-CTAAACCTATACTTTATTTCTGATATCTAAGAATCCAAACTAAGATGGC AGTGTTC

(A) Primers used for cloning *ETV1* and *KIT* short and long 3'UTR constructs. (B) Primers used for site mutagenesis of *ETV1* and *KIT* short and long 3'UTR constructs.

Supplemental Table 2: Differentially expressed miRNAs (p<0.05) between GIST and GI-LMS.

	miRNA ID	Parametric p-value	FDR	Fold change down in GIST	Fold change up in GIST	Genomic location
1	hsa-miR-222	< 1e-07	< 1e-07	5.18		X-p11.3
2	hsa-miR-29c	< 1e-07	< 1e-07		3.92	1-q32.2
3	hsa-miR-497	< 1e-07	< 1e-07		41.84	17-p13.1
4	hsa-miR-30a	< 1e-07	< 1e-07		3.91	6-q13
5	hsa-miR-603	< 1e-07	< 1e-07		47.65	10-p12.1
6	hsa-miR-221	< 1e-07	< 1e-07	2.28		X-p11.3
7	hsa-miR-382	< 1e-07	< 1e-07	1.80		14-q32.31
8	hsa-miR-938	< 1e-07	< 1e-07	3.51		10-p11.23
9	hsa-miR-330-3p	< 1e-07	< 1e-07		32.78	19-q13.32
10	hsa-miR-21	< 1e-07	< 1e-07	3.80		17-q23.1
11	hsa-miR-21*	< 1e-07	< 1e-07	1.79		17-q23.1
12	hsa-miR-96	< 1e-07	< 1e-07		17.60	7-q32.2
13	hsa-miR-155	< 1e-07	< 1e-07	2.93		21-q21.3
14	hsa-miR-645	1.00E-07	4.80E-06	2.76		20-q13.13
15	hsa-miR-297	1.00E-07	4.80E-06	3.73		4-q25
16	hsa-miR-518a-5p; hsa-miR-527	2.00E-07	8.50E-06		9.90	19-q13.41
17	hsa-miR-190b	2.00E-07	8.50E-06	2.25		1-q21.3
18	hsa-miR-653	3.00E-07	1.21E-05	1.49		7-q21.3
19	hsa-miR-338-5p	8.00E-07	3.06E-05	3.65		17-q25.3
20	hsa-miR-20a	9.00E-07	3.27E-05	2.10		13-q31.3
21	hsa-miR-410	1.10E-06	3.63E-05	1.66		14-q32.31
22	hsa-miR-15b	1.10E-06	3.63E-05		7.04	3-q26.1
23	hsa-miR-595	1.50E-06	4.73E-05	2.33		7-q36.3
24	hsa-miR-30d	1.70E-06	5.14E-05		1.77	8-q24.22
25	hsa-miR-216a	2.50E-06	7.26E-05	1.92		2-p16.1
26	hsa-miR-29b	2.80E-06	7.82E-05		2.49	7-q32.3 1-q32.2
27	hsa-miR-422a	3.20E-06	8.60E-05	2.40		15-q22.31
28	hsa-miR-7	3.70E-06	9.59E-05	1.51		9-q21.32 15-q26.1 19-p13.3
29	hsa-miR-624*	4.90E-06	0.000123	3.74		14-q12
30	hsa-miR-383	5.40E-06	0.000131	1.60		8-p22
31	hsa-miR-455-3p	5.60E-06	0.000131		2.48	9-q32
32	hsa-miR-509-3p	1.04E-05	0.000229	1.59		X-q27.3
33	hsa-miR-508-3p	1.07E-05	0.000229	1.57		X-q27.3
34	hsa-miR-31	1.07E-05	0.000229	2.00		9-p21.3
35	hsa-miR-9*	1.15E-05	0.000239	2.68		1-q22 5-q14.3 15-q26.1
36	hsa-miR-574-5p	1.19E-05	0.00024	3.10		4-p14
37	hsa-miR-145	1.26E-05	0.000247		3.06	5-q33.1



Supplemental Table 2: Differentially expressed miRNAs ($p < 0.05$) between GIST and GI-LMS. (Continued)

miRNA ID	Parametric p-value	FDR	Fold change down in GIST	Fold change up in GIST	Genomic location
38 hsa-miR-199a-5p	1.32E-05	0.000252		2.76	19-p13.2 1-q24.3
39 hsa-miR-148b	1.63E-05	0.000303		1.55	12-q13.13
40 hsa-miR-543	1.99E-05	0.000361	2.97		14-q32.31
41 hsa-miR-455-5p	2.09E-05	0.00037		2.03	9-q32
42 hsa-miR-30c	2.18E-05	0.000377		2.32	1-p34.2 6-q13
43 hsa-miR-933	2.36E-05	0.000399	1.83		2-q31.1
44 hsa-miR-490-3p	2.49E-05	0.000411	1.63		7-q33
45 hsa-miR-551b*	2.78E-05	0.000449	1.61		3-q26.2
46 hsa-miR-654-5p	3.44E-05	0.000543		1.25	14-q32.31
47 hsa-miR-342-5p	3.52E-05	0.000544	2.07		14-q32.2
48 hsa-miR-335	3.60E-05	0.000545		3.32	7-q32.2
49 hsa-miR-181a	4.60E-05	0.000682		1.80	1-q31.3 9-q33.3
50 hsa-miR-153	5.01E-05	0.000728		1.58	2-q35 7-q36.3
51 hsa-miR-451	5.87E-05	0.000831	1.87		17-q11.2
52 hsa-miR-30b	5.95E-05	0.000831		2.33	8-q24.22
53 hsa-miR-125a-5p	7.01E-05	0.00096		1.71	19-q13.33
54 hsa-miR-147	7.56E-05	0.001016	1.54		9-q33.2
55 hsa-miR-23a	7.76E-05	0.001024	1.76		19-p13.12
56 hsa-miR-574-3p	0.0001016	0.001317		3.93	4-p14
57 hsa-miR-195	0.0001118	0.001424		4.29	17-p13.1
58 hsa-miR-675	0.0001512	0.001893		2.14	11-p15.5
59 hsa-miR-143*	0.0002039	0.002509		2.39	5-q33.1
60 hsa-miR-18a	0.0002165	0.002565	1.41		13-q31.3
61 hsa-miR-518c	0.0002177	0.002565	1.56		19-q13.41
62 hsa-miR-208a	0.0002215	0.002565	1.65		14-q11.2
63 hsa-miR-138-1*	0.0002226	0.002565		4.05	3-p21.33
64 hsa-miR-379	0.0002653	0.00301	1.52		14-q32.31
65 hsa-miR-507	0.0002906	0.003246	1.52		X-q27.3
66 hsa-miR-154	0.0002989	0.003276		1.55	14-q32.31
67 hsa-miR-708*	0.0003023	0.003276	1.22		11-q14.1
68 hsa-miR-99b	0.0003286	0.0035		1.88	19-q13.33
69 hsa-miR-553	0.0003326	0.0035	1.73		1-p21.2
70 hsa-miR-500	0.0003567	0.0037	1.56		X-p11.23
71 hsa-miR-34a*	0.0003719	0.003803		4.61	1-p36.23
72 hsa-let-7c*	0.0003906	0.003939	1.57		21-q21.1
73 hsa-miR-517*	0.0004078	0.004056		1.25	19-q13.41
74 hsa-miR-708	0.0004416	0.004333	2.27		11-q14.1
75 hsa-miR-105	0.0005184	0.005018	1.23		X-q28

Supplemental Table 2: Differentially expressed miRNAs ($p < 0.05$) between GIST and GI-LMS. (Continued)

miRNA ID	Parametric p-value	FDR	Fold change down in GIST	Fold change up in GIST	Genomic location		
76 hsa-miR-199a-3p; hsa-miR-199b-3p	0.0005447	0.005137		2.19	19-p13.2	1-q24.3	9-q34.11
77 hsa-miR-15a	0.0005496	0.005137		3.15	13-q14.3		
78 hsa-miR-145*	0.0005519	0.005137		1.49	5-q33.1		
79 hsa-miR-329	0.0006264	0.005708		1.70	14-q32.31		
80 hsa-miR-181a-2*	0.000629	0.005708		1.30	9-q33.3		
81 hsa-miR-140-3p	0.0007306	0.006398		3.01	16-q22.1		
82 hsa-miR-506	0.0007368	0.006398	1.46		X-q27.3		
83 hsa-miR-148a	0.0007374	0.006398		1.45	7-p15.2		
84 hsa-miR-454*	0.0007403	0.006398	2.14		17-q22		
85 hsa-miR-140-5p	0.0008633	0.007374		2.31	16-q22.1		
86 hsa-miR-187*	0.0009113	0.007693		2.09	18-q12.2		
87 hsa-miR-1	0.000925	0.007716	2.12		20-q13.33	18-q11.2	
88 hsa-miR-16-2*	0.0009353	0.007716	1.31		3-q26.1		
89 hsa-miR-143	0.0009655	0.007876		2.08	5-q33.1		
90 hsa-miR-125b-2*	0.0010484	0.008457	1.29		21-q21.1		
91 hsa-miR-135a	0.0010601	0.008458	1.60		3-p21.1	12-q23.1	
92 hsa-miR-138	0.0011793	0.009306	1.64		3-p21.33	16-q13	
93 hsa-miR-298	0.0012295	0.009598	1.46		20-q13.32		
94 hsa-miR-431*	0.0013386	0.010339		1.41	14-q32.31		
95 hsa-miR-29b-2*	0.0016831	0.012862	1.40		1-q32.2		
96 hsa-miR-516a-5p	0.0018112	0.013697	1.39		19-q13.41		
97 hsa-miR-551a	0.0018559	0.013891		1.59	1-p36.32		
98 hsa-miR-185	0.0021398	0.015852	1.42		22-q11.21		
99 hsa-miR-29b-1*	0.0022412	0.016394	1.72		7-q32.3		
100 hsa-miR-586	0.0022719	0.016394	1.31		6-p12.3		
101 hsa-miR-493	0.0022807	0.016394	1.20		14-q32.31		
102 hsa-miR-888	0.0024732	0.01755	2.12		X-q27.3		
103 hsa-miR-626	0.0024899	0.01755	1.30		15-q15.1		
104 hsa-miR-17*	0.002534	0.017689	1.15		13-q31.3		
105 hsa-miR-93*	0.0025785	0.017829		1.18	7-q22.1		
106 hsa-miR-514	0.0026083	0.017864		2.17	X-q27.3		
107 hsa-miR-181d	0.0027104	0.01839	1.31		19-p13.12		
108 hsa-miR-518a-3p	0.0027783	0.018506	1.45		19-q13.41		
109 hsa-miR-629	0.0027785	0.018506	1.44		15-q23		
110 hsa-miR-361-3p	0.0028679	0.018928		1.74	X-q21.2		
111 hsa-miR-193a-3p	0.0029669	0.019405	1.46		17-q11.2		
112 hsa-miR-548b-3p	0.0029981	0.019434	1.15		6-q22.31		



Supplemental Table 2: Differentially expressed miRNAs ($p < 0.05$) between GIST and GI-LMS. (Continued)

miRNA ID	Parametric p-value	FDR	Fold change down in GIST	Fold change up in GIST	Genomic location		
113	hsa-miR-665	0.0030746	0.019754	1.41		14-q32.31	
114	hsa-miR-659	0.0032171	0.020488	1.36		22-q13.1	
115	hsa-miR-132	0.0033381	0.021074		1.37	17-p13.3	
116	hsa-miR-338-3p	0.0033714	0.0211	1.32		17-q25.3	
117	hsa-miR-452	0.0035591	0.022085	1.65		X-q28	
118	hsa-miR-17	0.0039755	0.024459	1.53		13-q31.3	
119	hsa-miR-181b	0.004499	0.02734		1.25	1-q31.3	9-q33.3
120	hsa-miR-648	0.004519	0.02734	1.20		22-q11.21	
121	hsa-miR-16-1*	0.0048092	0.028855	1.34		13-q14.3	
122	hsa-let-7a*	0.0048547	0.028889		1.22	9-q22.32	11-q24.1 22-q13.31
123	hsa-miR-340*	0.0049935	0.029474		1.57	5-q35.3	
124	hsa-miR-767-3p	0.0055134	0.03228	1.56		X-q28	
125	hsa-miR-25*	0.005654	0.032838		1.39	7-q22.1	
126	hsa-miR-891a	0.0058471	0.03369	1.34		X-q27.3	
127	hsa-miR-548c-5p	0.0060548	0.034613	1.18		12-q14.2	
128	hsa-miR-133b	0.0062592	0.035501	1.83		6-p12.2	
129	hsa-miR-10a*	0.0063659	0.035546	1.44		17-q21.32	
130	hsa-miR-133a	0.0064061	0.035546	1.66		18-q11.2	20-q13.33
131	hsa-miR-505*	0.0064139	0.035546	1.37		X-q27.1	
132	hsa-miR-9	0.0065122	0.035817	1.40		1-q22	5-q14.3 15-q26.1
133	hsa-miR-32*	0.0067005	0.036576	1.67		9-q31.3	
134	hsa-miR-615-3p	0.0067727	0.036645	1.46		12-q13.13	
135	hsa-miR-550	0.0068141	0.036645	1.40		7-p15.1	7-p14.3
136	hsa-miR-34b*	0.0069028	0.036849	1.23		11-q23.1	
137	hsa-miR-671-5p	0.0071393	0.037833	1.44		7-q36.1	
138	hsa-miR-488	0.0073843	0.038848	1.38		1-q25.2	
139	hsa-miR-671-3p	0.0075271	0.039085	1.21		7-q36.1	
140	hsa-miR-19a*	0.0075371	0.039085		1.20	13-q31.3	
141	hsa-miR-296-3p	0.0076491	0.03922	1.28		20-q13.32	
142	hsa-miR-100*	0.0076711	0.03922	1.15		11-q24.1	
143	hsa-miR-409-5p	0.0079124	0.039901		1.20	14-q32.31	
144	hsa-miR-331-3p	0.0079142	0.039901	1.45		12-q22	
145	hsa-miR-202	0.0083983	0.042049	1.34		10-q26.3	
146	hsa-miR-147b	0.0093471	0.046165	1.29		15-q21.1	
147	hsa-miR-19a	0.0093474	0.046165	1.34		13-q31.3	
148	hsa-miR-608	0.0097314	0.047737	1.44		10-q24.31	
149	hsa-miR-633	0.0101218	0.049318		1.14	17-q23.2	
150	hsa-miR-519b-3p	0.0102176	0.049453	1.14		19-q13.41	

Supplemental Table 2: Differentially expressed miRNAs ($p < 0.05$) between GIST and GI-LMS. (Continued)

miRNA ID	Parametric p-value	FDR	Fold change down in GIST	Fold change up in GIST	Genomic location
151 hsa-miR-33b*	0.0105164	0.050562		1.17	17-p11.2
152 hsa-miR-365	0.0107665	0.051424		1.37	16-p13.12 17-q11.2
153 hsa-miR-567	0.0110328	0.052352	1.29		3-q13.2
154 hsa-miR-503	0.0111954	0.052778		1.58	X-q26.3
155 hsa-miR-190	0.0119911	0.056165		1.38	15-q22.2
156 hsa-miR-500*	0.0124682	0.058025	1.31		X-p11.23
157 hsa-miR-877*	0.0128063	0.059219	1.35		6-p21.33
158 hsa-miR-219-2-3p	0.0128957	0.059255		1.22	9-q34.11
159 hsa-miR-146b-5p	0.0130367	0.059526		2.47	10-q24.32
160 hsa-miR-449b	0.0133274	0.060473	1.21		5-q11.2
161 hsa-miR-1307	0.0137505	0.061844	1.45		10-q24.33
162 hsa-miR-520d-5p	0.0138	0.061844	1.29		19-q13.41
163 hsa-miR-379*	0.0142728	0.063431		1.15	14-q32.31
164 hsa-miR-139-3p	0.0143288	0.063431	1.49		11-q13.4
165 hsa-miR-526b*	0.0145127	0.063856	1.20		19-q13.41
166 hsa-miR-542-5p	0.0151533	0.066273	1.38		X-q26.3
167 hsa-miR-100	0.0152667	0.066369		1.50	11-q24.1
168 hsa-miR-221*	0.0157629	0.068118	1.62		X-p11.3
169 hsa-miR-155*	0.0165619	0.071148		1.33	21-q21.3
170 hsa-miR-24-1*	0.0172539	0.073453	1.40		9-q22.32
171 hsa-miR-103-2*	0.0173009	0.073453	1.45		20-p13
172 hsa-miR-141*	0.0182249	0.076578	1.18		12-p13.31
173 hsa-miR-328	0.0182478	0.076578	1.39		16-q22.1
174 hsa-miR-544	0.0193201	0.080404	1.25		14-q32.31
175 hsa-miR-556-5p	0.0193811	0.080404	1.19		1-q23.3
176 hsa-miR-214*	0.0197509	0.081284	1.34		1-q24.3
177 hsa-miR-450b-5p	0.0198172	0.081284	1.19		X-q26.3
178 hsa-miR-377*	0.0203049	0.082637		1.34	14-q32.31
179 hsa-miR-936	0.0203746	0.082637		1.29	10-q25.1
180 hsa-miR-185	0.0205904	0.083048	1.29		22-q11.21
181 hsa-miR-644	0.0215981	0.086631	1.18		20-q11.22
182 hsa-miR-363*	0.0224241	0.08945		1.34	X-q26.2
183 hsa-miR-10a	0.0228451	0.090631		1.81	17-q21.32
184 hsa-miR-376a*	0.0233202	0.092013		1.52	14-q32.31
185 hsa-miR-583	0.0238761	0.093698	1.36		5-q15
186 hsa-miR-519c-3p	0.0240152	0.093737	1.14		19-q13.41
187 hsa-miR-580	0.024761	0.09609	1.18		5-p13.2
188 hsa-miR-542-3p	0.0248827	0.09609		1.25	X-q26.3



Supplemental Table 2: Differentially expressed miRNAs ($p < 0.05$) between GIST and GI-LMS. (Continued)

miRNA ID	Parametric p-value	FDR	Fold change down in GIST	Fold change up in GIST	Genomic location
189	hsa-miR-518f*	0.0271544	0.104307		19-q13.41
190	hsa-let-7g	0.0276734	0.105742	1.27	3-p21.1
191	hsa-miR-495	0.0285003	0.108331		14-q32.31
192	hsa-miR-573	0.029058	0.109876	1.12	4-p15.2
193	hsa-miR-125b	0.0293659	0.110465		11-q24.1 21-q21.1
194	hsa-miR-423-5p	0.0295403	0.110548	1.27	17-q11.2
195	hsa-miR-448	0.0310759	0.115698	1.09	X-q23
196	hsa-miR-101	0.0314363	0.116443	1.51	1-p31.3 9-p24.1
197	hsa-miR-300	0.0326548	0.1198	1.37	14-q32.31
198	hsa-miR-617	0.0326727	0.1198	1.31	12-q21.31
199	hsa-let-7i	0.0331424	0.120912	1.27	12-q14.1
200	hsa-miR-425*	0.0338918	0.12294	1.27	3-p21.31
201	hsa-miR-27a*	0.034037	0.12294	1.42	19-p13.12
202	hsa-miR-576-5p	0.0366166	0.131327	1.23	4-q25
203	hsa-miR-16	0.036721	0.131327	1.45	13-q14.3 3-q26.1
204	hsa-miR-220c	0.037615	0.133865	1.22	19-q13.32
205	hsa-miR-130b	0.0382793	0.135565	1.37	22-q11.21
206	hsa-miR-222*	0.0387693	0.136634	1.13	X-p11.3
207	hsa-miR-136*	0.0392342	0.137604		14-q32.31
208	hsa-miR-554	0.0405731	0.141616	1.12	1-q21.3
209	hsa-miR-636	0.0427149	0.148378		17-q25.2
210	hsa-miR-142-5p	0.0440717	0.152362	1.27	17-q22
211	hsa-miR-519a	0.0445061	0.153134		19-q13.41
212	hsa-miR-206	0.0447167	0.153134		6-p12.2
213	hsa-miR-941	0.0461752	0.156992	1.26	20-q13.33
214	hsa-miR-520c-3p	0.046276	0.156992	1.22	19-q13.41
215	hsa-miR-339-5p	0.047735	0.161145		7-p22.3
216	hsa-miR-192	0.0479439	0.161145	1.27	11-q13.1
217	hsa-miR-186*	0.0482783	0.161521	1.11	1-p31.1
218	hsa-miR-524-5p	0.0489574	0.163042		19-q13.41
219	hsa-miR-621	0.0497638	0.16497		13-q14.11

P-values of two-sample t-test and false discovery rate (FDR)-adjusted P-values as well as fold change in miRNA expression and miRNA genomic locations are indicated. The solid line indicates the cut-off value ($p < 0.005$, FDR $p < 0.03$) for the miRNAs used in the hierarchical clustering of Figure 1. The miRNAs of the miR-17-92 and miR-221/222 clusters are indicated in bold.

```

miR-20                GAUGGACGUGAUAUUCGUGAAAU 5'
                        | | |         |||||
miR-17                GAUGGACGUGACAUUCGUGAAAC 5'
                        | | |         |||||
KIT      m17/20a site  5' CTGTCTTTCTGAGAGCACACTTTA
                        x xx
KITshort m17/20a-mut  5' CTGTCTTTCTGAGAGCAAGCTTA

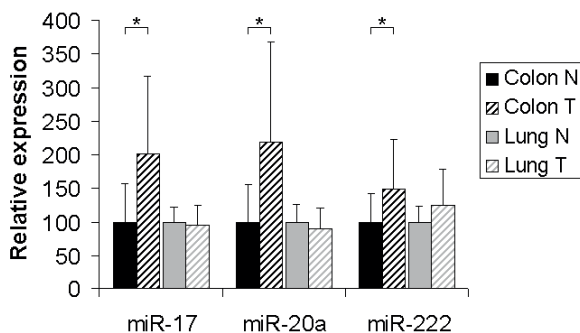
miR-222              UGGGUCAUCGGUCUACAUCGA 5'
                        | | |         |||||
KIT      m222 site    5' GTTTGGATTCTTATGTAGCA
                        xx x
KITshort m222-mut    5' GTTTGGATTCTTAGATATCA

miR-20a              GAUGGACGUGAUAUUCGUGAAAU 5'
                        |         | |||||
miR-17              GAUGGACGUGACAUUCGUGAAAC 5'
                        |         | |||||
ETV1      m17/20a site 5' TCTGCCATGGACTGTCACTTTA
                        x xx
ETV1short m17/20a-mut 5' TCTGCCATGGACTGTAGCTTA

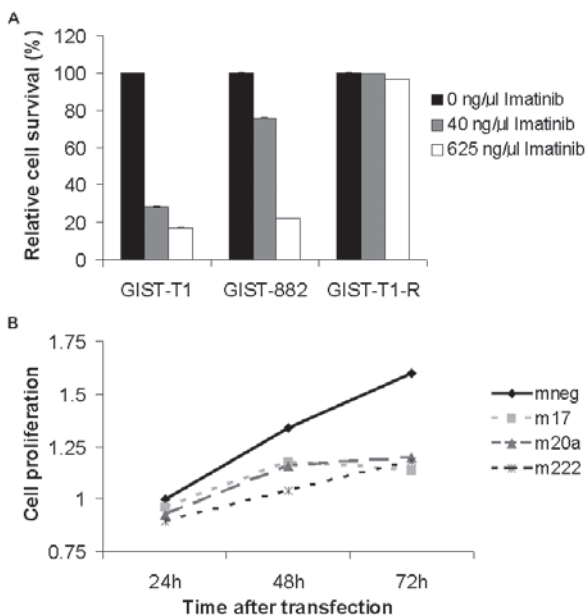
miR-222              UGGGUCAUCGGUCUACAUCGA 5'
                        | | |         |||||
ETV1      m222 site    5' GGAGGAGGAAGACTGTGTAGCAA
                        xx x
ETV1long  m222-mut    5' GGAGGAGGAAGACTGGATATCAA
    
```

Supplemental Figure 1: Predicted target sites for miR-17, miR-20a and miR-222 and mutations made in the 3'UTR of KIT and ETV1. Predicted 3'UTR target sites in KIT and ETV1 for miR-17, miR-20a and miR-222 and the mutations that have been generated in the target site sequence where the miRNA seed sequence (bold) binds. The vertical lines represent possible base pairing between miRNA and 3'UTR target site, and the x's indicate nucleotides that are mutated. For KIT, the miR-17/20a site and the miR-222 site that were present in the KITshort construct were mutated (KITsh m17/20a-mut, KITsh m222-mut). For ETV1, the miR-17/20a site that was present in the ETV1short and ETV1long construct, and the miR-222 site that was present in the ETV1long construct, were mutated (ETV1sh m17/20a-mut, ETV1lo m17/20a-mut, ETV1lo m222-mut). The resulting mutated 3'UTR fragments were tested in the context of the psiCHECK-2 luciferase reporter.

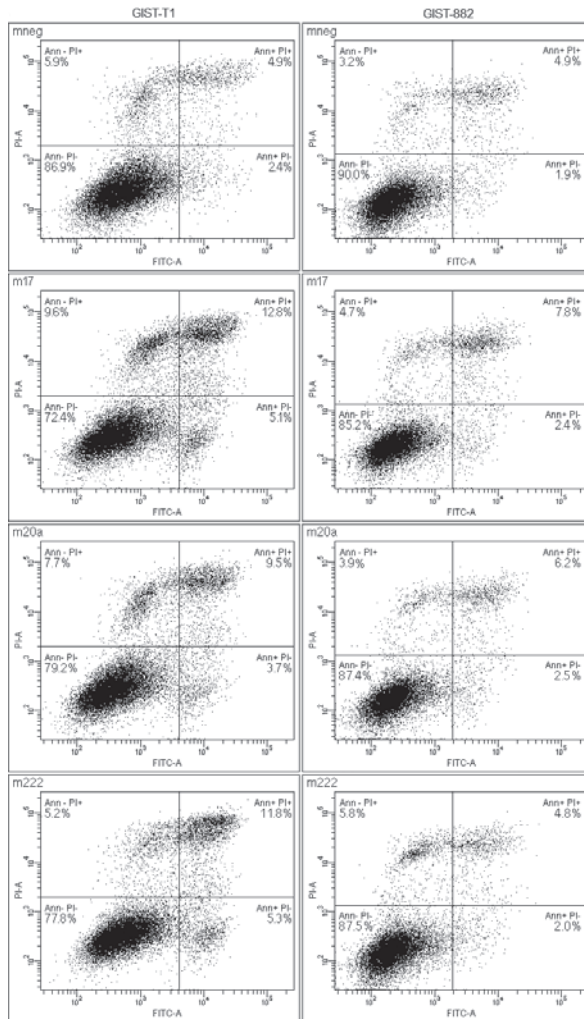




Supplemental Figure 2: Expression of miR-17, miR-20a, miR-222 in normal and tumor tissues. Bars represent miRNA microarray expression data of miR-17, miR-20a and miR-222 in normal (N) and tumor (T) tissues: colon (normal (n=26) vs. colorectal/adenocarcinoma (n=20)) and lung tissues (normal (n=14) vs. non-small cell lung cancer (n=18)). Depicted are average values \pm SD, average expression of the normal tissues is set at 100. Significant differences in miRNA levels are determined by student t-Test. * = $p < 0.05$

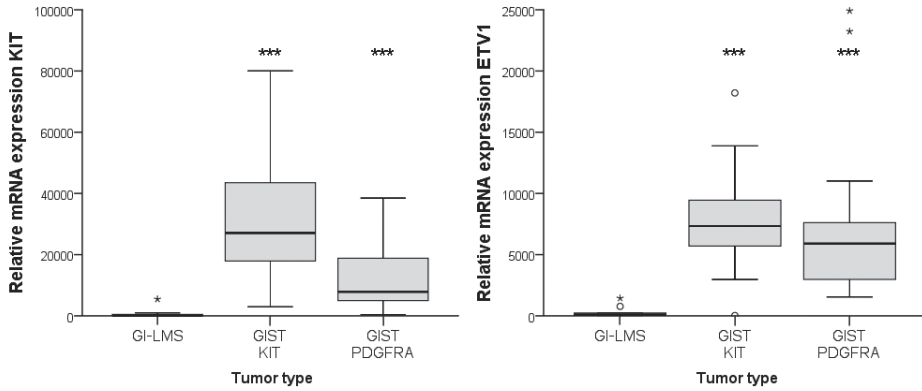


Supplemental Figure 3: Overexpression of miR-17, miR-20a and miR-222 causes reduced cell proliferation in imatinib resistant GIST. (A) GIST-T1, GIST-882 and GIST-T1-R cell lines were treated with 0 ng/ μ l, 40 ng/ μ l and 625 ng/ μ l imatinib for 72h after which cell density was measured by SRB assay. GIST-T1 and GIST-882 cells are sensitive to imatinib while the GIST-T1-R cell line is imatinib resistant. Bars depict average survival percentages \pm SD (n=2) relative to untreated cells which are set at 100% (B) Reduced cell proliferation of GIST-T1R cells transfected with miR-17, miR-20a and miR-222 mimics. Graphs depict average cell density (n=3) at 24h, 48h and 72h post-transfection, relative to the negative control (mneg; transfected with scrambled mimic) at 24h, which is set at 1.



Supplemental Figure 4: FACS plots from Annexin V/PI stainings of GIST-T1 and GIST-882 cell lines after transfection with miRNA mimics. GIST cell lines were transfected with scrambled (mneg), miR-17, miR-20a and miR-222 mimics, and harvested for Annexin V-FITC and PI staining after 72h. Viable cells end up in the lower left quadrant (Ann-/PI-), the lower right quadrant indicates the early apoptotic cells (Ann+/PI-), the upper right quadrant late apoptotic cells (Ann+/PI+) and the upper left quadrant dead cells (Ann-/PI+).





Supplemental Figure 5: *KIT* and *ETV1* expression is considerably higher in GIST compared to GI-LMS. Boxplots represent *KIT* and *ETV1* mRNA expression in GIST (n=50, either *KIT* or *PDGFRA* mutants) versus GI-LMS (n=10, median GI-LMS set at 100). *KIT* and *ETV1* expression was determined by qPCR and normalized to three housekeepers (*GAPDH*, *HPRT* and *HMBS*). Boxes represent 25th-75th percentile, line in the box represents median (50th percentile), whiskers represent lowest and highest values within 1.5x the interquartile range, circles are outliers (between 1.5-3x interquartile range), small asterisks are extreme values (>3x interquartile range). Significance differences in miRNA levels between GI-LMS and *KIT*- or *PDGFRA*-mutant GIST is determined by Mann Whitney U tests; *** = p<0.0005.

Chapter 5

MICRORNA RESPONSE TO HYPOXIC STRESS IN SOFT TISSUE SARCOMA CELLS: MICRORNA MEDIATED REGULATION OF HIF3A



Caroline M.M. Gits, Patricia F. van Kuijk, Jonneke C.W.M. de Rijck, Nikky Muskens, Moniek B.E. Jonkers, Wilfred F.J. van IJcken, Ron H.J. Mathijssen, Jaap Verweij, Stefan Sleijfer, Erik A.C. Wiemer

Submitted for publication

ABSTRACT

The state of hypoxia is often encountered in solid tumors and known to contribute to aggressive tumor behavior, radiation- and chemotherapy resistance and consequently a poor prognosis for the patient. MicroRNA (miRNAs) expression is regulated upon hypoxia, however, not much is known about the involvement of miRNAs in hypoxic signalling pathways in soft tissue sarcomas (STS). A panel of twelve STS cell lines was exposed to normal oxygen concentrations (normoxia) or 1% oxygen (hypoxia) for up to 48h. Hypoxic conditions were verified by upregulation of Hypoxia Inducible Factor (HIF) 1 α protein levels and increased mRNA expression of HIF1 target genes *CAIX* and *VEGFA*. Deregulation of miRNA expression after 24h of hypoxia was assessed by miRNA expression profiling using LNA™ oligonucleotide microarrays. The most differentially expressed miRNAs ($p < 0.001$) in response to hypoxia were miR-185*, miR-485-5p, miR-216a (upregulated) and miR-625 (downregulated). The well-known hypoxia responsive miR-210 was not detected by the microarray platform, but its upregulation upon hypoxic stress was verified by qPCR. Target prediction algorithms identified 11 potential binding sites for miR-485-5p and a single putative miR-210 binding site in the 3'UTR of *HIF3 α* , the least studied member of the HIF family. We showed that *HIF3 α* transcripts, expressing a 3'UTR containing the miR-485-5p and miR-210 target sites, are expressed in all sarcoma cell lines and upregulated upon hypoxia. Additionally, luciferase reporter constructs containing the 3'UTR of *HIF3 α* were used to demonstrate regulation of *HIF3 α* by miR-210 and miR-485-5p. In conclusion, here we provide evidence for the regulation of *HIF3 α* by hypoxia responsive miRNAs in STS which may help to tightly regulate and fine-tune the hypoxic response. This provides a better insight into the mechanisms underlying the hypoxic response in STS and may ultimately yield information on novel prognostic and predictive markers or targets for treatment.



INTRODUCTION

Hypoxia is a condition of reduced oxygen tension that is often encountered in solid tumors including soft tissue sarcomas (STS) when they outgrow their blood supply. The tumor cells respond to the hypoxic conditions by inducing genes that regulate various biological processes including cellular proliferation, apoptosis, metabolism, angiogenesis and migration.¹ A key element in the response to hypoxia is the upregulation of HIF1, a member of the family of hypoxia inducible factors (HIFs) also comprising HIF2 and HIF3.² These transcription factors consist of a tightly controlled alpha (HIF α), and a constitutively activated beta subunit (HIF β or ARNT family). Upon hypoxia, the alpha subunit is stabilized, translocated to the nucleus, where it dimerizes to the beta subunit. The HIF complex binds to hypoxia responsive elements (HREs) in gene promoters, thereby inducing the transcription of genes important for the adaption to low oxygen concentrations. HIF1 α and HIF2 α have similar protein domain structures, are regulated in a similar fashion and share several target genes,³ although their expression patterns differ in some tissues and some unique target genes have been identified.⁴ The function(s) of HIF3 α and the way it is regulated are still largely unknown. Complicating the study of *HIF3 α* is the fact that alternative splice variants are recognized coding for at least six isoforms, with structural and functional differences.⁵⁻⁷ *HIF3 α* is regulated by HIF1 at the transcriptional level and exerts an inhibitory effect on HIF1 α or HIF-dependent gene regulation, in a cell-type specific manner.⁵⁻¹¹

Tumor hypoxia and the accompanying biochemical and cellular changes in the tumor cells contribute to aggressive tumor behavior, and radiation- and chemotherapy resistance in many tumor types, including STS.¹²⁻¹³ STS is a group of relatively rare tumors of mesenchymal origin in which currently more than 50 different histological subtypes are recognized. STS have been reported to present with hypoxic areas resulting in increased tumor proliferation, distant metastases and shorter overall disease survival.¹⁴⁻¹⁵ Given the poor prognosis STS patients face with a median overall survival of only 1 year for patients presenting with metastatic disease, more insight is needed into the effects of hypoxia in STS and how hypoxia is regulated in STS.

MicroRNAs (miRNAs) are small (~ 23nt) non-protein coding RNA molecules that negatively regulate gene expression. MiRNAs play essential roles in a wide variety of cellular processes, such as differentiation, cell cycle regulation, metabolism, apoptosis and stem cell maintenance and are associated with various diseases including cancer.¹⁶ Most cancers display a deregulated miRNA expression profile when compared to relevant normal tissues. Some miRNAs may function as an oncomiR, having either a tumor suppressive or an oncogenic role.¹⁷⁻¹⁸ MiRNA expression can be influenced by changes in the tumor microenvironment,¹⁹⁻²⁰ including conditions like tumor hypoxia.²¹⁻²³ The miRNA response to hypoxia, which is often cell-type specific, suggests miRNAs are intimately involved in the cellular reaction to hypoxia²¹⁻²³ and some are in turn involved in feedback mechanisms that regulate *HIF*.²⁴⁻²⁹ Interestingly, many hypoxia responsive miRNAs



(HRMs) are also upregulated in cancer suggesting they also function in tumorigenesis and/or tumor progression.²¹ As opposed to the role of miRNAs in the major cancer types relatively little is known about the role of miRNAs in STS. In this study, we describe the miRNA response to hypoxic stress in sarcoma cell lines revealing the involvement of miRNAs in the hypoxic signalling in STS.

MATERIALS & METHODS

Cell culture

A panel of 12 soft tissue sarcoma cell lines was used, consisting of the fibrosarcoma cell lines HT1080, SW684 and BG-8, the liposarcoma cell line SW872, the leiomyosarcoma cell lines SK-UT-1 and SK-LMS-1, the synovial sarcoma cell line SW982 and the rhabdomyosarcoma cell lines RH30, A204, A673, RD and SJCRH30. Note that the A673 (ATCC®CRL-1598) cell line is now listed on the ATCC website as Ewing sarcoma. The myxoid fibrosarcoma cell line BG-8 was a kind gift from Dr. A. Carnero (Centro Nacional de Investigaciones Oncológicas, Madrid, Spain); HT1080, SK-UT-1, RD and RH-30 were acquired from Dr. M. Debiec-Rychter (KU Leuven, Leuven, Belgium) and SJCRH30 was obtained from Dr. L. Alberti (Université de Lyon, Centre Léon Bérard, Lyon, France). All further cell lines were obtained from the ATCC, Rockville, MD, USA. The cell lines were cultured in RPMI 1640/GlutaMAX (Invitrogen, Bleiswijk, The Netherlands) supplemented with 10% fetal bovine serum, at 37 °C, 5% CO₂, 21% O₂. Hypoxic experiments were carried out in an incubator at 37 °C, 5% CO₂, 1% O₂.

RNA isolation

Total RNA was isolated using RNAbee (Tel Test Inc., Friendswood, TX, USA) according to the manufacturer's recommendation. The RNA concentration and quality were determined on a Nanodrop-1000 (Nanodrop Technologies, Wilmington, DE, USA).

MiRNA microarray

MiRNA profiling was performed essentially as previously described.³⁰ In brief, 1 µg total RNA was fluorescently labeled with Cy3 using the ULS™ aRNA Labeling Kit (Kreatech Diagnostics, Amsterdam, The Netherlands). Labeled RNA was hybridized with locked nucleic acid (LNA™) modified oligonucleotide capture probes (Exiqon) spotted in duplicate on Nexterion E slides. The capture probe set (based on miRBase version 10, annotation version 13) contains 1344 probes of which 725 are capable of detecting human miRNAs. Hybridized slides were scanned and median spot intensity was determined using ImaGene software (BioDiscovery Inc., Hawthorne, CA, USA). After background subtraction, expression values were quantile normalized using R software, bad spots were deleted, and duplicate spots were averaged. For each expression value, the ratio to the geometric mean of the miRNA was log₂ transformed. These values were used to determine

differentially expressed miRNAs. Hierarchical clustering analyses were performed in Spotfire (Spotfire DecisionSite 9.1, Tibco Software, Somerville, MA, USA).

qPCR analysis of miRNA

MiR-210 expression was examined using TaqMan® MicroRNA Assays (Applied Biosystems, Nieuwerkerk aan den IJssel, The Netherlands). In brief, total RNA (50ng) was reverse transcribed using specific miRNA primers and the TaqMan® MicroRNA Reverse Transcription Kit (Applied Biosystems). The resulting cDNA was used as input in a quantitative real-time PCR (qPCR) using the miRNA specific primer/probe mix together with the TaqMan® Universal PCR Master Mix No AmpErase® UNG (Applied Biosystems) according to manufacturer's protocol. qPCR data were analyzed with SDS software (version 2.4, Applied Biosystems). MiRNA expression was normalized using RNU43 expression and the comparative C_T -method.³¹

cDNA-synthesis

RNA (1µg) was reversed transcribed using the High Capacity cDNA Reverse Transcription Kit (Applied Biosystems) according to the manufacturer's protocol. The resulting cDNA was used to perform qPCR and end-point PCR analysis.

qPCR analysis of mRNAs

cDNA (45ng) was used to perform qPCR using the primer/probe mix from the TaqMan® Gene Expression Assays of human *VEGFA* (assay ID Hs00900055_m1) and *CA-IX* (assay ID Hs00154208_m1) with exon spanning probes, and TaqMan® Universal PCR Master Mix using the 7500 Fast Real-Time PCR system (all Applied Biosystems) according to the manufacturer's protocol. *HPRT* was used as a housekeeper gene for normalization purposes using the comparative C_T -method.³¹ qPCR data was analyzed with SDS software (Applied Biosystems).

End-point PCR analysis

cDNA (50 ng) was used to perform endpoint PCR using 1x Green Go Taq Flexi Buffer, 1.25U Go Taq Flexi polymerase, 200 µM dNTP mix, 1.5 mM MgCl₂ and 300 nM forward and reverse primer of *HIF3α* (Supplemental Table 1a) on a thermal cycler using the following PCR-program: 2 min 95°C, 30-40 cycles of [45 sec 95°C, 45 sec 60-65°C, 45 sec 72°C], 5 min 72°C. PCR-products were analyzed on a 1.5% agarose gel in 0.5x TBE buffer with 0.5 µg/ml ethidium bromide.

Protein extraction

Cells were harvested in MCB lysis buffer (50 mM Tris-HCl pH 7.5, 50 mM NaCl, 10% glycerol, 1% NP-40, 0.5% Na-deoxycholate, 20 mM NaF) supplemented with a cocktail of protease and phosphatase inhibitors. Lysates were thoroughly vortexed and further lysed by two subsequent



freeze-thaw cycles using liquid nitrogen. Cell debris was spun down and protein concentration was determined by a Bradford assay (BioRad, Veenendaal, The Netherlands).

Western blotting

Twenty μg of total protein was subjected to SDS-PAGE. Proteins were transferred to a PVDF membrane followed by blocking of the membrane in 5% non-fat dry milk in PBS-Tween (Phosphate buffered saline, 0.05% Tween 20) to prevent non-specific antibody binding. Primary and secondary antibody incubations were carried out in the same buffer using anti-HIF1 α (610958, mouse monoclonal, 1:500, BD Biosciences, Breda, The Netherlands), anti-HIF3 α (ab10134, rabbit polyclonal, 1:500, Abcam, Cambridge, UK) and anti- β -Actin (AC-15, mouse monoclonal, 1:5000, Sigma-Aldrich, Zwijndrecht, The Netherlands) as a loading control. As secondary antibody HRP-conjugated goat-anti-mouse (1:10000, Santa Cruz Biotechnology, Heidelberg, Germany) or goat-anti-rabbit (1:10000, Jackson ImmunoResearch, Suffolk, UK) antibodies were used. Antibody incubations were followed by enhanced chemoluminescence (Supersignal West Pico Chemiluminescent Substrate, Thermo Scientific) and visualized on film (Amersham Hyperfilm ECL, GE Healthcare, Diegem, Belgium).

Mimic transfections

MiRIDIAN microRNA mimics (Thermo Scientific, Etten-Leur, Netherlands) of hsa-miR-210 and hsa-miR-485-5p and miRIDIAN microRNA Mimic Negative Control #1 (Thermo Scientific) were transfected in a final concentration of 50 nM using DharmaFECT1 transfection reagent (Thermo Scientific) 24h after cell seeding. For both cell lines transfection efficiency was optimized to >95% using fluorescent mimics.

Cloning

Fragments of the 3'UTR of *HIF3 α* (HIF3 α -short: 817 bp fragment, HIF3 α -long: 3807 bp fragment) were PCR amplified from human genomic DNA (Promega, Leiden, The Netherlands) introducing a XhoI (5'-end) and a NotI site (3'-end). The PCR products were cloned in PCR[®]-Blunt (Invitrogen), followed by a XhoI and NotI restriction and ligation in the psiCHECK[™]-2 vector (Promega) behind a *Renilla* luciferase gene. The psiCHECK-2 vector also contains a firefly luciferase gene, which was used for normalization. The resulting constructs are psiCHECK2/HIF3 α -short and psiCHECK2/HIF3 α -long. Site directed mutagenesis (QuickChange II XL, site directed mutagenesis kit, Agilent Technologies, Amsterdam, The Netherlands) was performed to mutate miR-210 and miR-485-5p target sites in the 3'UTR of *HIF3 α* in psiCHECK2/HIF3 α -short (Supplemental Figure 1). Primer sequences used for cloning and mutagenesis are listed in Supplemental Table 1b and 1c.

Luciferase assay

PsiCHECK-2/HIF3 α -short and psiCHECK2/HIF3 α -long were transfected using Fugene HD transfection reagent (Promega) 24h after cell seeding, or when mimics were used, 24h after miRNA mimic transfection, according to recommendations by the manufacturer. After 24 hours the cells were washed with PBS and lysed by Passive Lysis Buffer (Dual Luciferase[®] Reporter Assay System, Promega) for 30 min on a shaker platform. Lysates were transferred to white 96-wells microplates. Luciferase Assay Reagent II (Dual Luciferase[®] Reporter Assay System, Promega) was added, immediately followed by quantitation of the firefly luciferase activity on a luminometer (Aspekt Fluoroskan). Subsequently, Stop & Glo[®] Reagent (Dual Luciferase[®] Reporter Assay System, Promega) was added to the mixture, immediately followed by quantitation of the *Renilla* luciferase activity. Relative luciferase signals of duplicates were averaged, values (n=3) were normalized, and average and standard deviations were calculated. Significant differences in luciferase activity were determined by two-sample t-tests.

RESULTS

Hypoxia responsive miRNAs in soft tissue sarcoma cells

In order to examine the miRNA response to hypoxia in sarcomas, a panel of 12 soft tissue sarcoma cell lines was cultured for 0h, 6h, 24h and 48h under hypoxic (1% oxygen) or normoxic (21% oxygen) conditions. Exposure to hypoxic conditions was verified by the upregulation of HIF1 α protein levels, which is one of the earliest markers of hypoxia. HIF1 α protein, being degraded under normoxic conditions, is stabilized during hypoxia. As expected HIF1 α protein levels were significantly increased upon hypoxic stress (Figure 1A). At the 6h time point peak HIF1 α levels were observed which decreased after 24h and 48h of hypoxia. As a consequence of HIF1 α upregulation, the transcription of specific HIF1 target genes like *CA-IX* and *VEGFA* was slightly induced after 6h and further increased after 24-48h of hypoxia (Figure 1B, C).

Next, the miRNA expression profile was analyzed using microarrays containing LNA[™] oligonucleotide capture probes capable of detecting 725 human miRNAs. Since HIF1 target genes were clearly induced after 24h of hypoxia, miRNA expression levels of cell lines that were cultured for 24h under normoxic or hypoxic conditions were compared. Unsupervised hierarchical clustering based on the miRNA expression profiles grouped the cell lines on cell type rather than on exposure to hypoxia (Figure 2A), which implies that the changes in miRNA expression due to hypoxia are relatively minor. One major cluster branch contains the rhabdomyosarcoma cell lines and the synovial sarcoma cell line, the other branch contains the other cell lines (leiomyosarcoma, liposarcoma and fibrosarcoma cell lines). Supervised hierarchical clustering using the 32 most differentially expressed miRNAs ($p < 0.05$; Supplemental Table 2) between cell lines exposed to hypoxia or normoxia clearly separated the hypoxic from the normoxic samples (Figure 2B).



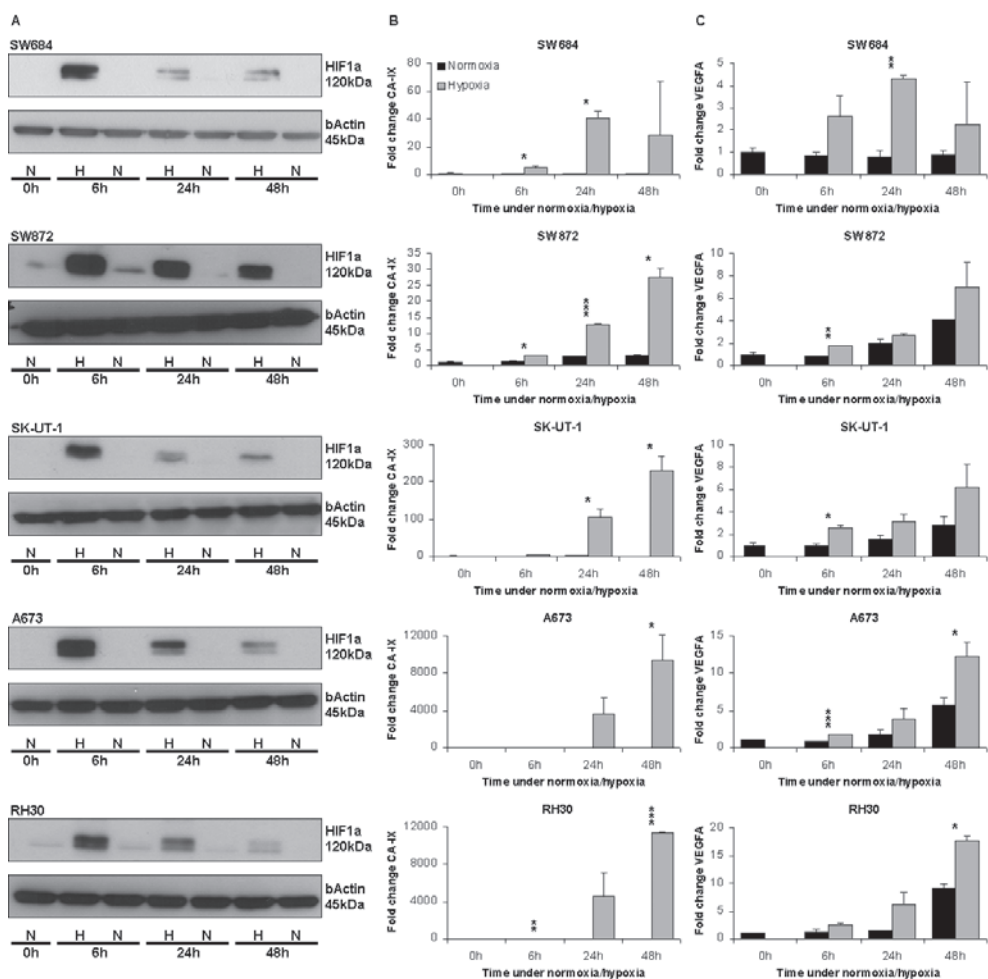


Figure 1: Hypoxia induces HIF1 α protein levels and CA-IX and VEGFA transcription in soft tissue sarcoma cell lines. A) HIF1 α protein levels are stabilized and increase during hypoxia. Cell lines were cultured under hypoxia (H) or normoxia (N) after the indicated times cell lysates were prepared and analysed by Western blotting for HIF1 α expression. HIF1 α levels peak at 6 hours of hypoxia. Upon prolonged hypoxia (24 and 48 hours) HIF1 α protein levels decrease, but remain increased compared to the HIF1 α levels detected in cells cultured under normoxic conditions. β -Actin was used as a loading control. B,C) mRNA levels of HIF1 target genes CA-IX (B) and VEGFA (C) are upregulated during hypoxia (grey bars) compared to normoxia (black bars). CA-IX and VEGFA expression was determined by RT-PCR and normalized to the expression of HPRT. Bars indicate average fold change of mRNA expression \pm S.D.(n=2) compared to the levels detected at 0h which are arbitrarily set at 1. Statistical significance between CA-IX and VEGF expression in normoxic and hypoxic samples at the various time points was determined by two-sample t-tests: *= p <0.05, **= p <0.005, ***= p <0.0005. The results obtained with five representative cell lines are shown.

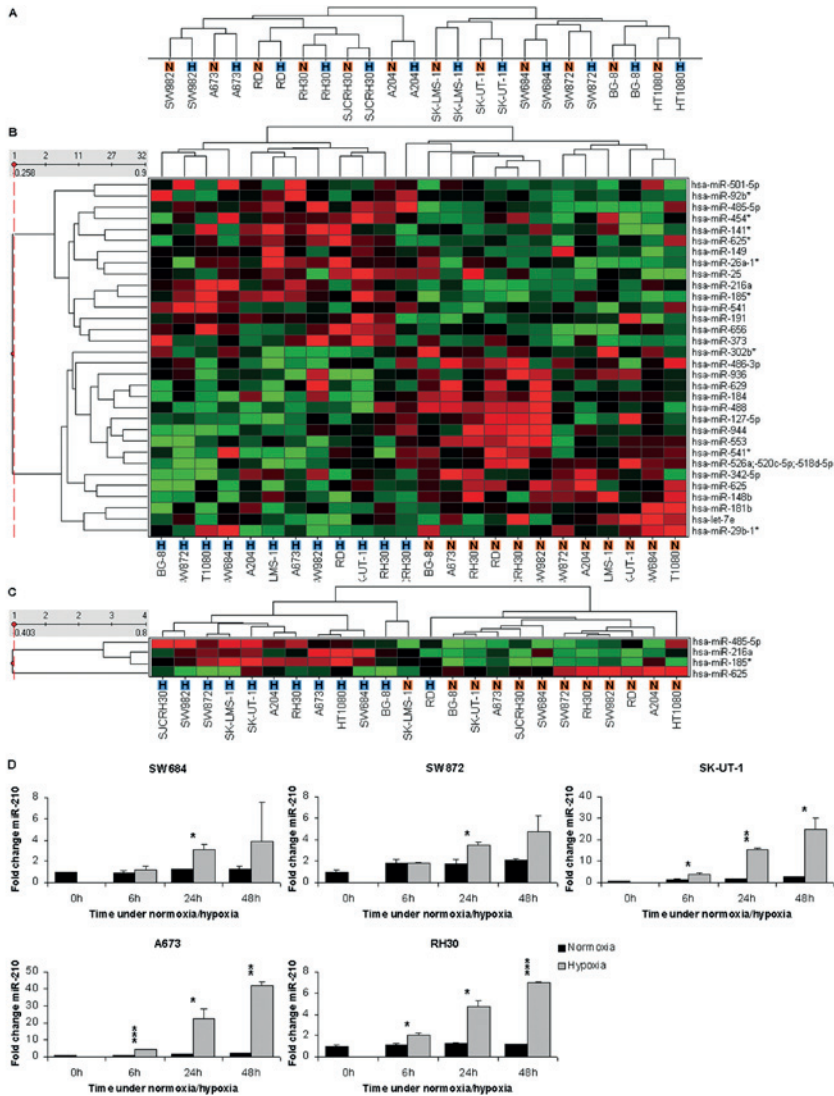


Figure 2: Hypoxia induces changes in miRNA expression. A) Unsupervised hierarchical clustering using miRNA expression data of hypoxic (H) and normoxic (N) cell line samples does not discriminate the hypoxic and normoxic samples. The hypoxic samples cluster together with their normoxic counterparts. B) The most significant differentially expressed miRNAs (two-sample t-test, $p < 0.05$) between cell lines that were cultured under normoxic and hypoxic conditions are used for a supervised hierarchical clustering. The expression of these 32 miRNAs can distinguish hypoxic from normoxic sarcoma cell line samples. C) The four most significant ($P < 0.001$) differentially expressed miRNAs (miR-485-5p, miR-216a, miR-185* and miR-625) discriminate sarcoma cell lines that were cultured under normoxic conditions from those cultured under hypoxic conditions in a supervised hierarchical clustering. D) MiR-210 is upregulated during hypoxia. RT-PCR was used to determine miR-210 levels in normoxic (black bars) and hypoxic (grey bars) samples from five representative sarcoma cell lines. Expression is normalized against RNU43 expression. Bars indicate average expression fold change \pm S.D. ($n=2$) of miR-210 compared to the expression at 0h. Statistical significance between expression in normoxic and hypoxic samples at a timepoint were determined by two-sample t-tests: *= $p < 0.05$, **= $p < 0.005$, ***= $p < 0.0005$.



Fifteen miRNAs were upregulated during hypoxia, while 17 miRNAs were downregulated. The SJCRH30 rhabdomyosarcoma cell line cultures under hypoxia was the only sample that misclustered, which indicates that the hypoxia induced miRNA response in this cell line was apparently weak. The top four differentially expressed miRNAs ($p < 0.001$) consisted of miR-185*, miR-485-5p, miR-216a and miR-625 (Figure 2C). Only miR-625 was downregulated in most hypoxic samples, whereas the other three miRNAs were predominantly upregulated. MiR-210, a commonly found hypoxia responsive miRNA (HRM), was undetectable on our microarray platform. Therefore the miR-210 expression in normoxic and hypoxic sarcoma cell line samples was separately determined by qPCR, which revealed a significant upregulation of miR-210 in all cell lines after 24h of hypoxia (Figure 2D).

HIF3 α transcripts are expressed and upregulated under hypoxia in sarcoma cell lines

Candidate target genes for the most differentially expressed miRNAs identified in the microarray analysis were predicted using TargetScanHuman 6.2 (<http://www.targetscan.org/>).³² When we focused on genes known to play a role in the hypoxic response it was noted that miR-485-5p has as much as 11 potential binding sites in the 3'UTR of HIF3 α , the less studied member of the family of hypoxia inducible factors. Also miR-210 has a single putative binding site in this transcript (Figure 3A).

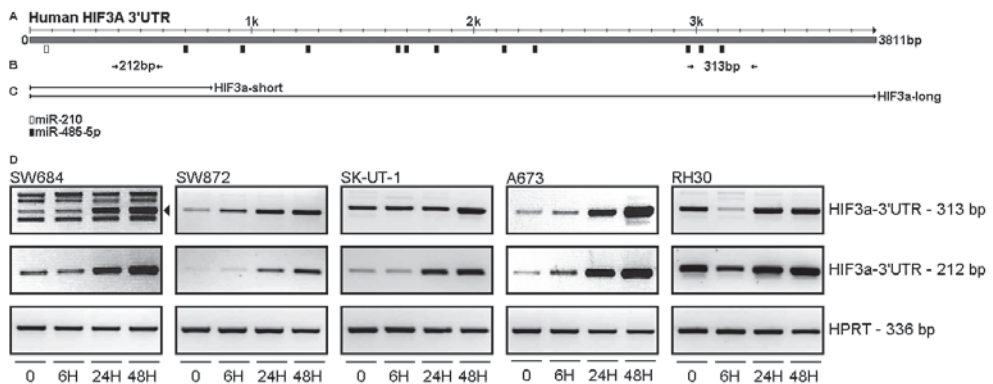


Figure 3: The 3'UTR of HIF3 α contains putative miR-210 and miR-485-5p binding sites and is expressed in sarcoma cell lines. A) Schematic representation of the 3'UTR of the HIF3 α transcript variants 003 and 201 (<http://www.ensembl.org>, release 72). Depicted are predicted target sites of miR-210 (open box) and miR-485-5p (black boxes). B) Arrows indicate location of primers used to detect the presence of HIF3 α 3'UTR transcripts. A 212 bp and 313 bp amplification product indicate expression of the 3'UTR of HIF3 α transcription variants 003 and 201. C) Lines designate the HIF3 α 3'UTR fragments (HIF3 α -short, HIF3 α -long) which were cloned into the psiCHECK-2 luciferase reporter to verify regulation of HIF3 α by miRNAs. D) End-point RT-PCR was used to determine the presence of HIF3 α 3'UTR transcripts and their induction upon hypoxia. Depicted are EtBr stained PCR amplification fragments of 212 and 313 bp derived from HIF3 α 3'UTR cDNA and an amplified 336 bp HPRT fragment as input control. The results obtained with five representative cell lines are shown.

Several human *HIF3α* transcripts exist due to alternative splicing, coding for different HIF3α isoforms.⁵⁻⁷ According to the Ensemble Genome Browser release 72 (<http://www.ensembl.org>) the *HIF3α* transcript variants 003 and 201 (consistent with HIF3α transcription variant 1, 2 and 3 according to GenBank (<http://www.ncbi.nlm.nih.gov/genbank>)) contain a long 3'UTR of 3811bp which includes the potential miR-210 and miR-485-5p binding sites. In order to determine whether these transcripts are expressed in our sarcoma cell line panel we used an adapted RT-PCR procedure involving an end-point PCR and specific primers located in the 3'UTR (primer sites are indicated in Figure 3B, primer sequences are listed in Supplemental Table 1a). *HIF3α* transcripts containing a long 3'UTR harboring the mentioned miRNA binding sites could be detected in all cell lines and were upregulated in time under hypoxic conditions (Figure 3D).

MiR-485-5p and miR-210 target HIF3α

The effects of miR-210 and miR-485-5p overexpression on HIF3α, protein levels were examined by immunoblotting. The sarcoma cell lines SW872 (liposarcoma) and SK-UT-1 (leiomyosarcoma) were transfected with mimics of miR-210, miR-485-5p or a scrambled negative control. 48h post-transfection the cells were exposed to hypoxia for 24h to induce HIF3α. Figure 4A clearly shows that overexpression of the miRNA mimics resulted in a reduced induction of HIF3α when compared to the HIF3α protein levels observed in cells transfected with a scrambled control mimic (mneg). The detected HIF3α protein has a relative molecular weight of approximately 70 kDa which is in line with the predicted molecular weight of the HIF3α proteins encoded by the 003 or 201 *HIF3α* transcript variants.

To demonstrate that during hypoxia HIF3α is regulated by hypoxia responsive miRNAs, a short (HIF3α-short, 817 bp) and a long (HIF3α-long, 3807 bp) fragment of the *HIF3α* 3'UTR (variants 003/ 201) (Figure 3C) were cloned in a psiCHECK2 luciferase reporter. The psiCHECK2/HIF3α-short construct encompassed the putative miR-210 binding site and the first miR-485-5p binding site. The psiCHECK2/HIF3α-long construct included an additional 10 potential binding sites for miR-485-5p. The SW872 and SK-UT-1 cell lines were transfected with the psiCHECK2/HIF3α-short and psiCHECK2/HIF3α-long constructs. The next day the cells were exposed to hypoxia for 24h, after which the luciferase activity in cell lysates was determined. Luciferase activity in SW872 hypoxic lysates was reduced to 57% and 65% in the HIF3α-short and HIF3α-long transfectants, respectively, when compared to the levels seen at normoxic circumstances (Figure 4B, left panel). In the hypoxic SK-UT-1 lysates the luciferase activity was decreased to 79% and 67% in the HIF3α-short and HIF3α-long transfectants, respectively (Figure 4B, right panel). These results indicate that during 24h hypoxia the 3'UTR of HIF3α is targeted, most likely by hypoxia responsive miRNAs, causing a reduction of the luciferase activity.



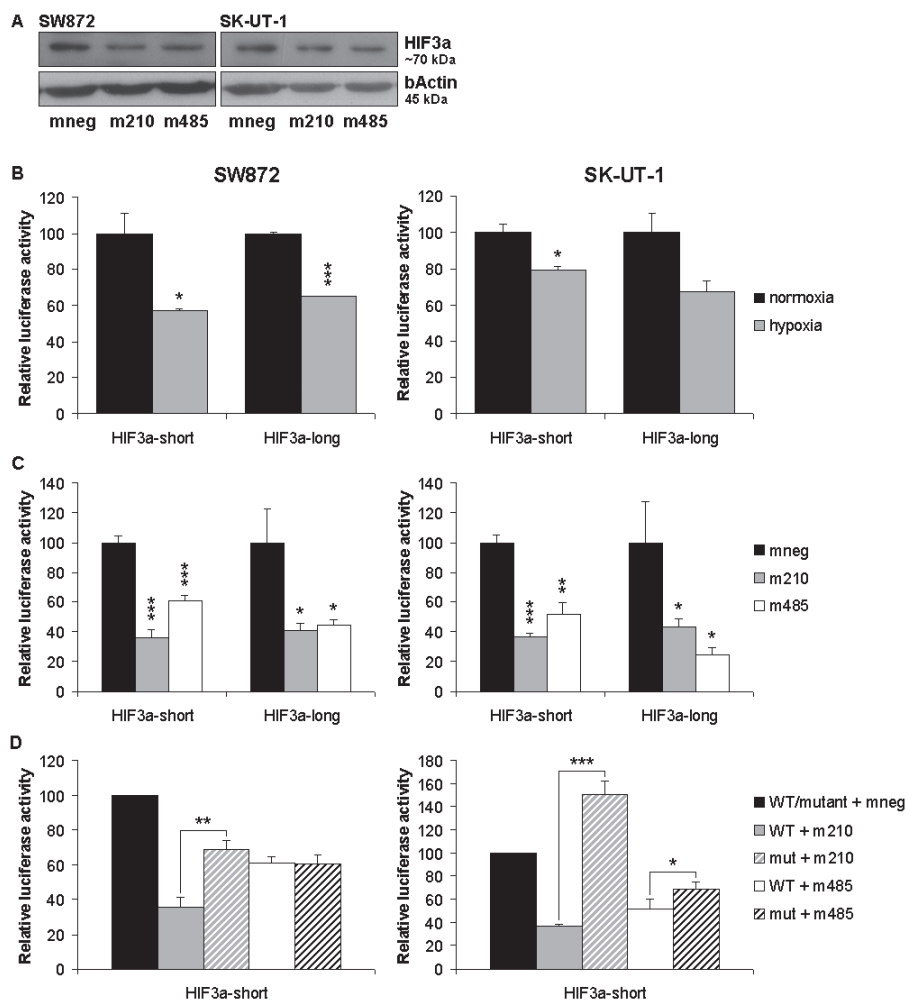


Figure 4: HIF3 α is regulated by miR-210 and miR-485-5p. A) MiR-210 and miR-485-5p mimic overexpression reduce HIF3 α protein induction under hypoxic conditions. Total protein lysates obtained from SW872 and SK-UT-1 cell lines, cultured for 24h under hypoxia and transfected with miR-210 mimic (m210), miR-485-5p mimic (m485) or a scrambled control mimic (mneg) were analysed by Western blotting for HIF3 α protein expression. β -Actin is used as a loading control. B) Hypoxia responsive miRNAs target HIF3 α 3'UTR. SW872 and SK-UT-1 cell lines were transfected with psiCHECK 2 constructs containing short and long 3'UTR fragments of HIF3 α . 48h later the cells were exposed to hypoxia for 24h. Bars indicate average luciferase activity \pm SD (n=3) measured in hypoxic cell lysates relative to the luciferase activity in normoxic cell lysates which is arbitrarily set at 100. C) MiR-210 and miR-485-5p regulate HIF3 α . SW872 and SK-UT-1 cell lines were transfected with mimics of miR-210, miR-485-5p or a scrambled control mimic (mneg) followed after 24h by a transfection with psiCHECK 2 constructs containing short and long fragments of the HIF3 α 3'UTR. Bars indicate average luciferase activity \pm SD (n=3) measured in cell lysates after 24h. D) MiR-210 and miR-485-5p regulate HIF3 α . SW872 and SK-UT-1 cell lines were transfected with mimics of miR-210, miR-485-5p or a scrambled control mimic (mneg) followed, after 24h, by a transfection with a psiCHECK 2-HIF3 α -short containing either wild-type(WT) or mutated (mut) miR-210 and miR-485-5p binding sites. Bars indicate average luciferase activity \pm SD (n=3) measured in cell lysates. Statistical significance was determined by two-sample t-tests: * p <0.05, ** p <0.005, *** p <0.0005.

To examine whether downregulation of HIF3 α is mediated by miR-210 and/or miR-485-5p we transfected miRNA mimics for miR-210 and miR-485-5p in SW872 and SK-UT-1 cells, after 24h followed by the transfection of the psiCHECK2/HIF3 α 3'UTR luciferase reporter constructs. Compared to the scrambled negative control (mneg), miR-210 overexpression decreased the luciferase activity to 36% and 41% in SW872 (Figure 4C, left panel) and 37% and 43% in SK-UT-1 (Figure 4C, right panel) in the HIF3 α -short and HIF3 α -long transfectants respectively. MiR-485-5p overexpression reduced the luciferase activity to 61% in the HIF3 α -short construct in the SW872 cell line. When ten additional putative binding sites for miR-485-5p were introduced in the HIF3 α -long transfectant, the luciferase activity dropped to 45% (Figure 4C, left panel). Overexpression of miR-485-5p decreased luciferase activity to 52% in SK-UT-1 cells transfected with psiCHECK2/HIF3 α -short and further reduced luciferase activity to 24% in the HIF3 α -long transfectants (Figure 4C, right panel).

To prove whether the regulation of HIF3 α is due to direct binding of miR-210 and miR-485-5p to target sites in the 3'UTR, the predicted binding sites were mutated to prevent miRNA binding (Supplemental Figure 1). Since the regulatory effect of the single miR-485-5p site present in the HIF3 α -short construct was greater than the effect of the additional miR-485-5p binding sites present in the HIF3 α -long construct, only the miR-485-5p target site in the HIF3 α -short construct was mutated. The presence of a mutated miR-210 binding site significantly increased (SW872) or restored (SK-UT-1) luciferase activity (Figure 4D). Mutation of the miR-485-5p target site did not affect luciferase activity in SW872 cells and restored luciferase activity to some extent in the SK-UT-1 cells. We conclude that miR-210 directly regulates HIF3 α whereas the regulation observed with miR-485-5p is primarily due to an indirect effect. However, we cannot rule out that direct regulation of HIF3 α does occur mediated by one or more of the additional miR-485-5p binding sites in the *HIF3 α* 3'UTR.

DISCUSSION

STS, like all solid tumors, can present with hypoxic areas, a state which is associated with disease progression and bad prognosis.¹⁴⁻¹⁵ To date, little is known about the involvement of miRNAs in the hypoxic response of STS. Greither et al. reported that the expression of miR-210, a well-known hypoxia responsive miRNA, is associated with poor survival in STS.³³ We identified 32 miRNAs that are deregulated upon hypoxia in a panel of 12 soft tissue sarcoma cell lines. Particularly, miR-185*, miR-485-5p, miR-216a were significantly upregulated, while miR-625 was significantly downregulated. In addition we detected induction of miR-210. A subset of the deregulated miRNAs, i.e. miR-185*, miR-191, miR-210, miR-373 (upregulated), miR-148b, miR-181b and miR-342-5p (downregulated), was previously identified as hypoxia responsive miRNAs (HRM) in other studies involving different cancer types.³⁴⁻³⁷ These miRNAs may be regarded as general responders to hypoxia. However the majority of miRNAs we detected has not been



previously associated with hypoxia suggesting a cell-type specific miRNA response, as has been reported before.³⁸⁻³⁹

The molecular mechanisms responsible for miRNA deregulation in response to hypoxia are for a large part still unclear as is the precise role of each of the HRM in the hypoxia response. As the key response to hypoxic conditions is the stabilization of HIF1, HRMs can be regulated by HIF-dependent or, alternatively, by HIF-independent mechanisms (reviewed in ³⁹⁻⁴⁰). Some HRMs, such as miR-210, contain hypoxia responsive elements (HREs) in their promoter region and are directly regulated by the HIF1 transcription factor in response to hypoxia.^{21, 41-42} Although HIF1 is generally known as a transcriptional activator, it can also function as a transcriptional repressor,⁴³ which could account for the downregulated miRNAs under hypoxic conditions. Another HIF-dependent mechanism by which hypoxia responsive miRNAs are regulated is via a HIF1 induced transcription factor, such as TWIST, which induces miR-10b expression.⁴⁴ A HIF-independent mechanism involved in the regulation of HRMs is e.g. the induction of Akt2 upon hypoxia, which in turn upregulates miR-21.⁴⁵ Also deregulation of the miRNA biogenesis during hypoxia could contribute to altered miRNA expression levels. Recently it was reported that hypoxia enhanced the association between EGFR and Ago2, resulting in increased Ago2-phosphorylation and reduced binding of Dicer to Ago2, thereby inhibiting miRNA processing.⁴⁶ In contrast, in another study hypoxia did not alter the expression of key miRNA machinery proteins (i.e. Drosha, Exp5, Dicer, Ago2 and DP103) in human trophoblasts.⁴⁷ In order to determine whether our top hypoxia responsive miRNAs (miR-185*; miR-485-5p; miR-216a and miR-625) contain HREs in their putative promoter region we screened 600 bp flanking sequences upstream of the transcription start site of the primary miRNA. With the exception of miR-485-5p of which the gene resides in a densely packed miRNA cluster on chromosome 14, the genes for miR-185, miR-216a and miR-625 are not clustered. No consensus HRE (A/GCGTG) could be detected upstream of miR-625 (which was downregulated during hypoxia), whereas miR-216a contains a 'ACGTGC'(position -42 to -37) and miR-185 contains a 'CCGTG'(position -305 to -301). Although the latter HRE does not perfectly match the consensus HRE sequence, imperfect HREs have been found to be functional.^{8, 48-49} Therefore it is possible that miR-216a and miR-185* are regulated by HIF1.

Since miR-210 is considered a general responder to hypoxia irrespective of cell-type and exact hypoxic conditions, its function is thought to be universal. MiR-210 has been demonstrated to have a role in e.g. cell proliferation, angiogenesis, apoptosis, DNA repair and mitochondrial metabolism (reviewed in ^{23, 50-51}). The function of other, less commonly deregulated HRMs is poorly understood, but these miRNAs are likely to have a cell-type specific function. Not much is known about miR-485-5p. This miRNA was downregulated in ependymomas⁵² and suppressed dendritic spine development in rats.⁵³ Furthermore miR-485-5p was downregulated in Alzheimers disease⁵⁴ and malignant serous ovarian tumors, and correlated with FIGO grade



in the latter.⁵⁵ Computational analysis predicted as much as eleven putative miR-485-5p binding sites in the 3'UTR of HIF3 α . Also miR-210 has a potential binding site in the 3'UTR of this member of the family of hypoxia inducible factors. Note that there are only two HIF3 α transcripts (variants 003 and 201) listed (<http://www.ensembl.org>; release 72) that harbor a 3'UTR long enough to encompass all miR-485-5p binding sites in addition to the miR-210 site. At least two other HIF3 α transcripts that contain a smaller 3'UTR (478 bp in variant 006 and 287 bp in variant 007) also contain the miR-210 binding site suggesting that the HIF3 α isoforms they encode may be controlled by miR-210. We demonstrated that HIF3 α is regulated by miR-210 and in an indirect fashion by miR-485-5p. We also showed that HIF3 α mRNA levels are induced upon hypoxia as expected of an hypoxia inducible factor. Under the same conditions, however, the expression of hypoxia responsive miRNAs like miR-210 and miR-485-5p is upregulated, which affects HIF3 α protein expression. We postulate that miRNAs help to fine-tune HIF3 α protein expression and in this way regulate the cellular hypoxic response. They can do so by affecting the translation of specific HIF3 α transcripts, however, we cannot rule out that part of the regulation takes place via HIF3 α mRNA degradation. Although HRMs targeting HIF3 α have never been documented before, miRNA regulation of HIFs is not uncommon: miR-155,⁴² mir-424,²⁸ and the miR-17-92 cluster²⁹ are known to target HIF1 α . Thus HIFs can induce the expression of miRNAs, and in turn, miRNAs can also target HIFs.

Our understanding of the regulation of HIF3 α and its role in the hypoxic response is still rather limited. Reports in the literature are sometimes contradictory or difficult to compare as they focus on different HIF3 α splice variants in different cell types. It is clear that HIF3 α can be regulated at different levels. Transcription of HIF3 α can be induced by HIF via HREs in the promoter region.⁶⁻⁸ This probably accounts for the increased HIF3 α mRNA expression upon hypoxia. In addition HIF3 α can be regulated at the protein level. HIF1 α and HIF2 α contain an oxygen dependent degradation domain (ODDD), which harbors two conserved prolines that can be hydroxylated by prolyl hydroxylases (PHDs) in presence of oxygen. This marks the proteins for proteasomal degradation via the von Hippel-Lindau (VHL) E3 ubiquitin ligase complex. It was postulated that HIF3 α , in contrast with HIF1 α and HIF2 α , is not regulated at the level of protein stability, since the longer HIF3 α transcripts miss part of the ODDD and the shorter isoforms lack the entire ODDD. This renders them less prone to hydroxylation and subsequent proteasomal degradation.⁸ However, other studies showed that the remaining proline residue in the ODDD of HIF3 α transcripts is targeted by VHL and subjected to proteasomal degradation in an oxygen dependent manner.^{5,7} Besides transcriptional regulation of HIF3 α by HIF1 and oxygen dependent degradation of HIF3 α proteins, we provide evidence for an additional layer of regulation of HIF3 α , i.e. miRNAs that act on the translational level. These different mechanisms can complement one another in fine tuning HIF3 α expression. This may be critical because of the versatile role HIF3 α plays in the hypoxic response.



None of the HIF3 α variants are likely to act as potent transcription factors, since they lack a C-terminal transactivation domain. However, they can have an effect on HRE-driven gene expression, depending on the level of HIF β .^{7, 10-11} When HIF β is not limiting, it will dimerize with HIF1 α , HIF2 α and HIF3 α to induce a subset of hypoxia regulated genes. HIF1 α /HIF β and HIF2 α /HIF β complexes will associate with HRE sequences, while the HIF3 α /HIF β complexes likely bind a response element different from the canonical HRE, to maximize hypoxia induced gene expression.⁷ When HIF β is limiting, HIF3 α will either compete with HIF1 α and HIF2 α for binding with HIF β ,¹⁰ or HIF3 α will associate with HIF1 α and HIF2 α ,^{7,11} both resulting in decreased capability to bind HRE sequences and diminished transcription of HIF target genes. As such, HIF3 α splice variants will not act as global regulators of gene expressions, but may modulate specific genes in a cell type dependent manner.⁷⁻⁸

In summary, this study describes, in addition to miR-210, a new panel of HRMs in hypoxic sarcoma cells. In turn, two of these HRMs, i.e. miR-210 and miR-485-5p, regulate HIF3 α in a direct or indirect fashion, respectively. Fine-tuning of HIF3 α expression is of great importance for the hypoxic response, since HIF3 α affects HIF1/2-induced gene expression. Keeping these negative feedback loops under tight control enables the cells to adapt to hypoxic conditions. Deregulation of these mechanisms, e.g. by therapeutic modulation of levels of miRNAs that are important for the hypoxic response, may inhibit the adaptive potential of the cells, and reduce their resistance against radiation and systemic agents. This could be beneficial not only against hypoxic tumors, but also in other diseases where low oxygen levels plays a role, e.g. in myocardial ischemia, stroke and chronic lung disease.⁵⁶

ACKNOWLEDGEMENTS

This study was funded by EC FP6 CONTICANET network of excellence (LSHC-CT-2005-018806) from the European Commission. We thank dr. A. Carnero, dr. M. Debiec-Rychter and dr. L. Alberti for providing cell lines.



REFERENCES

1. Harris AL. Hypoxia—a key regulatory factor in tumour growth. *Nat Rev Cancer*. 2002 Jan;2(1):38-47.
2. Wang GL, Semenza GL. General involvement of hypoxia-inducible factor 1 in transcriptional response to hypoxia. *Proc Natl Acad Sci U S A*. 1993 May 1;90(9):4304-8.
3. Ema M, Taya S, Yokotani N, Sogawa K, Matsuda Y, Fujii-Kuriyama Y. A novel bHLH-PAS factor with close sequence similarity to hypoxia-inducible factor 1alpha regulates the VEGF expression and is potentially involved in lung and vascular development. *Proc Natl Acad Sci U S A*. 1997 Apr 29;94(9):4273-8.
4. Hu CJ, Wang LY, Chodosh LA, Keith B, Simon MC. Differential roles of hypoxia-inducible factor 1alpha (HIF-1alpha) and HIF-2alpha in hypoxic gene regulation. *Mol Cell Biol*. 2003 Dec;23(24):9361-74.
5. Maynard MA, Qi H, Chung J, Lee EH, Kondo Y, Hara S, et al. Multiple splice variants of the human HIF-3 alpha locus are targets of the von Hippel-Lindau E3 ubiquitin ligase complex. *J Biol Chem*. 2003 Mar 28;278(13):11032-40.
6. Pasanen A, Heikkila M, Rautavuoma K, Hirsila M, Kivirikko KI, Myllyharju J. Hypoxia-inducible factor (HIF)-3alpha is subject to extensive alternative splicing in human tissues and cancer cells and is regulated by HIF-1 but not HIF-2. *Int J Biochem Cell Biol*. 2010 Jul;42(7):1189-200.
7. Heikkila M, Pasanen A, Kivirikko KI, Myllyharju J. Roles of the human hypoxia-inducible factor (HIF)-3alpha variants in the hypoxia response. *Cell Mol Life Sci*. 2011 Dec;68(23):3885-901.
8. Tanaka T, Wiesener M, Bernhardt W, Eckardt KU, Warnecke C. The human HIF (hypoxia-inducible factor)-3alpha gene is a HIF-1 target gene and may modulate hypoxic gene induction. *Biochem J*. 2009 Nov 15;424(1):143-51.
9. Maynard MA, Evans AJ, Hosomi T, Hara S, Jewett MA, Ohh M. Human HIF-3alpha4 is a dominant-negative regulator of HIF-1 and is down-regulated in renal cell carcinoma. *FASEB J*. 2005 Sep;19(11):1396-406.
10. Hara S, Hamada J, Kobayashi C, Kondo Y, Imura N. Expression and characterization of hypoxia-inducible factor (HIF)-3alpha in human kidney: suppression of HIF-mediated gene expression by HIF-3alpha. *Biochem Biophys Res Commun*. 2001 Oct 5;287(4):808-13.
11. Maynard MA, Evans AJ, Shi W, Kim WY, Liu FF, Ohh M. Dominant-negative HIF-3 alpha 4 suppresses VHL-null renal cell carcinoma progression. *Cell Cycle*. 2007 Nov 15;6(22):2810-6.
12. Airley RE, Phillips RM, Evans AE, Double J, Burger AM, Feibig HH, et al. Hypoxia-regulated glucose transporter Glut-1 may influence chemosensitivity to some alkylating agents: results of EORTC (First Translational Award) study of the relevance of tumour hypoxia to the outcome of chemotherapy in human tumour-derived xenografts. *Int J Oncol*. 2005 Jun;26(6):1477-84.
13. Hockel M, Schlenger K, Aral B, Mitze M, Schaffer U, Vaupel P. Association between tumor hypoxia and malignant progression in advanced cancer of the uterine cervix. *Cancer Res*. 1996 Oct 15;56(19):4509-15.
14. Brizel DM, Scully SP, Harrelson JM, Layfield LJ, Bean JM, Prosnitz LR, et al. Tumor oxygenation predicts for the likelihood of distant metastases in human soft tissue sarcoma. *Cancer Res*. 1996 Mar 1;56(5):941-3.
15. Nordsmark M, Hoyer M, Keller J, Nielsen OS, Jensen OM, Overgaard J. The relationship between tumor oxygenation and cell proliferation in human soft tissue sarcomas. *Int J Radiat Oncol Biol Phys*. 1996 Jul 1;35(4):701-8.
16. Wiemer EA. The role of microRNAs in cancer: no small matter. *Eur J Cancer*. 2007 Jul;43(10):1529-44.
17. Chen CZ. MicroRNAs as oncogenes and tumor suppressors. *N Engl J Med*. 2005 Oct 27;353(17):1768-71.
18. Lujambio A, Lowe SW. The microcosmos of cancer. *Nature*. 2012 Feb 16;482(7385):347-55.
19. Li X, Wu Z, Fu X, Han W. A microRNA component of the neoplastic microenvironment: microregulators with far-reaching impact. *Biomed Res Int*. 2013;2013:762183.
20. Wentz-Hunter KK, Potashkin JA. The Role of miRNAs as Key Regulators in the Neoplastic Microenvironment. *Mol Biol Int*. 2011;2011:839872.
21. Kulshreshtha R, Ferracin M, Wojcik SE, Garzon R, Alder H, Agosto-Perez FJ, et al. A microRNA signature of hypoxia. *Mol Cell Biol*. 2007 Mar;27(5):1859-67.
22. Kulshreshtha R, Davuluri RV, Calin GA, Ivan M. A microRNA component of the hypoxic response. *Cell Death Differ*. 2008 Apr;15(4):667-71.
23. Crosby ME, Devlin CM, Glazer PM, Calin GA, Ivan M. Emerging roles of microRNAs in the molecular responses to hypoxia. *Curr Pharm Des*. 2009;15(33):3861-6.



24. Yamakuchi M, Lotterman CD, Bao C, Hruban RH, Karim B, Mendell JT, et al. P53-induced microRNA-107 inhibits HIF-1 and tumor angiogenesis. *Proc Natl Acad Sci U S A*. 2010 Apr 6;107(14):6334-9.
25. Cha ST, Chen PS, Johansson G, Chu CY, Wang MY, Jeng YM, et al. MicroRNA-519c suppresses hypoxia-inducible factor-1alpha expression and tumor angiogenesis. *Cancer Res*. 2010 Apr 1;70(7):2675-85.
26. Xu Q, Liu LZ, Qian X, Chen Q, Jiang Y, Li D, et al. MiR-145 directly targets p70S6K1 in cancer cells to inhibit tumor growth and angiogenesis. *Nucleic Acids Res*. 2012 Jan;40(2):761-74.
27. Kelly TJ, Souza AL, Clish CB, Puigserver P. A hypoxia-induced positive feedback loop promotes hypoxia-inducible factor 1alpha stability through miR-210 suppression of glycerol-3-phosphate dehydrogenase 1-like. *Mol Cell Biol*. 2011 Jul;31(13):2696-706.
28. Ghosh G, Subramanian IV, Adhikari N, Zhang X, Joshi HP, Basi D, et al. Hypoxia-induced microRNA-424 expression in human endothelial cells regulates HIF-alpha isoforms and promotes angiogenesis. *J Clin Invest*. 2010 Nov;120(11):4141-54.
29. Taguchi A, Yanagisawa K, Tanaka M, Cao K, Matsuyama Y, Goto H, et al. Identification of hypoxia-inducible factor-1 alpha as a novel target for miR-17-92 microRNA cluster. *Cancer Res*. 2008 Jul 15;68(14):5540-5.
30. Pothof J, Verkaik NS, van IJcken W, Wiemer EA, Ta VT, van der Horst GT, et al. MicroRNA-mediated gene silencing modulates the UV-induced DNA-damage response. *EMBO J*. 2009 Jul 22;28(14):2090-9.
31. Schmittgen TD, Livak KJ. Analyzing real-time PCR data by the comparative C(T) method. *Nat Protoc*. 2008;3(6):1101-8.
32. Lewis BP, Burge CB, Bartel DP. Conserved seed pairing, often flanked by adenosines, indicates that thousands of human genes are microRNA targets. *Cell*. 2005 Jan 14;120(1):15-20.
33. Greither T, Wurl P, Grochola L, Bond G, Bache M, Kappler M, et al. Expression of microRNA 210 associates with poor survival and age of tumor onset of soft-tissue sarcoma patients. *Int J Cancer*. 2012 Mar 1;130(5):1230-5.
34. Guimbellot JS, Erickson SW, Mehta T, Wen H, Page GP, Sorscher EJ, et al. Correlation of microRNA levels during hypoxia with predicted target mRNAs through genome-wide microarray analysis. *BMC Med Genomics*. 2009;2:15.
35. Xu X, Jia R, Zhou Y, Song X, Wang J, Qian G, et al. Microarray-based analysis: identification of hypoxia-regulated microRNAs in retinoblastoma cells. *Int J Oncol*. 2011 May;38(5):1385-93.
36. Crosby ME, Kulshreshtha R, Ivan M, Glazer PM. MicroRNA regulation of DNA repair gene expression in hypoxic stress. *Cancer Res*. 2009 Feb 1;69(3):1221-9.
37. Hebert C, Norris K, Scheper MA, Nikitakis N, Sauk JJ. High mobility group A2 is a target for miRNA-98 in head and neck squamous cell carcinoma. *Mol Cancer*. 2007;6:5.
38. Kulshreshtha R, Ferracin M, Negrini M, Calin GA, Davuluri RV, Ivan M. Regulation of microRNA expression: the hypoxic component. *Cell Cycle*. 2007 Jun 15;6(12):1426-31.
39. Shen G, Li X, Jia YF, Piazza GA, Xi Y. Hypoxia-regulated microRNAs in human cancer. *Acta Pharmacol Sin*. 2013 Mar;34(3):336-41.
40. Nallamshetty S, Chan SY, Loscalzo J. Hypoxia: A Master Regulator of MicroRNA Biogenesis and Activity: Hypoxic Regulation of MicroRNAs. *Free Radic Biol Med*. 2013 May 24.
41. Huang X, Ding L, Bennewith KL, Tong RT, Welford SM, Ang KK, et al. Hypoxia-inducible mir-210 regulates normoxic gene expression involved in tumor initiation. *Mol Cell*. 2009 Sep 24;35(6):856-67.
42. Bruning U, Cerone L, Neufeld Z, Fitzpatrick SF, Cheong A, Scholz CC, et al. MicroRNA-155 promotes resolution of hypoxia-inducible factor 1alpha activity during prolonged hypoxia. *Mol Cell Biol*. 2011 Oct;31(19):4087-96.
43. Chen KF, Lai YY, Sun HS, Tsai SJ. Transcriptional repression of human cad gene by hypoxia inducible factor-1alpha. *Nucleic Acids Res*. 2005;33(16):5190-8.
44. Haque I, Banerjee S, Mehta S, De A, Majumder M, Mayo MS, et al. Cysteine-rich 61-connective tissue growth factor-nephroblastoma-overexpressed 5 (CCN5)/Wnt-1-induced signaling protein-2 (WISP-2) regulates microRNA-10b via hypoxia-inducible factor-1alpha-TWIST signaling networks in human breast cancer cells. *J Biol Chem*. 2011 Dec 16;286(50):43475-85.
45. Polytaichou C, Iliopoulos D, Hatziapostolou M, Kottakis F, Maroulakou I, Struhl K, et al. Akt2 regulates all Akt isoforms and promotes resistance to hypoxia through induction of miR-21 upon oxygen deprivation. *Cancer Res*. 2011 Jul 1;71(13):4720-31.
46. Shen J, Xia W, Khotskaya YB, Huo L, Nakanishi K, Lim SO, et al. EGFR modulates microRNA maturation in response to hypoxia through phosphorylation of AGO2. *Nature*. 2013 May 16;497(7449):383-7.



47. Donker RB, Mouillet JF, Nelson DM, Sadovsky Y. The expression of Argonaute2 and related microRNA biogenesis proteins in normal and hypoxic trophoblasts. *Mol Hum Reprod.* 2007 Apr;13(4):273-9.
48. Makino Y, Uenishi R, Okamoto K, Isoe T, Hosono O, Tanaka H, et al. Transcriptional up-regulation of inhibitory PAS domain protein gene expression by hypoxia-inducible factor 1 (HIF-1): a negative feedback regulatory circuit in HIF-1-mediated signaling in hypoxic cells. *J Biol Chem.* 2007 May 11;282(19):14073-82.
49. Augstein A, Poitz DM, Braun-Dullaeus RC, Strasser RH, Schmeisser A. Cell-specific and hypoxia-dependent regulation of human HIF-3alpha: inhibition of the expression of HIF target genes in vascular cells. *Cell Mol Life Sci.* 2011 Aug;68(15):2627-42.
50. Devlin C, Greco S, Martelli F, Ivan M. miR-210: More than a silent player in hypoxia. *IUBMB Life.* 2011 Feb;63(2):94-100.
51. Chan YC, Banerjee J, Choi SY, Sen CK. miR-210: the master hypoxamir. *Microcirculation.* 2012 Apr;19(3):215-23.
52. Costa FF, Bischof JM, Vanin EF, Lulla RR, Wang M, Sredni ST, et al. Identification of microRNAs as potential prognostic markers in ependymoma. *PLoS One.* 2011;6(10):e25114.
53. Cohen JE, Lee PR, Chen S, Li W, Fields RD. MicroRNA regulation of homeostatic synaptic plasticity. *Proc Natl Acad Sci U S A.* 2011 Jul 12;108(28):11650-5.
54. Faghihi MA, Zhang M, Huang J, Modarresi F, Van der Brug MP, Nalls MA, et al. Evidence for natural antisense transcript-mediated inhibition of microRNA function. *Genome Biol.* 2010;11(5):R56.
55. Kim TH, Kim YK, Kwon Y, Heo JH, Kang H, Kim G, et al. Deregulation of miR-519a, 153, and 485-5p and its clinicopathological relevance in ovarian epithelial tumours. *Histopathology.* 2010 Nov;57(5):734-43.
56. Semenza GL. Perspectives on oxygen sensing. *Cell.* 1999 Aug 6;98(3):281-4.



SUPPLEMENTAL TABLES AND FIGURES

Supplemental Table 1: Primers used for PCR and cloning.

A

Primer	Sequence	Product
HIF3 α Fw1	5'-AGAACAATGATCCACGGGT-3'	212 bp
HIF3 α Rv1	5'-GCCTCAATCGGAAGTCAC-3'	
HIF3 α Fw2	5'-GCCTCACAGCTTCCAAC-3'	313 bp
HIF3 α Rv2	5'-TGGGGCACAGAGATTGTAG-3'	
HPRT Fw	5'-ATGGGAGGCCATCACATTG-3'	336 bp
HPRT Rv	5'-GGTCCTTTCCACCAGCAAG-3'	

B

Primer	Sequence	Product
Fw	5'-GTCTCGAGCCGGCTCCTCTCCCATCTG-3'	817 bp
Rv-short	5'-GAGCGGCCGAGACCACATTGGAGGTTG-3'	
Rv-long	5'-GAGCGGCCGCTGCTACCAAGGTGAGGTCCTTAT-3'	

C

Primer Mutagenesis	Sequence
HIF3a-485-5p Fw	5'-CCTACTTCAGGGGCCGCGCCAGTTCCTCTGC-3'
HIF3a-485-5p Rv	5'-GCAGAGGAAGTGGCCGCGCCCTGAAGTAGG-3'
HIF3a-210 Fw	5'-CCACGCCGCGAGCAAAGCTTAGGATGGGGCG-3'
HIF3a-210 Rv	5'-CGCCCCATCCTAAGCTTTGGCTGCCGGCGTGG-3'

(A) Primers used for end-point RT-PCRs of HIF3 α 3'UTR fragments, resulting in amplification products of 212 bp (Fw/Rv1) and 313 bp (Fw/Rv2). Amplification of HPRT (product of 335 bp) was used as input control. (B) Primers used for cloning HIF3 α -short and HIF3 α -long 3'UTR constructs. (C) Primers used for site mutagenesis of predicted miR-485-5p and miR-210 binding sites in HIF3 α -short 3'UTR constructs.

Supplemental Table 2: Differentially expressed miRNAs ($p < 0.05$) between cell lines that were cultured under hypoxic and normoxic conditions. P-values of two-sample t-test as well as fold change in miRNA expression and miRNA genomic locations are indicated.

MiRNA	Parametric p-value	Fold-change Up in Hypoxia	Fold-change Down in Hypoxia	Genomic Location
1 hsa-miR-185*	4,60E-06	1,89		22-q11.21
2 hsa-miR-485-5p	1,42E-05	2,61		14-q32.31
3 hsa-miR-216a	0,0003276	1,91		2-p16.1
4 hsa-miR-625	0,0007143		1,38	14-q23.3
5 hsa-miR-553	0,0018115		1,33	1-p21.2
6 hsa-miR-526a; hsa-miR-520c-5p; hsa-miR-518d-5p	0,004425		1,19	19-q13.41
7 hsa-miR-148b	0,0076947		1,18	12-q13.13
8 hsa-miR-184	0,00935		1,24	15-q25.1
9 hsa-miR-656	0,0094883	1,22		14-q32.31
10 hsa-miR-488	0,0107997		1,24	1-q25.2
11 hsa-miR-127-5p	0,0110241		1,32	14-q32.31
12 hsa-miR-541*	0,0120157		1,26	14-q32.31
13 hsa-miR-181b	0,0163786		1,23	1-q31.3; 9-q33.3
14 hsa-miR-302b*	0,0227309		1,23	4-q25
15 hsa-miR-936	0,0258524		1,16	10-q25.1
16 hsa-miR-944	0,0281864		1,24	3-q28
17 hsa-let-7e	0,0291331		1,29	19-q13.33
18 hsa-miR-149	0,0297993	1,31		2-q37.3
19 hsa-miR-541	0,029902	1,30		14-q32.31
20 hsa-miR-26a-1*	0,0311843	1,16		3-p22.2
21 hsa-miR-92b*	0,034333	1,32		1-q22
22 hsa-miR-501-5p	0,0354958	1,23		X-p11.23
23 hsa-miR-342-5p	0,0370505		1,19	14-q32.2
24 hsa-miR-454*	0,0399102	1,21		17-q22
25 hsa-miR-191	0,0411142	1,19		3-p21.31
26 hsa-miR-625*	0,0424962	1,29		14-q23.3
27 hsa-miR-373	0,0433468	1,18		19-q13.41
28 hsa-miR-486-3p	0,043349		1,28	8-p11.21
29 hsa-miR-141*	0,0469436	1,17		12-p13.31
30 hsa-miR-25	0,0472339	1,18		7-q22.1
31 hsa-miR-29b-1*	0,0476345		1,22	7-q32.3
32 hsa-miR-629	0,049196		1,20	15-q23



```

5' ...CCACGCCGGCAGCCAACGCACAG... - HIF3α position 56-78 WT
      |||||      | |||||
3'   AGUCGGCGACAGUGUGCUGUC      - hsa-miR-210
      |||||      | |x| |xx|
5' ...CCACGCCGGCAGCCAAAGCTTAG... - HIF3α-m210-mut

5' ...CUCCUACUUCAGGGGCAGCCUCC... - HIF3α position 687-709 WT
      | |||| | | |||||
3'   CUUAAGUAGUGCCGGUCGAGA      - hsa-miR-485-5p
      | |||| | | |x| |xx|
5' ...CUCCUACUUCAGGGGCCGCGGCC... - HIF3α-m485-5p-mut

```

Supplemental Figure 1: Predicted target sites for miR-210 and miR-485-5p and the mutations made in the 3'UTR of HIF3α. Predicted 3'UTR target sites in HIF3α for miR-210 and miR-485-5p and the mutations that have been generated in the target site sequence where the miRNA seed sequence (bold) binds. The wild-type (WT) and mutated (mut) sites in HIF3α-short are shown. The vertical lines represent possible base pairing between miRNA and 3'UTR target site, and the x's indicate abrogated base pairing where nucleotides are mutated. The resulting mutated 3'UTR fragments were cloned into the psiCHECK-2 luciferase reporter.



Chapter 6

GENERAL DISCUSSION



Soft tissue sarcomas represent a diverse group of tumors comprising many histological subtypes. Because of the rare and heterogeneous nature of these tumors, histological classification and prediction of clinical behavior is often a challenge, which may result in ineffective treatment. Furthermore, the lack of specific molecular markers hinders treatment targeted on the characteristic aberrations present in the tumor. A better understanding of the biology of soft tissue sarcomas is necessary to find reliable diagnostic markers, elucidate prognostic and predictive factors, and improve treatment by finding new targets for therapy.

Molecular profiling

Molecular profiling has advanced dramatically since the use of microarrays became widespread at the end of the twentieth century. Among the first studies that used microarray technology to investigate gene expression, was a study on rhabdomyosarcoma cell lines.¹ The early gene expression profiling studies in sarcomas were mainly focused on segregating sarcomas from other tumor types or from their normal counterparts.¹⁻⁵ However, gene expression profiling did not always enable perfect discrimination of sarcoma subtypes, e.g. in a study of Fritz et al. where genomic profiling could better distinguish dedifferentiated from pleomorphic liposarcomas than mRNA profiling.⁶

Although the first miRNA, lin-4, was identified in the nematode *Caenorhabditis elegans* in 1993,⁷ it was not until the first years of the twenty-first century that more miRNAs were identified and that they were found to be conserved in many species.⁸⁻¹¹ Research then primarily focused on the identification of new miRNAs and their expression levels in different tissues. Soon it was demonstrated that miRNAs are key regulators of various biological processes, such as proliferation, differentiation, cell cycle regulation, metabolism, apoptosis and stem cell maintenance.¹² Also the role of miRNAs in cancer became apparent, with some miRNAs having an oncogenic or tumorsuppressive function.¹³ MiRNAs appeared good markers to discriminate healthy and diseased (e.g. tumor) tissues, and soon it was recognized that this new class of small RNA regulators of gene expression was superior to mRNA as molecular markers. Their small size, relative stability and resistance to RNases prevents miRNA degradation in isolated and long-term stored frozen samples.¹⁴ Furthermore, their superior stability enables miRNA detection in serum and plasma,¹⁵⁻¹⁶ and in exosomes.¹⁷ Moreover, miRNAs remain largely intact in formalin-fixed paraffin-embedded (FFPE) tissues.¹⁸ Therefore large collections of archived FFPE tissues can be used for miRNA profiling, whereas mRNA profiling ideally requires fresh or snap frozen tissue material. In addition to their better stability, miRNAs also proved to be better classifiers for tumors and tumor subtypes. Lu et al. showed that a small miRNA-based classifier was much better in establishing the correct diagnosis of poorly differentiated tumors than a larger mRNA classifier.¹⁹ Only a few miRNAs were needed to accurately predict the tumor tissue of origin. In another study by Rosenfeld et al. a miRNA classifier predicted tumor type with 90% accuracy.²⁰ Their miRNA



expression patterns correlated more accurately with cancer type, stage and clinicopathological variables than the mRNA profiles. Consequently, miRNA expression patterns are extremely useful for molecular profiling of tumors. This is particularly informative for soft tissue sarcomas, which are a rare and heterogeneous group of tumors. They are genetically complex, have a broad spectrum of biologic behaviors, and are sometimes hard to classify. MiRNAs can serve as molecular biomarkers for tumor diagnosis, prognosis of disease outcome and prediction of treatment response in soft tissue sarcomas. Since the levels of individual miRNAs can vary among patients, a signature of multiple miRNAs rather than a single miRNA would be more accurate and reliable as a diagnostic, prognostic, or predictive tool.

MiRNAs as diagnostic biomarkers

A miRNA that can be used as a diagnostic biomarker is characteristic for a certain group of tumors, either by its high expression or its relative absence, and helps distinguishing a tumor type from normal tissues, benign lesions, or other tumor types in diagnosis. Diagnostic miRNA biomarkers can be found by identifying differentially expressed miRNAs between established groups, e.g. tumor vs. normal, or different tumor subtypes.

We identified that the expression of the miR-17-92 cluster is significantly lower in gastrointestinal stromal tumors (GIST) than in gastrointestinal leiomyosarcomas (GI-LMS) and normal gastrointestinal tissues. The apparent downregulation of the miR-17-92 cluster in GIST is remarkable, since members of this miRNA cluster are often highly expressed in human malignancies, including gastric and colon cancers, neuroblastoma and B-cell lymphomas,²¹⁻²⁴ but also sarcomas such as osteosarcoma, angiosarcoma and rhabdomyosarcomas.²⁵⁻²⁷ Members of the miR-17-92 cluster can thus be used as diagnostic biomarkers in GIST. Although immunohistochemical staining of KIT is a widely used diagnostic tool to differentiate GIST from GI-LMS, not all GIST express high levels of KIT and a subset of LMS express KIT.²⁸⁻²⁹ Also a more recently described marker for GIST, DOG1, is not absolutely specific, since uterine LMS also showed DOG1 immunoreactivity.³⁰ Determining miR-17-92 cluster expression, in addition to using the currently present diagnostic tools, might enhance diagnostic accuracy in GIST.

Perhaps even more interesting than distinguishing different types of tumors, is the discrimination of different tumor subtypes based on miRNA expression. We examined the miRNA expression in all currently recognized liposarcoma subtypes (well differentiated, dedifferentiated, pleomorphic, myxoid and round cell liposarcomas), lipomas and normal fat, revealing subtype specific miRNAs as well as miRNAs that were aberrantly expressed in all liposarcomas. Other profiling studies usually focus on one or two liposarcoma subtypes and only compared the miRNA expression to the expression in normal fat.³¹⁻³⁴ Unique in our approach is, not only that we included all liposarcoma subtypes, but also that we compared miRNA expression levels of a single liposarcoma subtype to that of every other subtype. This way, only miRNAs that discriminated one subtype from multiple other subtypes and from control tissues were selected. Although the group sizes were small, subtype specific miRNAs were identified and validated in an independent sample



set, which proves that miRNA expression patterns are specific and emphasizes their diagnostic potential.

In addition to determining miRNA expression in established tumor entities, miRNA expression profiling can also be used for class discovery. Clustering may identify yet unrecognized tumor subtypes within morphologically similar, but genetically distinct tissues. In our analysis, some lipomas and well differentiated liposarcomas clustered together. This could imply there may be a subgroup of relatively benign well differentiated liposarcomas, which are less prone to dedifferentiate and have a more favorable outcome. As proposed before, lipomas and well differentiated liposarcomas could also represent different stages in a single biological continuum.³⁵⁻³⁷ Future investigation, with larger and well defined tumor sets, will have to demonstrate whether lipomas and well differentiated liposarcomas are two completely separate entities.

Diagnostic miRNA biomarkers can also be used for the early detection of cancer, since tumors display aberrant miRNA expression compared to normal cells. We demonstrated that the expression of miR-143, miR-144, miR-145 and miR-451 was already slightly reduced in benign lipomas, further decreased in low grade well differentiated liposarcoma, and lowest expressed in the more malignant liposarcoma subtypes, which shows that miRNA expression changes with malignancy in sarcoma development. Since tumors can shed miRNAs into the bloodstream, circulating miRNAs can be used as a powerful non-invasive biomarker for the early detection of cancer. Serum levels of muscle-specific miR-206 were significantly higher in patients with rhabdomyosarcoma than in patients with other tumors.³⁸ It is, however, of importance to establish during which stage of oncogenesis the miRNA expression changes, and prospective studies and studies on other sarcoma types still need to be conducted. Circulating miRNAs that can identify tumors at an early stage can be used for screening of high-risk groups, e.g. in individuals with hereditary syndromes associated with sarcoma development.

MiRNAs as prognostic biomarkers

A prognostic biomarker can be used to predict disease outcome. When the expression of a miRNA is specific for a certain (sub)type of cancer, it is potentially linked to a clinical parameter, such as progression, recurrence, metastasis or survival of that tumor type.

Expression of hypoxia-inducible factor-1 (HIF-1), vascular endothelial growth factor (VEGF) and carbonic anhydrase IX (CA-IX), correlates with metastasis and poor patient outcome in osteosarcoma.³⁹⁻⁴⁰ Alternatively, hypoxia induced miRNAs that are associated with the hypoxic response in soft tissue sarcoma, such as miR-210, miR-485-5p and miR-373, could be used as prognostic biomarkers. In breast cancer, miR-210 has shown to be a prognostic indicator of adverse prognosis, and circulating miR-373 showed potential to be a biomarker for lymph node involvement.⁴¹⁻⁴² Further research could demonstrate the potential role for these and other hypoxia regulated miRNAs as prognostic biomarkers in sarcomas.



We demonstrated that the miR-17 family was upregulated in myxoid/round cell liposarcomas, with the highest expression in liposarcomas with a high (>50%) round cell component. This miRNA family is associated with cell proliferation, suppressed apoptosis, tumor angiogenesis and aggressiveness in many tumor types,⁴³ which is in line with the more aggressive behavior of round cell liposarcomas. Although verification in a larger cohort is essential, the miR-17 family might potentially be used as prognostic miRNAs for aggressive behavior in myxoid/round cell liposarcomas.

MiRNAs as predictive biomarkers

A predictive biomarker is associated with therapy response, can identify subpopulations of patients who will most likely respond to a certain therapy, and can thereby aid in treatment decision making. We demonstrated that miR-24 levels are correlated to sensitivity to doxorubicin, a frequently used drug in sarcoma management, in different sarcoma cell lines. Low miR-24 levels were associated with doxorubicin sensitivity in myxoid liposarcomas, while miR-24 overexpression resulted in resistance to the drug. A non-myxoid liposarcoma cell line and a rhabdomyosarcoma cell line with high endogenous miR-24 levels were relatively resistant to doxorubicin and could be sensitized by miR-24 inhibitors. This indicates the potential of miR-24 as a predictive biomarker for doxorubicin treatment in sarcomas.

Hypoxia is associated with chemotherapy resistance, including doxorubicin, vincristine and actinomycin-D resistance in rhabdomyosarcoma and Ewing's sarcoma cells,⁴⁴ and cisplatin, doxorubicin and etoposide resistance in osteosarcoma cell lines.⁴⁵ Since determination of HIF1 α levels requires protein analysis of tumor tissue, which is invasive and time consuming, it would be easier to detect circulating hypoxia responsive miRNAs. Further studies are needed to determine if these circulating miRNAs are also associated with therapy resistance and can be used to better stratify patients for treatment of sarcomas.

MiRNAs with therapeutic potential in sarcomas

Given their important role in aberrant biological pathways contributing to sarcomagenesis, miRNAs have an incredible therapeutic potential. Re-expression of tumor suppressive miRNAs that are lost in the tumor tissue, or inhibition of highly expressed miRNAs with an oncogenic function, are two different strategies for miRNAs in anti-cancer therapy.

In liposarcomas, we identified subtype specific miRNAs, which can be used for diagnostic purposes. Whether this subtype specific miRNA expression profile is a causative factor in the disease, or merely occurs as a consequence of the pathological state is currently unknown. When the aberrantly expressed miRNAs are demonstrated to play a role in the oncogenic process, they have the potential to be used as therapeutic targets. This is especially interesting for non-myxoid liposarcomas, which are less susceptible for the present standard therapies.



We also identified downregulation of miR-143/145 and miR-144/451 in all liposarcoma subtypes. Re-expression of these miRNAs inhibited cell proliferation and induced apoptosis *in vitro*. Moreover, miR-143/-144/-145/-451 are frequently found underexpressed in other cancers and overexpression often affects cellular proliferation and apoptosis. This suggests a possible role for these miRNAs as novel therapeutic targets for multiple tumor types, including liposarcoma. Also the miR-17-92 and miR-221/222 clusters, which are downregulated in GIST, are potential therapeutic targets. Overexpression of these miRNAs in GIST cell lines dramatically inhibited cell proliferation, affected cell cycle progression, induced apoptosis, and suppressed KIT and ETV1 protein and RNA levels. The joined repression of these two essential GIST oncogenes could be promising for GIST treatment, especially for imatinib-resistant disease.

In addition to manipulating miRNAs levels as cancer treatment, modulation of miRNAs levels can also enhance efficacy of traditional cancer treatments. Modulation of miRNAs associated with the sensitivity to chemotherapeutic drugs can boost the response to these agents. Inhibition of miR-24 in liposarcoma, and possibly other tumors, could enhance the sensitivity for doxorubicin, a regularly used drug in sarcoma management. Combination therapy of doxorubicin and a miR-24 inhibitor should be further explored *in vivo*.

In myxoid liposarcomas, which express low levels of miR-24, further inhibition of miR-24 did not increase doxorubicin sensitivity. However, overexpression of miR-497 and miR-30a enhanced doxorubicin induced cell death. This effect is probably mediated via the IGF1R pathway. Blocking IGF1R signalling, which, as we have shown, can be achieved by miR-497/30a overexpression, is known to enhance chemosensitivity of cancer cells *in vitro* and *in vivo*.⁴⁶⁻⁴⁷ Although myxoid liposarcomas are more sensitive to radiotherapy and systemic treatments than other liposarcoma subtypes, the response rate is only 48%.⁴⁸ Combination therapy of doxorubicin and miR-497/30a can be promising for myxoid liposarcomas which do not respond well to standard treatment initially.

Therapeutic targeting of miRNAs that are involved in the hypoxic tumor response could deregulate the robust signalling pathways induced by hypoxia and convert radiation and chemotherapy resistance. This was demonstrated in a recent study which showed that inhibition of miR-210 could sensitize hepatoma cells to radiation therapy.⁴⁹

Approaches for miRNAs therapy

MiRNAs with a tumor suppressor-like function that are downregulated in cancer cells can therapeutically be re-introduced by means of miRNA replacement therapy. This can be achieved by introducing either a synthetic stem-loop primary/precursor-miRNA, which should be processed by the cells own miRNA biogenesis machinery, or a miRNA mimic (agomiR), a short chemically modified miRNA duplex which can directly be taken up by the RISC complex.⁵⁰ MiRNAs may target multiple genes at once, even by imperfect complementarity, which can enhance the therapeutic



effect when multiple genes from the same pathway are targeted, but can give unwanted side effects when tumor-unrelated genes are targeted. Since the miRNAs which are downregulated in the tumor are already present in the normal cells, miRNA replacement therapy is unlikely to induce serious adverse events. Alternatively, siRNAs are designed to target a single gene and to degrade this target,⁵¹ and small multiple-target artificial (SMART) RNAs can be used to specifically target multiple selected genes at once in a miRNA-like fashion, minimizing unexpected adverse events.⁵²

Replacement therapy of miR-34 and let-7 family members, and the miR-143/145 cluster, which are frequently downregulated in diverse cancers, has been studied *in vivo*. Therapeutic administration of let-7 mimics in a mice model of lung cancer reduced tumor growth, induced necrosis, and repressed direct let-7 targets.⁵³⁻⁵⁴ Systemic delivery of miR-34 mimics reduced tumor burden in murine models of lung, prostate and pancreatic cancer.⁵⁵⁻⁵⁷ MiR-143 and miR-145 reduced tumor growth in mice with pancreatic or colon cancer xenografts.⁵⁷⁻⁵⁹

MiRNAs with an oncogenic role, which are upregulated in tumors, can be repressed by anti-miRNA therapy, thereby derepressing their target mRNAs. Anti-miR oligonucleotides (AMOs) are single-stranded nucleotide sequences with direct complementarity to endogenous mature miRNAs, which can degrade the miRNA target upon binding.⁶⁰ AntagomiRs are also based on single stranded oligonucleotides, but they are modified with cholesterol-conjugated 2'-O-methyl or 2'-O-methoxyethyl groups to improve their stability, cellular uptake, and effectiveness.⁶¹ This enhances performance *in vivo*, as was shown by the inhibition of miR-16, miR-122, miR-192 and miR-194 in various tissues by intravenous administration of antagomiRs to mice.⁶² Furthermore, instead of having perfect complementarity to their target miRNAs, antagomiRs have base modification and mismatches that inhibit cleavage by Ago proteins but still enables a solid binding to the target miRNA.⁶¹ Locked nucleic-acid (LNAs) antisense oligonucleotides are also designed to increase stability. These RNA analogues bind complementary miRNAs with high affinity and specificity, and have been shown to exhibit adequate cellular uptake and low toxicity *in vivo*.⁶³ Additionally, LNA-modified oligonucleotide capture probes are being used for miRNA microarray platforms, providing high affinity binding and discrimination of miRNAs differing by a single nucleotide.⁶³ LNA-oligonucleotides have been used in several *in vitro* and *in vivo* studies, but the most successful example comes from a miR-122 inhibitor (miravirsen) which is the first miRNA-targeted drug to enter human clinical trials.⁶⁴ In a phase II clinical trial for the treatment of hepatitis C the patients received subcutaneous injections of miravirsen, which resulted in prolonged dose-dependent reductions in hepatitis C virus RNA levels without the occurrence of dose-limiting adverse events or evidence of viral resistance.⁶⁴ Another example of chemically modified oligonucleotides are morpholinos, which contain six-member morpholine rings instead of five-member (deoxy)ribose rings and are extremely resistant to the action of nucleases.⁶¹ Short morpholinos oligomers are very stable inside the cell and do not trigger immune responses.⁶⁵



They were initially used to block mRNA translation, but are now used to target pre-miRNAs or mature miRNAs, or conversely, to protect the mRNA by blocking the miRNA binding site.⁶¹ MiRNA sponges are synthetic mRNAs that act as miRNA decoys.⁶⁶ These competitive inhibitors consist of a strong promoter, driving the expression of an artificial transcript that carries multiple tandem repeats complementary to the seed sequence of a specific miRNA or a miRNA family sharing a common seed sequence, and can be temporarily expressed in cells.⁶⁶

Although miRNA-based therapy seems to be an effective strategy, some issues need further attention. MiRNA therapeutics should be protected from degradation by nucleases, delivered to tumor cells specifically, where they are taken up successfully, achieving ideally a long-lasting, sufficiently high effect with minimal toxicity and off-target effects. Since miRNAs can target many mRNAs, target specificity can be a problem. This raises the chance of off-target gene silencing and unwanted toxicity, which emphasizes the importance of target identification, chemically modified oligonucleotides that enhance specificity, and the need for tissue specific delivery methods. Poor cellular uptake can be solved by several systems that exist for the delivery of miRNAs therapeutics. Viral vector based systems show high gene transfer efficiency, although they lack tumor specific targeting and can trigger immune responses.⁶⁷ Nanoparticles, such as polymer- or lipid-based formulations, can encapsulate miRNAs and deliver them to cells with little toxicity, but they lack tumor specificity and are less efficient compared to viral vectors. However, liposome-based particles modified with a tumor-targeting monoclonal antibody successfully targeted lung metastases.⁶⁸ Atelocollagen is a promising carrier for miRNA therapy since it interacts with miRNAs to form a complex that has low antigenicity, is resistant to nucleases and can efficiently be transduced into cells.⁶⁹ A better understanding of miRNA biology and possibilities regarding stability, targeting and specificity will aid the development of more suitable strategies for miRNA therapeutics.

MiRNA target identification

Although more and more is known about the mechanism of action of miRNAs, and the (deregulation of) expression in many tissues, the identification of their targets is lagging behind. Target identification is important for the development of miRNA-based therapy and crucial for avoiding undesired side-effects by unexpected target regulation. Several computational algorithms have been developed to predict potential binding sites of specific miRNAs (reviewed in ⁷⁰⁻⁷¹). Most of these target prediction tools are based on pairing of the miRNA seed sequence (nucleotide 2-8, the most conserved part of metazoan miRNAs) to the mRNA target. A complicating factor is that perfect complementarity of the seed sequence is not essential, since additional base-pairing at the 3'end of the miRNA can compensate for mismatches in the seed sequence. Furthermore, most prediction algorithms only browse the 3'UTR of mRNAs for target prediction, while miRNAs can also bind sites in the 5'UTR or within the coding region.⁷²⁻⁷³ Due to



the diverse algorithms and criteria used and the chance of false positive or false negative findings, the different target prediction programs present only partially overlapping results, emphasizing the need of experimental validation of predicted miRNA targets. An inverse correlation between the miRNA expression and the mRNA/protein expression levels, or known involvement of certain genes in the disease of interest, can further increase the likelihood that the gene is regulated by the miRNA.

Experimental validation studies are essential to confirm miRNA-mRNA interactions. The most straightforward method for verification of miRNA function is by transfecting cells with miRNA mimics/inhibitors, followed by quantitative analyses of target mRNA and protein levels. Alternatively, as a high-throughput approach, changes in transcript levels can be measured by microarrays or sequencing techniques, and protein levels can be measured by proteome analysis. Newer techniques include HITS-CLIP or CLIP-seq (high-throughput sequencing after crosslinking immunoprecipitation), which are based on cross-linking of miRNA-mRNA complexes using ultraviolet irradiation, followed by their co-immunoprecipitation with RISC proteins (e.g. Ago2) and subsequent high-throughput sequencing.⁷⁴ PAR-CLIP (photo-activable-ribonucleoside-enhanced crosslinking and immunoprecipitation) is based on incorporating photoreactive ribonucleoside analogs into newly synthesized RNAs of living cells, followed by UV irradiation for efficient crosslinking, immunoprecipitation of RNA binding proteins of interest, and sequencing of the precipitated complexes.⁷⁵ Nevertheless, these techniques are expensive, technically challenging, and do not provide evidence for direct target regulation by the miRNA. Conversely, the use of relatively simple reporter assays can indicate whether the miRNA regulates the mRNA via direct binding of the predicted target site. 3'UTR fragments of the gene of interest, containing the putative miRNA target sites, are cloned into an expression vector carrying a reporter gene (e.g. luciferase reporter). As a negative control 3'UTR fragments with a mutated target site, unable to bind the miRNA, are used. Transfection of cells with these reporter constructs in combination with miRNA mimics/inhibitors, and subsequent measurement of reporter activity enables validation of predicted miRNA-mRNA interactions.

The identification of miRNA targets can be a big challenge, but is very essential. Since miRNAs can have different targets and elicit different effects in other tissues, miRNA-based therapy can have undesired side effects. On the other hand, the fact that miRNAs can target multiple genes involved in the same or other oncogenic pathways provides an opportunity to affect many pathways simultaneously, which could enhance the therapeutic effect. Therefore, the identification of miRNA targets will not only enhance our understanding of the deregulated biological pathways in tumors, but also provide opportunities for the development of miRNA-based therapeutics.



Future recommendations for miRNA research in soft tissue sarcoma

In order to get miRNAs from bench to bedside, we need to understand the function of these small regulators in health and disease. As demonstrated by our studies and others, there is a lot of potential in the use of miRNAs as biomarker or therapeutic strategy in soft tissue sarcomas. However, as soft tissue sarcomas comprise such a rare and heterogeneous tumor type, larger studies, preferably by multicenter efforts and (inter)national collaborations, are mandatory to bring this potential to the next level. This would enable the analysis of large tumor sample sets, which are ideally well annotated and diagnosed by expert soft tissue sarcoma pathologists. Tumor samples should be classified using standard criteria involving morphological appearance, immunohistochemistry and genetic analyses, taking possible tumor heterogeneity into account. Also the analysis of blood samples of sarcoma patients would be interesting in order to identify circulating miRNAs and to determine their role as biomarker. Combining miRNA profiling with genomic, transcriptomic and proteomic analyses provides a full spectrum of information, which should be deposited in publically available databases to facilitate the comparisons between studies and the validation of findings in other sample sets. Bio-informaticians can link the expression data to obtain clues on miRNA regulation and potential target genes, which should be followed by experimental validation in the laboratory. *In vitro* studies in human sarcoma cell lines can be used to determine the role of miRNAs in the tumor cells and to establish whether modulation of miRNA expression has therapeutic potential. These results should subsequently be verified *in vivo*, in xenograft models or in animal models of primary soft tissue sarcomas.⁷⁶ Promising “miRNA-drugs” can be examined for safety, specificity, and effectivity as single agent as well as in combination with other miRNAs mimics and inhibitors, or known chemotherapeutic agents.

The results of profiling studies and the recognition that miRNAs can be used as biomarkers for classification, prognosis and clinical response, are encouraging. MiRNAs can give new insights into the biology of soft tissue sarcomas, and provide promising opportunities for future management of these rare mesenchymal tumors.



REFERENCES

1. Khan J, Simon R, Bittner M, Chen Y, Leighton SB, Pohida T, et al. Gene expression profiling of alveolar rhabdomyosarcoma with cDNA microarrays. *Cancer Res.* 1998 Nov 15;58(22):5009-13.
2. Nielsen TO, West RB, Linn SC, Alter O, Knowling MA, O'Connell JX, et al. Molecular characterisation of soft tissue tumours: a gene expression study. *Lancet.* 2002 Apr 13;359(9314):1301-7.
3. Wolf M, El-Rifai W, Tarkkanen M, Kononen J, Serra M, Eriksen EF, et al. Novel findings in gene expression detected in human osteosarcoma by cDNA microarray. *Cancer Genet Cytogenet.* 2000 Dec;123(2):128-32.
4. Allander SV, Nupponen NN, Ringner M, Hostetter G, Maher GW, Goldberger N, et al. Gastrointestinal stromal tumors with KIT mutations exhibit a remarkably homogeneous gene expression profile. *Cancer Res.* 2001 Dec 15;61(24):8624-8.
5. Nagayama S, Katagiri T, Tsunoda T, Hosaka T, Nakashima Y, Araki N, et al. Genome-wide analysis of gene expression in synovial sarcomas using a cDNA microarray. *Cancer Res.* 2002 Oct 15;62(20):5859-66.
6. Fritz B, Schubert F, Wrobel G, Schwaenen C, Wessendorf S, Nessling M, et al. Microarray-based copy number and expression profiling in dedifferentiated and pleomorphic liposarcoma. *Cancer Res.* 2002 Jun 1;62(11):2993-8.
7. Lee RC, Feinbaum RL, Ambros V. The *C. elegans* heterochronic gene *lin-4* encodes small RNAs with antisense complementarity to *lin-14*. *Cell.* 1993 Dec 3;75(5):843-54.
8. Pasquinelli AE, Reinhart BJ, Slack F, Martindale MQ, Kuroda MI, Maller B, et al. Conservation of the sequence and temporal expression of *let-7* heterochronic regulatory RNA. *Nature.* 2000 Nov 2;408(6808):86-9.
9. Lee RC, Ambros V. An extensive class of small RNAs in *Caenorhabditis elegans*. *Science.* 2001 Oct 26;294(5543):862-4.
10. Lau NC, Lim LP, Weinstein EG, Bartel DP. An abundant class of tiny RNAs with probable regulatory roles in *Caenorhabditis elegans*. *Science.* 2001 Oct 26;294(5543):858-62.
11. Lagos-Quintana M, Rauhut R, Lendeckel W, Tuschl T. Identification of novel genes coding for small expressed RNAs. *Science.* 2001 Oct 26;294(5543):853-8.
12. Wiemer EA. The role of microRNAs in cancer: no small matter. *Eur J Cancer.* 2007 Jul;43(10):1529-44.
13. Lujambio A, Lowe SW. The microcosmos of cancer. *Nature.* 2012 Feb 16;482(7385):347-55.
14. Mraz M, Malinova K, Mayer J, Pospisilova S. MicroRNA isolation and stability in stored RNA samples. *Biochem Biophys Res Commun.* 2009 Dec 4;390(1):1-4.
15. Madhavan D, Cuk K, Burwinkel B, Yang R. Cancer diagnosis and prognosis decoded by blood-based circulating microRNA signatures. *Front Genet.* 2013;4:116.
16. Mitchell PS, Parkin RK, Kroh EM, Fritz BR, Wyman SK, Pogosova-Agadjanyan EL, et al. Circulating microRNAs as stable blood-based markers for cancer detection. *Proc Natl Acad Sci U S A.* 2008 Jul 29;105(30):10513-8.
17. Hannafon BN, Ding WQ. Intercellular Communication by Exosome-Derived microRNAs in Cancer. *Int J Mol Sci.* 2013;14(7):14240-69.
18. Li J, Smyth P, Flavin R, Cahill S, Denning K, Aherne S, et al. Comparison of miRNA expression patterns using total RNA extracted from matched samples of formalin-fixed paraffin-embedded (FFPE) cells and snap frozen cells. *BMC Biotechnol.* 2007;7:36.
19. Lu J, Getz G, Miska EA, Alvarez-Saavedra E, Lamb J, Peck D, et al. MicroRNA expression profiles classify human cancers. *Nature.* 2005 Jun 9;435(7043):834-8.
20. Rosenfeld N, Aharonov R, Meiri E, Rosenwald S, Spector Y, Zepeniuk M, et al. MicroRNAs accurately identify cancer tissue origin. *Nat Biotechnol.* 2008 Apr;26(4):462-9.
21. Guo J, Miao Y, Xiao B, Huan R, Jiang Z, Meng D, et al. Differential expression of microRNA species in human gastric cancer versus non-tumorous tissues. *J Gastroenterol Hepatol.* 2009 Apr;24(4):652-7.
22. Volinia S, Calin GA, Liu CG, Ambs S, Cimmino A, Petrocca F, et al. A microRNA expression signature of human solid tumors defines cancer gene targets. *Proc Natl Acad Sci U S A.* 2006 Feb 14;103(7):2257-61.
23. Schulte JH, Marschall T, Martin M, Rosenstiel P, Mestdagh P, Schlierf S, et al. Deep sequencing reveals differential expression of microRNAs in favorable versus unfavorable neuroblastoma. *Nucleic Acids Res.* 2010 Sep;38(17):5919-28.
24. He L, Thomson JM, Hemann MT, Hernando-Monge E, Mu D, Goodson S, et al. A microRNA polycistron as a potential human oncogene. *Nature.* 2005 Jun 9;435(7043):828-33.

25. Thayanyithy V, Sarver AL, Kartha RV, Li L, Angstadt AY, Breen M, et al. Perturbation of 14q32 miRNAs-cMYC gene network in osteosarcoma. *Bone*. 2012 Jan;50(1):171-81.
26. Italiano A, Thomas R, Breen M, Zhang L, Crago AM, Singer S, et al. The miR-17-92 cluster and its target THBS1 are differentially expressed in angiosarcomas dependent on MYC amplification. *Genes Chromosomes Cancer*. 2012 Jun;51(6):569-78.
27. Reichel JL, Duan F, Smith LM, Gustafson DM, O'Connor RS, Zhang C, et al. Genomic and clinical analysis of amplification of the 13q31 chromosomal region in alveolar rhabdomyosarcoma: a report from the Children's Oncology Group. *Clin Cancer Res*. 2011 Mar 15;17(6):1463-73.
28. Medeiros F, Corless CL, Duensing A, Hornick JL, Oliveira AM, Heinrich MC, et al. KIT-negative gastrointestinal stromal tumors: proof of concept and therapeutic implications. *Am J Surg Pathol*. 2004 Jul;28(7):889-94.
29. Raspollini MR, Amunni G, Villanucci A, Pinzani P, Simi L, Paglierani M, et al. c-Kit expression in patients with uterine leiomyosarcomas: a potential alternative therapeutic treatment. *Clin Cancer Res*. 2004 May 15;10(10):3500-3.
30. Sah SP, McCluggage WG. DOG1 immunoreactivity in uterine leiomyosarcomas. *J Clin Pathol*. 2013 Jan;66(1):40-3.
31. Borjigin N, Ohno S, Wu W, Tanaka M, Suzuki R, Fujita K, et al. TLS-CHOP represses miR-486 expression, inducing upregulation of a metastasis regulator PAI-1 in human myxoid liposarcoma. *Biochem Biophys Res Commun*. 2012 Oct 19;427(2):355-60.
32. Zhang P, Bill K, Liu J, Young E, Peng T, Bolshakov S, et al. MiR-155 is a liposarcoma oncogene that targets casein kinase-1alpha and enhances beta-catenin signaling. *Cancer Res*. 2012 Apr 1;72(7):1751-62.
33. Tap WD, Eilber FC, Ginther C, Dry SM, Reese N, Barzan-Smith K, et al. Evaluation of well-differentiated/de-differentiated liposarcomas by high-resolution oligonucleotide array-based comparative genomic hybridization. *Genes Chromosomes Cancer*. 2011 Feb;50(2):95-112.
34. Ugras S, Brill E, Jacobsen A, Hafner M, Socci ND, Decarolis PL, et al. Small RNA sequencing and functional characterization reveals MicroRNA-143 tumor suppressor activity in liposarcoma. *Cancer Res*. 2011 Sep 1;71(17):5659-69.
35. Dei Tos AP, Doglioni C, Piccinin S, Sciort R, Furlanetto A, Boiocchi M, et al. Coordinated expression and amplification of the MDM2, CDK4, and HMGI-C genes in atypical lipomatous tumours. *J Pathol*. 2000 Apr;190(5):531-6.
36. Italiano A, Cardot N, Dupre F, Monticelli I, Keslair F, Piche M, et al. Gains and complex rearrangements of the 12q13-15 chromosomal region in ordinary lipomas: the "missing link" between lipomas and liposarcomas? *Int J Cancer*. 2007 Jul 15;121(2):308-15.
37. Mentzel T. Biological continuum of benign, atypical, and malignant mesenchymal neoplasms - does it exist? *J Pathol*. 2000 Apr;190(5):523-5.
38. Miyachi M, Tsuchiya K, Yoshida H, Yagyu S, Kikuchi K, Misawa A, et al. Circulating muscle-specific microRNA, miR-206, as a potential diagnostic marker for rhabdomyosarcoma. *Biochem Biophys Res Commun*. 2010 Sep 10;400(1):89-93.
39. Kaya M, Wada T, Akatsuka T, Kawaguchi S, Nagoya S, Shindoh M, et al. Vascular endothelial growth factor expression in untreated osteosarcoma is predictive of pulmonary metastasis and poor prognosis. *Clin Cancer Res*. 2000 Feb;6(2):572-7.
40. Yang QC, Zeng BF, Dong Y, Shi ZM, Jiang ZM, Huang J. Overexpression of hypoxia-inducible factor-1alpha in human osteosarcoma: correlation with clinicopathological parameters and survival outcome. *Jpn J Clin Oncol*. 2007 Feb;37(2):127-34.
41. Camps C, Buffa FM, Colella S, Moore J, Sotiriou C, Sheldon H, et al. hsa-miR-210 is induced by hypoxia and is an independent prognostic factor in breast cancer. *Clin Cancer Res*. 2008 Mar 1;14(5):1340-8.
42. Chen W, Cai F, Zhang B, Barekati Z, Zhong XY. The level of circulating miRNA-10b and miRNA-373 in detecting lymph node metastasis of breast cancer: potential biomarkers. *Tumour Biol*. 2013 Feb;34(1):455-62.
43. Mendell JT. miRiad roles for the miR-17-92 cluster in development and disease. *Cell*. 2008 Apr 18;133(2):217-22.
44. Kilic M, Kasperczyk H, Fulda S, Debatin KM. Role of hypoxia inducible factor-1 alpha in modulation of apoptosis resistance. *Oncogene*. 2007 Mar 29;26(14):2027-38.
45. Adamski J, Price A, Dive C, Makin G. Hypoxia-Induced Cytotoxic Drug Resistance in Osteosarcoma Is Independent of HIF-1Alpha. *PLoS One*. 2013;8(6):e65304.



46. Min Y, Adachi Y, Yamamoto H, Imsumran A, Arimura Y, Endo T, et al. Insulin-like growth factor I receptor blockade enhances chemotherapy and radiation responses and inhibits tumour growth in human gastric cancer xenografts. *Gut*. 2005 May;54(5):591-600.
47. D'Cunja J, Shalaby T, Rivera P, von Buren A, Patti R, Heppner FL, et al. Antisense treatment of IGF-IR induces apoptosis and enhances chemosensitivity in central nervous system atypical teratoid/rhabdoid tumours cells. *Eur J Cancer*. 2007 Jul;43(10):1581-9.
48. Jones RL, Fisher C, Al-Muderis O, Judson IR. Differential sensitivity of liposarcoma subtypes to chemotherapy. *Eur J Cancer*. 2005 Dec;41(18):2853-60.
49. Yang W, Sun T, Cao J, Liu F, Tian Y, Zhu W. Downregulation of miR-210 expression inhibits proliferation, induces apoptosis and enhances radiosensitivity in hypoxic human hepatoma cells in vitro. *Exp Cell Res*. 2012 May 1;318(8):944-54.
50. Henry JC, Azevedo-Pouly AC, Schmittgen TD. MicroRNA replacement therapy for cancer. *Pharm Res*. 2011 Dec;28(12):3030-42.
51. Bakhtiyari S, Haghani K, Basati G, Karimfar MH. siRNA therapeutics in the treatment of diseases. *Ther Deliv*. 2013 Jan;4(1):45-57.
52. De Guire V, Caron M, Scott N, Menard C, Gaumont-Leclerc MF, Chartrand P, et al. Designing small multiple-target artificial RNAs. *Nucleic Acids Res*. 2010 Jul;38(13):e140.
53. Esquela-Kerscher A, Trang P, Wiggins JF, Patrawala L, Cheng A, Ford L, et al. The let-7 microRNA reduces tumor growth in mouse models of lung cancer. *Cell Cycle*. 2008 Mar 15;7(6):759-64.
54. Trang P, Medina PP, Wiggins JF, Ruffino L, Kelnar K, Omotola M, et al. Regression of murine lung tumors by the let-7 microRNA. *Oncogene*. 2010 Mar 18;29(11):1580-7.
55. Wiggins JF, Ruffino L, Kelnar K, Omotola M, Patrawala L, Brown D, et al. Development of a lung cancer therapeutic based on the tumor suppressor microRNA-34. *Cancer Res*. 2010 Jul 15;70(14):5923-30.
56. Liu C, Kelnar K, Liu B, Chen X, Calhoun-Davis T, Li H, et al. The microRNA miR-34a inhibits prostate cancer stem cells and metastasis by directly repressing CD44. *Nat Med*. 2011 Feb;17(2):211-5.
57. Pramanik D, Campbell NR, Karikari C, Chivukula R, Kent OA, Mendell JT, et al. Restitution of tumor suppressor microRNAs using a systemic nanovector inhibits pancreatic cancer growth in mice. *Mol Cancer Ther*. 2011 Aug;10(8):1470-80.
58. Ibrahim AF, Weirauch U, Thomas M, Grunweller A, Hartmann RK, Aigner A. MicroRNA replacement therapy for miR-145 and miR-33a is efficacious in a model of colon carcinoma. *Cancer Res*. 2011 Aug 1;71(15):5214-24.
59. Akao Y, Nakagawa Y, Hirata I, Iio A, Itoh T, Kojima K, et al. Role of anti-oncomirs miR-143 and -145 in human colorectal tumors. *Cancer Gene Ther*. 2010 Jun;17(6):398-408.
60. Weiler J, Hunziker J, Hall J. Anti-miRNA oligonucleotides (AMOs): ammunition to target miRNAs implicated in human disease? *Gene Ther*. 2006 Mar;13(6):496-502.
61. Sotillo E, Thomas-Tikhonenko A. Shielding the messenger (RNA): microRNA-based anticancer therapies. *Pharmacol Ther*. 2011 Jul;131(1):18-32.
62. Krutzfeldt J, Rajewsky N, Braich R, Rajeev KG, Tuschl T, Manoharan M, et al. Silencing of microRNAs in vivo with 'antagomirs'. *Nature*. 2005 Dec 1;438(7068):685-9.
63. Stenvang J, Silahatoglu AN, Lindow M, Elmen J, Kauppinen S. The utility of LNA in microRNA-based cancer diagnostics and therapeutics. *Semin Cancer Biol*. 2008 Apr;18(2):89-102.
64. Janssen HL, Reesink HW, Lawitz EJ, Zeuzem S, Rodriguez-Torres M, Patel K, et al. Treatment of HCV infection by targeting microRNA. *N Engl J Med*. 2013 May 2;368(18):1685-94.
65. Summerton J. Morpholino antisense oligomers: the case for an RNase H-independent structural type. *Biochim Biophys Acta*. 1999 Dec 10;1489(1):141-58.
66. Ebert MS, Neilson JR, Sharp PA. MicroRNA sponges: competitive inhibitors of small RNAs in mammalian cells. *Nat Methods*. 2007 Sep;4(9):721-6.
67. Liu YP, Berkhout B. miRNA cassettes in viral vectors: problems and solutions. *Biochim Biophys Acta*. 2011 Nov-Dec;1809(11-12):732-45.
68. Chen Y, Zhu X, Zhang X, Liu B, Huang L. Nanoparticles modified with tumor-targeting scFv deliver siRNA and miRNA for cancer therapy. *Mol Ther*. 2010 Sep;18(9):1650-6.
69. Minakuchi Y, Takeshita F, Kosaka N, Sasaki H, Yamamoto Y, Kouno M, et al. Atelocollagen-mediated synthetic small interfering RNA delivery for effective gene silencing in vitro and in vivo. *Nucleic Acids Res*. 2004;32(13):e109.

70. Witkos TM, Koscianska E, Krzyzosiak WJ. Practical Aspects of microRNA Target Prediction. *Curr Mol Med*. 2011 Mar;11(2):93-109.
71. Saito T, Saetrom P. MicroRNAs--targeting and target prediction. *N Biotechnol*. 2010 Jul 31;27(3):243-9.
72. Orom UA, Nielsen FC, Lund AH. MicroRNA-10a binds the 5'UTR of ribosomal protein mRNAs and enhances their translation. *Mol Cell*. 2008 May 23;30(4):460-71.
73. Fang Z, Rajewsky N. The impact of miRNA target sites in coding sequences and in 3'UTRs. *PLoS One*. 2011;6(3):e18067.
74. Licatalosi DD, Mele A, Fak JJ, Ule J, Kayikci M, Chi SW, et al. HITS-CLIP yields genome-wide insights into brain alternative RNA processing. *Nature*. 2008 Nov 27;456(7221):464-9.
75. Hafner M, Landthaler M, Burger L, Khorshid M, Hausser J, Berninger P, et al. Transcriptome-wide identification of RNA-binding protein and microRNA target sites by PAR-CLIP. *Cell*. 2010 Apr 2;141(1):129-41.
76. Dodd RD, Mito JK, Kirsch DG. Animal models of soft-tissue sarcoma. *Dis Model Mech*. 2010 Sep-Oct;3(9-10):557-66.



Chapter 7

SUMMARY
SAMENVATTING



SUMMARY

Soft tissue sarcomas represent a rare, heterogeneous group of mesenchymal tumors, comprising many histological subtypes that can occur almost anywhere in the body. Histological classification and prediction of clinical behaviour and prognosis in sarcomas is often a challenge. Furthermore, the lack of specific molecular markers hinders treatment targeted on the characteristic aberrations present in the tumor. A better understanding of the biology of soft tissue sarcomas is necessary to find reliable diagnostic markers, elucidate prognostic and predictive factors, and improve treatment by finding new targets for therapy.

Genomic aberrations and gene expression profiles involved in the pathobiology of soft tissue sarcoma aided in diagnostic decision making and in the elucidation of novel therapeutic targets. However, not much is known about the involvement of microRNAs (miRNAs) in soft tissue sarcoma biology. These evolutionarily conserved, small, non protein-coding RNA molecules can target (near-) complementary sequences in the 3'UTR of mRNA molecules, thereby inhibiting their translation into functional proteins. One gene can be targeted by multiple miRNAs and a single miRNA can regulate multiple mRNA molecules, which underlines the complexity and widespread effects of miRNA function. MiRNAs play important roles in diverse cellular processes and their expression is often changed in cancer. This thesis addresses the role of miRNAs in the tumor biology of soft tissue sarcoma.

In **chapter 2** we examined miRNA expression in all liposarcoma subtypes, lipomas and fat. We demonstrated that miRNAs can discriminate liposarcoma subtypes and identified subtype specific miRNAs which may aid diagnostics. The distinction between well differentiated liposarcomas and benign lipomas was blurred, suggesting these tumor types may represent a biological continuum. Myxoid/round cell liposarcomas (MRCLS) showed a very distinct miRNA expression profile. Furthermore we demonstrated that overexpression of miR-145 and miR-451 in liposarcoma cell lines decreased cellular proliferation rate, impaired cell cycle progression and induced apoptosis. We therefore suggest that these miRNAs act as tumor suppressors in adipose tissue and that re-expression of these miRNAs could be a promising therapeutic strategy for liposarcomas.

In **chapter 3** we focused on MRCLS, which displayed a very distinct miRNA expression pattern. The miR-23a~27a~24-2 and miR-23b~27b~24-1 cluster members were all significantly downregulated in MRCLS. Overexpression of miR-24 in myxoid liposarcoma cell lines with low endogenous miR-24 levels induced doxorubicin resistance, while miR-24 inhibition in sarcoma cell lines with high endogenous miR-24 levels sensitized to doxorubicin treatment. By modulation of the MRCLS specific fusion gene *FUS-CHOP*, we identified that miR-497, miR-30a and miR-34b expression is controlled by this fusion protein. Overexpression of miR-497 and miR-30a considerably downregulated protein expression of IGF1R (insulin-like growth factor receptor) and its substrates IRS1 and IRS2. We demonstrated that IRS1 is directly regulated by miR-497, IRS2 by miR-30a, and IGF1R by both miRNAs. Furthermore miR-497 and miR-30a overexpression significantly sensitized myxoid liposarcoma cell lines to doxorubicin treatment, which is possibly



mediated via the IGF1R pathway. Hence, combination therapy of miR-497 and miR-30a with chemotherapeutic or targeted agents in MRCLS should be further explored.

In **chapter 4** we determined the miRNA expression profile of gastrointestinal stromal tumors (GIST). We identified that several miR-17-92 and miR-221/222 cluster members were significantly lower expressed in GIST compared to gastro-intestinal leiomyosarcomas and normal gastrointestinal control tissues. Overexpression of miR-17, miR-20a and miR-222 in GIST cell lines strongly inhibited cell proliferation, interfered with cell cycle progression and induced apoptosis. In addition, these miRNA strongly downregulated protein and (to a lesser extent) mRNA levels of their predicted target genes *KIT* and *ETV1*, two key players in GIST oncogenesis. We confirmed direct regulation of *KIT* and *ETV1* by miR-222 and miR-17/20a, respectively. Delivering these miRNAs therapeutically could hold great potential for GIST management, especially in imatinib-resistant disease, as two essential GIST oncogenes could be repressed simultaneously.

MiRNAs expression can be influenced by changes in the tumor microenvironment, such as tumor hypoxia, which is known to contribute to aggressive tumor behavior, and radiation- and chemotherapy resistance. In **chapter 5** we identified hypoxia responsive miRNAs (HRMs) in a panel of sarcoma cell lines. We demonstrated that two of these HRMs, i.e. miR-210 and miR-485-5p, regulate *HIF3 α* in a direct and indirect manner respectively, which results in reduced HIF3 α protein levels. Regulation of *HIF3 α* by hypoxia responsive miRNAs may help to tightly regulate and fine-tune the hypoxic response. A better understanding of the mechanisms underlying the hypoxic response in soft tissue sarcomas may ultimately yield information on novel prognostic and predictive markers or targets for treatment.

In conclusion, miRNA profiling and the functional characterization of miRNAs gave more insight into the role of miRNAs in the tumor biology of soft tissue sarcoma. We identified miRNAs that can potentially be used as diagnostic, prognostic, or predictive biomarkers in soft tissue sarcomas, or could serve as a target for therapy. These results show that miRNAs hold great potential for future management of soft tissue sarcomas.



SAMENVATTING

Weke delen sarcomen vormen een zeldzame, heterogene groep mesenchymale tumoren, die bestaat uit vele histologische subtypes die bijna overal in het lichaam kunnen voorkomen.

Histologische classificatie en het voorspellen van klinisch gedrag en prognose is in sarcomen vaak ingewikkeld. Bovendien maakt het gebrek aan specifieke moleculaire markers het moeilijk de behandeling te richten op karakteristieke afwijkingen die in de tumor aanwezig zijn. Door een beter begrip van de biologie van weke delen sarcomen kunnen betrouwbare diagnostische, prognostische en voorspellende factoren, alsmede nieuwe aangrijpingspunten voor therapie geïdentificeerd worden, waardoor behandelingen kunnen verbeteren.

Genomische afwijkingen en genexpressieprofielen die betrokken zijn in de pathobiologie van weke delen sarcomen helpen bij het stellen van diagnoses en het vinden van nieuwe therapeutische targets. Er is echter weinig bekend over de rol van microRNAs (miRNAs) in de biologie van weke delen sarcomen. Deze korte, evolutionair geconserveerde, niet voor eiwit coderende RNA moleculen richten zich op (vrijwel) complementaire sequenties in de 3'UTR van mRNA moleculen. Hierdoor kunnen ze de translatie van mRNA naar functionele eiwitten remmen. Één gen kan door meerdere miRNAs gereguleerd worden, terwijl een enkele miRNA meerdere mRNA moleculen kan reguleren, wat benadrukt hoe complex en groots het effect van miRNAs is. MiRNAs spelen een belangrijke rol in diverse cellulaire processen, en de mate waarin ze voorkomen (expressie) is vaak veranderd in kanker. Dit proefschrift behandelt de rol van miRNAs in de tumorbiologie van weke delen sarcomen.

In **hoofdstuk 2** hebben we de miRNA expressie in alle subtypen van liposarcomen, lipomen en normaal vetweefsel onderzocht. We hebben laten zien dat miRNAs de verschillende subtypen kunnen onderscheiden, en hebben subtype specifieke miRNA geïdentificeerd die kunnen helpen bij diagnosestelling. Het verschil tussen goed gedifferentieerde liposarcomen en lipomen was onduidelijk, wat suggereert dat deze tumortypen wellicht een aaneengesloten biologische spectrum vormen. Myxoïde/rondcel liposarcomen (MRCLS) hadden een erg onderscheidend miRNA expressieprofiel. Verder hebben we aangetoond dat overexpressie van miR-145 en miR-451 in liposarcoomcellijnen leidt tot verminderde celproliferatie, een tragere celcyclus en de inductie van apoptose. Daarom suggereren we dat deze miRNAs in vetweefsel als tumorsuppressors werken en dat het weer tot expressie brengen van deze miRNAs een veelbelovende therapeutische strategie kan zijn voor liposarcomen.

In **hoofdstuk 3** hebben we gefocust op de MRCLS, die een karakteristiek miRNA expressieprofiel vertoonden. De leden van de miR-23a~27a~24-2 en miR-23b~27b~24-1 clusters kwamen allemaal significant lager tot expressie in MRCLS. Overexpressie van miR-24 in myxoïde liposarcoomcellijnen met lage endogene miR-24 niveaus induceerden doxorubicine resistentie, terwijl miR-24 inhibitie in sarcoomcellijnen met hoge endogene miR-24 niveaus leidde tot gevoeligheid voor doxorubicine behandeling. Door het moduleren van het MRCLS specifieke fusiegen *FUS-CHOP* hebben we kunnen vaststellen dat miR-497, miR-30a en miR-34b door dit



fusie-eiwit gereguleerd worden. Overexpressie van miR-497 en miR-30a resulteerde in sterk verminderde eiwitexpressie van IGF1R (*insulin-like growth factor receptor*) en haar substraten IRS1 en IRS2. We hebben laten zien dat IRS1 direct gereguleerd wordt door miR-497, IRS2 door miR-30a, en IGF1R door beide miRNAs. Bovendien zorgde overexpressie van miR-497 en miR-30a voor verhoogde gevoeligheid van myxoid liposarcomcellijnen voor doxorubicine, wat waarschijnlijk door de IGF1R signaleringsroute gemedieerd is. Daarom moeten combinatietherapieën van miR-497 en miR-30a met chemotherapie of gerichte medicatie in MRCLS verder onderzocht worden. In **hoofdstuk 4** hebben we de miRNA expressieprofielen van gastrointestinale stromale tumoren (GIST) bepaald. We vonden een significant lagere expressie van diverse miR-17-92 en miR-221/222 clusterleden in GIST ten opzichte van gastrointestinale leiomyosarcomen en normale gastrointestinale controleweefsels. Overexpressie van miR-17, miR-20a en miR-222 in GIST cellijnen remde de celproliferatie, verstoorde de celcyclus en induceerde apoptose. Bovendien zorgden deze miRNAs voor sterk verlaagde eiwit en (in mindere mate) RNA niveaus van hun voorspelde targetgenen *KIT* en *ETV1*, twee belangrijke spelers in het ontstaan van GIST. We bevestigden dat *KIT* en *ETV1* direct gereguleerd worden door respectievelijk miR-222 en miR-17/20a. Doordat twee essentiële GIST oncogenen gelijktijdig geremd worden, kan het therapeutisch toedienen van deze miRNAs grote implicaties hebben voor de behandeling van GIST, vooral in het geval van imatinib-resistentie.

MiRNA expressie kan beïnvloed worden door veranderingen in de tumor micro-omgeving, zoals tumorhypoxia, wat bijdraagt aan agressief tumorgedrag, en resistentie tegen stralings- en chemotherapie. In **hoofdstuk 5** hebben we hypoxia responsieve miRNAs (HRMs) geïdentificeerd in een groep sarcomcellijnen. We hebben aangetoond dat twee van deze HRMs, miR-210 en miR-485-5p, op een respectievelijk directe en indirecte manier *HIF3α* reguleren, wat leidt tot verlaagde HIF3α eiwit niveaus. Regulatie van *HIF3α* door HRMs kan helpen de hypoxische respons heel specifiek te reguleren. Een beter begrip van de mechanismen die ten grondslag liggen aan de hypoxische respons in weke delen sarcomen kan uiteindelijk nieuwe prognostische en predictieve markers en therapeutische targets opleveren.

In conclusie kan miRNA profilering en het functioneel karakteriseren van miRNAs meer inzicht geven in de rol van miRNAs in de tumorbiologie van weke delen sarcomen. We hebben miRNAs geïdentificeerd die in weke delen sarcomen potentieel als diagnostische, prognostische of predictieve biomarkers gebruikt kunnen worden, of kunnen dienen als therapeutisch target. Deze resultaten laten zien dat miRNAs veelbelovend zijn in de toekomstige behandeling van weke delen sarcomen.



Chapter 8

ACKNOWLEDGEMENTS

CURRICULUM VITAE

PUBLICATION LIST

PHD PORTFOLIO



DANKWOORD

Na al het plannen, verzamelen, pipetteren, incuberen, isoleren, analyseren, interpreteren, documenteren, presenteren en publiceren, nu eindelijk tijd om iedereen die hieraan heeft bijgedragen te bedanken. Ondanks dat dit hoofdstuk de wetenschappelijke journals niet zal halen hoop ik toch dat het een hoge impactfactor en citatiescore weet te bewerkstelligen.

Allereerst mijn promotieteam. Prof. dr. Verweij, beste Jaap, hartelijk dank dat ik op de afdeling Interne Oncologie, wat bij de start van mijn onderzoek nog onder jouw leiding stond, mocht beginnen aan mijn promotietraject. Ik dank je voor je toegankelijkheid, je enorme kennis van weke delen sarcomen, en je immer snelle respons op vragen en manuscripten.

Prof. dr. Sleijfer, beste Stefan, tijdens mijn promotietraject ben je zelf ook ‘gepromoveerd’ van mijn co-promotor tot promotor, en heb je de functie van afdelingshoofd van Jaap overgenomen. Bedankt dat je me (net als jezelf) van een uithoek van het land naar de grote stad haalde, wat ongetwijfeld goed is geweest voor mijn persoonlijke ontwikkeling. Ik heb veel geleerd van je klinische input en je schrijfkunsten en heb je (voetbal)humor altijd erg gewaardeerd. Dr. Wiemer, beste Erik, veel dank voor je vertrouwen om mij in jouw lab als eerste aan de slag te laten gaan met sarcoomonderzoek. Ik heb het erg gewaardeerd dat ik altijd bij je binnen kon lopen en wil je danken voor je ‘vaderlijke’ wetenschappelijke adviezen. Ik wil jullie alle drie hartelijk bedanken voor jullie inzet, met name met betrekking tot de afronding van mijn promotietraject.

I also want to thank the members of the doctoral committee, Prof. dr. Fodde, Prof. dr. Jenster and Prof. dr. Debiec-Rychter for reading and judging my thesis in a short time span.

Dear Maria, thank you for your collaboration on the GIST chapter. Your tumor samples and your expertise on the topic were very much appreciated. Dr. Michael den Bakker, bedankt voor je toegankelijkheid, je kennis, en het verzamelen en nakijken van de vele sarcoom- en controleweefsels. Ontzettend fijn om met zo’n top-patholoog te hebben kunnen samenwerken. Ook dank aan Prof. dr. Kees Verhoef voor het verzamelen van weefsels. Marcel Smid en Anouk Heine, hartelijk dank voor al jullie hulp bij de statistische vraagstukken en analyses. Andrea Sacchetti, many thanks for the FACS analyses. Ik dank de mensen van Center for Biomics, met name dr. Wilfred van IJcken, Christel Kockx, Zelia Ozgur en Antoine van der Sloot, voor de faciliteiten en support rondom de microarray experimenten. Dank aan dr. Joris Pothof, Maikel Wouters en Kasper Derks van Genetica voor discussies en troubleshooting met betrekking tot de microarrays. I would also like to thank our Conticanet collaborators, especially dr. Agnieszka Wozniak and Prof. dr. Patrick Schöffski (Catholic University Leuven), Prof. dr. Philipp Ströbel and Katharina Mößinger (University Medical Center Göttingen), Prof. dr. Jean-Michel Coindre, dr. Frédéric Chibon and dr. Isabelle Hostein (Institut Bergonié, Bordeaux), and other collaborators.



Natuurlijk ook veel dank aan mijn (oud-)collega's van de Interne Oncologie. Moniek (Mniekiej!), ontzettend bedankt voor al je hulp de eerste twee jaar van mijn project. We waren een goede match in het lab en daarbuiten en ik vond het dan ook erg jammer dat je ons moest verlaten. Gelukkig was daar Patricia (Patries!), ongelofelijk hoeveel werk jij verzet hebt! Bedankt dat voor al je hulp en gezelligheid op het lab. Ik vind het fijn dat je mij (in een 'verloren uurtje' ;) bij mijn promotie wilt vergezellen als paranimf! Marijn, roomy, bedankt voor je wijze raad, gezelligheid en bemoedigende woorden. Als aio's konden we niet alleen voor labzaken, maar ook voor de highlights van de laatste afleveringen van A/HNTM bij elkaar terecht. Ook bedankt voor alle informatie omtrent de promotieplanning! Labgirls, jullie hebben ervoor gezorgd dat zelfs honderden epjes schrijven en eindeloos pipetteren leuk bleef. Fijn dat we elkaar nog regelmatig blijven zien met de MoCaJoMaParties! Xander, ook jij was altijd in voor gezelligheid, ijsjes en eindeloze discussies. Bedankt voor je hulp met de tlda's. Herman, bedank voor je enthousiasme, tips en vele verhalen. Ron, bedankt voor je input bij de manuscripten. Ook dank aan andere (oud-)collega's, Ton, Robert, Najat, Walter, Peter, Inge, Mei, Lisette, Annemieke, Anne-Joy, Jacqueline, Sander, Jessica en Karel. Jonneke (Jonny!), je hebt je als mijn eerste student niet alleen als bekwaam analist maar ook als gezellig vriendinneke ontplooid. Hartelijk dank voor je werk aan het hypoxia project. Nikky, ook jij bedankt voor je werk aan het hypoxia project, met name natuurlijk het HIF3 α gedeelte. Ook voor de studenten die niet bij mij stage hebben gelopen (Nathalie, Iris, Solmaz en Sandra), het was altijd leuk studenten in het lab te hebben en te zien groeien tijdens hun stage. Veel succes allemaal met jullie verdere carrières.

Many thanks to de meiden van de 4^e die het werk net even een stukje leuker maken: Katharina, Ronak, Marcia, Lale, Diana, Esther, Renée, Wendy, Charlotte, of het nou om koffiepauze, swirls, phd-ladies nights, of regular hallway chitchats ging, bedankt voor de gezelligheid! Ook dank aan de rest van het JN1 voor alle belangstelling en hulp.

Ook dank aan mijn oud-collega's/opleiders in Maastricht (MaastRO en MolGen). Jullie hebben met jullie enthousiasme en gedrevenheid het plezier voor het labwerk in mij aangewakkerd en mij de skills geleerd die mij als PhD-student goed van pas kwamen. Hartelijk dank hiervoor!

En natuurlijk wil ik ook al mn vriendjes en vriendinnetjes bedanken voor alle slappe lach/klaag/shop/vreet/luisterend oor/enz momenten. Marieke (Mriekske!) het meisje met de Dr Martens die op de eerste dag van de uni naast me kwam zitten en nooit meer weg is gegaan. Samen de bachelor doorlopen (ik schrijven jij vroeten) en heel wat pannenkoepjes, arretjescakes en roze koeken verder nog steeds vriendinnetjes. Bedankt dat je altijd voor me klaar staat (near or far) om te lachen en te huilen. Superfijn dat je mijn paranimf wil zijn! Marjolein en Yvette, super om nog regelmatig af te spreken en alle oh zo herkenbare phd-perikelen te kunnen bespreken. Of juist helemaal nergens aan te denken en lekker lol te hebben. Leintje, je hebt ons voorgedaan



hoe het allemaal moet en mag al een tijdje van je doctors bestaan genieten. Je doet het super! Yv, fijn dat je alles met goed gevolg hebt afgerond en nu helemaal op je plaats zit in je nieuwe baan, succes! Bart, Felix, we zien elkaar iets minder vaak, maar wanneer we ons zien is het weer als vanouds. Dat hou ik er graag in! Vriendinnetjes uit 'Echt', Evi, Kim, Vera, Chantal, Marjo, ik waardeer het enorm dat we elkaar ondanks de afstand nog niet uit het oog verloren zijn. Bedankt voor alles! Anita, ongelofelijk hoe we van TGFR via lassie, soldaatjes en eindeloze shopsessies tot deze vriendschap gekomen zijn. Fniekyness rulezz!

Papa en mama, bedankt voor alles wat jullie ooit voor me gedaan hebben. Bedankt dat jullie me altijd gestimuleerd hebben het beste uit mezelf te halen, en me de mogelijkheid gegeven hebben te studeren. Ik vind het fijn dat ik altijd bij jullie terecht kan voor wijze raad. Papsie, ik bewonder je optimisme en je doorzettingsvermogen. Het spijt me dat ik niet meer voor je kan doen dan je trots maken. Miemoe, ik bewonder je warmte en zorgzaamheid. Jullie liefde voor elkaar is een groot voorbeeld voor me. Bedankt voor alles. Ik hou van jullie. De rest van de familie en schoonfamilie, bedankt voor alle interesse, steun, kaarsjes en aanmoedigingen. Altijd fijn om jullie om me heen te hebben.

Last but not least, Paulo, bedankt dat je er altijd voor me bent. Bedankt voor je positiviteit en relativeringsvermogen, voor de ontelbare keren dat je me hebt weggebracht en opgehaald, voor je begrip als ik het weer eens druk had, voor je humor waarmee je me altijd aan het lachen maakt, en natuurlijk voor je liefde, je warmte, en je armen om me heen. Wanneer ik bij jou ben kan ik alles loslaten, volledig mezelf zijn, ultiem tot rust komen, en genieten. I love you hunn.



CURRICULUM VITAE (English)

Caroline Maria Margarita Gits was born on March 4th 1986 in Sittard. She obtained her VWO diploma (secondary education), including a Latin course testimony, from the Bisschoppelijk College Echt in 2003. In September 2003 she started the study Molecular Life Sciences at Maastricht University, for which she obtained her Bachelor of Science degree in 2006. During her master Clinical Molecular Sciences she focused on oncology research. She performed her junior internship in the MaastRO (Maastricht Radiation Oncology) lab under supervision of dr. R.K. Chiu, where she investigated the effects of hypoxia on DNA damage by carcinogens. After her internship, in the summer of 2007, she continued this research as a student assistant. Caroline performed her senior internship at the department of Molecular Genetics of Maastricht University under supervision of dr. J.W. Voncken. Here she investigated the epigenetic regulation of Polycomb Group proteins in hypoxic tumor cells. In 2008 she obtained her Master of Science degree *cum laude*. In August 2008 Caroline started her PhD project at the department of Medical Oncology of the Erasmus MC in Rotterdam. Supervised by her promotores, Prof. dr. J. Verweij and Prof. dr. S. Sleijfer, and co-promotor dr. E.A.C. Wiemer, she investigated the role of microRNAs in the tumor biology of soft tissue sarcomas. The research was carried out in the context of ConTiCaNet, a European Network of Excellence, which involved collaborations with a number of European research groups. Her research describes the expression of miRNAs in diverse soft tissue sarcoma (sub)types and the functional characterization of the tumor-specific miRNAs. Caroline presented her work on various (inter)national meetings, for which she received a travel grant of the Vereniging Trustfonds Erasmus Universiteit Rotterdam in 2011. She also followed a number of additional courses, considering biomedical research, scientific communication and statistics. The results of her PhD project are described in this thesis.



CURRICULUM VITAE (Nederlands)

Caroline Maria Margarita Gits werd geboren op 4 maart 1986 in Sittard. Ze behaalde haar VWO diploma, inclusief certificaat basisvorming Latijn, in 2003 aan het Bisschoppelijk College Echt. In september 2003 begon ze aan de opleiding Moleculaire Levenswetenschappen aan de Universiteit Maastricht, waarvoor ze in 2006 haar Bachelor diploma behaalde. Tijdens de masteropleiding Clinical Molecular Sciences richtte zij zich op oncologisch onderzoek. Ze volgde haar junior stage bij het MaastRO (Maastricht Radiation Oncology) lab onder leiding van dr. R.K. Chiu, waar ze de invloed van hypoxia op DNA schade door kankerverwekkende stoffen onderzocht. Na afloop van haar stage heeft Caroline in de zomer van 2007 dit onderzoek als student-assistent voortgezet. Haar senior stage heeft ze uitgevoerd op de afdeling Moleculaire Genetica van Universiteit Maastricht, onder leiding van dr. J.W. Voncken. Hier heeft ze de epigenetische regulatie van Polycomb Groep eiwitten in hypoxische tumorcellen onderzocht. In 2008 verkreeg zij *cum laude* haar Master of Science diploma. In augustus 2008 begon Caroline haar promotieonderzoek op de afdeling Interne Oncologie van het Erasmus MC te Rotterdam. Onder leiding van haar promotores, Prof. dr. J. Verweij en Prof. dr. S. Sleijfer, en co-promotor dr. E.A.C. Wiemer, onderzocht ze de rol van microRNAs in de tumor biologie van weke delen sarcomen. Het onderzoek werd uitgevoerd in het kader van ConTiCaNet, een Europees Netwerk van Excellentie, waarbij werd samengewerkt met diverse Europese onderzoeksgroepen. Haar onderzoek beschrijft de expressie van miRNAs in diverse (sub)typen weke dele sarcomen en de functionele karakterisatie van de tumor-specifieke miRNAs. Ze presenteerde haar werk op meerdere (inter)nationale meetings, waarvoor ze in 2011 een reisbeurs ontving van de Vereniging Trustfonds Erasmus Universiteit Rotterdam. Ook volgde ze verschillende aanvullende cursussen, onder andere omtrent biomedisch onderzoek, wetenschappelijke communicatie en statistiek. De bevindingen van haar onderzoek zijn beschreven in dit proefschrift.



PUBLICATION LIST

Gits C.M.M., van Kuijk P.F., Jonkers M.B.E., Smid M., van IJcken W.F., Coindre J.-M., Chibon F., Verhoef C., Mathijssen R.H.J., den Bakker M.A., Verweij J., Sleijfer S., Wiemer E.A.C. MicroRNA expression profiles distinguish liposarcoma subtypes and implicate miR-145 and miR-451 as tumor suppressors. *Submitted*

Gits C.M.M., van Kuijk P.F., Jonkers M.B.E., Smid M., van IJcken W.F., Coindre J.-M., Chibon F., Mathijssen R.H.J., den Bakker M.A., Verweij J., Sleijfer S., Wiemer E.A.C. MicroRNAs in myxoid/round cell liposarcomas: FUS-CHOP regulated miR-497 and miR-30a target the Insulin-like Growth Factor 1 Receptor pathway. *In preparation*

Gits C.M.M., van Kuijk P.F., Jonkers M.B.E., Boersma A.W.M., van IJcken W.F., Wozniak A., Sciort R., Rutkowski P., Schöffski P., Taguchi T., Mathijssen R.H.J., Verweij J., Sleijfer S., Debiec-Rychter M., Wiemer E.A.C. Mir-17-92 and miR-221/222 cluster members target KIT and ETV1 in human gastrointestinal stromal tumors. *Accepted. Br J Cancer (2013)*

Gits C.M.M., van Kuijk P.F., de Rijck J.C.W.M., Muskens N., Jonkers M.B.E., van IJcken W.F., Mathijssen R.H.J., Verweij J., Sleijfer S., Wiemer E.A.C. MicroRNA response to hypoxic stress in soft tissue sarcoma cells: microRNA mediated regulation of HIF3 α . *Submitted*

Prickaerts P.*, Adriaens M.E.*, Van den Beucken T., Gits C.M.M., Dahlmans V.E., Zuzarte P., McPherson J., Wouters B.G.*, Voncken J.W.* (*equal contributions). Hypoxia induces bivalent chromatin domains by specific gain of H3K27me3. *In preparation*

Moessinger K., Kueffer S., Sticht C., Gits C.M.M., Simon-Keller K., Bohlender A.-L., Coindre J.-M., Sciort R., Wiemer E.A.C., Hohenberger P., Marx A., Stroebel P. The miR-17-92 cluster regulates proliferation and apoptosis in MYC amplified angiosarcomas. *In preparation*



PHD PORTFOLIO

	Year	Workload (Hours/ECTS)
General academic skills		
- Biomedical English Writing and Communication (Sep-Oct 07, Maastricht University)	2007	1.0 ECTS
- Laboratory animal science (incl assignments, presentation, final exam) (Art. 9, 19 Nov – 6 Dec 07, CPV Maastricht, MUMC+)	2007	5.0 ECTS
In-depth courses (e.g. Research school, Medical Training)		
- Radiation Hygiene 5b (Jan 07, Maastricht University)	2007	1.5 ECTS
- Course on Safe Microbiological Techniques (7-9 Feb 07, Maastricht University/Hogeschool Zuyd, Heerlen)	2007	1.5 ECTS
- Biomedical Research Techniques VII (13-17 Oct 08, MolMed, Erasmus MC)	2008	1.0 ECTS
- Epigenetics course (+held presentation+poster presentation+discussion) (17-21 Nov 08, GROW, MUMC+)	2008	5.0 ECTS
- Basic data analysis of gene expression array course (18 Dec 08, MolMed, Erasmus MC)	2008	1.2 ECTS
- Browsing genes and genomes with Ensembl (16-17 Sep 09, MolMed, ErasmusMC)	2009	0.6 ECTS
- SPSS (22-23 Oct 09, MolMed, ErasmusMC)	2009	0.6 ECTS
- Course Basic and Translational Oncology (9-12 Nov 09, MolMed, ErasmusMC)	2009	1.8 ECTS
- Course Molecular Medicine (2-3 Mar 10, MolMed, ErasmusMC)	2010	0.7 ECTS
- Course on Photoshop CS3 (12+14 Apr 10, MolMed, ErasmusMC)	2010	0.3 ECTS
- Course Systems Biology Applied Bioinformatics, Sequences and Variations (28-29 Oct 10, MolMed, ErasmusMC)	2010	0.7 ECTS



	Year	Workload (Hours/ECTS)
Presentations		
- Poster Presentation @ CTOS Annual Meeting (6 Nov 09, Bold New Eden Roc, Miami Beach)	2009	0.5 ECTS
- Oral presentation @ JNI Scientific Lab Meetings (7 Dec 09, JNI, ErasmusMC)	2009	0.5 ECTS
- Oral presentation @ Conticanet Annual General Assembly 2010 (29 Jan 10, Faculty Club, Leuven)	2010	0.5 ECTS
- Poster presentatie @ 14 th Molecular Medicine Day (4 Mar 10, MolMed, Congress Centre Engels, Rotterdam)	2010	0.1 ECTS
- Oral presentation @ Symposium on Translation Oncology, KWF (27 Sep 10, De Reehorst, Ede)	2010	0.1 ECTS
- Oral presentation @ Scientific meeting Medical Oncology (1 Oct 10, Erasmus MC Woudestein, Rotterdam)	2010	0.1 ECTS
- Oral presentation @ JNI Scientific Lab Meetings (29 Nov 10, JNI, ErasmusMC)	2010	0.5 ECTS
- Poster presentation @ 15 th Molecular Medicine Day (3 Feb 11, MolMed, Congress Centre Engels, Rotterdam)	2011	0.5 ECTS
- Poster presentation @ AACR International Conference on Frontiers in Basic Cancer Research	2011	0.5 ECTS
- Oral presentation @ JNI Scientific Lab Meetings (20 Feb 12, JNI, ErasmusMC)	2012	0.5 ECTS
- Poster presentation @ 16 th Molecular Medicine Day (29 Feb 12, MolMed, Congress Centre Engels, Rotterdam)	2012	0.5 ECTS
- Oral presentation PhD-Meeting (5 Apr 12, Erasmus MC, Rotterdam)	2012	0.1 ECTS
- Oral presentation PhD-Meeting (18 Oct 12, Erasmus MC, Rotterdam)	2012	0.2 ECTS
- Poster presentation @ 17 th Molecular Medicine Day (13 Feb 13, MolMed, Congress Centre Engels, Rotterdam)	2013	0.5 ECTS



	Year	Workload (Hours/ECTS)
International conferences		
- Conticanet Annual General Assembly 2009 (8-9 Jan 09, Institute Curie, Paris)	2009	0.6 ECTS (16h)
- CTOS Annual Meeting (5-7 Nov 09, Bold New Eden Roc, Miami Beach)	2009	0.8 ECTS (22h)
- Conticanet Annual General Assembly 2010 (29 Jan 10, Faculty Club, Leuven)	2010	0.3 ECTS (8h)
- Conticanet Annual General Assembly 2011 (13 Jan 11, Hotel Novotel Charenton, Paris)	2011	0.3 ECTS (8h)
- AACR International Conference on Frontiers in Basic Cancer Research (14-18 Sep 11, Intercontinental San Francisco, San Francisco)	2011	1.3 ECTS (37h)
Seminars and workshops		
- Molecular Mechanisms and Mouse Models in Cancer (27-28 Nov 08, Royal Tropical Institute, Amsterdam)	2008	0.6 ECTS (16h)
- 13 th Molecular Medicine Day (5 Feb 09, MolMed, Congress Centre Engels, Rotterdam)	2009	0.2 ECTS (6h)
- Workshop Pharmacokinetics & Pharmacodynamics (09 Mar 09, JN1 ErasmusMC, Rotterdam)	2009	0.2 ECTS (6h)
- Get Out Of Your Lab Days (12-14 Mar 09, Molmed, Soest)	2009	1.0 ECTS (28h)
- 14 th Molecular Medicine Day (4 Mar 10, MolMed, Congress Centre Engels, Rotterdam)	2010	0.3 ECTS (10h)
- Symposium on Translational Oncology (27 Sep 10, KWF, De Reehorst, Ede)	2010	0.3 ECTS (8h)
- Molecular Mechanisms in Cancer (11-12 Nov 10, Royal Tropical Institute, Amsterdam)	2010	0.6 ECTS (16h)
- 15 th Molecular Medicine Day (3 Feb 11, MolMed, Congress Centre Engels, Rotterdam)	2011	0.3 ECTS (10h)
- Emergency Service - Fire Extinguishing Systems (24 Mar 11, ErasmusMC, Rotterdam)	2011	0.1 ECTS (2h)
- Epigenetics and noncoding RNAs (10-11 Nov 11, Royal Tropical Institute, Amsterdam)	2011	0.6 ECTS (16h)
- 16 th Molecular Medicine Day (29 Feb 12, MolMed, Congress Centre Engels, Rotterdam)	2012	0.3 ECTS (10h)
- Poster presentation @ 17 th Molecular Medicine Day (13 Feb 13, MolMed, Congress Centre Engels, Rotterdam)	2013	0.2 ECTS (6h)



	Year	Workload (Hours/ECTS)
Supervising Master's theses		
- Supervising BSc student 30wks internship (Nov 10 – Jun 11, ErasmusMC, Rotterdam)	2010-2011	4.3 ECTS (120h)
- Co-Supervising BSc student 40wks internship (Aug 11 – May 12, ErasmusMC, Rotterdam)	2011-2012	1.4 ECTS (40h)



